The role of Endothelial Cell Specific Chemotaxis Regulator (ECSCR) in endothelial cell biology

By Ana Raquel Andrade Veríssimo

A Thesis submitted to The University of Birmingham for the degree of
DOCTOR OF PHILOSOPHY

School of Immunity and Infection

College of Medical and Dental Sciences

The University of Birmingham

September 2012

ABSTRACT

Angiogenesis, although a natural process, when deregulated can be associated with many human pathologies, including cancer. The endothelial cells play a crucial role in the growth and remodelling of the vasculature. A novel unique endothelial marker, endothelial cell specific chemotaxis regulator (ECSCR), has been identified and the aim of this project was to characterise its expression patterns and mechanism of action.

In HUVECs the interaction with filamin A was confirmed and immunoprecipitation has pulled down several cytoskeletal proteins involved in cell movement, including moesin, that binds to ECSCR. ECSCR loss causes cytoskeleton to be disorganised and overexpression induces filopodia in HEK 293T cells, but not M2 cells, that do not contain filamin A.

In zebrafish ECSCR is restricted to the major trunk and head vasculature, whereas in mouse it appears to be present also in the intersegmental vessels. Morpholino mediated knockdown of zebrafish Escr caused disruption of intersegmental vessel sprouting from the trunk vessels. The original phenotype was successfully rescued. A null Ecscr knockout mouse has been produced and preliminary data show that the deletion is not lethal and ECSCR is present in some small vessels, but not all vasculature. Loss of ECSCR may result in respiratory complications.

ACKNOWLEDGEMENTS

First and foremost, I would like to express my gratitude to my supervisor, Professor Roy Bicknell. Thank you very much for all your patience, support and advice. It was a great pleasure and a privilege to be a part of your team.

I thank Rajeeb, my supervisor for a year, who taught me a great deal about fish and my other fish supervisor, Dr, Ferenc Mueller.

Many thanks to all the Bicknell lab members, past and present, effective and extended, by neighbouring effect. Life would not have been the same without the lunchtime daily crosswords.

Thank you to my friends, especially Anabela and Vanessa, for all your friendship and support.

Finally, I would like to thank my family, especially my parents, for being there, always.

TABLE OF CONTENTS

LIST OF FIGURES

ABBREVIATIONS

aa – amino acid

APS – ammonium persulfate

BAC – bacterial artificial chromosome

BSA – bovine serum albumin

cDNA – complimentary deoxyribonucleic acid

CKO – conditional knock out

cRNA – complimentary ribonucleic acid

Cy3 – cyanine 3-cytosine triphosphate

Cy5 – cyanine 5-cytosine triphosphate

DEPC – diethylpyrocarbonate

dH_2O – distilled water

DNA – deoxyribonucleic acid

DNase – deoxyribonuclease

dNTP – 2'-Deoxyribonucleoside-5'-tri- phosphate

DTT – dithiothreitol

ecd – extracellular domain

ECSCR – (human) endothelial cell specific chemotaxis regulator

EDTA – ethylenediamine tetra-acetic acid

fc – final concentration

FCS – foetal calf serum

HEK – human embryonic kidney

hpf – hours post fertilization

HUVEC – human umbilical vein endothelial cell

icd – intracellular domain

KO – knock out

mECSCR – mouse endothelial cell specific chemotaxis regulator

MMLV-RT – murine Moloney leukaemia virus reverse transcriptase

NCBI – National Center for Biotechnology Information

NTP – nucleoside triphosphate

PEG – polyethylene glycol

PBS – phosphate buffered saline

PBST – phosphate buffered saline with tween

PCR – polymerase chain reaction

PFA – paraformaldehyde

PMSF – phenylmethylsulfonyl fluoride

RNA – ribonucleic acid

RNase –ribonuclease

RS – restriction site

TEMED – N,N,N',N'-tetramethylethylenediamine

SDS – sodium dodecyl sulphate

SEND – (mouse) skin endothelial

siRNA – small interference ribonucleic acid

SMART – simple modular architecture research tool

SSC – saline sodium citrate

TBS – tris buffered saline

TBST – tris buffered saline with tween

WISH – Whole-mount *in situ* hybridization

1 GENERAL INTRODUCTION

1.1 The role of endothelial cells in angiogenesis

The endothelium is a single layer of simple squamous epithelial cells that line the interior surface of blood vessels of the entire human vascular system. The development of new blood vessels from existing vasculature is known as angiogenesis or neovascularisation (Risau, 1997). This complex and organised process comprises vascular initiation, formation, maturation, remodelling and regression (Gilbert, 2006). The endothelial cells forming new vessels are stimulated with angiogenic factors which make them more permeable. Then, they start secreting proteolytic enzymes that breakdown the basement membrane to create space for the new vessel (Mignatti and Rifkin, 1996). Some cells from the vessel wall start migrating towards the gradient of angiogenic factors and form a tube, that merges with another vessel and a lumen is formed. This vessel will then mature and be stabilised by the recruitment of pericytes (Carmeliet, 2003; Jain, 2003; Adams and Alitalo, 2007).

1.2 Developmental and pathological angiogenesis

Angiogenesis is fundamental for normal development and healing (inflammation, wound healing), but it also occurs in over 70 different disease states, due to loss of regulation of normal processes. Diabetic retinopathy, rheumatoid arthritis, psoriasis and cancer are some examples of these pathologies (Pandya *et al*., 2006).

For over 30 years researchers have been studying developmental and pathology-associated vascularisation in quest for angiogenesis-stimulating factors that could be used as targets for anti-angiogenic therapies (Folkman, 1971; Denekamp, 1982; Folkman and Klagsbrun, 1987; Kidd and Weinstein, 2003). However, these two kinds of vessel development differ from each other.

Although the heart is the first functional organ of the body, it only begins to beat after the embryonic first circulatory loops are formed. A primitive vascular plexus is originated by a process called vasculogenesis when the embryo is still being nourished by diffusion. Therefore, the embryonic vasculature is different from the adult one, since it must adapt to the changes occurring in the embryo. This plexus is connected to the heart tube and when this organ starts to pump, this initial network is irrigated and the first circulation is established. The link between vasculogenesis and angiogenesis is made by the expression of VEGF receptors by pluripotent precursors in response to FGF. This is how the pluripotent precursors become hemangioblastic precursors. After vasculogenesis, the primary capillary networks are remodelled and veins and arteries are formed, by angiogenesis (Gilbert, 2006; Flamme *et al*, 1997).

The initial formation of a tumour is not dependent of blood vessels. Only when it reaches a volume of 2 mm^3 neovascularisation occurs in response to the tumour oxygen and nutrient demands. This vascularisation is called tumour angiogenesis, since it differs from developmental and normal angiogenesis (Sacewicz *et al*., 2009). Due to these differences, tumour vasculature can be described as immature vasculature. The walls are poorly developed, with few vascular smooth muscle cells and pericytes, which results in higher permeability and the networks are chaotic and lack a hierarchy (Tozer *et al*., 2005; Neri and Bicknell, 2005). Apart from recruiting neighbouring blood vessels and vascular endothelial cells to support their own nourishment, tumours also have the ability to produce angiogenic factors to mobilise bone marrow-derived endothelial precursor cells into the developing vasculature (Rafii *et al*., 2002).

1.3 Targeting angiogenesis

The quest for factors that promote tumour angiogenesis as therapeutic targets for cancer has begun many decades ago, with the study of vascular endothelial growth factor (VEGF)

(Ferrara, 2002). Although VEGF plays a pivotal role in vascular development, it has become clear that it has a function in other non-vascular processes such as organogenesis and patterning and therefore new targets are needed without this kind of side effects (Coultas *et al*., 2005; Greenberg and Jin, 2005). Additionally, although showing some therapeutic efficacy in mouse models and some human cancers, relapse and tumour progression follow the transitory positive effects of anti-VEGF therapies (Bergers and Hanahan, 2008). Free radicals, such as reactive oxygen species, are created by hypoxic conditions in tumours. These, in combination with hypoxia- reoxygenation cycling and immune cell infiltration after chemotherapy affect hypoxia- inducible factor 1 (HIF1) activity, which is implicated in endothelial and tumour cell survival (Dewhirst *et al*., 2008). Hypoxic and necrotic regions found in tumours offer the opportunity for cancer-selective therapy (Brown and Wilson, 2004). Nitric oxide is also a highly reactive free radical that regulates several physiological functions, such as angiogenesis, blood flow, vascular permeability, leukocyte-endothelial interaction, platelet aggregation, microlymphatic flow, as well as neurological and cytotoxic functions (Fukumura *et al*., 2006). This molecule is produced by endothelial nitric oxide synthase (eNOS) which is present, together with other signalling proteins, at the endothelial cell surface in microdomains called caveolae. Caveolin 1 seems to have the capacity to inactivate eNOS and act as a tumour suppressor *in vitro* although *in vivo*, at later stages, it appears to play a role in cancer chemoresistance, survival and metastasis (Carver and Schnitzer, 2003). Tumour blood vessels express markers not present in normal vasculature, but shared by angiogenic vessels in non-malignant conditions. Thus, a better understanding of tumour cells is needed, as well as caution regarding normal angiogenesis, when designing anti-angiogenic therapies (Rouslahti, 2002). Since vascular endothelium is not a homogeneous tissue, Kuzu *et al*. (1992) reported the diagnostic usefulness of using a panel of antibodies against vWF, CD31 and CD34 to identify

tumours of vascular origin, as they gave reliable immunostaining even for formalin fixed, paraffin wax embedded sections. Other known endothelial markers are the transcription factor Fli-1, several receptors including the VEGF receptors (FLT1, KDR) and the angiopoetin receptors TIE1 and TIE2/TEK (Verissimo *et al*., 2009).

The advent of modern sequencing and expression analysis combined with advances in bioinformatics datamining has led to the recent discovery of several novel endothelial genes. Our group has used a bioinformatics datamining strategy that combined expressed sequence tags (EST) cluster expression analysis in the human Unigene index and SAGEmap xProfiler to identify novel endothelial-specific genes. Four novel genes were identified: endothelial cell-specific molecules (ECSM) 1-3 and magic roundabout (similar to the axon guidance protein roundabout Robo1). We have also identified endothelial protein-disulfide isomerase (EndoPDI), highly expressed in endothelial cells. mRNA and protein levels of EndoPDI are induced by hypoxic conditions and it was shown to have a protective role only in cells exposed to hypoxia, in contrast to PDI which displayed no differences between cell protection under hypoxic or normoxic conditions. Furthermore, we showed by *in situ* hybridization that EndoPDI expression is very rare in normal tissues, being expressed preferentially in tumour endothelium and other hypoxia-associated lesions. These data indicate that EndoPDI is a potential target for tumour endothelial therapies (Verissimo *et al*., 2009).

On the other hand, pro-angiogenic therapies are also useful in treating diseases such as ischaemic disorders and some therapies have already been approved for use in several countries (Ferrara and Kerbel, 2005).

1.4 The identification and characterization of endothelial cell specific chemotaxis regulator (ECSCR)

Expressed sequence tags (EST) of endothelial cell specific chemotaxis regulator (ECSCR – formerly ECSM2) were found to be enriched in endothelium by bioinformatics datamining (Huminiecki and Bicknell, 2000). It was described as an endothelial marker for the first time in a study by Pelosi *et al*. (2002), where they showed that ECSCR was present in a postnatal population of $CD34^{+}KDR^{+}$ cells comprising hemangioblasts and endothelial progenitors. The endothelial specificity of ECSCR has also been confirmed by quantitative polymerase chain reaction using a range of endothelial and non-endothelial cell lines (Herbert *et al*., 2008; Armstrong *et al*., 2008), as well as *in situ* hybridization on a variety of human tissues (Armstrong *et al.*, 2008). By applying a novel method of differential gene expression analysis using multiple cDNA libraries, Herbert *et al*. (2008) have identified ECSCR within the top nine predicted tumour endothelial markers. More recently, this protein has been found to be upregulated in another type of disease, colitis, where increased pathological angiogenic activity plays a role (Fang *et al*., 2011). ECSCR is a glycosylated type I transmembrane protein, present especially in spike-like cell protrusions termed filopodia. Reduced chemotaxis and impaired tube formation on Matrigel™ were observed when ECSCR was knocked down by siRNA. Filamin A was identified in a yeast-two-hybrid screen as an interacting protein for its intracellular domain. This was confirmed by GST (glutathione-s-transferase) pull down. Taken together, these data implicate a role for ECSCR in angiogenesis through modulation of the actin cytoskeleton. Mouse and zebrafish orthologs were identified (Figure 1.1) (Armstrong *et al*., 2008). The predicted structure for these three proteins using SMART software indicates the presence of a signal peptide, and extracellular, transmembrane and intracellular domains, as shown on figure 1.2.

The chromosomal location of the human, mouse and zebrafish genes is 5q31.2, 18 B2 and chromosome 21, respectively. The NCBI accession numbers for cDNA and proteins for *Homo sapiens*, *Mus musculus* and *Danio rerio* are NM_001077693/NP_001071161.1, NM_001033141.1/NP_001028313.1 and XM_002666009.1/XP_002666055.1, respectively. Other names for the protein are ECSM2/ARIA (human), Ecsm2/Riken1110006O17 (mouse) and hypothetical LOC100006714 (zebrafish).

The data produced by Armstrong *et al.* (2008) were rapidly independently confirmed by Ma *et al*. (2009). They observed that in HEK293 cells transfected with ECSCR-GFP overall tyrosine phosphorylation signalling was reduced compared to the controls. ECSCR may have a role in attenuating the epidermal growth factor (EGF)-induced cell migration by cross talking with its receptor (EGFR), possibly by inhibiting the Shc-Ras-ERK (MAPKinase) pathway. In these transfected cells actin stress fibres formed by filament bundling were destroyed and the formation of filopodia was induced. In addition to its location to the plasma membrane and enrichment in filopodia in isolated cells, the same group has shown that ECSCR is also present in cell-cell junctions in confluent cells (Shi *et al*., 2011). ECSCR promotes cell aggregation and seems to inhibit basic fibroblast growth factor (bFGF)-mediated cell migration via the FGFR-ERK-FAK pathway (Shi *et al*., 2011).

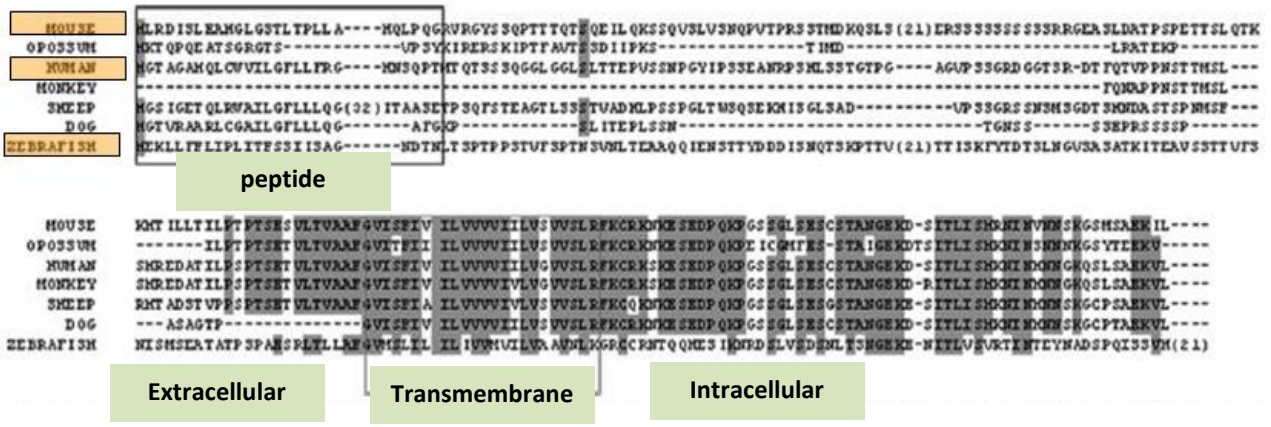

Figure 1.1 – Alignment of ECSCR orthologs.

To search for ECSCR orthologs, the human gene was aligned with genomes of different species using the Ensembl website (www.ensembl.org/). The correspondent proteins were then aligned using the online multiple sequence alignment tool Clustalw2 (http://www.ebi.ac.uk/Tools/msa/clustalw2/). Conserved regions are highlighted in grey. The transmembrane and intracellular domains show greater conservation than the extracellular domain (adapted from Armstrong *et al.*, 2008).

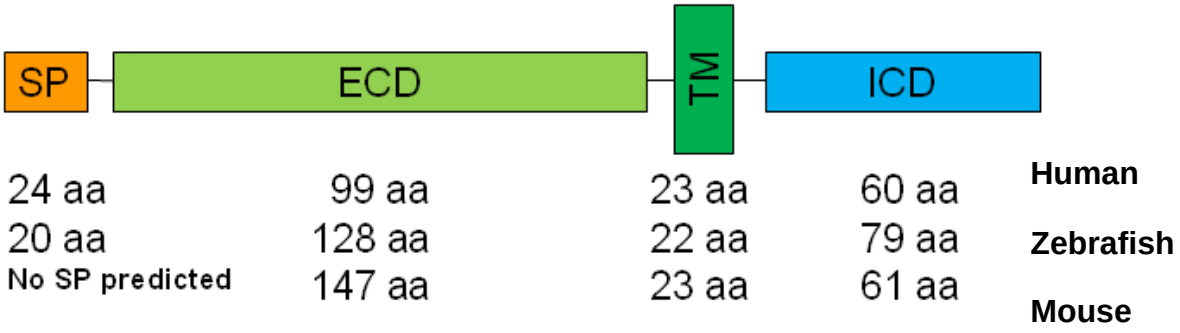

Figure 1.2 – Predicted structure for human, zebrafish and mouse ECSCR using SMART.

The predicted sequences of the human, zebrafish and mouse ECSCR proteins were obtained from NCBI (http://www.ncbi.nlm.nih.gov/) and analysed using SMART (Simple Modular Architecture Research Tool) (http://smart.embl-heidelberg.de/) to search for architectural features. It was predicted that these proteins contained a signal peptide (SP) (except the murine version), an extracellular domain (ECD), a single transmembrane domain (TM) and an intracellular domain (ICD).

aa – amino acids.

In a second study published in 2009 the authors did not acknowledge the existence of ECSCR and submitted their work on a "novel" endothelial protein called ARIA (apoptosis regulator through modulating IAP expression) (Ikeda *et al.*, 2009). They described that ARIA (ECSCR) interacted with proapoptotic proteins cIAP-1 and cIAP-2, modulating their degradation by the proteasome and thus regulating endothelial cell survival. They found that ARIA is expressed in mouse embryonic vasculature and also in endothelial cells *in vivo* and *in vitro*. ARIA siRNA knockdown in HUVECs resulted in significant reduction of apoptosis. More recently, the same group has produced an ARIA knockout mouse and described that this molecule regulates the PTEN/PI3K/Akt/eNOS pathway. The mice display non-lethal bleeding during embryogenesis and increased small vessel density, as well as altered expression of vascular growth factors, such as angiopoetins and VEGF receptors. Post-natal neovascularisation was enhanced using the critical limb ischemia model and more bone marrow-derived endothelial cells were found in ischemic muscle. ARIA was found to be enriched in endothelial progenitor cells (Koide *et al*., 2011).

Ecscr knockdown in zebrafish developing embryos slows down angioblast migration towards the midline (posterior lateral plate mesoderm) (Verma *et al*., 2010). In HUVECs ECSCR partially co-localises with KDR and its knockdown results in lower VEGF-induced phosphorylation of KDR (lower sensitivity to VEGF).

A summary of the current knowledge of ECSCR proposed signalling is depicted on figure 1.3. So far, even though there is discrepancy in some results, ECSCR seems to be an interesting and promising target for angiogenesis therapies, due to its endothelial specificity and role in cell motility, adhesion and apoptosis.

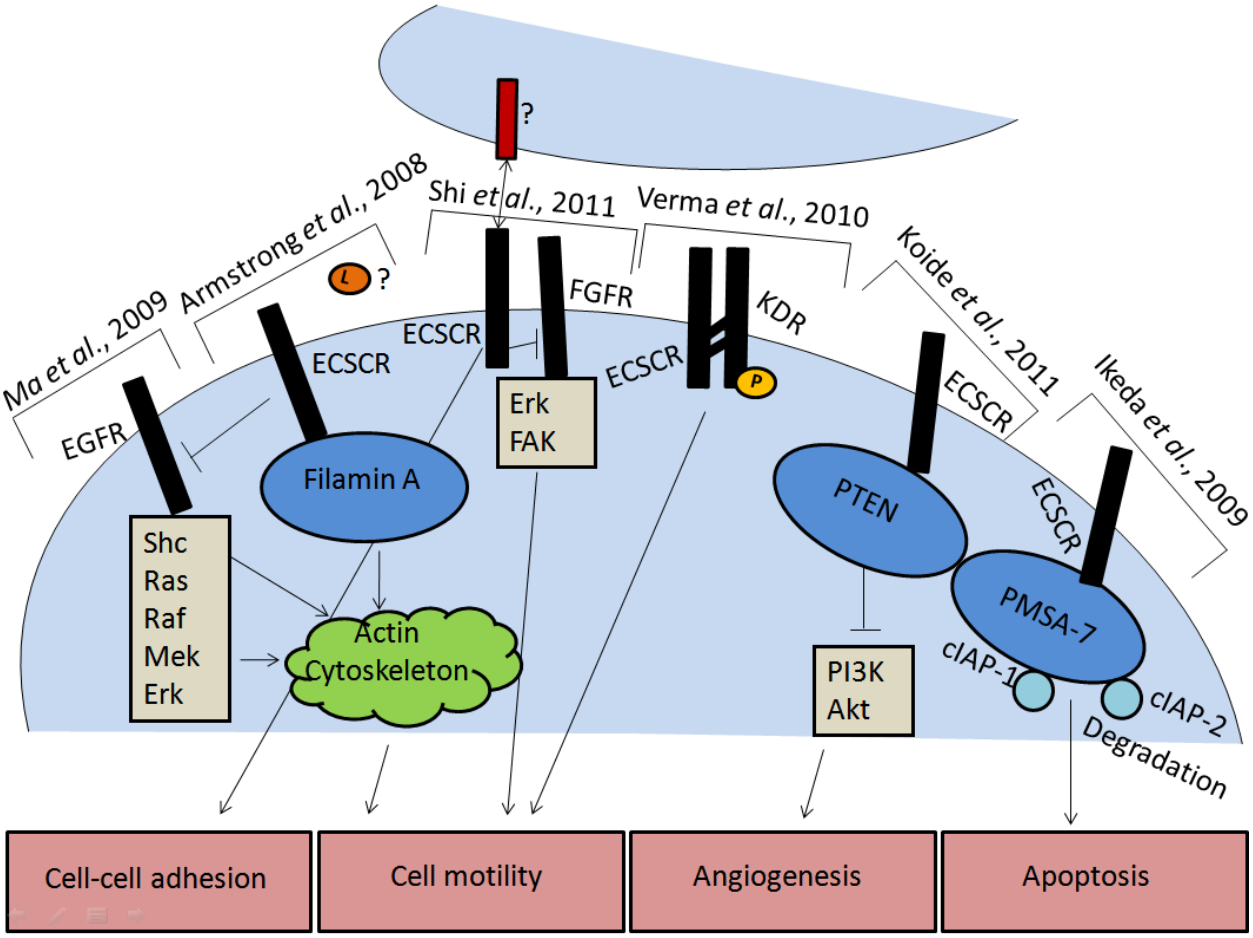

Figure 1.3 – Proposed models describing the current knowledge of ECSCR signalling in endothelial cells

Although the literature on ECSCR is still limited, different studies suggest distinct roles for the protein in endothelial cells: apoptosis, via direct interaction with cIAP, angiogenesis through PTEN, cell motility by directly interacting with Filamin A or contributing to phosphorylation of EGFR or KDR and cell-cell adhesion through interaction with a possible ligand or the ECSCR molecule itself. KDR - Kinase insert domain receptor; EGFR – epidermal growth factor receptor; L – ligand; P – phosphorylation; FAK – focal adhesion kinase; PTEN – phosphatase and tensin homolog; cIAP – cellular inhibitor of apoptosis protein; PMSA-7 – proteasome subunit α7. (adapted from Verissimo *et al.*, 2009).

1.5 Cell migration: the fine orchestration between protrusion, retraction and adhesion

Cell migration is essential for both physiological and pathological processes. During embryonic development intensive migration occurs so that different lineages of cells can reach a proper location (Kurosaka and Kashina, 2008). Throughout life, certain cell types continue to migrate in order to be able to perform their roles, such as those from the immune system (Madri and Graesser, 2000). In pathological conditions, such as cancer, metastatic cells are highly motile (Seol *et al*., 2012). Migration is a multi-step, dynamic, cyclic process, that comprises the extension of protrusions at the leading edge, substrate adhesion and rear retraction. All these are achieved by rapid modulation and coordination of complexes of cytoskeletal proteins.

1.5.1 Filopodia and lamellipodia at the leading edge of migrating cells

In response to external signals cells polarise, acquiring a conspicuous morphology, characterised by flat membrane protrusions, termed lamellipodia, and spike-like protrusions called filopodia at the leading edge (figure 1.4). The formation of two distinct protrusive actin structures with different architectures and dynamics in close spatial proximity is due to the activation of two separate nucleation pathways, Arp2/3 and formins (Gomez *et al.*, 2007).

Actin filaments polymerise at the leading edge and depolymerise at the rear of lamellipodia, in a process named treadmilling (Wang, 1985). The fast-moving and short-lived lamellipodial actin speckes are preceded by slow-moving, long-lived speckles that form the lamella. Actin is arranged in branched filaments in lamellipodia, whereas in the lamella it is presented as loose, unbranched filaments containing tropomyosin and myosin II (figures 1.4 A and 1.4 D)

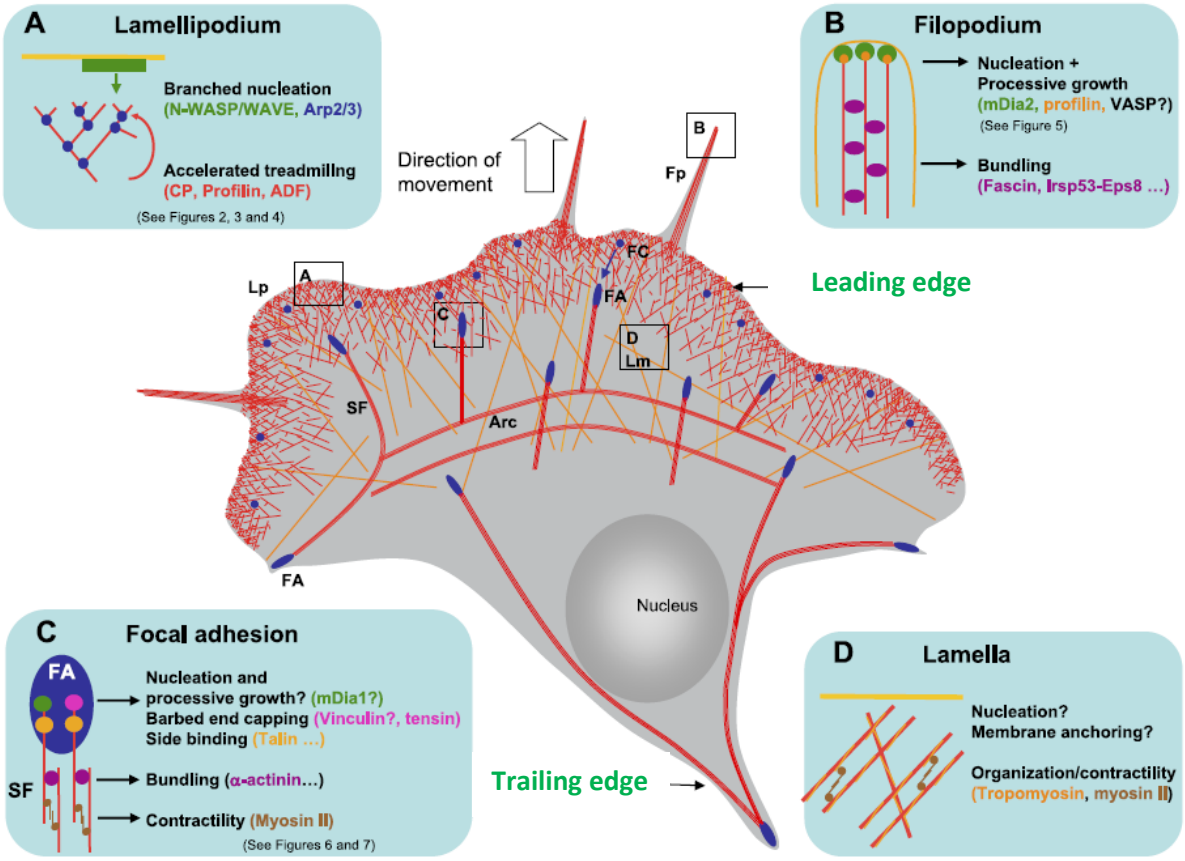

Figure 1.4 - Processes involving the actin cytoskeleton during cell migration

In lamellipodia, branched actin filaments are formed at the plasma membrane by WASP-Arp2/3 and regulated by a set of regulatory proteins (ADF, capping proteins, profilin) (A). When migrating, cells extend finger-like protrusions called filopodia beyond the protruding lamellipodia to sense the environment. At the tip, formins like mDia2 catalyze the processive assembly of profilin-actin. The resulting non-branched actin filaments are tightly bundled by several proteins including fascin and the Irsp53-Eps8 complex (B). Slow moving cells form focal adhesions, that connect the extracellular matrix to contractile bundles made of actin filaments, myosin II, and bundling proteins including alpha-actinin (C). The lamella contains tropomyosin and myosin II. The nucleating and anchoring at the plasma membrane mechanisms are unknown (D). Lp - lamellipodium; Fp - filopodium; Lm - lamella; SF - stress fiber; FA - focal adhesion; FC - focal complex (adapted from Le Clainche and Carlier, 2008)

(Le Clainche and Carlier, 2008). Surprisingly, injection of tropomyosin resulted in loss of lamellipodia but increased leading edge protrusions and accelerated migration. This suggests that lamellipodia may be more important in other processes, such as pathfinding (Gupton *et al.*, 2005). At low concentrations, cofilin promotes actin depolymerisation by cleavage and at high concentrations it nucleates actin filaments, (Adrianantoadro and Pollard, 2006), whereas profilin binds monomeric actin (Yarmola and Bubb, 2006). Treadmilling is a dynamic process that involves and depends on the balance of many proteins that contribute to actin filaments progression and regression, such as severing, nucleating and capping proteins (Le Clainche and Carlier, 2008).

As cells migrate, actin filaments need to be continuously polymerised at one end and disassembled at the other. In the lamellipodium the Wiskott–Aldrich Syndrome Proteins (WASP) activate the actin related proteins (Arp)2/3 complex, which works in coordination with cofilin, profilin and capping proteins to achieve branched nucleation. The Arp2/3 complex, located at the leading edge, determines the direction of the protrusion (Goley and Welch, 2006). Actin assembly by Arp2/3 through WASP activation occurs downstream from Rac1 and Cdc42 (responsible for the formation of ruffles and filopodia, respectively) (Nobes and Hall, 1995).

Contrasting with the branched architecture of lamellipodia, filopodia are formed of 15-20 parallel filaments tightly packed (figure 1.4 B). They locate exteriorly to lamellipodia, at the leading edge of protrusions (Lewis and Bridgman, 1992). Actin assembly and retrograde flow control extension and retraction in these structures, respectively. Although Cdc42 controls filopodia formation, some authors argue that the Arp2/3 complex does not contribute to actin nucleation in this context, supported by the fact that N-WASP null fibroblasts possess normal filopodia and the Arp2/3 complex promotes branched rather than linear actin nucleation (La

Clainche and Carlier, 2008). In the same year our group has described a role for the Arp2/3 complex in filopodia formation (Sheldon *et al*., 2008). In order to investigate the role of roundabout proteins in endothelial cell biology, Robo1 and Robo4 siRNA knockdown was performed in HUVECs and it was found that both resulted in impaired cell migration and tube formation. Yeast-two-hybrid analysis, confirmed by glutathione-s-transferase pull down, has identified WASP and Arp2/3 as interacting partners for Robo4 intracellular domain, as well as Mena, which signals downstream from Cdc42 and IRSp3 (insulin receptor substrate fo 53 kDa) to initiate filopodia. The heterodimer Robo1-Robo4 is essential for the formation of filopodia. It was hypothesised that Slit 2 binds to Robo1 when in a complex with Robo4 thus eliciting the formation of filopodia. Furthermore, in zebrafish endothelial cells, Robo4 activates and controls the levels of Cdc42 and Rac1. Angioblasts isolated from zebrafish embryos where Robo4 was knocked down search actively for direction, which suggests a role for Robo4-Rho GTPases in attractive vascular guidance (Verissimo *et al*., 2009).

Formins are another group of actin-nucleating proteins downstream of Rho GTPases that are present at the tip of filopodia and induce their formation (diaphanous-related formin, mDia2). In *Dyctiostelium* dDia2 is required for filopodial extension (Schirenbeck *et al*., 2005). In a study in *Drosophila*, Homem and Peifer (2009) have shown that activated Dia mobilises enabled (Ena) to the deading edge. Although each of these proteins is sufficient to induce filopodia, jointly they induce lamellipodia. Taken together, these observations suggest that the ratio between Dia and Ena regulate the balance between these protrusive structures. Clearly, cytoskeletal rearrangements are complex and multifactorial, contemplating fine equilibria and perhaps some redundancy, as well as cell type-specificity.

Phosphorylated ERM (ezrin, radixin, moesin) actin-binding proteins also locate at filopodia (Bretscher *et al.*, 2002).

1.5.2 The role of cell-matrix adhesions in cell migration

Cell migration starts with the emission of cytoplasmatic protrusions and also includes the traction of the cell body and tail retraction. Adhesion to the matrix is key in controlling the dynamics between protrusion (achieved by actin assembly at the leading edge) and the traction of the cell body and retraction of the tail (achieved by actomyosin contractile force) (La Clanche and Carlier, 2009). There are three types of adhesion structures: focal complexes, focal adhesions and fibrillar adhesions (figure 1.5) (La Clanche and Carlier, 2009). Focal complexes are dot-like, Rac1 activated, nascent adhesions that disassemble and reassemble at the leading edge during protrusion and contain a loose actin network (Rottner *et al.*, 1999). Proteins such as PAK-interacting exchange factor PIX and G-protein-coupled receptor kinase (GRK)-interacting target 1 (GIT1) participate in focal complex disassembly (Zhao *et al*., 2000). In response to RhoA these structures stabilise, mature and give origin to focal adhesions. These are associated with the end of stress fibres and contain vinculin, talin, paxillin, alpha-actinin, focal adhesion kinase (FAK) and integrin αvβ3 (Zaidel-Bar *et al*., 2003). In turn, fibrillar adhesions arise from focal adhesions, although much less complex, and contain tensin and integrin α5β1, taking the shape of thin actin cords (Zamir *et al.*, 2000).

Vinculin is present in focal adhesions and is able to bind actin and talin. Its regulation seems to be important for angiogenesis, as low levels are required for *in vitro* tube formation (as well as integrin α2, talin, α-actinin and actin, although these proteins don't decrease as much) (Deroanne *et al.*, 1996). Integrins are a large family of transmembrane receptors formed of alpha and beta chains that play a major role in mediating interactions between the intracellular compartment and the extracellular matrix. Eighteen α subunits and eight β subunits can combine to form 24 functional heterodimers. Thus, they are involved in a variety of physiological processes, such as cell migration, embryogenesis and haemostasis. Ligand

binding leads to clustering and recruitment of actin filaments through the interaction with cytoskeletal proteins, such as talin, vinculin, α-actinin and filamin (Hemler, 1999). Integrins have the ability to signal bidirectionally, allowing a dynamic exchange between the intracellular and extracellular compartments (Legate *et al*., 2009). Signalling involving integrins is very complex as there are, to date, 156 proteins known to be part of the integrin adhesome (Moser and Legate, 2009). Focal adhesion kinase plays a crucial role in focal adhesions (and therefore in regulating cell motility), by switching between Rho GAPs and GEFs. RhoA activation leads to increased cell contractility and trailing edge retraction, whereas RhoA inactivation results in decreased cell contractility and lamellipodia formation (Tomar and Schlaepfer, 2009).

Stress fibres are essential to achieve retraction of the rear of the cell, by applying contractile force on focal adhesions (Small and Resch, 2005). These structures are formed of actin and myosin and are found both in association with focal adhesions and independent from focal adhesions. Stress fibre formation associated with focal adhesions is activated by RhoA (Small *et al*., 1998).

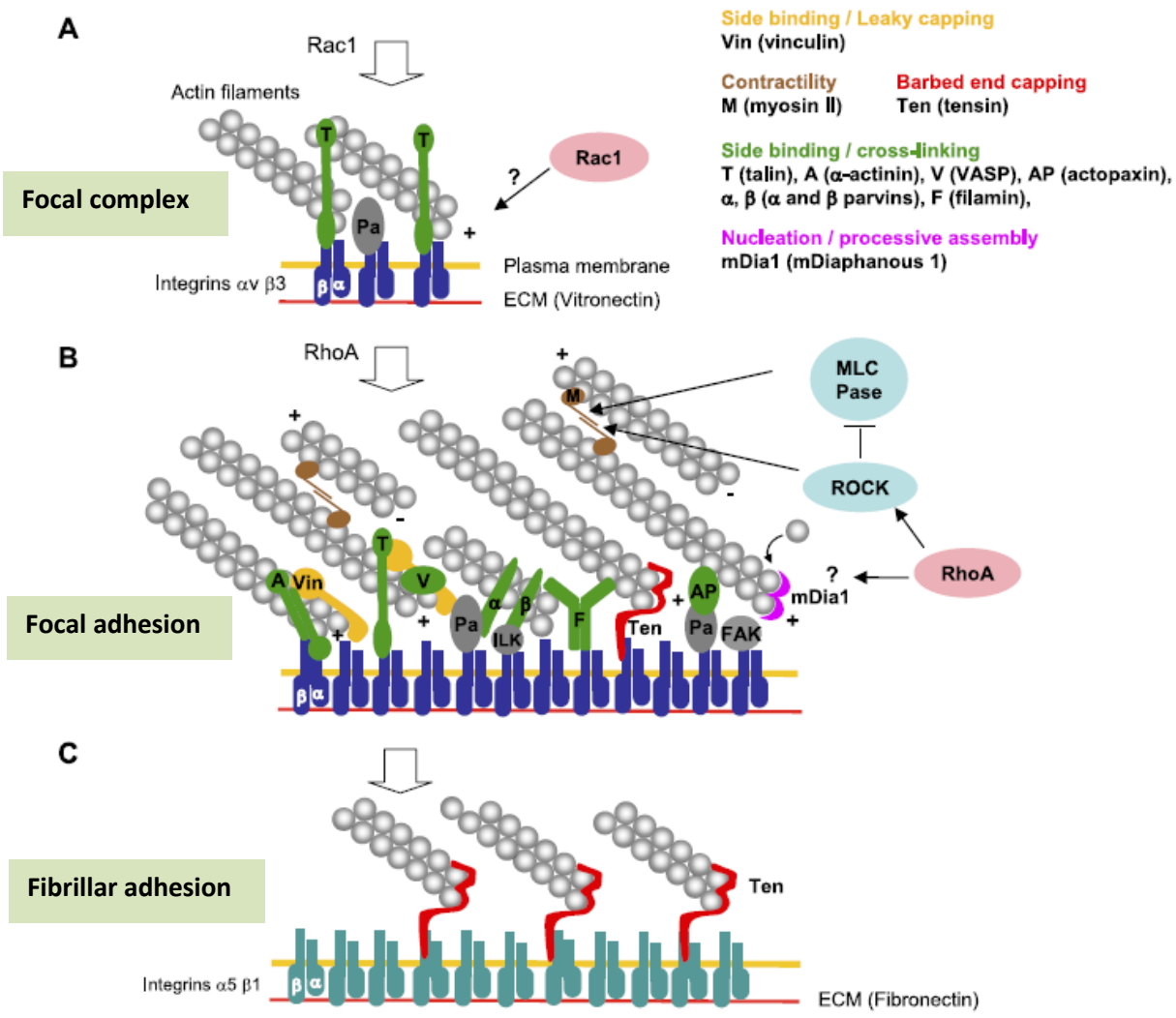

Figure 1.5 - Adhesion structures.

Depending on their composition, size, shape, dynamics and location, adhesion structures are classified as focal complexes (A), focal adhesions (B) or fibrillar adhesion (C). Rac1 signaling elicits the formation of focal complexes, that contain integrin beta-3, talin (Ta), and Paxillin (Pa). Focal complexes mature into focal adhesions in response to RhoA signalling, which activates ROCK, resulting in stress fibre contractility. Fibrillar adhesions contain high levels of tensin (adapted from Le Clainche and Carlier, 2009)

1.6 Cell-cell adhesion

Endothelial integrity is maintained by intercellular adherence, that regulates transendothelial migration of blood cells, as well as permeability. This is achieved through tight and adherens junctions. The first are maintained by claudin 5, junctional adhesion molecule and endothelial cell adhesion molecule (Schnittler, 1998). The latter are particularly important in this process and are essentially composed of vascular endothelial cadherin (VE-cadherin). It forms dimers *via* the extracellular domain and recruits proteins, such as catenins, to the membrane, through the cytoplasmic tail (Lampugnani *et al*., 1992). Catenins serve as a link between VE-cadherin and the cytoskeleton (Bogatcheva *et al*., 2008). Initial contacts between two cells are thought to be made through the extension of filopodia and subsequent cell migration. Almagro *et al*. (2010) have shown that VE-cadherin is also present in the tip and body of filopodia in non-confluent cells. The motor protein myosin X co-localises with and transports VE-cadherin along actin filaments towards the membrane, thus contributing to cell-cell junction formation.

Non-muscle myosin II participates in cytoskeletal rearrangements implicated in cell adhesion, migration and division. As well as participating in cell-matrix adhesion, this protein also promotes the formation and stabilization of cell-cell junctions, as it is required for cadherin clustering. Active RhoA drives contraction and compactation and activates non-muscle myosin IIa. At a later stage, myosin II stabilises the junctions by pulling inwards in both cells involved in the junction (Ivanov *et al*., 2007).

1.7 Filamins and cytoskeleton

Filamins are a family of large actin-binding proteins that stabilise filamentous (F)-actin networks, link actin to the intracellular domain of transmembrane proteins and serve as a scaffold for many cytosolic proteins. Thus, they participate in many processes, such as signal

transduction, gene transcription and receptor translocation. There are three isoforms, A, B and C, and many splice variants have been described, that influence their crosslinking pattern, as well as the proteins that bind to them. Filamins A and B are ubiquitous, whereas filamin C has a more restricted distribution to skeletal and cardiac muscle cells (Zhou *et al*., 2009). Filamins are formed of 24 repeats of approximately 96 amino acid each that fold into anti-parallel beta-sheets that overlap to generate rods. They form homo or heterodimers *via* immunoglobulin-like (Ig) domain 24 and bind to actin through the N-terminal actin binding domain (ABD). There are two hinge regions, between repeats 15 and 16 and also between repeats 23 and 24. These sites are susceptible to calpain and caspase cleavage (Stossel *et al*., 2001) (figure 1.6).

Many proteins have been found to interact with Filamin A that are involved in diverse processes, such as transcription factors (androgen receptor), cell motility (migfilin, FILIP), cell adhesion (integrins β1, β2, β7), cell signalling (caveolin-1, Rho-associated protein kinase), lymphocyte function (CD28, calcineurin), proteolysis (caspase-3, epithin), metabolic function (insulin receptor) and vascular function (calmodulin, calcitonin receptor, ECSCR) (figure 1.7) (Popowicz *et al*., 2006; Zhou *et al.*, 2007; Zhou *et al*., 2009). This multitude of functions highlights the importance of filamin A (and filamins in general, as the other members have been found to also interact with a variety of partners, although less studied) in cellular processes and implicates its malfunction in many diseases. For example, humans with mutations in filamin A develop central nervous system and skeletal disorders, as well as cardiovascular malformations. Filamin A knockout mice die at E14 and display disrupted epithelial and endothelial organization, altered adherens junctions in many tissues, as well as cardiovascular abnormalities and haemorrhage (Feng *et al*., 2006).

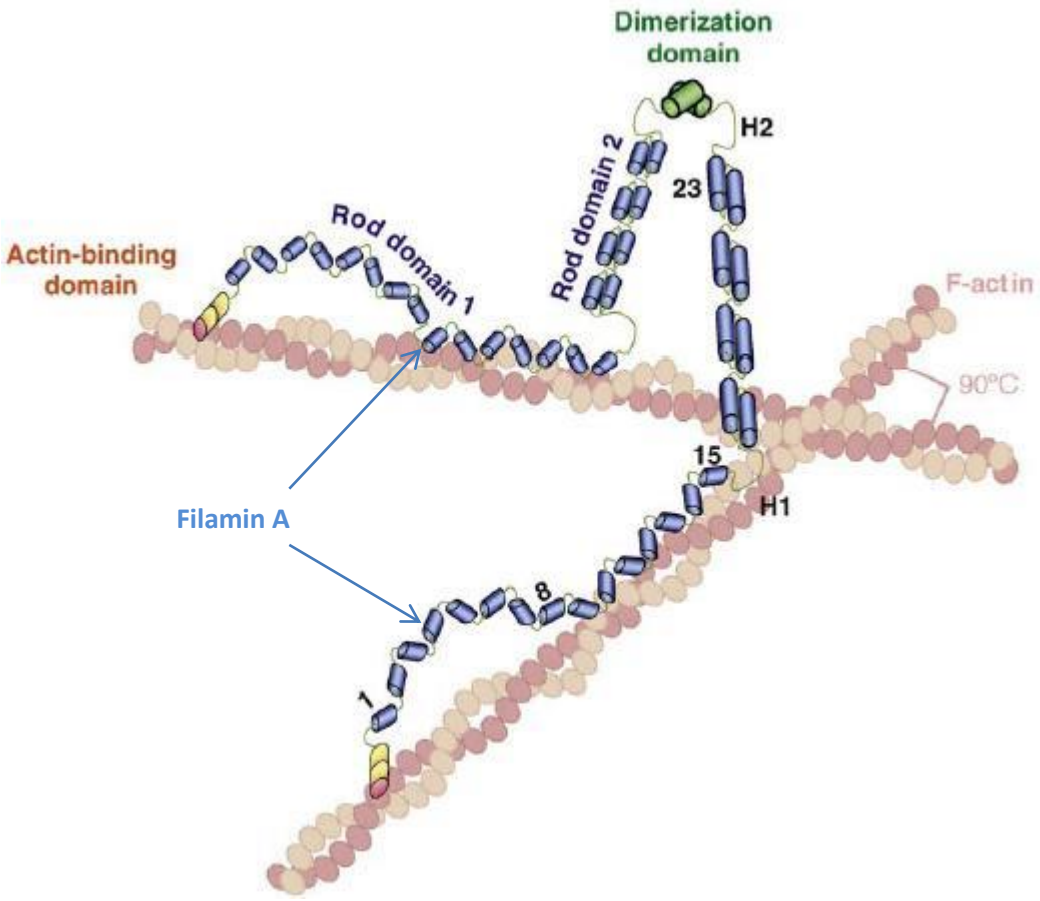

Figure 1.6 - Interaction of filamin A with filamentous actin.

Filamin dimerisation promotes orthogonal bundling of the actin filaments. The Ig repeats 9-15 of rod domain 1 are very avid for actin, whereas rod domain 2 is responsible for binding of most partners, as can be seen in more detail on figure 1.7 (adapted from Zhou *et al*., 2009)

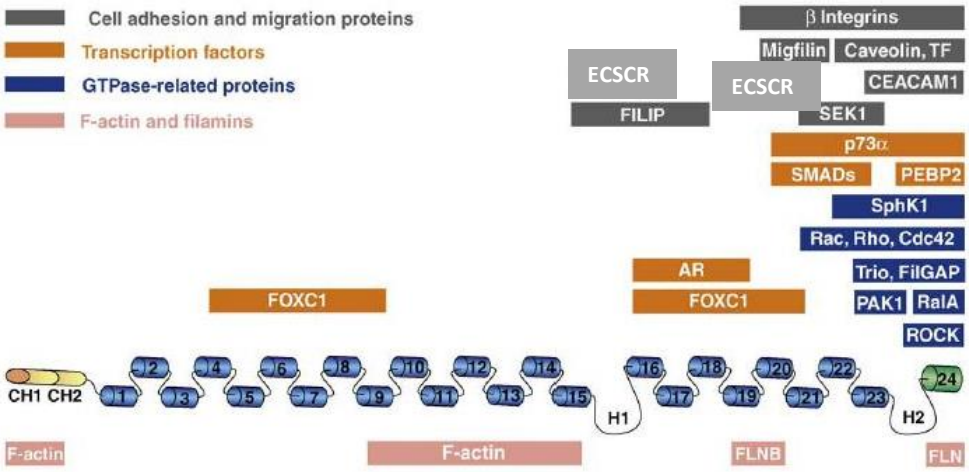

Figure 1.7 - Structure of filamin A and mapping of binding of some interacting proteins. Filamin A encompasses 24 repeats that fold into antiparallel β-sheets and function as interfaces for protein–protein interactions. At the N terminus there is an actin-binding domain that contains two calponin-homology domains (CH1 and CH2). Most of binding partners interact with FLNA at the C-terminus, as depicted. These partners are divided into groups of transcription factors, GTPase-related proteins, other filamins and filamentous actin, and cell adhesion and migration proteins (adapted from Zhou et al., 2009)

CH – calponin homology domains (actin binding domain); 1-14 – Ig repeats; H1 and H2 – hinge regions, susceptible to calpain cleavage. AR – androgen receptor; ECSM – ECSCR

Filamin C knockout causes perinatal lethality, but does not seem to cause cardiovascular malformations (Dalkilic *et al*., 2006). Filamin B, that has recently been implicated in VEGF-induced endothelial cell migration *via* Rac-1 and Vav-2, seems to indeed have a role in the formation of the vascular system, as knockout mice for this protein have impaired microvascular development (as well as in other larger vessels, such as the middle cerebral artery). The embryos die at stage E11 (Valle-Perez *et al*., 2010; Zhou *et al*. a, 2007).

To perform so many distinct functions, not only does filamin A have several splice variants, but it also can be cleaved into different fragments, that allow migration into different cell compartments and further interactions. The full-length 280 kDa protein can be cleaved to 170 kDa (actin-binding domain plus Ig repeats 1-15) and 110 kDa (Ig repeats 16-24). The latter can be further cleaved to a 90 kDa fragment (loses Ig repeat 24) that has the ability to translocate into the nucleus and interact with the androgen receptor, which results in repression of its transcriptional activity (Gorlin *et al*., 1990; van der Flier and Sonnenberg, 2001; Loy *et al*., 2003).

Filamin A is essential for cell migration, as cells deficient in this protein fail to undergo locomotion in response to migration-stimulating factors. These cells are able to protrude and retract multiple spherical processes termed blebs, as a result of the inability of enduring internal hydrostatic pressure. Bleb protrusions start with monomeric actin, and some weak polymerization and crosslinking occurs, but the lack of filamin A and proper crosslinking limits the growth of these protrusions and they eventually retract (Cunningham, 1995). Transfection of filamin A re-establishes migratory capacity (Cunningham *et al*., 2002).

Filamin A localizes to filopodia, lamellipodia, stress fibers and focal adhesions (Campbell, 2008). During spreading this protein is enriched near the cell membrane and adhesion sites

(Kim *et al*., 2008). It regulates intracellular traffic of β1 integrins, thus controlling cell adhesion. Cells that lack filamin A show reduced expression of cell-surface β1 integrins during the initial period of adhesion to matrix, that is rescued by the re-introduction of filamin A (Meyer *et al*., 1998; Kim *et al*., 2010). In turn, blocking β1 integrin function reduces cell spreading and the localization of filamin A to cell extensions (Meyer *et al*., 1998). The fine regulation of the integrin-filamin interaction results in two different phenotypes: some binding is required to stabilise cell-matrix adhesions, whereas excessive binding prevents proper actin remodelling and cell motility (Kim *et al*., 2008). In order to achieve signalling and movement, filamin A must be replaced by talin in the β-chain of integrins. Cell adhesion and spreading depend on the integrity of actin filaments, intermediate filaments and microtubules and the stability of these three complexes depends on each other. Although the precise mechanism underlying this interdependence is not yet fully understood, filamin A seems to act as a bridge between these systems, as it is present in all of them (Kim and McCulloch, 2010). More evidence for the importance of filamin A in adhesion comes from the fact that siRNA-mediated knockdown of filamin A results in reduction of vinculin and paxilin recruitment to focal adhesion sites (Kim *et al*, 2010).

Filamin A is present in the extremities of spreading and migrating cells, in lamellipodia during early stages of cell spreading and is enriched in filopodia upon cell migration stimulation. Cells that do not possess filamin A fail to respond to these stimuli and are unable to form filopodia (Ohta *et al*., 1999). Filamins control the nature of cell protrusions and retractions because they are located both at the leading edge as well as the rear of polarised cells (figure 1.8). Filamin A interacts with small GTPases of the Rho family, which are activated upon integrin binding to the extracellular matrix. These signalling cascades lead to the formation of filopodia and lamellipodia through actin porlymerization (Zhou *et al*., 2009). Filamin A is necessary for

RalA-mediated filopodial protrusion (Ohta *et al*., 1999). Another process, membrane ruffling, is mediated by p21-activated kinase-1 (PAK1), that is activated by binding to and phosphorylation of filamin A. PAK1 is a downstream effector of Rac1 and Cdc42. In addition, filamin A is capable of associating with the Rho downstream effector ROCK in areas or membrane protrusions, as well as sphingosine kinase 1, which further stimulates PAK1, through the production of sphingosine-1-phosphate (Zhou *et al*., 2009). For a tighter regulation of Rho signalling, filamin A is also able to bind guanine nucleotide-exchange factors (GEFs), such as Trio, and GTPase-activating proteins (GAPs), such as FilGAP.

Accumulation of p190RhoGAP in the cell membrane leads to Rho inactivation and Lbc stimulates ROCK activity which inactivates Rac through phosphorylation and stimulation of FilGAP. This causes protrusions at the leading edge to be suppressed and cell retraction is promoted. Furthermore, ROCK phosphorylates and activates myosin II, which is responsible for contractile activity (Tseng *et al.*, 2004).

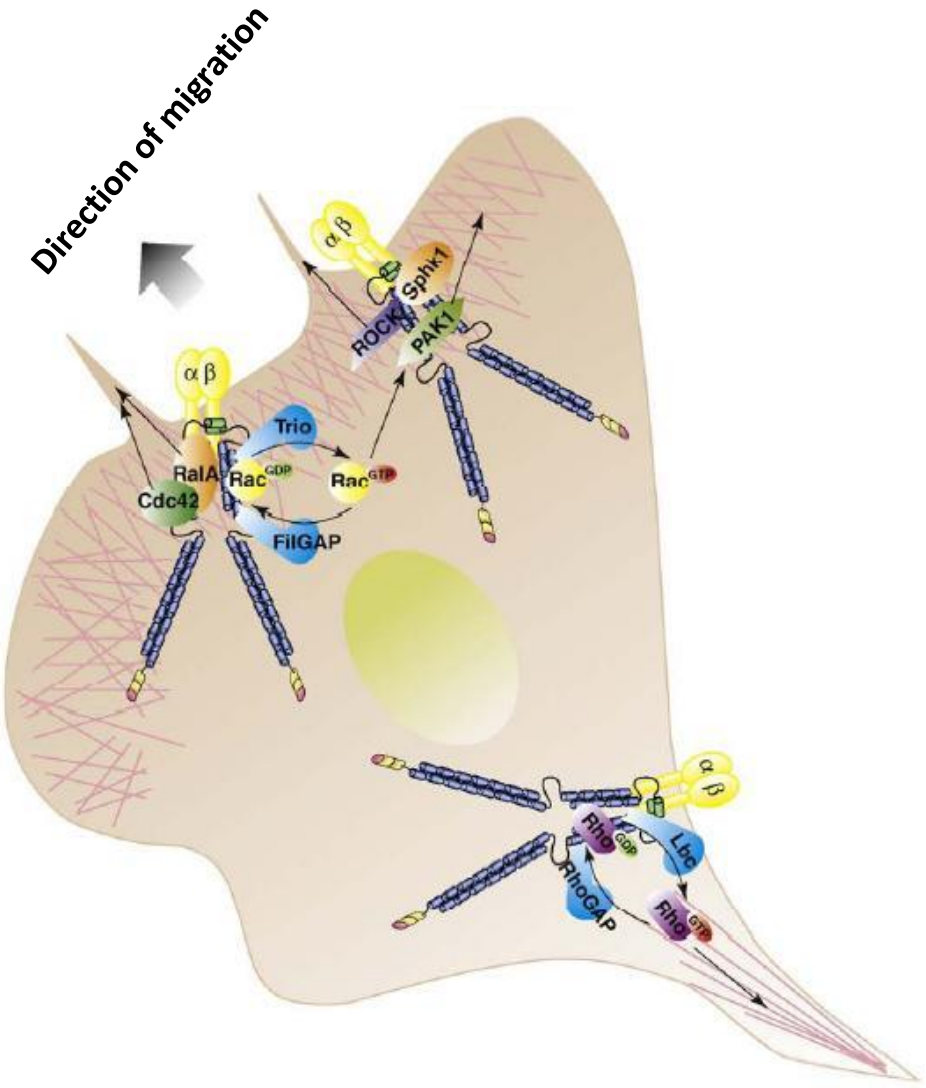

Figure 1.8 - Interaction of filamin A with filamentous actin.

During cell migration FLNA acts as a scaffold for small GTPases. The lamellar membrane at the leading edge of motile cells participates in a series of complex movements that involve the assembly and reorganization of actin bundles and networks, both formed by FLNA. FLNA crosslinks actin filaments and engages transmembrane proteins (β-integrins), as well as small GTPases (Cdc42, Rho, Rac, RalA) and their upstream (Trio, Lbc, FilGAP, RhoGAP) and downstream (ROCK, PAK1) factors (adapted from Zhou *et al*., 2009)

1.8 Angiogenesis assays and models

In vitro assays allow the study of endothelial cell proliferation, migration, tube formation, fluid shear stress and flow, intracellular signalling and cell interactions (single or co-culture studies) (Auerbach *et al*., 2003; Staton *et al*., 2006; Martin and Murray, 2009). The endothelial cell tube formation assay on basement membrane is very easy to perform and allows the study of angiogenic and antiangiogenic factors, to define mechanisms and pathways involved in angiogenesis and to define endothelial populations. Basically, upon seeding on an appropriate matrix, endothelial cells undergo a series of differentiation processes that lead to the establishment of vessel-like structures (Arnaoutova *et al*., 2009). A step closer to a more complete strategy is the quantitative-three dimensional *ex vivo* mouse aortic ring angiogenesis assay, as the vessel contains other cell types that interact with the endothelium *in vivo* (Baker *et al.*, 2012). After dissection, aortic rings are serum-starved and embedded in a matrix of choice, according to the objectives of the study. Then, the rings are fed and allowed to develop sprouts for about 5-9 days. Before embedding, the rings can be treated with siRNA and during regular media changes throughout the assay drugs, growth factors, etc. can be added. Subsequently, the rings can be analysed for a variety of parameters, such as sprout number and length, pericyte coverage, as well as used for immunofluorescent staining and confocal imaging. Although this assay can be informative, one of its limitations is the fact that it may not be physiologically relevant, as normal aorta does not really sprout. Retina has also proved to be a good and widely used model in angiogenesis research to investigate neurovascular relationships and developmental and pathological angiogenesis (Gariano and Gardner, 2005). Although very informative, cell cultures and *ex vivo* models don't account for the whole picture, and need to be complemented with *in vivo* assays.

In vivo comparative studies of normal and pathological conditions, such as subcutaneous implantation of matrigel plugs or sponge and subsequent analysis of vascularisation, as well as the use of transgenic mice and zebrafish help to better understand the mechanisms of angiogenesis and to develop and predict the effect of antiangiogenic drugs (Staton *et al*., 2006; Martin and Murray, 2009).

The mouse (*Mus musculus*) has been used as a mammalian model for a very long time. More recently, the zebrafish (*Danio rerio*) has proven to be a suitable model to human angiogenesis and its use over the last years has increased. Zebrafish embryos have an external development and are transparent, being suitable for very simple microscopy analysis with much detail (Lessman, 2011). Being a vertebrate, the vasculature is similar to the mammalian one (Gore *et al*., 2012). The molecular mechanisms regulating vasculogenesis and haematopoiesis are conserved throughout vertebrate evolution as demonstrated, for example, by studies using the *cloche* and *spadetail* mutants. In brief, both mutants display defects in haematopoiesis, but only the *cloche* mutants have altered vascular gene expression. In these fish no vasculature at all develops (Thompson *et al*., 1998). Transgenic lines are already available and they can be used to directly assess the effect of morpholino knock down of genes of interest. The fact that the genome is sequenced is another advantage (Weinstein, 2000).

The zebrafish model has contributed to finding novel endothelial-specific genes, uncover gene function, understand developmental processes, as well as disease pathogenesis, progression and regression. Sumanas *et al*. (2005) have identified several endothelial specific genes using the zebrafish *cloche* mutant. They analysed over 15,000 zebrafish genes or ESTs in mutants affected at a very early step of haematopoiesis and vasculogenesis. These fish lack almost all blood cells, head and trunk endothelial cells and the endocardium, as well as markers for both lineages, such as scl, gata1, flt1 and flt4. Dual specificity phosphatase 5, cadherin 5 (VE-

cadherin), aquaporin 8 and ETS1-like protein (etsrp) were found to be significantly down-regulated in these mutants and their expression pattern has shown their endothelial specificity. The same authors have then characterised etsrp and demonstrated that it is necessary and sufficient for the initiation of vasculogenesis (Sumanas and Lin, 2006). Etsrp morpholino knockdown *in vivo* resulted in the impairment of angioblast migration, differentiation and functional blood vessel formation. Vascular endothelial markers were highly reduced in these morphants and overexpression of etsrp restored their expression in the *cloche* mutants. More vascular-specific genes were identified in the zebrafish by microarray analysis of etsrp overexpressing zebrafish embryos, such as angiotensin II type 2 receptor, endothelial cell specific adhesion molecule and stabilin 2 (Wong *et al*., 2009).

Zebrafish have been found to develop almost any tumour type known in humans, with comparable morphology and acting through similar signalling pathways (Feitsma and Cuppen, 2008). Given all the manipulation and imaging advantages of zebrafish, a model for hypoxia-induced pathological angiogenesis that mediates tumour cell dissemination, invasion and metastasis has been created (Lee *et al*., 2009). Under hypoxia implanted murine fibrosarcoma cells were disseminated from primary sites, invaded neighbouring tissues and metastasised to distal parts of the body, whereas under normoxic conditions this did not happen.

Over the years many mouse models have been developed to study angiogenesis (both normal and pathological), as well as cancer and many other conditions. These models can be wild type mice that are surgically or otherwise physically modified or transgenic mice, which are genetically altered. For example, the acute murine hind limb ischemia and reperfusion model entails simultaneous occlusion of several branches of the femoral and iliac arteries to achieve limb ischemia, followed by loosening of the pressure source to allow reperfusion (Crawford *et al*., 2006). Knockout mouse models for endothelial genes have provided many insights into

vascular cell biology. The models available can be more or less complex, ranging from null knockouts of the gene of interest obtained by gene targeting to conditional or inducible knockouts, where the disruption of the occurs only in certain tissue types or upon stimulation. An example of the former is the creation of the Tie2Cre deleter strain, that allows the study of gene deletions specifically in the endothelium (Kisanuki *et al*., 2001). Another type of transgenic mice include the expression of specific proteins fused to GFP, to allow visual analysis, as well as cell isolation (Hillen *et al.*, 2008). A new transgenic line can also be created by crossing and combining pre-existing ones.

With the development of new laboratorial techniques and tools, software and equipment, the available amount of data for mouse tumour models is enormous. In order to facilitate the integration, location and visualisation these data, the Mouse Tumour Biology database has been created (Kupke *et al*., 2008).

1.9 Hypothesis

With evidence showing that ECSCR is specifically expressed in endothelium and is involved in cytoskeletal processes, the hypothesis being tested is that ECSCR promotes specific endothelial cells events and its absence leads to defective vasculature formation.

1.10 Aim of the study

Our group has shown that ECSCR is specific to the endothelium, binds to filamin A and its absence in HUVECs causes impairment of chemotactic migration and tube formation. It locates to the plasma membrane and is enriched in filopodia. This suggested a role for ECSCR in modulating cell migration through the modulation of the actin cytoskeleton (Herbert *et al*., 2008; Armstrong *et al*., 2008). However, to the date of the start of this project nothing else was known about this interesting molecule.

For this study, three models were used to establish molecular mechanisms by which ECSCR regulates endothelial cell chemotaxis and angiogenesis, one *in vitro*: primary human umbilical vein endothelial cells (HUVECs), and two *in vivo*: zebrafish and mice. The main objectives were:

1– To identify ECSCR binding partners and reveal downstream signalling. The elucidation of ECSCR-filamin A interaction was pursued and other binding partners were investigated and uncovered. The effect of ECSCR loss on the distribution of these proteins was assessed.

2– To determine the role of Ecscr during zebrafish vascular development.

The endothelial specificity of Ecscr in zebrafish was confirmed by *in situ* hybridization (it seems to be located only in the zebrafish head and major trunk vasculature) and RT-PCR has shown that Ecscr expression increases at the onset of vasculogenesis (around 15 hpf). When

Ecscr is knocked down with morpholino antisense oligonucleotides, the sprouting of intersegmental vessels is disrupted.

3– To develop and characterise an Ecscr knockout mouse model

In order to further characterise the role of Ecscr during mammal development and, potentially, during adult life in healthy and pathological andgiogenesis conditions, an Ecscr null knockout mouse was generated. Preliminary data from LacZ staining show endothelial specificity. Interestingly, Ecscr seems to be present only in some vessels and not all vasculature.

4 – To investigate if the function of ECSCR is conserved across species

Evidence from qPCR and *in situ* hybridization shows that endothelial specificity of ECSCR is conserved in human, mouse and zebrafish. Taking data together from this work and published literature, ECSCR seems to have a role in the development of vessels of smaller calibre (mouse and zebrafish).

2 MATERIALS AND METHODS

2.1 Reagents and equipment

All chemicals used were of analytical or molecular biology grade and purchased from Sigma-Aldrich (Gillingham, UK), unless otherwise specified.

Different centrifuges were used, according to the volumes, temperatures and centrifugation speeds required:

- Biofuge Pico Heraeus (Kendro Laboratory Products GmbH, Langenselbold, Germany) for 1.5 ml tubes and up to 16060 x g;

- Hettich Mikro 22R (refrigerated) (Andreas Hettich GmbH, Tuttlingen, Germany) for 1.5 ml tubes and up to 21910 x g;

- Biofuge Primo Heraeus (Thermo Electron Corporation, Waltham, USA) for 15 or 50 ml tubes and up to 2576 x g;

- AvantiTM J-20XP (refrigerated) (Beckman Coulter, Brea, CA, USA) for up to 500 ml bottles and up to 26000 x g. Depending on the tube/bottle size, JLA-10.5 or JA-25.5 rotors were used.

All other equipment used is listed throughout this chapter, within the respective sections.

2.1.1 Buffers and solutions

The general use buffers and solutions utilised are listed and described below, on table 2.1.1. Any other specific or commercial solutions are referred in the respective sections.

Table 2.1 - Buffers and solutions

Solution name	Contents
NP40 lysis buffer	0.02% (w/v) NaN_3, 2% (v/v) NP40, 20mM Tris-HCl pH7.5, 300mM NaCl, 2mM EDTA, 1x Protease inhibitor mix
E. coli lysis buffer	50 mM Tris-HCl, pH 7.5, 100 mM NaCl, 2 mM EGTA, 2mM EDTA, 1 mM DTT, 1 mM PMSF, 1x protease inhibitor mix
E. coli washing buffer	20 mM Tris-HCl, pH 7.4, 0.2 M NaCl, 1 mM EDTA, 10 mM b-mercaptoethanol
Elution buffer	20 mM Tris-HCl, pH 7.4, 0.2 M NaCl, 1 mM EDTA, 10 mM b-mercaptoethanol, 10 mM maltose
TBST (Tris-buffered saline Tween)	20 mM Tris-HCl, pH 7.5, 150 mM NaCl, 0.1 % (v/v) Tween-20
6x DNA sample loading buffer	30 % (v/v) glycerol, 0.25 % (w/v) bromophenol blue, 0.25 % (w/v) xylene cyanol FF
2x SDS-PAGE sample loading buffer	100 mM Tris-Cl, pH 6.8, 20% (v/v) β-mercaptoethanol, 4% (w/v) SDS, 0.2% (w/v) bromophenol blue, 20% (v/v) glycerol
TAE buffer	40 mM Tris-base, 18 mM glacial acetic acid, 1 mM EDTA

Solution name	Contents
SDS-PAGE running buffer (1x)	25 mM Tris-base, 0.25 M glycine, 0.1 % (w/v) SDS
Western blotting transfer buffer (1x)	6 mM Tris-base, 47.6 mM glycine, 20 % (v/v) methanol, pH 8.3
Stripping buffer	1M Tris pH7.5, 10% (v/v) SDS
Coomassie staining buffer	40 % (v/v) methanol, 10 % (v/v) acetic acid, 0.2 g Coomassie Briliant Blue dye
Coomassie destaining buffer	10 % (v/v) acetic acid, 12.5 % (v/v) isopropanol
PBS	0.14 M NaCl, 2.68 mM KCl, 10 mM Na_2HPO_4, 1.76 mM KH_2PO_4, pH 7.4
Hybridization buffer	50% (v/v) formamide, 5x SSC, 0.5 mg/ml tRNA, 0.05 mg/ml heparin, 9.2 mM citric acid, 1% (v/v) Tween 20
MABT	0.1M maleic acid, 0.15M NaCl, pH7.5, 0.1% (v/v) Tween 20
BCL buffer III	0.1M Tris-HCl, 0.1M NaCl, 0.05M $MgCl_2$, 1% (v/v) Tween 20

2.1.2 Antibodies

The antibodies used are listed and described on tables 2.2 and 2.3. Unless another species is stated, the antibodies were raised against human antigens.

Table 2.2 – Primary antibodies

Antibody	Optimisation range	Working concentration	Source
Rabbit anti-ECSCR icd pAb	1:200 – 1:10000 5 – 30 µl	1:5000 (WB) 10 µl (IP)	CRUK
Rabbit anti-ECSCR pAb	1:200 – 1:10000	1:1000 (WB)	Harlan, UK
Rabbit serum pre-bleed (IgG control)	-	Same as test antibody	CRUK/Harlan, UK
Rabbit anti-zebrafish Ecscr icd pAb	1:200 – 1:10000	1:500 (WB)	CRUK
Goat anti-moesin pAb	1:500 – 1:5000 1:100 – 1:500	1:2500 (WB) 1:200 (IF)	Abcam, Cambridge, UK
Mouse anti-talin1 mAb	2-8 µg/ml	4 µg/ml (WB)	Abcam, Cambridge, UK
Mouse anti-vinculin mAb	1-5 µg/ml	2 µg/ml (WB)	Abcam, Cambridge, UK
Rabbit anti-T-plastin pAb	1:500 – 1:5000	1:1000 (WB)	Abcam, Cambridge, UK

Antibody	Optimisation range	Working concentration	Source
Mouse anti-filamin A mAb	1:250 – 1:1000 1:50 – 1:200	1:500 (WB) 1:100 (IF)	Millipore
Mouse anti-tubulin mAb	1:10000*	1:10000	Sigma, Poole, UK
Anti-digoxigenin	1:5000*	1:5000	Roche

Abbreviations: pAb – polyclonal antibody; mAb – monoclonal antibody; WB – western blot; IP – immunoprecipitation; IF – immunofluorescence.

The antibody concentrations marked with an asterisk on tables 2.2 and 2.3 had previously been optimised and validated by other people in the lab.

Table 2.3 - Secondary antibodies

Abbreviations: WB – western blot; IP – immunoprecipitation; IF – immunofluorescence; HRP – horseradish peroxidase.

Antibody	Working concentration	Source
Donkey anti rabbit-HRP conjugated	1:5000 (WB)*	GE Healthcare, Chalfont St Giles, UK
Goat anti mouse-HRP conjugated	1:5000 (WB)*	Dako, Ely, UK

Table 2.3 (cont.) – Secondary antibodies

Antibody	Working concentration	Source
Mouse anti-rabbit light chain specific-HRP conjugated	1:1000 (WB)*	Millipore
Donkey anti-rabbit-Alexa 488 conjugated	4 µg/ml (IF)*	Invitrogen
Goat anti-rabbit-Alexa 546 conjugated	4 µg/ml (IF)*	Invitrogen
Goat anti-mouse-Alexa 488 conjugated	4 µg/ml (IF)*	Invitrogen
Goat anti-mouse-Alexa 546 conjugated	4 µg/ml (IF)*	Invitrogen

2.1.3 Cloning vectors

The plasmids used to insert various complete or partial open reading frames are listed and described on table 2.4.

Table 2.4 - Cloning vectors

Plasmid	Source	Use
Pmal	New England Biosciences	MBP-fusion proteins
Pgex	Amersham Biosciences	GST-fusion proteins
PCR Topo blunt	Invitrogen	General blunt end cloning
pCS2	DL Turner, Michigan	*In situ* probes synthesis
pACT2	Clontech	Yeast-two-hybrid assay
pGBT9	Clontech	Yeast-two-hybrid assay
Zipper-hGLuc[1]93	Gift from Remy and Michnick, 2006	Luciferase complementation assay
Zipper-hGLuc[2]93	Remy and Michnick, 2006	Luciferase complementation assay
pRGFP-N1	Clontech	C-terminus GFP fusions

2.1.4 Oligonucleotides

All the primers, as well as the siRNA duplexes were purchased from Eurogentec (Southampton, UK). Probes for qPCR were purchased from Roche Applied Science, UK and RNA antisense morpholinos were obtained from Gene Tools, USA.

Table 2.5 - Oligonucleotides used for sequencing, cloning, colony PCR screen and site-directed mutagenesis (SDM)

Primer	Oligonucleotide sequence (5'-3')	Application
SP6	CATACGATTTAGGTGACACTATAG	Sequencing
T7	TAATACGACTCACTATAGGG	Sequencing
EGFP-N	CGTCGCCGTCCAGCTCGACCAG	Sequencing
pGEXF	CACGTTTGGTGGTGGCGACC	Sequencing

Primer	**Oligonucleotide sequence (5'-3')**	**Application**
PGEXR	CCGGGAGCTGCATGTGTCAGAGG	Sequencing
pGBT9F	GAGTAGTAACAAAGGTCAAAGACA	Sequencing
pGBT9R	GAGTCACTTTAAAATTTGTATACAC	Sequencing
pACT2F	AATACCACTACAATGGATGATGTA	Sequencing
pACT2R	GTTTTTCAGTATCTACGATTC	Sequencing
pGEX/pMALzECSCRF	TAGTAGGGATCCGGACGCTGTTGTAGAAACAC	Ecscr icd PCR
pGEX/pMALzECSCRR	CTACTAGTCGACTCATGAACCCAGTGAAATCA	Ecscr icd PCR
mECSCR-insitu-F	AAGTCTTCTCAGGTCTCCTTGGTAT	*In situ* probe PCR
mECSCR-insitu-R	TGGACAATCTACCTCATTATTTCCTTA	*In situ* probe PCR
zECSCRatg	CATTTGGACTTAGCCATGGAGAAACTGCTC	Ecscr PCR
zECSCRtag	TCATGAACCCAGTGAAATCAGCTGGTCTCT	Ecscr PCR
InsituF	AAGTCTTCTCAGGTCTCCTTGGTAT	Genotyping
WTintron3R	CCATTTCCCTCCTCCATCTGTTCTTT	Genotyping
UNeoF	GCAGCCTCTGTTCCACATACACTTCA	Genotyping
InsituR	TGGACAATCTACCTCATTATTTCCTTA	Genotyping
ECSCREcoRIF	GAATTCAGCCTGAGGTTCAAGTGTCGG	ECSCR icd PCR
ECSCRSalIF	GTCGACTTAAAGAACCTTCTCTGCTGAG	ECSCR icd PCR
ECSCRicdBamHIR	CTACTAGGATCCTAAGAACCTTCTCTGCTGAG	ECSCR icd PCR
BamHIFLNA1F	TAGGGATCCAGATTGGGGAGGAGACGGTGATCACTG	Filamin A 1 PCR
EcoRIFLNA1R	GAATTCTTAGCTTCCTGGGATGTGCATGTT	Filamin A 1 PCR
BamHIFLNA2F	TAGGGATCCAGCGGACGTGCAGGGTCACCTACTGCC	Filamin A 2PCR
EcoRIIFLNA2R	GAATTCTTAGTCGGGAATGTGTTCCTCGTT	Filamin A 2PCR
MoesinSacIR	CTACTAGAGCTCTTACATAGACTCAAATTCGTC	Moesin PCR
EzrinXhoIR	CTACTACTCGAGTTACAGGGCCTCGAACTCGTC	Ezrin PCR
ECSCRicd1BamH1R	CTACTAGGATCCTTAGGCTGTGGAGCAGCTTTCAGAC	ECSCR icd 1 PCR
ECSCRicd2EcoRIF	TAGTAGGAATTCAATGGAGAGAAAGACAGCATCAC	ECSCR icd 2 PCR
ECSCRicd2BamH1R	CTACTAGGATCCTTAAAGAACCTTCTCTGCTGAG	ECSCR icd 2 PCR

Primer	Oligonucleotide sequence (5'-3')	Application
MoesinNotIF	TAGTAGGCGGCCGCACCATGCCCAAAACGATCAGTGTGC GTGTG	Moesin PCR
MoesinClaIR	CTACTAATCGATCATAGACTCAAATTCGTCATTGCGC	Moesin PCR
ECSCRNotIF	TAGTAGGCGGCCGCACCATGGGCACCGCAGGAGCCATGC AGCTG	ECSCR PCR
ECSCRClaIR	CTACTAATCGATAAGAACCTTCTCTGCTGAGAGACTTTG	ECSCR PCR
Beta-actinF	GCACCCAGCACAATGAAGA (Probe 63)	qPCR
Beta-actinR	CGATCCACACGGAGTACTTG (Probe 63)	qPCR
ECSCRF	AGCTGTGCTGGGTGATCCT (Probe 69)	qPCR
ECSCRR	ATTGTGGGCTGGGAGTTGT (Probe 69)	qPCR

Table 2.6 - siRNA duplexes for *in vitro* knock-down

siRNA Duplex	Gene knock-down	Duplex sense strand (5'-3')
D1	Human ECSCR	ACAAUGACCCAGACCUCUA99
NCD	No interaction	Eurogentec keep this sequence private

Table 2.7 - RNA antisense morpholinos for *in vivo* translation or splice interference

Morpholino	Gene affected	Antisense sequence (5'-3')
5'UTR	Zebrafish Ecscr	GCGTAAGTCCAAATGACGTTCAATC
5'UTR mismatch	None	GGCAAACTCGAAATCACCTTCAATC
Splice	Zebrafish Ecscr	CATCAGTAGAAAACCTACCAAAGGC
Splice mismatch	None	CATGACTACAAAACCTACGAAACGC

2.2 Mammalian cell culture and related techniques

2.2.1 Mammalian cells

Human umbilical vein endothelial primary cells (HUVECs) were isolated from cords obtained through Birmingham Women's Health Care NHS Trust, donated with informed consent. They were prepared according to Jaffe *et al.*, (1973). These cells were cultured in M199 complete medium.

Human embryonic kidney 293T (HEK 293T) cells were obtained from Cancer Research UK Central Services (Clare Hall, Hertfordshire). These cells were cultured in complete DMEM medium.

2.2.2 Cell culture

All cell culture techniques were performed using sterile plastic culture dishes or plates (Falcon, Becton Dickinson Labware, Franklin Lakes, USA) and the cells were incubated in a humidified atmosphere with 5 % CO_2 supply at 37 °C (Sanyo CO_2 incubator, Sanyo Electric CO, Japan). The media and gelatine were filtered through sterile 0.22 μm pore filters (Millipore) prior to use and PBS was sterilised by autoclaving.

HEK 293T cells don't require surface coating. Before seeding HUVECs, the Petri dishes, coverslips or wells were coated with 0.1% (w/v) gelatine from porcine skin (Fluka, BioChemika, Seelze, Germany) in PBS and incubated at 37ºC for 30 minutes. After that time the gelatine was removed and the cells were plated, covered with warm complete M199 medium and incubated at 37ºC.

To culture HUVECs M199 medium (CRUK Central Services or Sigma-Aldrich) was supplemented with 10% (v/v) foetal calf serum (FCS) (PAA Cell Culture Company), 0.3% (v/v) bovine brain extract (prepared according to Maciag *et al*., 1979), 90 μg/ml of heparin, 4 mM of L-glutamine and penicillin/streptomycin (Invitrogen), if required. Complete DMEM was made by adding 10% (v/v) FCS, 4 mM of L-glutamine and penicillin/streptomycin (Invitrogen), if required, to Dulbecco's Modified Eagle's Medium.

HUVEC primary cells should be used within five passages, split once a week at a 1:3 ratio. In order to split them, the medium was removed, the cells were washed with PBS and 1.5 ml of trypsin (20 mg/ml) were added to a 10 cm dish. After 5 minutes the reaction was stopped by adding 4.5 ml of warm medium. The suspension was then centrifuged at 195 x g, the supernatant containing trypsin was discarded and the cells were ressuspended in warm medium and seeded. HEK 293T cells were split in the same fashion, 1:10, twice a week.

Cell counting, when necessary, was performed after exposing the cells to trypsin and quenching the reaction with complete medium, by mixing 10 μl of the cell suspension and 10 μl of Trypan blue (Stratagene). 10 μl of this mixture were loaded into a haemocytometer counting chamber (Neubauer, Paul Marienfeld GmbH & CO, Germany) and counted according to the manufacturer's instructions, on an inverted Leica DM IL microscope (Leica Microsystems, Houston, USA).

2.2.3 siRNA knock down of ECSCR in HUVECs

The siRNA duplexes were designed according to the rules described by Reynolds *et al.* (2004). One million HUVECs were seeded on gelatine coated 10 cm plates and incubated for 24 hours at 37ºC. The next day transfections were performed with Mock (sterile water), ECSCR duplex 1 (D1) and negative control duplex (NCD) siRNA at 10 nM with 0.3% (v/v) lipofectamine™ RNAiMAX (Invitrogen). Two mixes were setup, the first containing 2 µl of 20 µM duplex / water (Mock) in 678 µl of OptiMEM (Gibco BRL, UK) and the second containing 12 µl of RNAiMAX lipofectamine™ and 108 µl of OptiMEM medium. Both mixtures were homogenised and incubated separately for 10 min at room temperature and then combined, gently mixed and incubated for another 10 min at room temperature. Meanwhile, the cells were washed twice with PBS. The transfection mixtures were added to 3200 µl of OptiMEM medium, mixed and the cells were covered with this solution. The plates were incubated for four hours at 37ºC. After that time, the transfection mix was replaced with normal complete M199 medium (without antibiotics). Two days after transfection the cells were used for various assays.

2.2.4 Polyethylenimine (PEI) transfection of HEK 293T cells

Conventional transfection protocols rely on the calcium phosphate precipitation technique. However, large variability in transfection efficiency is observed ans it is difficult to scale-up the precipitation reactions (Naldini *et al*., 2006). Polyethylenimine is a hydrophilic polymer that condenses DNA into positively charged particles, which bind to anionic cell surface residues and are imported into the cell via endocytosis. Once inside, protonation of the amines results in an influx of counter-ions and a lowering of the osmotic potential. Osmotic swelling causes the vesicles to burst and release the polymer-DNA complex (polyplex) into the cytoplasm. When the polyplex unpacks the DNA diffuses to the nucleus (Rudolph *et al*., 2000;

Akinc *et al*., 2004). Toledo *et al*. (2009) have shown that HEK293T transfections with PEI after 24h display an efficiency of 94.3% (±3.2), compared to 66.2 (±5.6) to those made with calcium phospate. Another advantage is that PEI transfections, unlike those that use calcium phosphate, do not require a medium change 16-20h after transfection. This protocol was described for transfection of lentiviral vectors and optimised for smaller plasmids by Dr. Mike Tomlinson (University of Birmingham, UK).

Three million HEK 293T cells were seeded on 10 cm plates, covered with complete DMEM medium and incubated at 37ºC for 24 hours. On the next day the medium (without antibiotics) was replaced 2 hours before the transfection. For the transfection 9 μg of DNA plasmid were mixed with 1 ml of OptiMEM medium and 36 μl of PEI (1 mg/ml). The tubes were briefly vortexed and left to rest for 10 min, to allow the PEI/DNA complexes to form. This solution was then added to the medium and gently mixed in. The cells were incubated at 37ºC for 48h and used for different assays.

2.2.5 Scratch wound assay

The scratch wound assay allows the observation of cell migration *in vitro* after a scratch is made on a confluent monolayer. It is a quick, easy and inexpensive method (Liang *et al*., 2007). For that purpose, HUVECs were plated and transfected with siRNA as described in section 2.2.3. After 36 h the cells were treated with trypsin and seeded at a 7.5 x 10^4 cells/well density on glass coverslips (13 mm diameter, VWR International), pre-coated with 0.1% gelatine (in 24-well cell culture plates, covered with 1 ml of complete M199 medium). At 48 h two scratches were made across each monolayer and the cells were allowed to migrate for eight hours. After that time, the cells were fixed and immunostained for various proteins, as described on section 2.2.6. In the classical scratch wound assay the cells are allowed to migrate for 24h, with images being taken at 4, 6, 8, 12 and 24h to monitor the speed of wound closure.

In this case, the cells were allowed to migrate for only 8h because the aim was to stain cells that were confluent as well as cells that were in the process of migration.

2.2.6 Immunofluorescent staining

The cells were seeded and treated as described on section 2.2.5. The medium was removed from the wells and the cells were washed with PBS. Then, they were fixed with 4% PFA (w/v) in PBS for 15 min at room temperature and permeabilised with 0.1% (v/v) Triton X100 in PBS for 4 min. One more PBS wash was performed and the cells were incubated with 100 µl of blocking buffer (10% (v/v) FCS, 3% (w/v) BSA in PBST – PBS with 0.1% (v/v) Tween 20) for 1 h at room temperature. All the subsequent incubations were done at this temperature. The primary antibodies were added in the concentrations described on table 2.1.2, in blocking buffer and incubated for 1 h. After that time, the cells were washed 3 times with PBST for 5 min each and incubated for one more hour with secondary antibody with an appropriate fluorescent tag diluted in blocking buffer (4 µg/ml). This solution was washed out with PBST for 5 min, 3 times. The coverslips were then mounted on glass slides (Menzel-Glaser GmbH, Braunschweig, Germany) using 5 µl of ProLong Gold Antifade reagent with DAPI (Invitrogen) per coverslip. The stained cells were observed and images were acquired using an Axiovert 100M confocal microscope and LSM 510 software (Zeiss). LSM Image Browser software (Zeiss) was used to open, edit and export the images.

2.3 Protein analyses and assays

2.3.1 Cell lysis and protein extraction

10 cm confluent plates of cells were washed with 1x PBS, exposed to trypsin, quenched with medium and centrifuged at 195 x g. The pellet was ressuspended and lysed in 100µl of NP40 buffer by pipetting up and down (on ice). Alternatively, after the PBS wash, the cells were treated with 150 µl of lysis buffer and scraped and collected into tubes on ice. The samples

were centrifuged at 10000 rpm for 5 min and the supernatant was transferred into a new tube containing 1 V of 2x SDS-PAGE sample loading buffer. This mixture was boiled for 5 min at 100ºC and loaded on an SDS-PAGE gel or stored at -80ºC.

2.3.2 Immunoprecipitation using an anti-ECSCR intracellular (icd) domain antibody

To precipitate possible binding partners for ECSCR, 1050 µl of HUVECs lysate from seven 10 cm plates for each assay were incubated for 2 hours at 4ºC on a wheel with 10 µl of antibodies (either the polyclonal antibody against the icd of ECSCR or rabbit IgG as a control) and 30 µl of packed G-protein beads (Sigma). After that period the supernatant was removed and the beads were washed with 1ml of NP40 buffer 3 times. SDS-PAGE loading buffer was added 1:1 and the samples were boiled at 100ºC for 5 min and loaded on a polyacrylamide gel, ran, and stained with brilliant blue coomassie.

2.3.3 SDS-PAGE

Protein samples were boiled for 5 min at 100ºC, spun down for 10 s and loaded on 6-10% polyacrylamide gels (Protogel, National Diagnostics, Hessle Hull, UK), according to the size of the proteins of interest. These gels were prepared according to Sambrook and Russel (2001). All the electrophoresis equipment used was from Invitrogen (Carlsbad, USA). Electrophoresis was performed in 1x running buffer at 80 V until the samples reached the resolving buffer and then the voltage was increased to 120 V. After the electrophoresis the gels were Coomassie stained or used for western blotting.

2.3.4 Gel staining of proteins with Coomassie Brilliant Blue

For protein staining, polyacrylamide gels were placed in coomassie brilliant blue staining buffer and rocked for at least 1 hour at room temperature (or overnight). The gel was then de-stained at room temperature using Coomassie Brilliant Blue de-staining buffer. For the preparation of samples for mass spectrometry analysis, gels were stained with Protoblue Safe

(National Diagnostics) colloidal stain (1 part of ethanol plus 9 parts of the colloidal solution) and de-stained with distilled water.

2.3.5 In-gel digestion of proteins separated on SDS-PAGE gel for mass spectrometry analysis

All tubes, boxes, ruler and glass plate were rinsed with 0.1% formic acid (Fluka)/50% acetonitrile. The stained gel was placed the glass plate and the bands were excised with a sterile scalpel blade (about 5 mm each) and placed in individual 1.5 ml tubes. The gel pieces were washed 2x with 100 µl of 50% acetonitrile/50 mM ammonium bicarbonate for 45 minutes at 37^{o}C with agitation and then dried down in the speedvac. 50 µl of 50 mM DTT (made up in 10% acetonitrile/50 mM ammonium bicarbonate) were added and an incubation at 56^{o}C for 1h followed. The supernatant was discarded and 50 µl of 100 mM iodoacetamide (made up in 10% acetonitrile/50 mM ammonium bicarbonate) were added. The tubes were covered in foil and incubated at room temperature for 30 minutes. The supernatant was removed and the bands were washed 3x with 10% acetonitrile in 40 mM ammonium bicarbonate for 15 minutes at room temperature with agitation. The pellets were dried down in the speedvac and rehydrated in 20 µl or 1.5x the gel volume (if greater than 20 µl) of 12.5 µg/ml Promega seq. Grade modified trypsin in 10% acetonitrile/40 mM ammonium bicarbonate for 1h at room temperature. 20 µl of 10% acetonitrile/40 mM ammonium bicarbonate were added and the bands were incubated at 37^{o}C overnight.

On the following day the supernatant was collected and saved and 30 µl of 3% formic acid in water were added to the pellet and incubated at 37^{o}C for 1h. This supernatant was added to the one previously collected. This step was repeated for 30 min and the three supernatants containing the digested peptides were combined. The samples were stored at -20^{o}C and ran by Dr. Douglas Ward from Cancer Sciences, University of Birmingham.

2.3.6 Expressing zebrafish Ecscr intracellular domain (icd) fused to MBP

Zebrafish Ecscr icd was amplified by PCR from cDNA and cloned into pMAL. This plasmid was used to transform chemically competent BL21(DE3) pLys S *E. coli*. One colony was inoculated in LB-broth (Ampicillin, Chloramphenicol), incubated over night at 37 ºC and then diluted 100-fold into LB-broth (Ampicillin, Chloramphenicol). The bacteria were cultured at 37 ºC until OD_{600nm} = 0.4-0.6, when they were induced with 1 mM IPTG for 3 hours. To minimise protein degradation, 0.5 mM PMSF was added. After the induction, the bacteria were centrifuged (10 min, 6000 rpm), washed with *E. coli* washing buffer and centrifuged again. Pellets were stored in -80 ºC. After that, the bacteria were thawed on ice, lysed with ice-cold *E. coli* lysis buffer (2 ml per 100 ml of bacterial culture) and ultra-sonicated for 3 min (Ultrasonicator Vibra CellTM, Sonics & Materials, Newtown, USA). Triton X100 to 1% was added and the samples were incubated on ice for 30 min. The lysates were centrifuged (10 min, 14000 rpm, 4 ºC), the supernatant was collected and mixed with glycerol to give a final concentration of glycerol 50% (v/v) and stored at -20 ºC.

To purify the zebrafish Ecscr-MBP protein, bacterial lysate was incubated with packed amylose beads on a rotating wheel for 2 hours at 4 °C. After that time beads were washed with *E. coli* washing buffer and eluted with elution buffer and de-salted through a PD10 column. To roughly assess the efficacy of purification and the amount of protein that was bound to amylose-agarose beads, 10 µl of each sample was run on a polyacrylamide gel alongside with the BSA samples as mass standards. The purified samples were sent to CRUK to immunise two rabbits and produce a polyclonal antibody (1x 1200 µl of 50-100 µg and 5x 1200 µl of 200-400µg).

2.3.7 GST pull down

Human ECSCR icd was amplified by PCR from cDNA and cloned into pGEX, to make a GST fusion protein, that was expressed and purified in the same way as described in 2.3.6, but using glutathione beads instead of amylose ones. As a control, GST alone was also expressed (pGEX vector alone). The pulldown was performed using 300 µl of bacterial lysates and 1050 µl of HUVECs lysates, as described on section 2.3.2 for immunoprecipitation, but using glutathione beads instead of protein G ones. After the final wash, 2x SDS-PAGE sample buffer was added 1:1 and the samples were boiled, ran on an SDS-PAGE gel and analysed by western blot.

2.3.8 Western Blot

After the SDS-PAGE, the gels, blotting paper and blotting pads were soaked in transfer buffer for 10 min prior to assembling the transfer apparatus in the X cell II™ Mini cell, X cell II™ Blot Module and X cell sure lock™ (Invitrogen, Carlsbad, USA). PVDF membrane (Immobilon-P, 0.45 µm, Millipore, Billerica, USA) was activated by pre-wetting in methanol (Fisher Scientific) for 30 s and then placed also in 1x transfer buffer. Wet transfer was performed at 30 V for 2 hours at 4 ºC. The membranes were stained with Ponceau S dye (Sigma) to check the transfer and then blocked with 5 % dried milk (prepared in TBST buffer) for 1 hour at room temperature or overnight at 4ºC. The membranes were briefly washed in TBST and placed in appropriate primary antibody solution probing at room temperature for 1h on a rotator. After this incubation, the membranes were washed for 30 min in TBST with 4 buffer changes and incubated with appropriate secondary antibodies conjugated with horseradish peroxidase (HRP). After 1 hour of incubation at room temperature, the membranes were washed for 30 min as above and developed with ECL Western Blotting Detection Reagents (GE Healthcare, Little Chalfont, UK) for 1 minute. The blots were

visualized by autoradiography on Hyperfilm ECL (GE Healthcare) which was exposed to the membrane for different times, in the dark.

When reprobing with another antibody was required, the membranes were stripped. For that purpose, the membranes were incubated for 30 min at 65ºC in 50 ml of stripping buffer supplemented with 350 µl of beta-mercaptoethanol (Sigma), washed with TBST for 30 min changing the buffer every 10 min, blocked and probed as described above.

2.3.9 Yeast-two-hybrid assay

In order to assess direct interactions between ECSCR and candidate binding partners identified by mass spectrometry, yeast-two-hybrid assays were performed.

2.3.9.1 Yeast strain and media

The yeast strain used for this assay was PJ69-4A (genotype: MATa, trp1-901, leu2-3,112, ura3-52, his3-200, gal4Δ, gal80Δ, GAL2-ADE2, LYS2::GAL1-HIS3, met2::GAL7-lacZ).

PJ69-4A yeast was grown on yeast-peptone-dextrose (YPD) full medium (1 % (w/v) bacto-yeast extract, 2 % (w/v) bacto-peptone, 2 % (w/v) dextrose, 0.01 % (w/v) tryptophan (Trp) and 2 % (w/v) bacto-agar (when solid medium was required).

For the assay, selective media were used. Special synthetic complete dextrose (SCD) medium contained 0.67 % (w/v) yeast nitrogen base without amino acids, 2 % (w/v) dextrose and 0.14 % (w/v) yeast synthetic drop-out media supplement lacking histidine (His), leucine (Leu), uracil (Ura) and Trp and 2 % (w/v) bacto-agar (for solid medium). Before the final screening, as described below, SCD medium was supplemented with 100 mg/L Trp, 50 mg/L Leu, 40 mg/L His or 20 mg/L Ura. Except for Trp and Ura, that were sterilised by filtering through 0.22 µm-pore filters (Millipore), all the stock solutions were autoclaved.

2.3.9.2 Yeast-two-hybrid method

The entire method was carried out using aseptic technique.

ECSCR icd was cloned into pGBT9 (to be fused to the binding domain of Gal4p) and the interacting candidates were cloned into pACT2 (to be fused to the activation domain of Gal4p). These constructs were transformed into the yeasts sequentially and the positive clones were selected by SCD medium lacking Trp (for clones containing pGBT9), Leu (for clones containing pACT2) or both (for double transformants). This yeast strain contains a Gal4 promoter-His3 reporter gene. Once the double transformants were obtained, they were grown on SCD-Leu^--Trp^- at 30ºC and diluted to an OD_{600} of 0.5. Then, five ten-fold serial dilutions were made and 10 µl of each were carefully placed on agar plates of SCD-Leu^--Trp^- and SCD-Leu^--$Trp^-$$His^-$(3AT) and allowed to grow for 3-7 days at 30ºC. All spots should grow on the former plates and in the latter only the ones where an interaction occurs should survive.

For the transformations yeasts were grown overnight at 30ºC with agitation from a single colony in 3 ml of YPD or SCD lacking the appropriate ingredients. The lithium acetate / single stranded carrier DNA / polyethylene glycol method by Gietz and Woods (2002) was used. Briefly, on the following morning the cultures were diluted to an OD_{600} of 0.25 and allowed to grow for two more generations up to OD_{600} of 0.5-1. An OD_{600} of 1 is approximately 2×10^7 yeast/ml. For this protocol, 2×10^8 yeasts were used per transformation. These were centrifuged for 2 min at 5000 x g and the pellets washed with 1 ml of sterile water and transferred into 1.5 ml tubes. Another centrifugation as before followed and the water was removed. In this order, 240 µl of 50 % (w/v) polyethylene glycol (PEG, molecular weight of 3350 g), 36 µl of 1 M lithium acetate, 10 µl of 10 mg/ml single-stranded-carried DNA from salmon sperm (Invitrogen) (previously boiled for 5 min and chilled on ice), and 34 µl of plasmid DNA diluted in water (0.1 to 1 µg of DNA) were added to the yeast pellet, that was then ressuspended in this

mixture. The yeasts were agitated at 30ºC for 30 min and then a 15 min heat-shock at 42ºC was performed. The yeasts were centrifuged as previously and the pellets were washed with 1 ml of water. In the end, they were plated in the appropriate media, after ressuspending in 150-200 µl of water.

2.3.10 Luciferase complementation assay

When the yeast-two-hybrid method was unable to provide a more specific answer, protein-protein interaction was studied using the luciferase complementation assay, where ECSCR was cloned into Zipper-hGLuc[1]93 (to replace the zipper protein and make a fusion to the first half of *Gaussia* luciferase) and the interacting candidates were cloned into Zipper-hGLuc[2]93 (to replace the zipper protein and make a fusion to the second half of *Gaussia* luciferase) (Remy and Michnick, 2006). When an interaction occurs, the two halves of luciferase come together to form an active enzyme, and this activity can be measured using a luminometer upon supply of an appropriate substrate (the *Renilla* luciferase assay system, from Promega was used).

The complementing plasmids were transfected into HEK 293T cells, following the PEI protocol on section 2.2.4. As a transfection efficiency control, a third plasmid expressing beta-galactosidase was co-transfected (1/10th of the concentration of the other plasmids, as advised by Dr. Michael Tomlinson). After 48 h the medium was removed and the cells were washed with PBS. For a 6-well plate 500 µl of 1x lysis buffer (Promega) were added to each well and the plates were placed on a rocker and incubated at room temperature for 15 min.

The lysates were collected into 1.5 ml tubes. For the luciferase assay, it is not necessary to remove the cell debris, but for other applications the lysates were spun down at 16,000 x g and the clear supernatant was collected. 100 µl of 1x *Renilla* luciferase substrate in *Renilla* luciferase assay buffer (Promega) were aliquoted into each well of an opaque, white, shiny,

clean 96-well plate and 20 µl of cell lysate were added and mixed thoroughly. This was done in triplicates. Untransfected cells, as well as water and lysis buffer only were used as controls. The plates were placed in the luminometer and the bioluminescence was read. Luminescence was integrated over 10'' with a 2'' delay.

To normalise the luminescence data, a beta-galactosidase assay was also performed. For that, 900 µl of phosphate buffer (60 mM Na_2HPO_4, 40 mM NaH_2PO_4, 10 mM KCl, 1 mM $MgSO_4$) were added to 200 µl of ONPG (4 mg/ml dissolved in phosphate buffer 0.1 M, pH 7) and 40 µl of cell lysate. This mixture was incubated 37^{o}C for about 1h, until yellow. The reaction was stopped by adding 200 µl the Na_2CO_3 1M and the tubes were spun down for 10 minutes at 13000 rpm. The OD was measured at 420 nm. The normalised activity was calculated as follows: normalised activity = luciferase activity/β-gal activity.

2.4 Molecular biology methods

All molecular biology methods were performed according to either the manufacturer's insctructions when kits were used or according to protocols existing in the laboratory that have been optimised over time by various scientists, based on Sambrook and Russell (2001).

2.4.1 Bacterial strains and media

For transformation with various plasmids, fusion protein expression and site-directed mutagenesis, chemically competent *Escherichia coli* strains DH5α, BL21(DE3) pLys S or XL1-Blue Supercompetent Cells (Stratagene, La Jolla, USA) were used. All bacteria were cultured in liquid Luria Bertani (LB) broth or plated on LB agar (both from Cancer Research UK Central Services, Clare Hall, Hertfordshire or Sigma). According to the antibiotics resistance carried by the different plasmids, 0.1 of mg/ml ampicillin (Amp, Sigma, Poole, UK),

0.02 mg/ml chloramphenicol (Sigma) and/or 0.03 mg/ml kanamycin (Sigma) were added to the media.

2.4.2 DNA amplification by PCR

DNA fragments were amplified by polymerase chain reaction (PCR) using a high fidelity polymerase. 25 µl of reaction contained 5.8 µl of water, 4 µl of 5x Phusion HF Buffer (New Engalnd Biolabs (NEB), Herts, UK), 2 µl of dNTP (2 mM, Bioline, London, UK), 2 µl of each primer (10 µM) and 0.2 µl of Phusion™ High-Fidelity DNA Polymerase (NEB). In the end 500 ng of template were added to the mixture. For the negative control, the template was replaced by water. The PCR reaction conditions were as follows: initial denaturation (98ºC, 30 s), 30 cycles of denaturation (98ºC, 10 s), annealing (appropriate temperature for each pair of primers, 30 s) and elongation (72 ºC, for the time necessary for the fragment to be amplified – ca. 1000 bp/min). A final elongation step at 72ºC for 5 min was included.

2.4.3 DNA digestion using restriction enzymes

Restriction enzyme digestion was used either to confirm the presence of inserts in plasmids or to digest inserts and vectors for ligation (sticky ends). Purified PCR product or plasmid were incubated in 50 µl of digestion mixture, containing 5 µl of suitable 10x NEBuffer, 5 µl of 10x BSA (if necessary, NEB), 3-5 units of each restriction enzyme (NEB) per microgram of DNA and water. Digestion was carried out for 2 hours at the appropriate temperature for each enzyme.

2.4.4 Nucleic acids electrophoresis in agarose gel

DNA/RNA gel electrophoresis was performed in 0.8 – 1.5% agarose (VWR International, Lutterworth, UK) gels made up with TAE buffer and containing 1:10000 DNA Sybr Safe (Invitrogen). The separation was carried out in TAE buffer, at 90 V. Gels were visualised and imaged using Gene Genius Bio Imaging System (Syngene, Cambridge, UK).

2.4.5 Plasmid ligation and bacterial transformation

Inserts obtained directly by PCR or restriction digestion were ligated into the appropriate digested plasmids using T4 Ligase (400000 U/ml, NEB). To 16 µl of insert/vector ratio of 3:1, 2 µl of enzyme and 2 µl of T4 Ligase Buffer (NEB) were added. Ligations were performed at room temperature for 1 hour or overnight for greater efficiency. Chemically competent *E. coli* (25 µl) were mixed with 5 µl of ligation mix or 50-500 ng of plasmid (for protein expression) and incubated on ice for 30 min. Subsequently, the bacteria were heat shocked at 42ºC for 1.5 min and incubated on ice for further 2 min. 250 µl of room temperature SOC medium (or LB) were added to the bacteria and they were incubated at 37ºC for 1 hour, with 200 rpm shaking (Sanyo/Gallenkamp, Loughborough, UK). Bacteria were plated on LB-agar plates (containing appropriate antibiotics) and incubated overnight at 37 ºC.

Positive colonies were screened by PCR or digestion with the appropriate restriction enzymes. For further confirmation of ligation and sequence integrity, the plasmids were sent out to Functional Genomics and Proteomics (School of Biosciences, University of Birmingham) for sequencing.

Glycerol stocks of bacteria containing all constructs were produced by mixing saturated bacterial cultures with an equal volume of 30 % (v/v) glycerol and stored at -80 ºC.

2.4.6 Plasmid preparation and purification

Large scale preparation of plasmids was performed from 200 ml cultures grown overnight using the GenElute^{TM} Plasmid Maxiprep Kit (Sigma, Poole, UK) according to the manufacturer's instructions. For small-scale plasmid preparations DNA was isolated from 5 ml cultures according to the GeneJET^{TM} Plasmid Miniprep Kit (Fermentas, UK). DNA concentration was measured using the NanoDrop ND-1000 Spectrophotometer (Labtech, Ringmer, UK).

2.4.7 Cell lysis and RNA extraction

The medium was removed from the cells growing in 10 cm dishes and 1 ml of Tri Reagent (Ambion) was added. The cells were lysed by pipetting up and down, the lysate was collected in 1.5 ml tubes and frozen at -20ºC. To extract the RNA the samples were thawed, incubated at 30ºC for 10 min and vortexed. After that, the solutions were centrifuged at 12000 rpm for 5 min, 200 µl of chloroform (per 1 ml of Tri Reagent) were added and the tubes were agitated. Following a 10 min incubation at room temperature, the samples were centrifuged at 12000 rpm for 10min and the supernatant was transferred into a new tube containing 0.7 V of ice cold isopropanol. This mixture was incubated at -20ºC for 30 min, centrifuged at 12000 rpm for 10 min, the pellet was washed with 70% ethanol and the final pellet was suspended in nuclease-free water and quantified using NanoDrop ND-1000 Spectrophotometer (Labtech, Ringmer, UK).

2.4.8 cDNA synthesis

cDNA synthesis was performed using the High Capacity cDNA Reverse Transcription kit (Applied Biosystems) for qPCR or the Superscript III for RT-PCR kit for cloning. For the first one, per reaction, 2 µl of 10x RT buffer, 0.8 µl of 25x dNTP mix, 2 µl of 10x random primer, 1 µl of multiscribe RT, 4.2 µl of RNase free water and 10 µl of RNA sample were added in a tube. The reaction was carried out at 25ºC for 10 min followed by 2 hours at 37ºC. For the latter, 1 µl of 0.5 µg/µl oligo(dT)12-18 primers, 1 µl of 10 mM dNTP mix, 5 µg of RNA and water up to 13 µl were added to a nuclease-free tube. The mixture was heated at 65ºC for 5 min and incubated on ice for 1 min. Then, 4 µl fo 5x first strand buffer, 1 µl of 0.1 M DTT, 1 µl of RNase out (40 U/µl) and 1 µl of Superscript III RT (200 U/µl) were added and after homogeneising, the reaction was incubated at 50ºC for 1 hour. Finally, the reaction was inactivated by heating at 70ºC for 15 min.

2.4.9 Quantitative RT-PCR (qPCR)

To quantify relative gene expression, 12.5 µl of sensi mix (Abgene, Epsom, UK), 1 µl of each primer (10 µM), 0.25 µl of each probe (Exiqon, Vedbaek, Denmark) and 0.25 µl of nuclease-free water were mixed in a hood. On the lab bench, 10 µl of each sample dilution (1:10, 1:100) were added to the previous mixture (in triplicates). The qPCR reaction was performed on Rotor-Gene RG-3000 qPCR machine (Corbett Research Ltd, Australia).

2.4.10 Microarray

Unless otherwise stated, the reagents used to perform the microarray were purchased from Agilent Technologies.

For the microarray three 10 cm plates of ECSCR siRNA transfected and three plates of negative control duplex transfected HUVECs were used (after 48h of transfection). Total RNA was extracted and purified. Cy3 dye was used for knock down samples and Cy5 dye for the controls.

To generate the microarray the Agilent Two Colour Microarray-Based Gene Expression Analysis (Quick Amp Labelling) kit was used, following the manufacturer's instructions. The protocol comprises the following steps: cDNA synthesis, cRNA synthesis and labelling, purification and quantification of the labelled/amplified cRNA, hybridization, washing, reading, extracting data and data analysis.

In brief, a total of 1µg of each RNA sample was mixed with the T7 promoter primer, spike mix (A for Cy3 or B for Cy5) and nuclease-free water. The samples were denatured and first strand buffer, DTT, dNTP mix, MMLV-RT, RNase out and water were added for the cDNA synthesis reaction. cRNA was synthesized and labelled by adding nuclease-free water, transcription buffer, DTT, NTP mix, PEG, RNase out, inorganic pyrophosphatase, T7 RNA polymerase and Cy3 or Cy5 to the previous reaction. Labelled and amplified cRNA was purified and washed

using RNeasy mini spin columns (Quiagen) and quantified on Nanodrop ND-1000 UV-VIS Spectrophotometer version 3.2.1.

The microarray data were analysed using two different programs: SAM (statistical analysis of microarrays) contained in a program called MeV (multiexperiment viewer) from Tigr – the institute for genomics research (http://www.tm4.org/mev/) and R, a free statistical program from Bioconductor (http://www.bioconductor.org). The workflow for both programmes is equivalent and includes quality control, normalisation and differential expression analysis. The final list of genes was obtained for a fold change above 2 and a p value below 0.01.

In order to put the results into context, the lists of up and downregulated genes were analysed using Ingenuity Pathway Analysis (Quiagen) (www.ingenuity.com).

2.5 Methods employed for *in vivo* analyses

2.5.1 Species and strains

To study the function of ECSCR *in vivo*, two model species were used, *Danio rerio* (zebrafish, vertebrate fish model) and *Mus musculus* (common mouse, mammalian model). The animals were reared and bred at the Biomedical Services Unit, University of Birmingham.

Two strains of zebrafish were used, wild type AB* and transgenic tg[fli1:EGFP]. The mouse strain used as background was black C57Bl/6JOlaHsd, the white strain used to obtain blastocysts and do germline transmission testing was albino C57Bl/6 and the strain used implant blastocysts injected with ES cells was CD-1.

2.5.2 Zebrafish and mouse whole mount *in situ* hybridization (WISH)

The *in situ* hybridization technique allows the detection of sites of expression of a certain gene. For that purpose, a digoxigenin-labelled anti-sense RNA probe (complementary to the mRNA

to be detected) is synthesized and hybridized against paraffin sections or, in this case, whole embryos to detect expression of the target gene (Thisse and Thisse, 2008).

For the WISH E9.5 C57Bl/6JOlaHsd mouse embryos and 24 hours post-fertilization (hpf) AB* zebrafish embryos were used. The protocol was done according to Thisse and Thisse (2008).

2.5.2.1 Mouse RNA probe synthesis

SEND cells were cultured and RNA was extracted. cDNA was synthesized using the high capacity cDNA reverse transcription kit. An 857 bp fragment was amplified by PCR and cloned into PCR TOPO blunt (using 0.5 µl of salt solution, 0.5 µl of TOPO vector, 2 µl of DNA and 0 µl of nuclease-free water). The purified plasmid was linearised with NotI (for antisense RNA) and BamH1 (for sense RNA). For the transcription of the sense and antisense RNA probes, by this order, 1 µg of linear plasmid (10 µl), 2 µl of 10x transcription buffer (Roche), 2µl of 10x digoxigenin label mix (Roche), 2 µl of 10x SP6 (for antisense probe) or T7 (for sense probe) RNA polymerase, 1 µl of ribolock RNase inhibitor (Fermentas) and 3 µl of nuclease-free water, to a total of 20 µl were added. The solutions were mixed and incubated at 37C for 2.5 hours. 1 µl of DNaseI was added and the tubes were incubated at 37ºC for 15 min. The probes were then purified using the Mini Quick spin columns (Roche Applied Science), according to the manufacturer's instructions. The probes were quantified and 10 µl aliquots were stored at -80ºC. The probes were visualised on a 2% (w/v) agarose gel.

2.5.2.2 Whole-mount *in situ* hybridization

On the first day the embryos were rehydrated through a methanol series of 75%, 50% and 25% (in DEPC-treated PBS), for 5min each and rinsed twice (5 min) in PBST (0.1% v/v of Tween 20 in DEPC-treated PBS). The embryos were then incubated with freshly made proteinase k 10 µg/ml (Sigma) for 30 min and the reaction was stopped with 2 mg/ml of glycine (Sigma) in PBST for 5 min. After that the embryos were washed twice with PBST for 5 min, post-fixed

in 4% (w/v) PFA (in DEPC-treated PBS) and washed again with PBST. Subsequently, they were incubated with 50% PBST/50% hybridization buffer for 3 min at room temperature and with 100% hybridization buffer at 70ºC for 4 hours, with a change after 2 hours. The probes were denatured at 95ºC for 5 min and diluted in the hybridization buffer to 500 ng/ml. The embryos were incubated with this solution overnight at 70ºC.

On the following day the hybridization buffer was removed and the embryos were washed through a series of hybridization buffer: 2xSSC (100:0, 75:25, 50:50, 25:75 and 0:100), 10 min each. They were then washed with 0.2% SSC and another series of 0.2% SSC: MABT (75:25, 50:50, 25:75 and 0:100) for 5 min each. The embryos were blocked in 2% Boehringer blocking agent, 5% goat serum (in MABT) at room temperature for 1 hour. After that time, another 2 hour incubation as described before took place, with fresh solution. The embryos were then incubated overnight with gentle shaking at 4ºC with 1:5000 anti-digoxigenin antibody in the same solution.

On the last day of the protocol the tubes containing the embryos were transferred to room temperature for 1 hour. The antibody mix was removed and the embryos were were washed 8x with MABT, 15 min each. After one quick wash with BCL buffer III, two 15 min washes followed. Finally, colour was developed by using 400 µl of BM purple at room temperature (the tubes were wrapped in foil). After two hours the embryos were checked for development of colour. The reaction was stopped by washing with 20mM EDTA in PBST, the embryos were post-fixed with 4% PFA and stored at 4ºC.

2.5.3 Injection of antisense zebrafish Ecscr morpholino oligonucleotides

Antisense morpholino zebrafish Ecscr oligonucleotides were microinjected into the yolk of 1-cell transgenic tg[fli1:EGFP] zebrafish embryos. As controls, uninjected embryos and embryos injected with mismatched morpholinos were used. The concentrations tested were 0.2, 0.4 and

0.8 ng of morpholino per embryo (1 nl of 0.25, 0.5 and 1 mM). The transgenic embryos were observed, photographed and counted at 28 hpf. They were divided into three categories, according to the severity of the effects caused by the morpholino injections, compared to the controls: no abnormal phenotype, mild and severe. The percentages of embryos in each category were calculated. This experiment was done three times and at least 100 embryos were counted each time, for each condition.

2.5.3.1 Zebrafish Ecscr morpholino phenotype rescue assay

In order to assess the specificity of the morpholinos, a rescue assay was performed, by co-injecting zebrafish Ecscr mRNA.

Zebrafish Ecscr was amplified by PCR from cDNA and cloned into the pCS2 vector, that contains an RNA polymerase promoter, SP6. The plasmid was linearised with *Not* I (New England Biosciences) and mRNA was synthesized with SP6 RNA polymerase using the MmessageMmachine kit (Ambion). This mRNA was microinjected into one cell zebrafish embryos alone (to optimise the right concentration to be used) or in combination with the zebrafish Ecscr translation or splicing blocking morpholinos.

All animal work was carried out under approved Home Office projects and personal licenses. The PhD student's personal license number for both zebrafish and mice was PIL 40/9557 and the two project licenses held by Prof. Roy Bicknell were PPL 40/3131 ("An analysis of tissue development in zebrafish") and PPL 80/2217 ("Validation of novel endothelial genes as vascular targets").

2.6 Statistical analyses

Unless otherwise stated, all experiments were repeated at least three times with similar results. Data were plotted with error bars representing the standard deviation. A Shapiro-Wilk

normality test was performed on data sets to confirm a normal distribution. For this test, data are normally distributed when $p \geq 0.05$. P values were determined using GraphPad Prism 5 to test for significant differences in data. Unpaired, two-tailed Student's t-test was used to determine the significance of experiments. When the calculated p value was less than 0.05, the hypothesis that the means of the two compared groups differed significantly was accepted. On chapter 4 (figures 4.7 and 4.8) a chi-squared test was performed, as the data sets are lists of counts. Differences between conditions were also considered significant when $p \leq 0.05$.

3 IDENTIFICATION OF PROTEINS INTERACTING WITH ECSCR

3.1 Introduction

Endothelial cell specific molecule 2 (ECSM2) was first identified in 2000 (Huminiecki and Bicknell, 2000) but until 2008 there were no other publications concerning ECSCR. Armstrong *et al.* (2008) used siRNA knockdown and implicated a role for ECSM2 in cell migration and tube formation and identified a molecular interaction with filamin A. In the light of these findings, ESCM2 was renamed by the Human Genome Organization (HUGO) Gene Nomenclature Committee (HGNC) endothelial cell specific chemotaxis regulator (ECSCR). In 2009, two further independent studies were published. The first showed that ECSCR can attenuate the epidermal growth factor receptor (EGFR)-induced cell migration, possibly by inhibition of the Shc-Ras-ERK (MAPKinase) pathway (Ma *et al*., 2009). The second identified the role of ECSCR in cell survival by interaction with the cIAP-1 and cIAP-2 pro-apoptotic proteins and modulation of their degradation by the proteasome (Ikeda *et al*., 2009). More recently, a zebrafish developmental study by Verma *et al*. (2010) has proposed that ECSCR enhances endothelial VEGF receptor 2 sensitivity to VEGF, thus in turn promoting migration of zebrafish angioblasts.

The endothelial specificity of ECSCR and its effect on cell migration suggests a role in endothelial cell biology. Although some possible interactions between ECSCR and other molecules are starting to emerge, the exact mechanism of action and signalling pathways are yet to be clarified.

3.2 Identification of binding partners for ECSCR

To capture and identify ECSCR interacting proteins/complexes a co-immunoprecipitation (co-IP) analysis was performed. This used anti-ECSCRicd antiserum (rabbit serum was used as an IgG control). Co-IPs were run on a gradient gel (4-12%), stained and processed for mass

spectrometry (MS) analysis. The results were analysed, proteins were ranked by number of hits/differences between the ECSCR and negative control IPs and grouped by function, using the DAVID software. Principal functional groups were cytoskeletal processes, trafficking, protein folding, apoptosis and metabolism (figure 3.1 A). As ECSCR had been previously implicated in cytoskeletal modulation, this cluster was analysed in more detail. (figure 3.1 B). The analysis of the MS data has also revealed a good peptide diversity for each hit, *i.e.*, each protein was identified by several different peptides, which adds confidence to the results. Identification of filamin A (with 34 peptides for the specific IP *versus* 5 for the control), confirmed earlier work by Armstrong *et al.* (2008). Putative interacting proteins were chosen for confirmation of the MS data by GST pull down (ECSCRicd-GST and GST alone, as a control) and subsequent western blot – talin 1, vinculin, filamin A, moesin, myosin 9 (myosin II) and plastin 3. Briefly, there are no apparent differences in myosin II, talin and vinculin, and there seems to be more filamin A (as shown by the Armstrong *et al*., 2008), moesin and plastin 3 in the pull down with ECSCRicd-GST than with GST alone (figure 3.2)**.**

Filamin A, moesin and plastin 3 were chosen for further studies, as the two latter ones are present in filopodia, which is where ECSCR is enriched. Filamin A and moesin were analysed for direct interactions with ECSCRicd by yeast-two-hybrid. Bioinformatics analysis of the ECSCR protein primary structure using the tools available at www.expasy.com, such as SMART, revealed no conserved domains or structural features similar to other proteins contained in public databases. However, ECSCRicd contains a cluster of basic amino acids RK(S)K, immediately after the transmembrane domain, which has been shown to interact with ezrin-radixin-moesin (ERM) family of proteins in other proteins (Yonemura *et al*., 1998). As for filamin A, the interaction with ECSCRicd had already been found by others

A

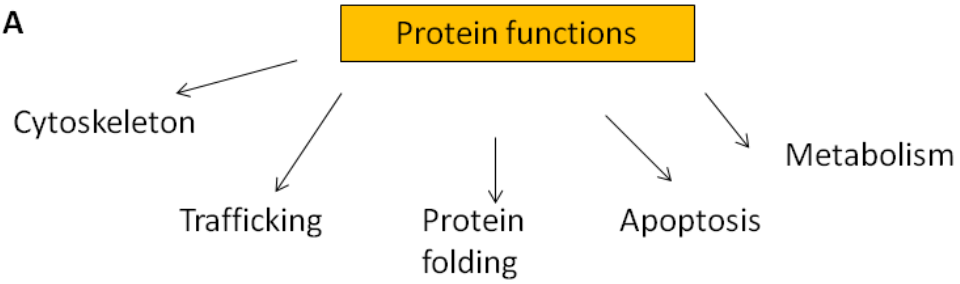

B

Protein	IP	IgG
Filamin A	34	5
Myosin II	35	5
Vinculin	22	4
Moesin	17	9
Talin	11	4
Alpha-actinin-4	14	0
Alpha-actinin-1	13	1
Ras GTPase-activating-like protein	8	0
Plastin-3	3	0

Figure 3.1 - Proteins that co-immunoprecipitate with ECSCR from HUVECs lysate.

The list of proteins that co-IP with ECSRicd was submitted to DAVID, to obtain functional clusters (A). The cytoskeletal fraction was chosen for study in further detail (B). IP – number of peptides obtained for each protein upon immunoprecipitation using an antibody against ECSCR icd; IgG – number of peptides obtained for each protein upon immunoprecipitation using rabbit serum. The lines in green show proteins present in filopodia.

(Armstrong *et al.*, 2008), so the aim was to confirm these results and try to map the interaction to the ECSCRicd.

The ultimate goal, after finding direct interactions with specific regions, would be to mutate them and to show that the proteins no longer interacted, as well as using those mutants in functional assays (like the Boyden chamber, for example, since it was demonstrated by Armstrong *et al*. (2008) that the lack of ECSCR significantly reduces HUVECs migration through a pore).

For the yeast-two-hybrid assay, the complete intracellular domain of ECSCR was amplified by PCR and inserted into the pGBT9 plasmid using *EcoR*I and *BamH*I restriction enzymes. The candidate interactors, full length moesin and two fragments of filamin A corresponding to Ig repeats 15-16 and 19-21 (Armstrong *et al.*, 2008) were inserted into pACT2, using *BamH*I and *EcoR*I restriction enzymes. Ezrin full length was also cloned in the same way and was used as a negative control, as it is very closely related to moesin (both part of the ERM family) but did not appear in the MS results. Combinations of ECSCRicd and the potential interactors were transfected into yeast (as well as combinations of ECSCRicd and empty pACT2 as a control). The two plasmids encode for an activating domain and a binding domain of Gal4p which, upon binding of the fused interacting proteins, come together to activate a reporter gene (HIS3). For more details see section 2.3.9.

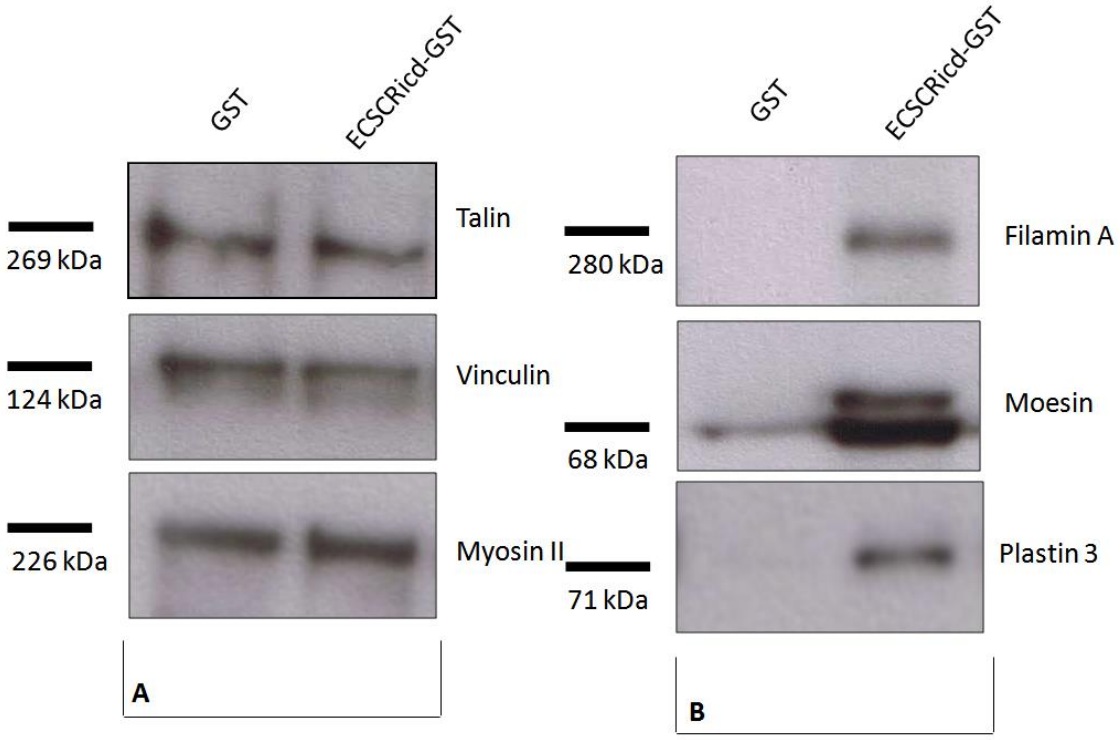

Figure 3.2 - Assessment of the results of mass spectrometry by GST pull down and western blot analysis

GST pull down was control for ECSCRicd-GST. There were proteins that showed no difference between the test and the control (A) and others that were specifically pulled down with ECSCRicd-GST (B). This experiment was performed 3 times with similar findings. GST – glutathione-S-transferase; ECSCRicd-GST – ECSCR intracellular domain fused to GST.

After seeding the double transformants in the appropriate selective media, all contained both plasmids (as they grew on SCD Trp^- Leu^-) (Figure 3.3). However, only the colonies containing ECSCRicd and either fragment of filamin A grew on the medium that selected for interactions (SCD His^- (3AT) Trp^- Leu^-) (figure 3.3). This confirmed that Filamin A and ECSCRicd directly interact. To look further into this result, yeast containing ECSCRicd and moesin, ezrin (and pACT2 as a control) were grown and total protein was extracted and analysed by western blot. This revealed that neither moesin nor ezrin were expressed by the yeast. Therefore, other methods were employed to test for this interaction, as described below.

After confirmation of binding between ECSCRicd and filamin A, an attempt was made to map the region of ECSCRicd responsible for it. Since there are no conserved domains, two halves of ECSCR (the first 30 amino acids and the second 30 amino acids) were amplified by PCR and inserted into pGBT9 using *EcoR*I and *BamH*I restriction enzymes. These constructs were then co-transfected into yeast with the pACT2 plasmids containing either fragment of filamin A. The yeast-two-hybrid assay revealed that neither of the two halves of ECSCRicd was able to bind either of the filamin A fragments (figure 3.4). This study was abandoned because this technique didn't seem to be the most appropriate to determine the region of filamin A where ECSCR binds. Making a construct where ECSCR becomes much smaller than the protein it is fused to may result in occlusion of the amino acids that bind to filamin A, leading to a false result. On the other hand, since neither half of ECSCR seems to bind to Filamin A, the next step would be to test a region in the junction between the two. This could also lead to false results, as often proteins need to be in a certain conformation to be able to interact with other molecules. Therefore, it cannot be ruled out that instead of the middle region, actually both halves of ECSCR are important for binding to filamin A, as they may interact with each other via distant amino acids to confer a certain secondary structure necessary for interaction. An

alternative but time consuming method would be to mutate individual amino acids and evaluate the effect upon binding. The fact that ECSCR bares no homology to any other protein makes this study more difficult, as there is no obvious candidate region to start with.

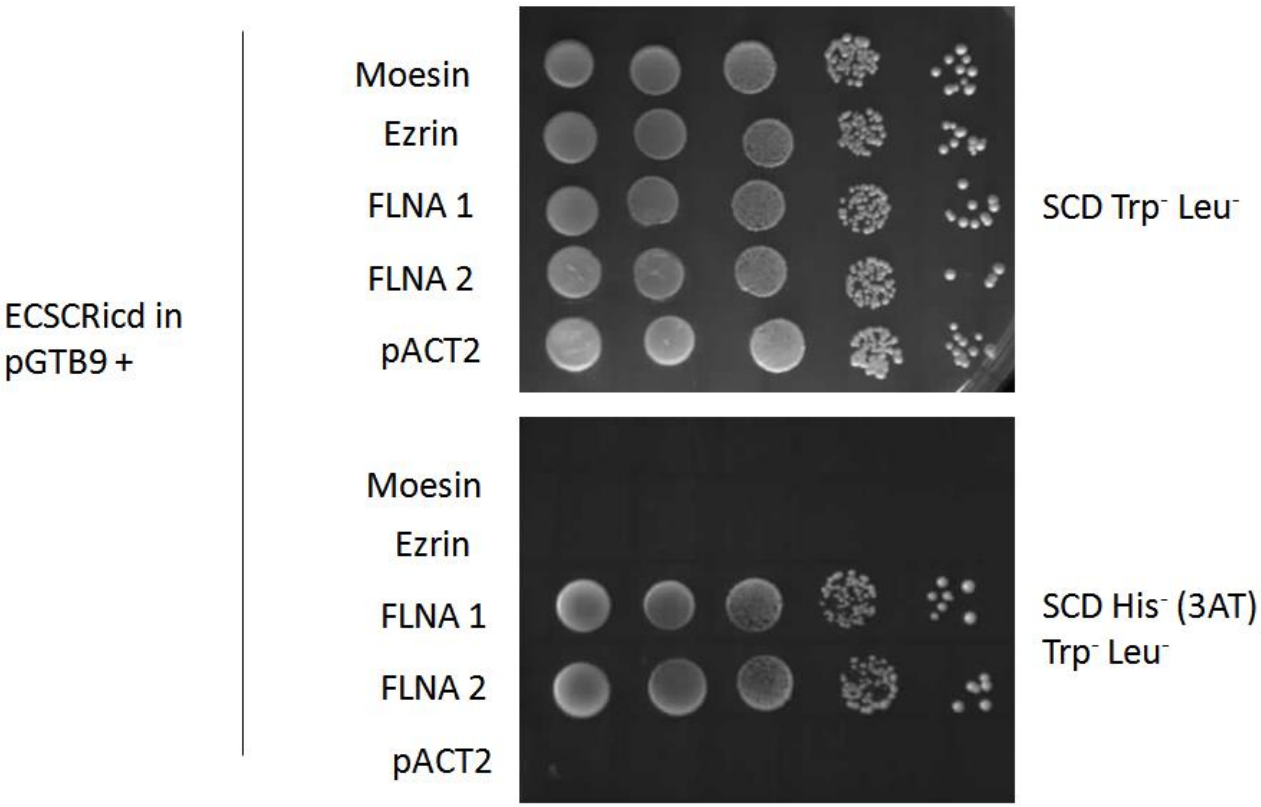

Figure 3.3 - Yeast-two-hybrid assay to assess protein interactions between ECSCRicd and filamin A

A yeast-two-hybrid assay was performed using ECSCR intracellular domain to look for interactions with filamin A fragments corresponding to repeats 15-16 (FLNA 1) and 19-21 (FLNA 2), as well as moesin and ezrin. The assay confirmed direct interaction between ECSCRicd and filamin A, but not moesin or ezrin. SCD – synthetic complete dextrose; Trp^- - lacks tryptophan; Leu^- - lacks leucine; His^- - lacks histidine; 3AT – 3-amino-1,2,4-triazole.

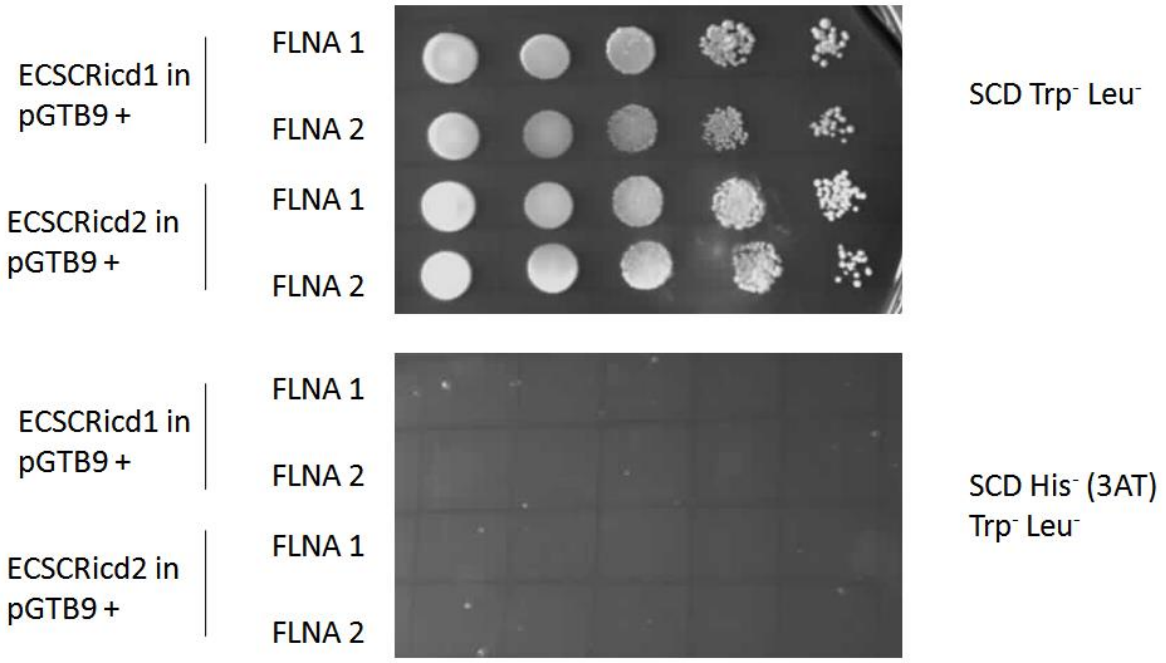

Figure 3.4 - Yeast-two-hybrid assay to assess protein interactions between the two halves of ECSCRicd and filamin A

To further investigate the interaction between ECSCR and filamin A, a yeast-two-hybrid assay was performed using either the first 30 amino acids (ECSCRicd1) or the last 30 amino acids (ECSCRicd2) of ECSCR intracellular domain to look for interactions with filamin A fragments corresponding to repeats 15-16 (FLNA 1) and 19-21 (FLNA 2). The assay showed that either half of ECSCRicd is insufficient to bind to either fragments of filamin A. SCD – synthetic complete dextrose; Trp^- - lacks tryptophan; Leu^- - lacks leucine; His^- - lacks histidine; 3AT – 3-amino-1,2,4-triazole.

To obtain a more conclusive answer about the ECSCRicd-moesin interaction, a luciferase complementation assay was performed. This assay is similar to the yeast-two-hybrid, in the sense that the two potential interactors are fused to two halves of a protein that becomes functional upon binding. In this case, luciferase is an enzyme that is able to degrade a substrate and the interaction is measured by a luminometer, as the degradation product is bioluminescent. The method was developed by Remy and Michnick (2006), who kindly provided the Zipper-hGLuc[1]93 and Zipper-hGLuc[2]93 plasmids, which were used as a positive control. Moesin and ECSCRicd were amplified by PCR and inserted into these plasmids using the *Not*I and *Cla*I restriction enzymes, which resulted in the replacement of the zipper protein by these two. Instead of yeast, for this method mammalian cells (HEK 293T) were tansfected with the appropriate combinations of plasmids (and also each one plus either Zipper-hGLuc[1]93 or Zipper-hGLuc[2]93 to assess specificity). In addition, all cells were transfected with a third plasmid, encoding beta-galactosidase, to normalise the trasnfection efficiency.

The results indicate a positive interaction between ECSCRicd and moesin ($p < 0.05$) (figure 3.5). However, marginal significance was obtained only after five repeats, as there is a big variation between replicates and the negative controls containing moesin fused to the first half of luciferase co-transfected with the second half of luciferase fused to a zipper protein (which should not interact with either ECSCR or moesin) produce high levels of background, having luminescence reads close to those of the ECSCR-moesin interaction. The same result was observed for the other negative control, where ECSCR intracellular domain is fused to the second half of luciferase co-transfected with the first half of luciferase fused to a zipper protein.

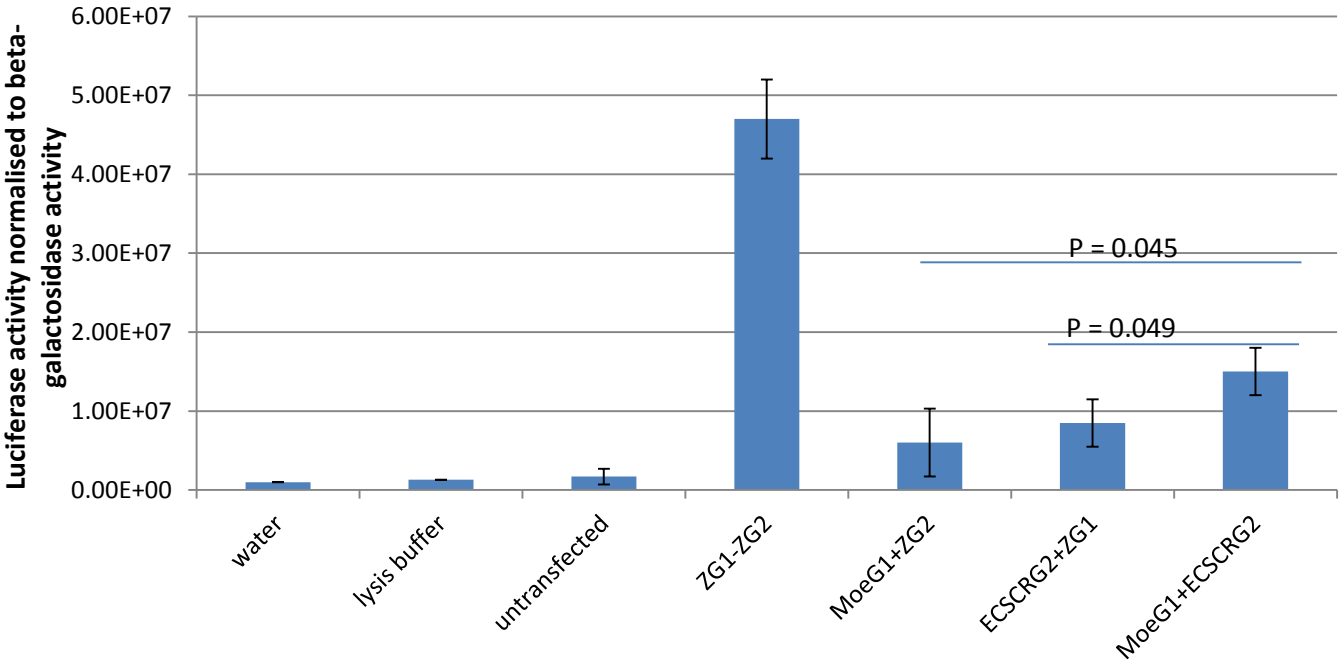

Figure 3.5 - Luciferase complementation assay to assess the interaction between ECSCR and moesin in HEK 293T cells

To assess the interaction between ECSCR and moesin, full length moesin and the intracellular domain of ECSCR were inserted into two complementary plasmids that contain half of the luciferase enzyme sequence each. Two zipper proteins known to interact with each other were used as a positive control. Water, lysis buffer and untransfected cells were used as negative controls, as well as combinations of each test plasmid (MoeG1, ECSCRG2) with the respective complementary half of luciferase fused to a non-specific interactor. The experiment was repeated 5 times. This assay demonstrates that the interaction between ECSCRicd and moesin is specific, as it is significantly higher than the interaction of either with a zipper protein ($p < 0.05$, two tailed unpaired t-test). The error bars represent the standard deviation from the mean. ZG1 – Zipper-hGLuc[1]93; ZG2 – Zipper-hGLuc[2]93; MoeG1 – moesin fused to first half of luciferase; ECSCRG2 – ECSCR fused to the second half of luciferase.

3.3 The effect of ECSCR on the cytoskeletal arrangement

It has been shown that the knockdown of ECSCR by siRNA in HUVECs causes impaired tube formation and migration in a Boyden chamber assay and that ECSCR probably modulates the cytoskeleton organization via filamin A (Armstrong *et al*., 2008).

In the present study the interaction with filamin A has been confirmed and other cytoskeletal proteins involved in filopodia formation have been co-immunoprecipitated with endogenous full length ECSCR, as well as pulled down by its intracellular domain.

To further investigate the role of ECSCR at a cellular level, siRNA knockdown was performed in HUVECs and cytoskeletal proteins such as plastin 3, talin1, VE-cadherin, F-actin (phalloidin), moesin, filamin A and non-muscle myosin II were visualised using immunofluorescence (figure 3.6). These proteins were chosen because they have been specifically co-immunoprecipitated with ECSCR (figure 3.1). Additionally, VE-cadherin was stained because ECSCR also localises to cell-cell junctions (Shi *et al*., 2011). The aim was to evaluate if the lack of this protein would somehow disrupt cell-cell adhesion. Phalloidin was used to stain stress fibres (F-actin) because Ma *et al*. (2009) have reported that in HEK 293T cells transfected with ECSCR-GFP stress fibres were largely destructed compared to the GFP control. Phalloidin was used in cells treated with ECSCR siRNA (and negative control duplex control) to assess if ECSCR knockdown would result in an increase of stress fibres.

Plastin 3 locates to cell protrusions and seems to be less evident in cells where ECSCR is depleted. Talin 1 locates near the cell edges in adhesion points, which seem to be lost when ECSCR is absent. VE-cadherin locates to cell-cell junctions and ECSCR knockdown does not seem to have an effect on this protein. When ECSCR is knocked down, stress fibres seem to be less organised (F-actin). Moesin is located at cell protrusions and seems to have a more diffused distribution when ECSCR is knocked down. Both filamin A and myosin II are

arranged in fibre-like structures along the cells, which seem disorganised in the absence of ECSCR. In general, the lack of ECSCR seems to result in a less organised cytoskeleton in terms of protrusions and fibre-like structures, that seem to be disconnected from the membrane. This is consistent with a role for ECSCR in anchoring the cytoskeleton to the membrane. Although the immunofluorescence protocol was optimised for each antibody and the experiment was done 3 times, some antibodies still did not produce a very good staining. Some further optimisation could be attempted or different antibodies could be purchased to generate results that are clearer.

On the other hand, the opposite experiment was performed, where ECSCR-GFP was overexpressed in cells that do and do not contain filamin A. ECSCR is located at the plasma membrane and filopodia in HEK 293T cells. The construct was able to induce the formation of filopodia in HEK 293T cells (that contain filamin A), but not in and M2 cells (that do not express filamin A) (figure 3.7). The experiment was done 3 times for HEK 293T cells and only once for M2 cells. In the latter ECSCR also seems to locate at the plasma membrane. However, these cells seem to be blebbing (even the GFP control). The experiment should be repeated to obtain reproducible results.

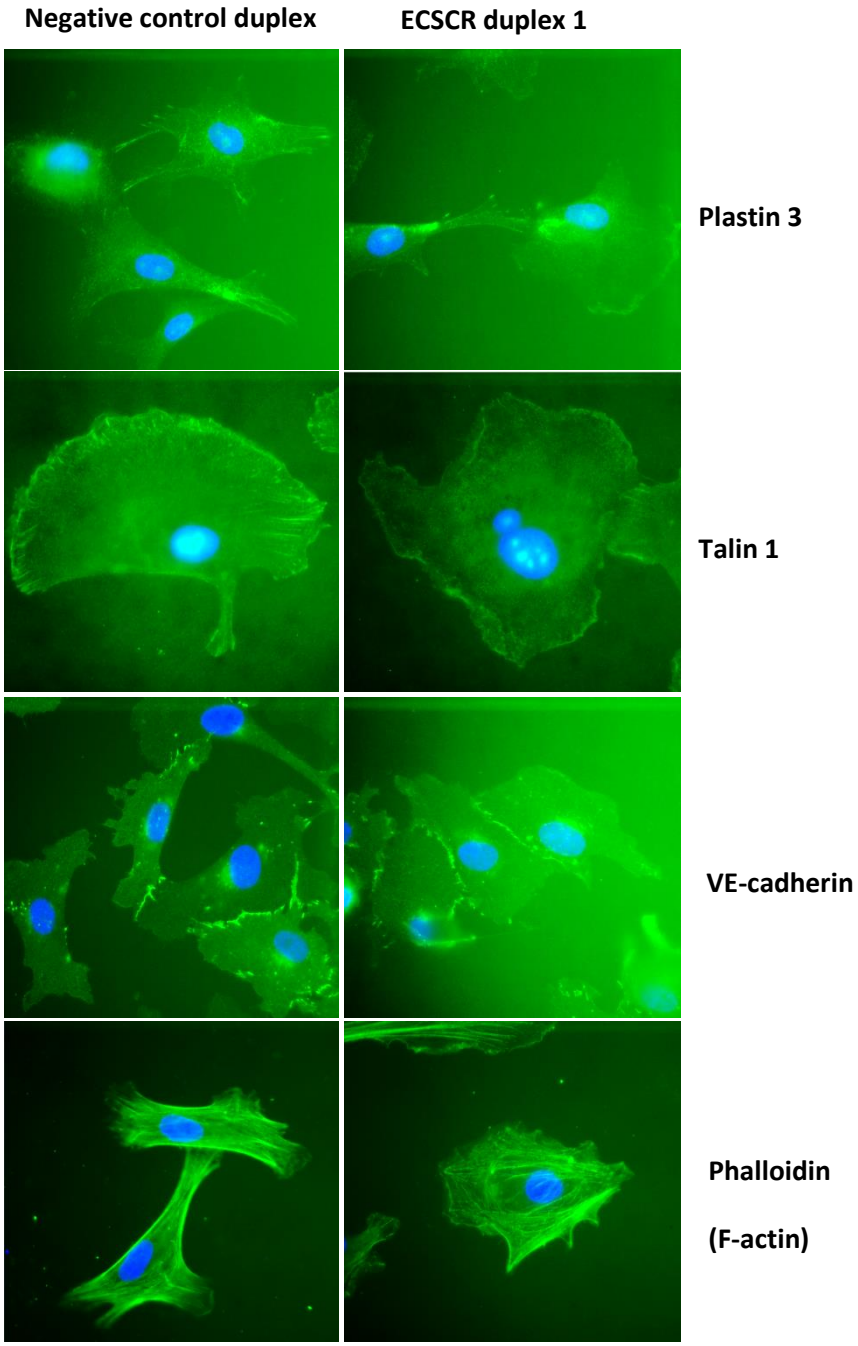

Figure 3.6 (part 1) – Immunofluorescent staining of cytoskeletal proteins upon ECSCR siRNA knockdown

siRNA knockdown was performed in HUVECs and cytoskeletal proteins such as plastin 3, talin1, VE-cadherin and F-actin (phalloidin) were visualised using immunofluorescence (green). DAPI was used to stain the nuclei (blue). Plastin 3 locates to cell protrusions and seems to be less evident in cells where ECSCR is depleted. Talin 1 locates near the cell edges in adhesion points, which seem to be lost when ECSCR is absent. VE-cadherin locates to cell-cell junctions and ECSCR knockdown does not seem to have an effect on this protein. When ECSCR is knocked down, stress fibres seem to be less organised (F-actin).

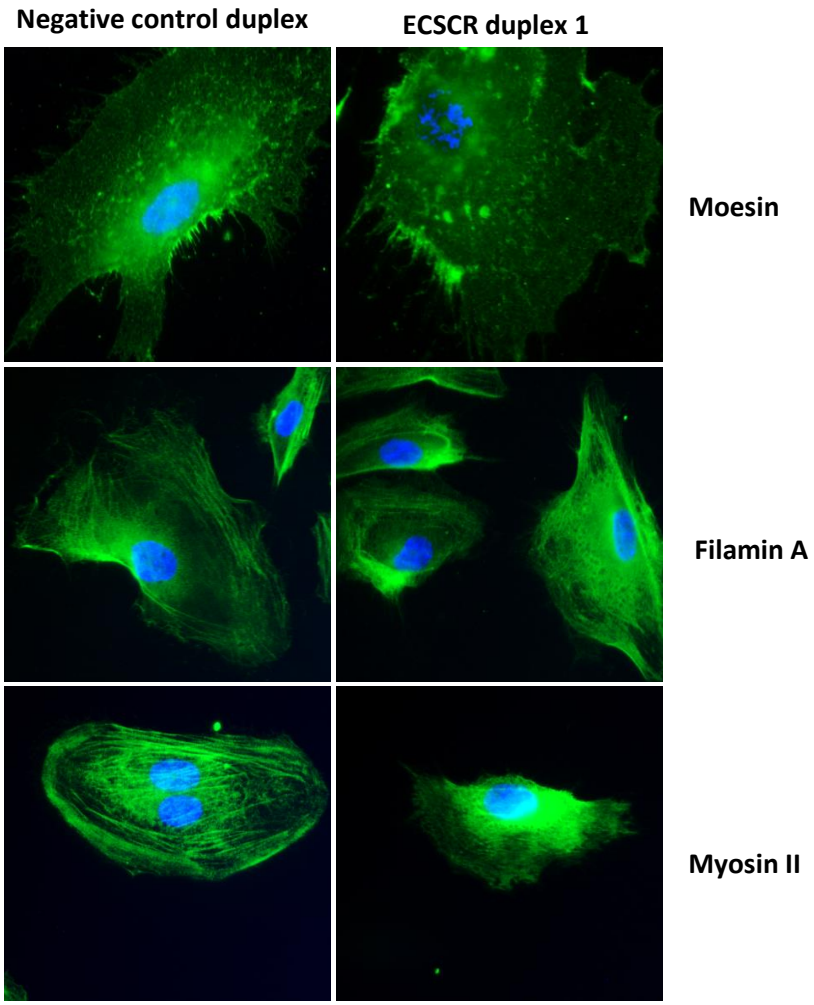

Figure 3.6 (part 2) – Immunofluorescent staining of cytoskeletal proteins upon ECSCR siRNA knockdown

siRNA knockdown was performed in HUVECs and cytoskeletal proteins such as moesin, filamin A and myosin II were visualised using immunofluorescence (green). DAPI was used to stain the nuclei (blue). Moesin is located at cell protrusions and seems to have a more diffused distribution when ECSCR is knocked down. Both filamin A and myosin II are organised in fibre-like structures along the cells, which seem disorganised in the absence of ECSCR.

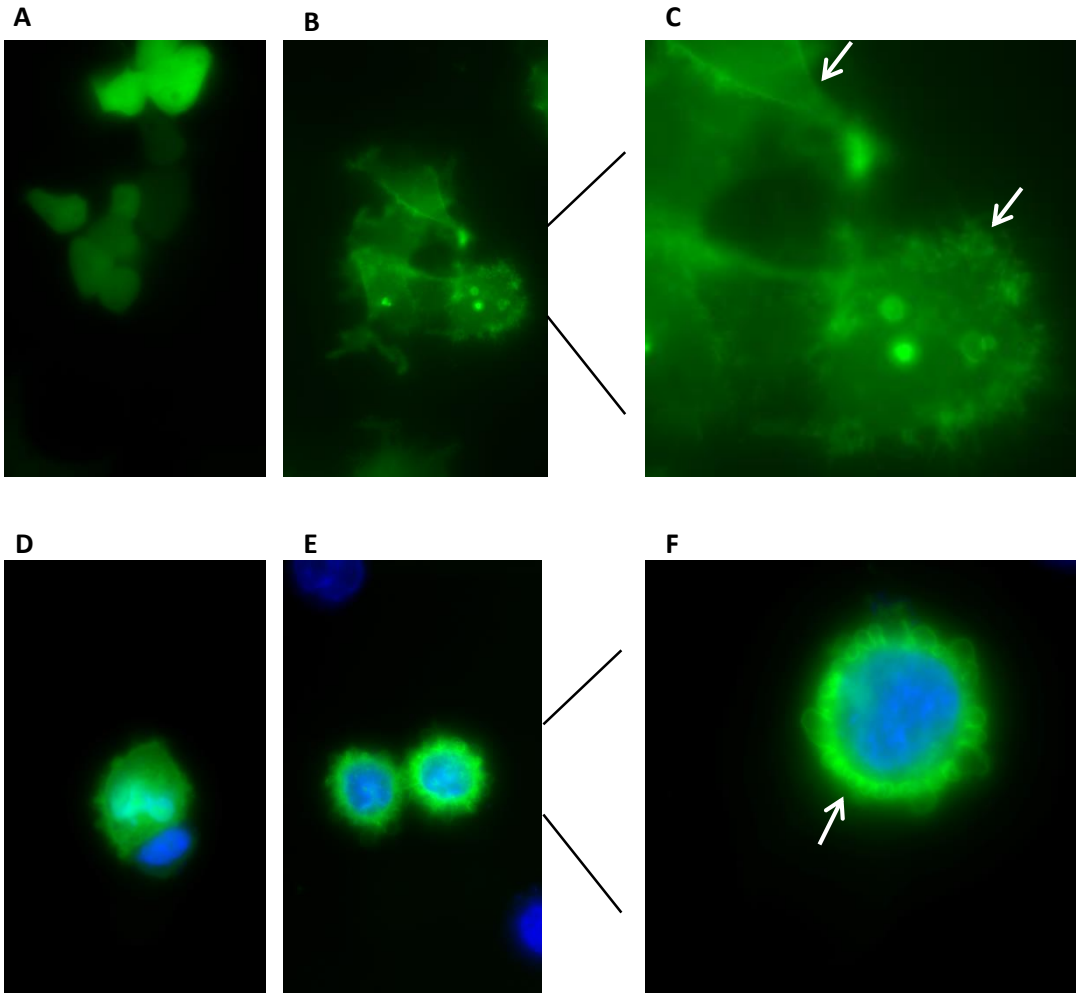

Figure 3.7 – ECSCR overexpression in HEK 293T and M2 cells

ECSCR-GFP was transfected into HEK 293T and M2 cells (B, C, E, F). GFP was used as a control (A, D). C and F are magnifications of B and E, respectively. The white arrows point at the location of ECSCR. ECSCR is able to induce filopodia in HEK 293T cells, but not in M2 cells. The experiment was repeated 3 times with similar results for HEK 293T cells and once for M2 cells. Total magnification: 400x.

3.4 siRNA duplex titration and transfection stability assessment

In order to study the role of ECSCR, siRNA-mediated knock down can be performed to evaluate the loss of function of this molecule in various assays.

The siRNA duplex 1 (D1) had already been used by Armstrong *et al.* (2008), at a concentration of 50 nM, but no titration had been done to assess the minimum concentration that could be used. For that purpose, HUVECs were transfected with 1, 10, 30 and 50 nM of D1 (mock transfection was used as a control) and the ECSCR mRNA and protein were quantified by qPCR and western blot, respectively (figures 3.8 and 3.9). ECSCR has a molecular weight of 55 kDa. From the two figures it is possible to verify that all the concentrations of D1 tested had a significant effect on knocking down ECSCR.

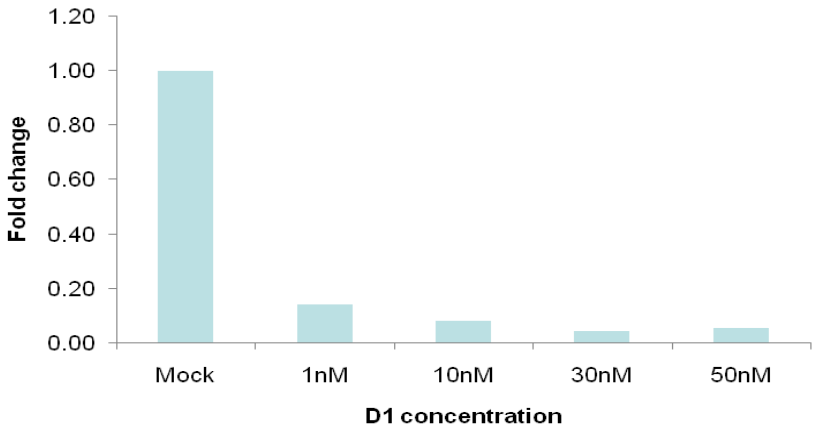

Figure 3.8 - Relative ECSCR expression of siRNA transfected HUVECs assessed by qPCR.

In order to assess the minimum concentration of siRNA duplex (D1) that could be used to knock ECSCR down, HUVECs were treated with 1, 10, 30 and 50 nM of D1. Mock-treated cells were used as a control. RNA was collected, converted to cDNA and amplified by qPCR. ECSCR expression was normalised to that of actin for each sample and ECSCR relative expression in the treated cells is presented relative to that of the mock control. The experiment was done 3 times and qPCR for each sample was performed in triplicate. All concentrations tested were able to produce an ECSCR knock down. A two-tailed unpaired t-test was performed between each treated sample and the control and all p-values were <0.005.

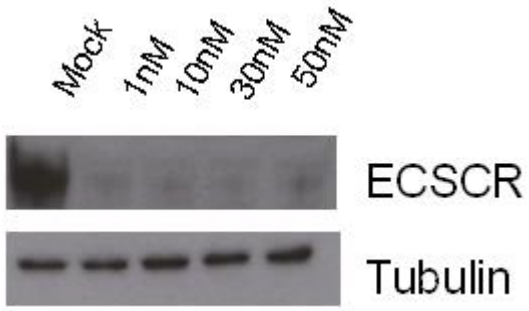

Figure 3.9 - Relative ECSCR expression of siRNA tranfected HUVECs assessed by western blot

In order to assess the minimum concentration of siRNA duplex (D1) that could be used to knock ECSCR down, HUVECs were treated with 1, 10, 30 and 50 nM of D1. Mock-treated cells were used as a control. Total protein was collected, ran on a 12% acrylamide gel, transferred onto a PVDF membrane and blotted for ECSCR and tubulin, as a control. The experiment was done 3 times. As for the mRNA levels, all D1 concentrations have successfully knocked down the ECSCR protein.

3.5 Microarray

In addition to finding molecules that interact directly with ECSCR, in order to have an insight on its role on endothelial cell biology, a microarray was performed using cells transfected with ECSCR siRNA and cells transfected with an unspecific duplex. The RNA quality was analysed using Bioanalyser (Agilent Technologies) and all the samples had a RIN (RNA Integrity Number) above 9.4. The maximum value on this scale is 10 and the closer to this number the RIN of a sample is the better. Samples with RIN values below 6 or 7 should not be considered. After labelling, the specific activity was above 13 in all samples. This value should be between 10 and 14.

The slides were scanned and the data were extracted. The microarray data were analysed using two different programs: SAM (statistical analysis of microarrays) contained within the MeV (multiexperiment viewer) from Tigr (the institute for genomics research) and R, a free statistical program from Bioconductor. The lists of up and downregulated genes obtained from both programs were very similar, and the one produced by R had the advantage of containing information about the fold change. All the genes considered had a fold change equal to or greater than 2. 342 genes were found to be upregulated and 354 downregulated. The most upregulated gene was CCL20 (a chemokine involved in attracting lymphocytes and dendritic cells towards endothelial cells) and the most downregulated gene was CYP26B1 (a member of the cytochrome P450 family of metabolism enzymes, responsible for inactivating all-trans retinoic acid to hydroxylated forms). The full lists of up and downregulated genes can be found on appendix 1.

From these lists, 15 random genes (8 upregulated and 7 downregulated) were chosen to validate the microarray by qPCR. The six original samples (RNA from three controls and three ECSCR knocked down HUVECs) plus six new ones (also RNA from D1 and negative control duplex-

treated HUVECs) were analysed by qPCR (in triplicate). Gene expression was normalised to that of actin for each sample and a fold change between the samples treated with ECSCR-targeting duplex and negative control duplex was calculated using the delta delta CT method (Livak and Schmittgen, 2001). Although the fold change value is different from that obtained from the microarray analysis, all genes show the same trend as they do in the microarray results (figure 3.10). CD 36 was not detected in any samples by qPCR.

The two lists of genes were analysed separately in a program that creates clusters of genes according to their common structural features or role in a certain pathway or process. This program is called DAVID (Database for Annotation, Visualization and Integrated Discovery) (Dennis *et al*., 2003). 123 upregulated and 90 downregulated clusters were identified. Most of the genes, both up- and downregulated, fell into the categories of adhesion molecules, glycoproteins, cytoskeleton-related, chemotaxis and apoptosis (figure 3.11). Figure 3.11 does not show the category "glycoproteins" because this is a structural feature common to many unrelated proteins, rather than a more specific grouping according to function.

Within each general cluster several others could be found. For example, upregulated genes involved in adhesion are specifically involved in cell-cell adhesion, whereas downregulated gens in this category are involved in both cell-cell adhesion and cadherin-mediated adhesion (figure 3.11). Upregulated cytoskeletal genes are involved in actin processes and cell projection, whereas downregulated genes interact with actin mostly via a kelch domain (β-propeller tertiary structure) or are associated with microtubules. Regarding chemotaxis, the absence of ECSCR seems to increase inflammation and decrease locomotive behaviour. Negative regulators of apoptosis are upregulated, whereas positive modulators of apoptosis seem to be both up and downregulated, in cells treated with ECSCR-targeting siRNA duplex compared to cells expressing normal levels of this protein.

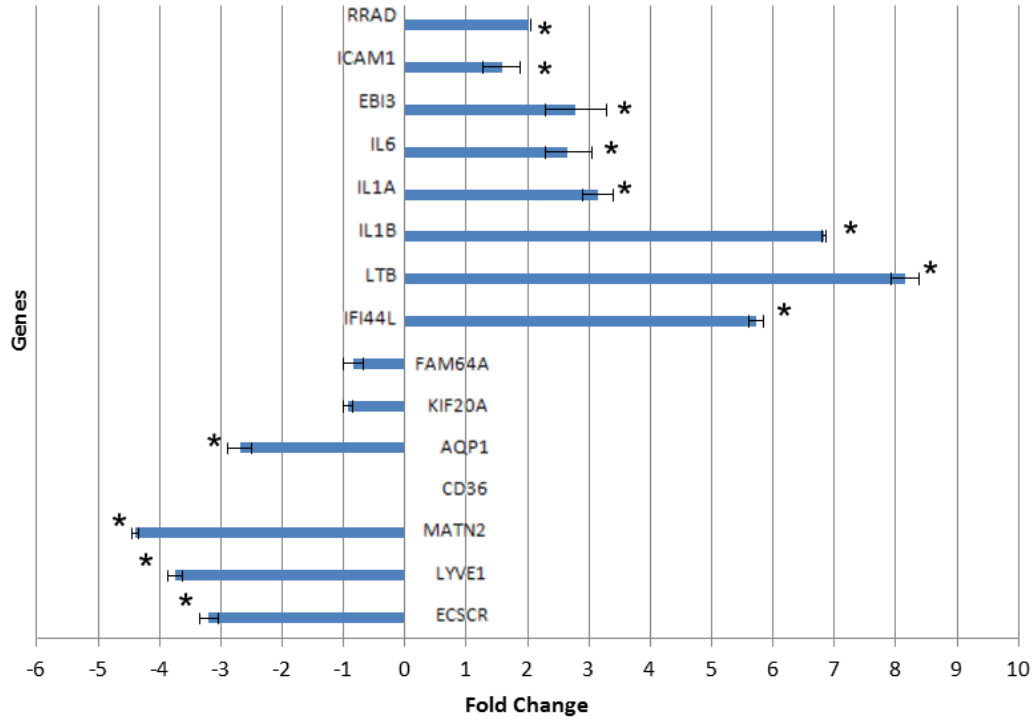

Figure 3.10 – Gene expression validation by qPCR of 15 random genes differentially expressed in the microarray

To validate the results obtained from the microarray analysis, the same 3 samples and 3 new ones of RNA from HUVECs treated with ECSCR-targeting siRNA duplex or a negative control duplex were analysed by qPCR. Fold change between gene expression in controls and ECSCR knocked down cells was calculated using the delta delta CT method. The results largely validate the microarray, as all show the same trend. CD36 was not detected in any sample. The error bars represent the standard deviation from the mean. A two-tailed unpaired t-test was performed to assess significant differences between gene expression of HUVECs treated with D1 and negative control duplex. * - $p < 0.05$ two tailed unpaired t-test.

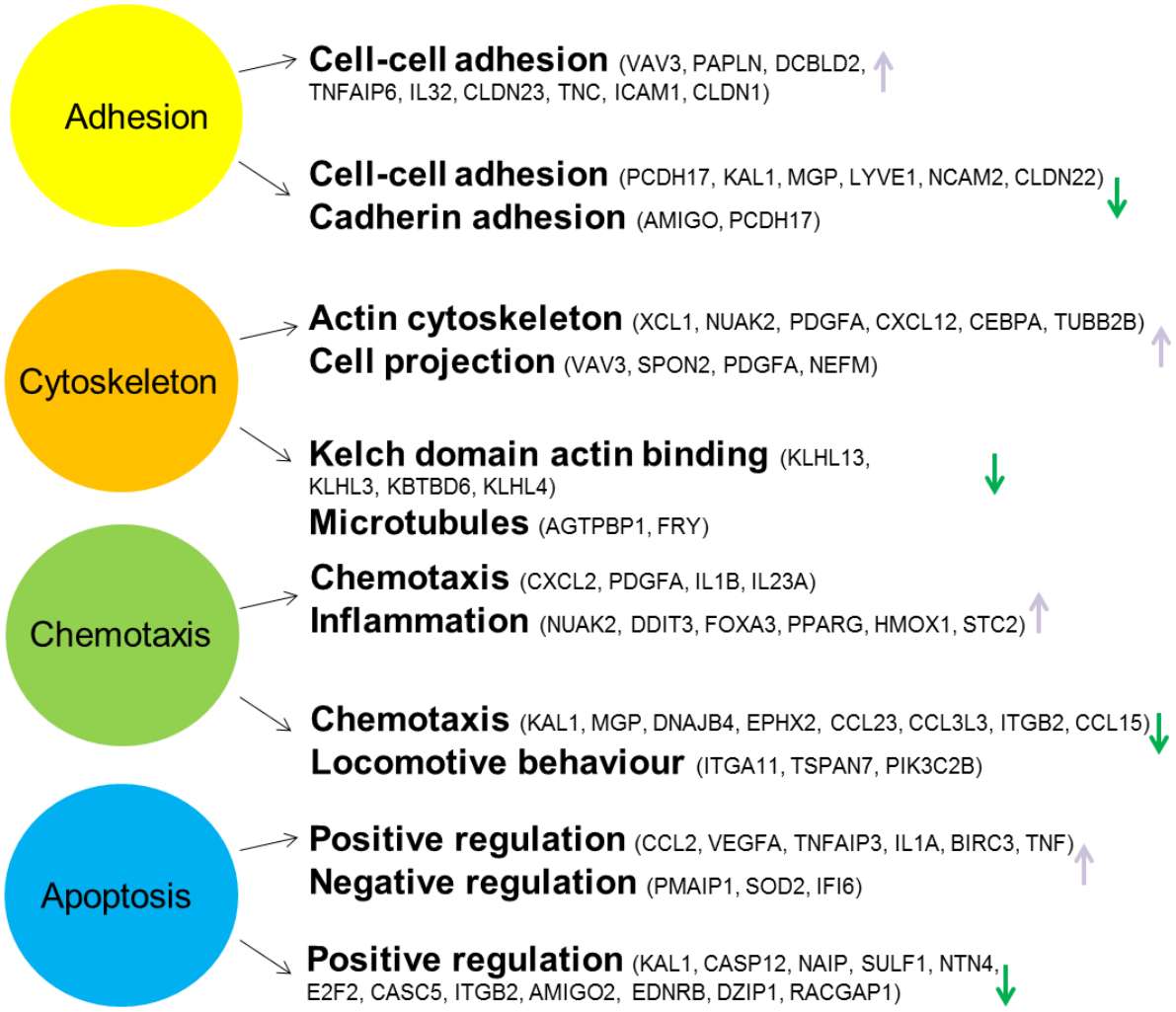

Figure 3.11 – Main functional clusters of up and downregulated genes when ECSCR is knocked down

The lists of up- and downregulated genes found using R were submitted to DAVID so that genes could be grouped by function. The main clusters were adhesion, cytoskeleton, chemotaxis and apoptosis. Purple arrows pointing up refer to clusters containing upregulated genes; green arrows pointing down refer to clusters containing downregulated genes. Examples of genes contained in each cluster were included in brackets.

To have an idea of what pathways may be altered when ECSCR is depleted, the results from R (gene accession number, log ratio, fold change and p-value) were also analysed on the Ingenuity Pathway Analysis program (Quiagen). A cut off of 2 fold (either up or downregulated) and $p < 0.01$ were selected. This software clusters genes according to how they relate to each other in specific interaction networks. Figure 3.12 illustrates the initial outputs once the data are analysed. The different pathways are represented by blue bars, identified on the x axis and are ordered by the proportion of genes in a certain pathway that were contained in the supplied results list (from R) compared to the total number of genes in that pathway (figure 3.12 A). The whole data sets can be viewed in different formats, such as a network connecting the different pathways (figure 3.12B).

By clicking on each blue bar, the up and donwregulated genes from the list obtained from R that are on a specific pathway can be seen. Furthermore, the pathway itself can also be visualised. Figures 3.13 and 3.14 illustrate two of those pathways: granulocyte adhesion and diapedesis and atherosclerosis. Genes represented in grey are part of the pathway, but were not on the list of significantly differentially expressed genes between HEVECs treated with negative control duplex and ECSCR-targeting siRNA duplex. Green represents downregulation and red represents upregulation. Stronger or weaker shades of these colours represent higher or lower fold change, respectively.

Although very informative, the actual interpretation of the pathways provided is difficult, as some molecules in the same pathway are downregulated and others that are affected by those are upregulated. Also, many of the molecules are expressed (or more described) in other cell types. However, only HUVECs were used for this experiment, so not much can be concluded about other cells.

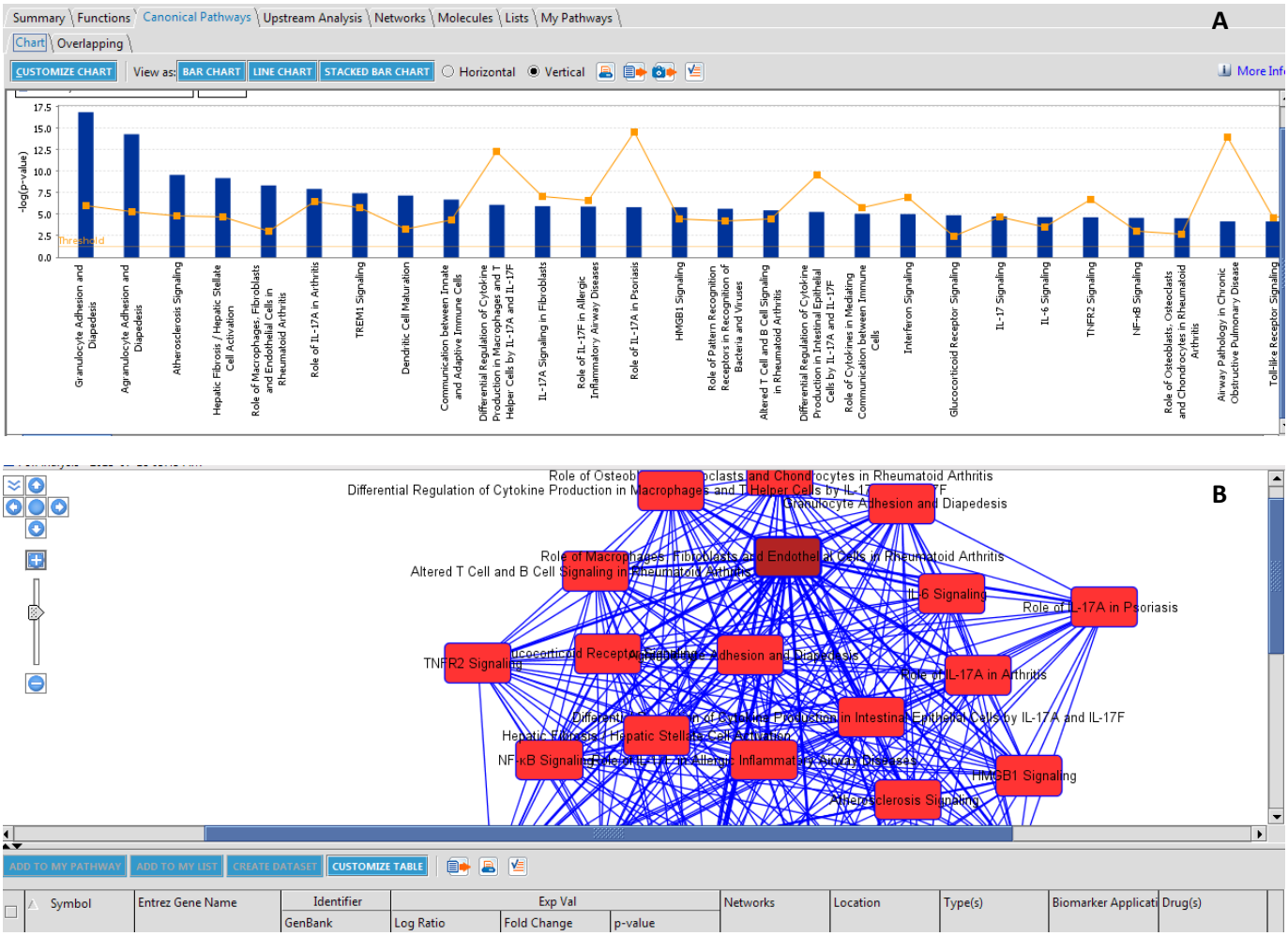

Figure 3.12 – Examples of Ingenuity Pathway Analysis initial outputs

The lists of up and downregulated genes found using R were submitted to Ingenuity Pathway Analysis to look for altered pathways when ECSCR is depleted. The initial outputs once the data are analysed are illustrated. The different pathways are represented by blue bars, identified on the x axis and are ordered by the proportion of genes in a certain pathway that were contained in the supplied results list compared to the total number of genes in that pathway (A). The whole data sets can be viewed in different formats, such as a network connecting the different pathways (B).

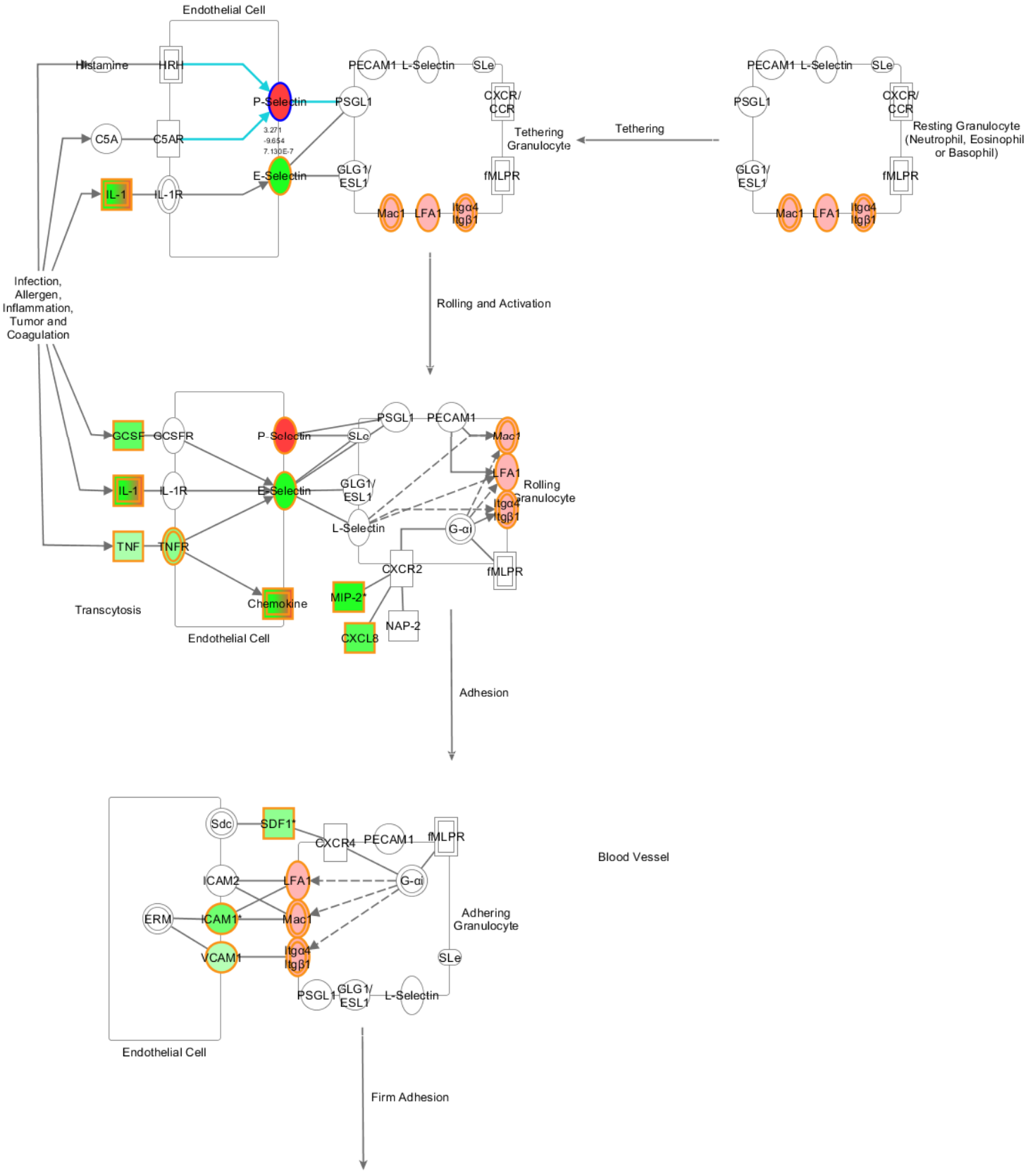
Endothelial Cell
Histamine
HRH
P-Selectin
PSGL1
PECAM1
L-Selectin
SLe
CXCR/
CCR
C5A
C5AR
3.27E-1
-9.65E-4
7.13E-7
E-Selectin
GLG1/
ESL1
fMLPR
IL-1
IL-1R
Mac1
LFA1
Itgα4
Itgβ1
Tethering
Tethering
Granulocyte
Resting Granulocyte
(Neutrophil, Eosinophil
or Basophil)
Infection,
Allergen,
Inflammation,
Tumor and
Coagulation
Rolling and Activation
GCSF
GCSFR
TNF
TNFR
L-Selectin
G-αi
CXCR2
Rolling
Granulocyte
Transcytosis
Chemokine
MIP-2*
CXCL8
NAP-2
Endothelial Cell
Adhesion
Blood Vessel
Sdc
SDF1*
CXCR4
ICAM2
ERM
ICAM1*
VCAM1
Adhering
Granulocyte
Endothelial Cell
Firm Adhesion

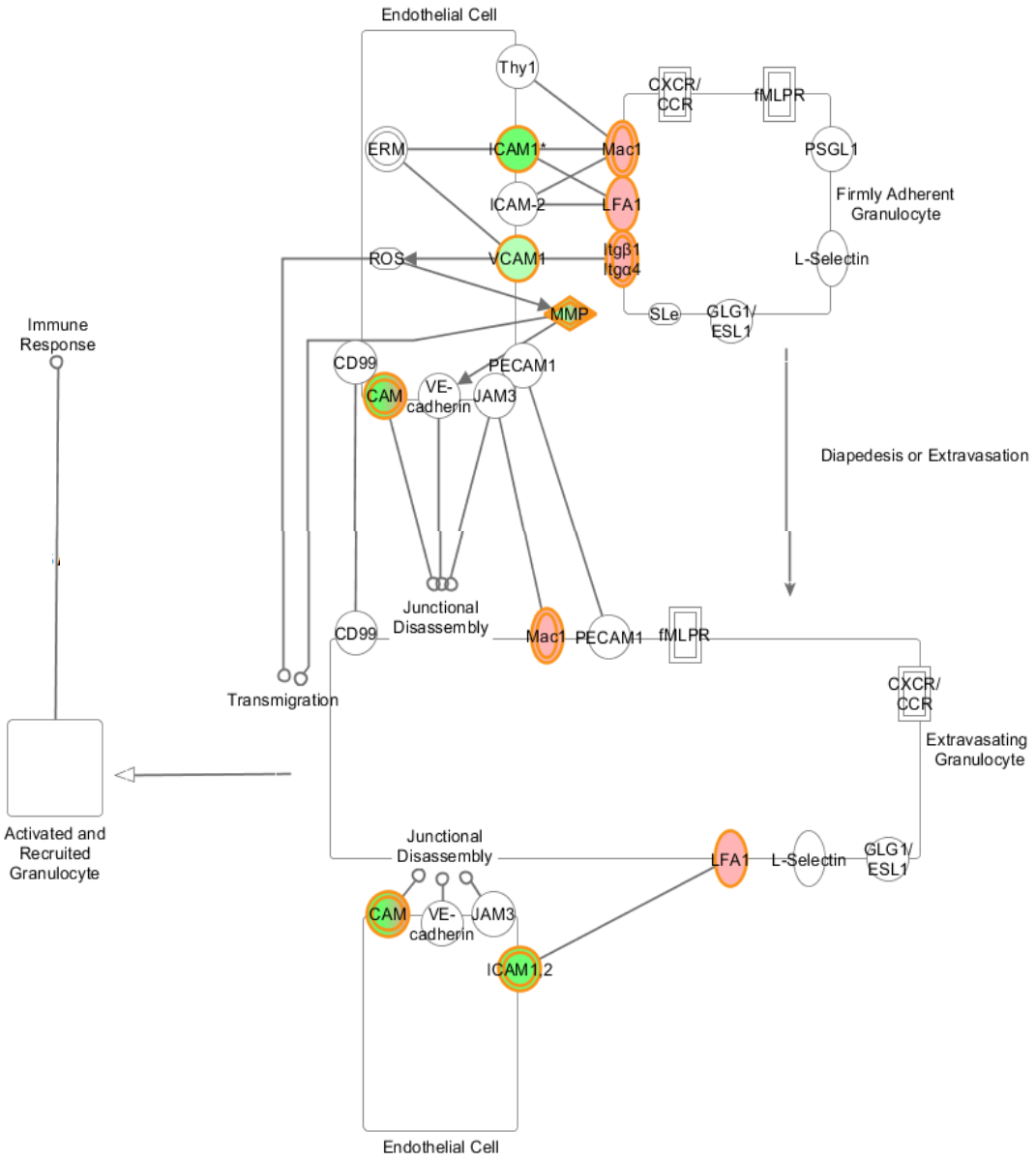

Figure 3.13 – Granulocyte adhesion and diapedesis pathway (this page and previous page)

Granulocyte adhesion and diapedesis was the pathway with the highest proportion of submitted genes compared to the total amount of genes in the pathway. Genes represented in grey are part of the pathway, but were not on the list of significantly differentially expressed genes between HEVECs treated with negative control duplex and ECSCR-targeting siRNA duplex. Green represents downregulation and red represents upregulation. Stronger or weaker shades of these colours represent higher or lower fold change, respectively.

Figure 3.14– Atherosclerosis signalling (next page)

This pathway was chosen as another example because endothelial cells are known to play a role in atherosclerosis and also to illustrate the different information the program can provide. In this figure, not only the pathways are shown, including molecules and different types of cells/compartments, but also a diagram with a series of events that lead to atherosclerosis is provided. Part of the pathway is cut out from the figure, so that it can be legible, as the aim of this image was to show what types of analyses the program can perform. Genes represented in grey are part of the pathway, but were not on the list of significantly differentially expressed genes between HEVECs treated with negative control duplex and ECSCR-targeting siRNA duplex. Green represents downregulation and red represents upregulation. Stronger or weaker shades of these colours represent higher or lower fold change, respectively.

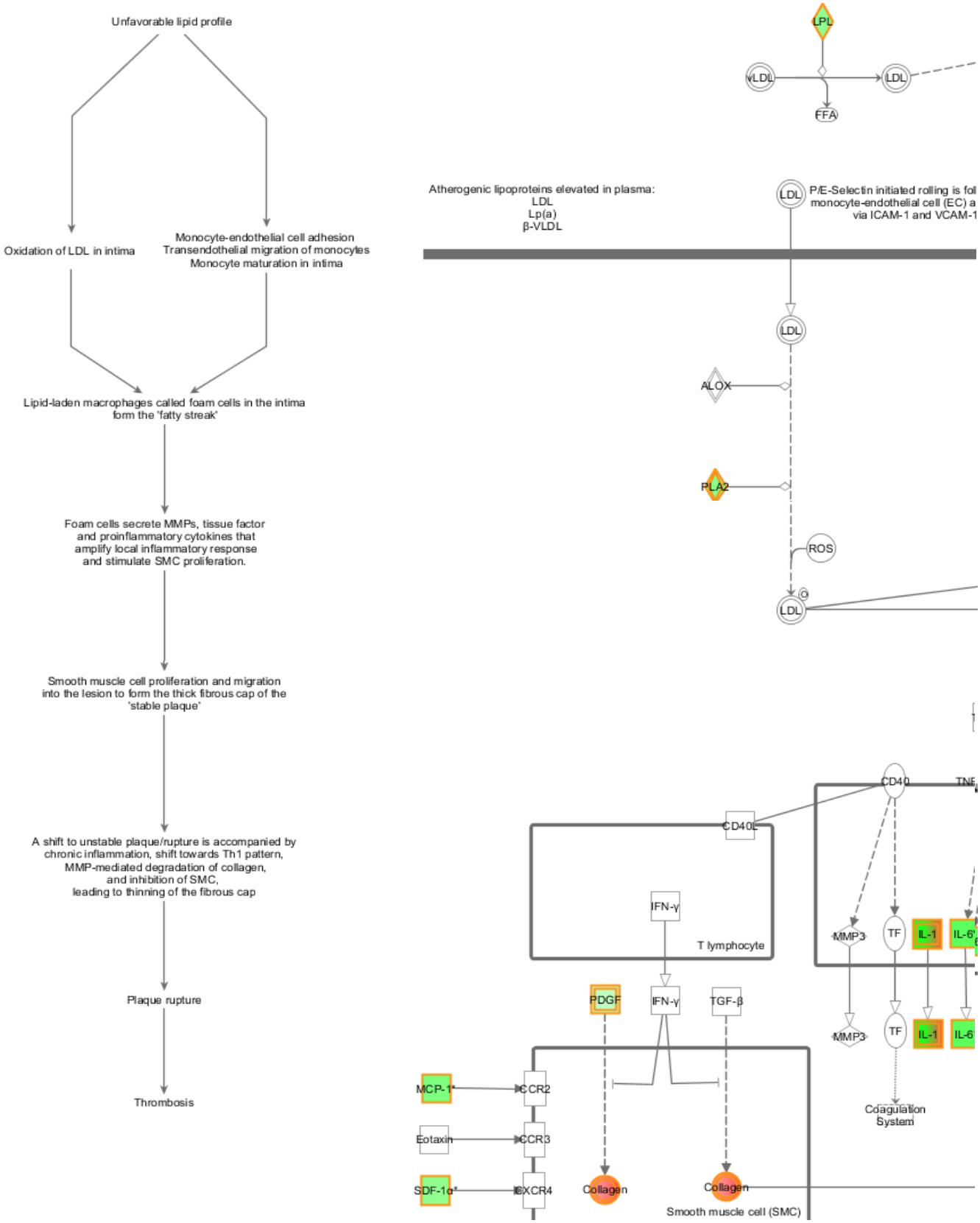
Unfavorable lipid profile
Oxidation of LDL in intima
Monocyte-endothelial cell adhesion
Transendothelial migration of monocytes
Monocyte maturation in intima
Lipid-laden macrophages called foam cells in the intima form the 'fatty streak'
Foam cells secrete MMPs, tissue factor and proinflammatory cytokines that amplify local inflammatory response and stimulate SMC proliferation.
Smooth muscle cell proliferation and migration into the lesion to form the thick fibrous cap of the 'stable plaque'
A shift to unstable plaque/rupture is accompanied by chronic inflammation, shift towards Th1 pattern, MMP-mediated degradation of collagen, and inhibition of SMC, leading to thinning of the fibrous cap
Plaque rupture
Thrombosis
LPL
vLDL
LDL
FFA
Atherogenic lipoproteins elevated in plasma:
LDL
Lp(a)
β-VLDL
LDL
P/E-Selectin initiated rolling is foll
monocyte-endothelial cell (EC) a
via ICAM-1 and VCAM-1
LDL
ALOX
PLA2
ROS
LDL
CD40
TNF
CD40L
IFN-γ
T lymphocyte
MMP3
TF
IL-1
IL-6
PDGF
IFN-γ
TGF-β
MMP3
TF
IL-1
IL-6
MCP-1*
CCR2
Eotaxin
CCR3
SDF-1α*
CXCR4
Collagen
Collagen
Coagulation System
Smooth muscle cell (SMC)

Additionally to this work, a monoclonal antibody produced against ECSCR by Phusion Antibodies (Belfast) was used to detect ECSCR in normal and cancer human tissues and in angiogenesis assays. The results are presented as appendix 2, as only in the end it was discovered that the antibody does not recognise ECSCR after all and this work cannot be published. However, it represented many months of work towards this thesis. The antibody has blocks endothelial cell migration on a scratch wound assay and tube formation on matrigel. *In situ* hybridization on human paraffin-embedded normal and cancer specimens done by Bicknell and Nagy (University of Birmingham, UK) seemed to show that ECSCR was upregulated in some cancers. Based on this, the antibody was used to stain tissue arrays containing human normal and cancer samples. This antibody recognises the naked protein, but not endogenous endothelial glycosylated ECSCR on a western blot. The final proof was provided by FACS analysis, where the antibody induced a shift in the population compared to that not treated with antibody, but there was no difference between HUVECS expressing ECSCR and not expressing ECSCR (knocked down by siRNA). In conclusion, this antibody recognises endothelium specifically and has biological effects on angiogenesis assays. However, its target is unknown.

3.6 Discussion

3.6.1 Finding binding partners for ECSCR

Previously to the present study, Laura Armstrong (2005), a PhD student in the same laboratory, had isolated, cloned and characterised full length ECSCR cDNA, as the only available sequence at the time was derived from alignment of EST sequences. Then, she verified the endothelial specificity by detecting the transcript in several cell lines by qPCR, as well as human tissue paraffin sections, by *in situ* hybridization. A range of endothelial cell stimuli were tested, alone or in combination, to identify which ones regulated ECSCR expression. Hypoxia (0.1% oxygen), oxidative stress (1 mM H_2O_2), confluence (250,000 cells seeded on each plate and harvested at different times), VEGF (10 ng/ml), FGF (10 ng/ml), VEGF + FGF (10 ng/ml each), IFN-gamma (100 units/ml), TNF-alpha (100 ng/ml), IFN-gamma + TNF-alpha (100 units/ml and100 ng/ml, respectively) and IL1-beta (10 ng/ml). The conditions were tested at 4, 8, 16 and 24h. None has had a significant effect on ECSCR expression. Much effort was also dedicated to producing an antibody that would recognise ECSCR, which was largely unsuccessful. Filamin A was identified as a binding partner for the intracellular domain of ECSCR using yeast-two-hybrid on an endothelial cell library.

Ikeda *et al.* (2009) reported that cIAP-1 and cIAP-2 also interacted with this domain. So far, no other interacting molecules for the intracellular domain have been described and no attempt made to find interacting partners or even a ligand for the extracellular domain. That is a crucial step to understand the mechanism by which ECSCR signals.

Protein co-immunoprecipitation using a polyclonal antibody against ECSCR and subsequent analysis of the samples by mass spectrometry (MS) showed that ECSCR potentially interacted with proteins involved in cytoskeletal processes (actin bundling and anchorage of cytoskeletal proteins to the plasma membrane), trafficking (endosomes), protein folding, apoptosis

(ubiquitin and ubiquitin-related proteins) and metabolism (glycolytic proteins) (figure 3.1). The protein with most specific hits in the co-immunoprecipitation with ECSCR *versus* IgG control was Filamin A, which is in line with the work by Armstrong *et al*. (2008). Curiously, filamin A is ubiquitous whereas filamin B expression is more restricted to endothelial cells. Filamin B, but not filamin A knockdown by siRNA has impaired VEGF-induced cell migration of HUVECs through the increase of the number of focal adhesions. This seemed to be achieved by changes in activity and location of Rac-1, a small GTP-binding protein, with consequences on downstream signalling. This indicated a possible pathway involving filamin B, Rac-1 and Vav-2 (an activating guanine nucleotide exchange factor for Cdc42/Rac-activated kinase kinase (PAK)-4/5/6) (Valle-Perez *et al*., 2010). The fact that filamin B is somehow more specific to endothelium than filamin A and this isoform but not filamin A is involved in VEGF-induced cell migration, indicates they have different roles and participate in distinct signalling pathways. This is reinforced by the current data, where filamin A strongly associates with ECSCR and, although very structurally similar, no filamin B was co-immunoprecipitated.

The co-immunoprecipitation results were subsequently confirmed by GST-pull down, where moesin, filamin A and plastin 3 were pulled specifically with ECSCR, whereas talin-1, vinculin and myosin II were not (figure 3.2). The GST pull down is considered to be a more stringent method than immunoprecipitation. The latter can yield entire complexes of proteins that bind to the target of the antibody, whereas the former relies on more specific affinity, as the fusion protein is competing with the endogenous one for potential interacting partners. This explains why there were more proteins associated with ECSCR using co-immunoprecipitation compared to GST-pull down. These two techniques are complementary, as immunoprecipitation can give a broader insight into signalling complexes, as it is able to capture them to the beads, conserving true endogenous interactions. GST-pull down is then a

refinement, capturing proteins that interact with ECSCR more directly. By combining these two techniques it is possible to start building networks, where Filamin A, moesin and plastin 3 are more directly associated with ECSCR (not necessarily in the same pathway) and other molecules, such as talin-1 or myosin II may still be part of the same pathways, but are separated by several other proteins.

The current study differs from that performed by Armstrong (2005) in the number of candidate interactors found. This is because distinct methods were applied. In this study, co-immunoprecipitation was followed by GST-pull down and yeast-two-hybrid, which first give a general view of what proteins may be involved (directly and indirectly) with ECSCR signalling and then direct interactions can be confirmed to establish the role and position of ECSCR within the network. Laura has used BD matchmaker two hybrid system (Clontech, UK) to look for ECSCR interacting proteins. The 58 amino acids of ECSCR intracellular domain were expressed as bait, in pGBKT7 and a placental cDNA library was inserted into pGADT7. Placental polyA$^+$ RNA was used to make cDNA. Colonies that contained several inserts were excluded, as well as unlikely partners for the intracellular domain, such as secreted proteins. Colonies containing only one insert were selected to re-confirm interactions that were consistently reproducible and most expressed filamin A. PIAS1 (protein inhibitor of activated STAT1), a nuclear protein, was also identified. There is a possibility that ECSCR is cleaved and translocated into the nucleus in a similar manner to Notch, a membrane-bound transcription factor (Kopan, 2002) or PIAS1 can translocate into the cytoplasm. However, this protein was not further analysed. In the present study this protein was not found in ECSCR immunoprecipitation. Although a library holds potential to find interactors for Ecscr, Laura has encountered various technical difficulties related to several constructs being present in the same colony, false positives and low reproducibility. As discussed below, yeast may not be able to

express some human proteins at all or with the correct post-translation modifications that are essential for signalling or binding. Also, it is a more artificial system than using actual endothelial cells and trying to capture endogenous interactions using an antibody. The latter method captures endothelial molecules produced in endothelial cells, bound to each other in a way that is closest to what may be physiological than any other method using yeast or non-endothelial cells.

ECSCR shows no structure homology to any known protein. However, its intracellular domain contains a cluster of basic amino acids, that was shown to be critical for the binding of other proteins to moesin (Martin-Villar *et al*., 2010). In the light of these findings and given that ECSCR selectively pulled down moesin, this protein was chosen to proceed to more specifically test a possible direct interaction. As yeast-two-hybrid failed to answer this question (the yeast did not express moesin), a luciferase complementation assay was performed (figures 3.3 and 3.5). The two methods are similar in the sense that the two candidates for interaction are each fused to one half of a reporter protein that is only expressed if an interaction occurs. However, yeast-two-hybrid uses yeast, whereas the luciferase complementation assay uses mammalian cells. Yeast are not able to reproduce many post-translational modifications present in mammalian cells, which may be important for interactions (Luo *et al*., 1997). Also, due to toxicity or other species incompatibilities, yeast may not be able to produce the protein of interest at all, which was the case for moesin. The luciferase complementation assay has successfully demonstrated an interaction between ECSCR intracellular domain and moesin. However, minimal significance ($p < 0.05$) was only obtained after 5 replicates. Negative controls were included where either moesin or ECSCR were co-expressed with a zipper protein fused to the complementary luciferase half for each case. No interaction between the zipper protein and moesin or ECSCR was expected to happen. However, the luminescence values for

these controls, although lower than those for the specific interaction between moesin and ECSCR, were quite high. HEK 293T cells are a popular cell line to use for protein expression, as they can produce most post-translational mammalian modifications and yield high amounts of protein expression (Thomas and Smart, 2005). In the case of the luciferase complementation assay, however, this may not be an advantage. Too much protein being overexpressed may mean that non-specific interactions start to occur due to excessive amounts of protein, rather than real interactions. To obtain cleaner results, perhaps HeLa cells could be used instead of HEK 293T.

The interaction between ECSCR and filamin A found by Armstrong (2005) was also confirmed in this study using yeast-two-hybrid (figure 3.3). The two regions from filamin A (repeats 15-16 and 19-21) have been shown to bind many other proteins (Zhou *et al*., 2009). These are involved in a variety of functions, from intracellular signalling to cell cycle, transcription and adhesion. Protein kinase C (PKC) also binds to filamin A, this interaction occurs at the plasma membrane and is believed to lead to lead to the phosphorylation of filamin A, influencing its interaction with cell surface molecules. As for ECSCR, PKC was shown to bind to filamin A at two separate sites in repeats 1-4 and 22-24 (Tigges *et al*., 2003). ECSCR localises to the plasma membrane and filamin A is known to interact with several other membrane bound proteins, many of which are involved in cell adhesion and coagulation pathways. For example, filamin A can promote and inhibit adhesive functions. When bound to the integrin cytoplasmic domain, it restricts integrin-dependent cell migration by inhibiting transient membrane protrusion and cell polarisation (Calderwood *et al*., 2001). The multitude of filamin A interactors involved in many different pathways may implicate a diverse role for ECSCR, controlling the filamin A availability not only to bind to other molecules but also to be anchored to the membrane, thus modulating these pathways.

3.6.2 The role of ECSCR in modulating the cytoskeleton

To further investigate the role of ECSCR in modulating the cytoskeleton siRNA knockdown was performed and several cytoskeletal proteins found in the co-immunoprecipitation assay were visualised by immunofluorescence (figure 3.6). VE-cadherin, a molecule present in cell-cell adhesion regions was also stained, as Shi *et al*. (2001) have reported that ECSCR also localizes to cell-cell junctions. Although ECSCR promotes cell aggregation *in vitro* (Shi *et al*., 2001) its loss does not seem to be sufficient to affect cell-cell adhesion, as there seems to be no difference between VE-cadherin staining in HUVECs transfected with ECSCR siRNA or negative control duplex.

Additionally, Armstrong (2005) has demonstrated that ECSCR co-localises with F-actin, which also binds filamin A. Co-localisation around the membrane was expected, but clusters of co-localised proteins were also observed at the base of cell protrusions. This suggests that ECSCR has a role in the development of these protrusions through its interaction with filamin A and possible coupling to F-actin, in a migratory or adhesive function. F-actin was stained using phalloidin. Although subtle, there seems to be a difference in stress fibres of cells transfected with ECSCR siRNA compared to those treated with negative control duplex. Loss of Ecscr seems to result in more disorganised fibres, that are more distant from the cell edges. Ma *et al*. (2009) have reported that the transfection of ECSCR-GFP into HEK 293T cells had resulted in the destruction of stress fibres. In accordance to that observation, loss of ECSCR should result in increased stress fibres, however the opposite was observed. This can be due to differences between the two cell types, where different binding partners may be available, thus influencing distinct pathways. Also, ECSCR produced in HEK 293T cells is slightly smaller than the

endothelial one (Armstrong, 2005), which means it may lack important post-translational modifications, such as a specific glycosylation pattern of carbohydrate, which affects its role in stress fibre formation.

As for the other proteins studied, the loss of ECSCR results in a similar phenotype: filamin A and myosin II are present in fibre-like structures, which become destructed and disorganised when ECSCR is lost, in a similar fashion to F-actin. This is consistent with a role for ECSCR in anchoring the cytoskeleton to the membrane. Talin-1 and plastin 3 also seem to be lost at cell-surface adhesions and cell protrusions, respectively. Actin-bundling proteins not only structure the cortical actin cytoskeleton, but also control actin dynamics. Plastin 3 has been shown to decrease F-actin disassembly rate and inhibit cofilin-mediated depolymerisation of actin filaments *in vitro* (Giganti *et al*., 2005). If upon ECSCR loss plastin 3 is dislocated, then its role in keeping actin fibres assembled may be impaired. Moesin, rather than lost, seems to be more distant from the membrane and to have a more diffused distribution, compared to the very well-defined spike-like structures observed in HUVECs treated with negative control duplex. The staining protocol for this antibody could still be further optimised, as it has produced a clearer staining when used by Martin-Villar *et al*. (2010). ERM proteins, such as moesin, link membrane proteins to the underlying cortical cytoskeleton and control the distribution of and signalling from membrane receptors (McClatchey and Fehon, 2009). Since many proteins work cooperatively, loss of ECSCR may affect their distribution, regardless of interacting directly or indirectly with them. Additionally, ECSCR may have specific roles in adhesion, protrusion or migration that are only revealed in a particular context. Armstrong *et al*. (2008) have shown that lack of ECSCR results in slower migration through a membrane pore. Myosin II has been demonstrated to have a very specific role in contraction only during passage through narrow gaps, where squeezing contraction of the trailing edge propels the rigid

nucleus (Lämmermann *et al*., 2008). To further investigate the interaction of ECSCR with these proteins (or its influence in a signalling pathway where they are important), context-specific assays could be performed, such as the Boyden chamber assay to assess migration through a pore rather than migration on a flat surface, where myosin II has no role.

To further elucidate any role for ECSCR, the opposite experiment was performed, where ECSCR-GFP was overexpressed. The M2 cell line is deficient in filamin A and the cells display defects in membrane stability and migration. When filamin A is re-introduced, these functions are restored (Cunningham *et al.*, 1992). Other studies in these cells have also revealed that filamin A is essential for the maintenance of protrusions or lamellae which enable the cells to crawl (Flanagan *et al*., 2001). In the current study, M2 cells were transfected with ECSCR. The cells were still unable to form filopodia, whereas in HEK cells (that contain filamin A), ECSCR was able to induce the formation of these structures (figure 3.7). This shows that ECSCR has the ability to induce the formation of filopodia and needs filamin A to do so.

Interestingly, M2 cells contain filamin B, which does not appear to have a redundant function to that of filamin A, as demonstrated by these cells' inability to form cell protrusions (Cunningham *et al.*, 1992). ECSCR seems to require specifically filamin A but not filamin B for tube formation. This is reinforced by the fact that filamin A was specifically co-immunoprecipitated with ECSCR (34 hits for ECSCR versus 5 for the IgG control) and filamin B, although very similar in structure, was not found to be associated to ECSCR.

Consistent with its role in cytoskeleton modulation, ECSCR knockdown resulted in less stress fibres and displacement of cytoskeletal components and its overexpression has induced the formation of filopodia. The overexpression experiments were performed in both cells that express filamin A and cells that do not. It had been reported that M2 cells, due to the lack of

filamin A, were unable to respond to RalA and Cdc42 to form filopodia. The current study shows that ECSCR, which interacts directly with filamin A, is also not able to induce filopodia in the absence of filamin A. The M2 experiments, nevertheless, should be repeated to confirm these results. The cells were a kind gift from Dr. Jo Morris (University of Birmingham, UK). However, they were found to be contaminated with fungus. They were subject to treatment with anti-fungal agents and after two weeks seemed to be contamination-free. There were no apparent morphological changes under bright field microscopy, but when transfected with GFP, even the controls showed very small blebs. ECSCR was still able to locate to the membrane, but it is unclear whether blebs were caused by these cells not being healthy, or due to ECSCR expression (as they were much more evident in ECSCR-containing cells). For many years blebbing has been associated with cell death. However, it also constitutes a mode of locomotion that is actin-free and completely dependent on myosin, as demonstrated by Blaser *et al*. (2008) in zebrafish primordial germ cells *in vivo*.

3.6.3 Microarray to test the effect of ECSCR knockdown

A microarray was performed to assess the effect of ECSCR knockdown in the gene expression of HUVECs. All the genes considered had a fold change equal to or greater than 2. 342 genes were found to be upregulated and 354 downregulated. The most upregulated gene was CCL20 (a chemokine involved in attracting lymphocytes and dendritic cells towards endothelial cells) and the most downregulated gene was CYP26B1 (a member of the cytochrome P450 family of metabolism enzymes, responsible for inactivating all-trans retinoic acid to hydroxylated forms). 15 up and downregulated genes were chosen to confirm the microarray data by qPCR (figure 3.10). They have shown the same trend as the microarray. CD36 was not detected by qPCR. The reason why CD36 was detected in samples from HUVECS by microarray but not

by qPCR may have to do with the sensitivity of each technique. The microarray chip was designed for very low-input samples. HUVECs have been reported as being CD36 negative (McCormick *et al*., 2000), as well as CD36 positive (Sölder *et al*., 2012). The latter authors have also found that HUVECs are negative for LYVE-1, whereas the in the current study the message for this protein was found elevated (and, therefore, present) in HUVECs with low levels of ECSCR, both by microarray and qPCR.

Most of the genes, both up- and downregulated, fell into the categories of adhesion molecules, glycoproteins, cytoskeleton-related, chemotaxis and apoptosis (analysis done using DAVID) (figure 3.11). When possible pathways were analysed using ingenuity pathway analysis, the more apparent role for ECSCR in these functions seemed to be diluted (figures 3.12-3.14). The first method groups proteins by function regardless of a specific pathway, whereas the second one groups them by pathway and the result was not as useful as anticipated in interpreting the effects of ECSCR loss. Also, most of the figures show other types of cells that are not endothelial, as that particular pathway is either specific to them or has been more extensively studied in those cell types.

VEGFA and FGF13, well known angiogenesis stimulators, were found to be upregulated (4.2 and 8.9 fold, respectively). This cell response to the loss of ECSCR appears to make HUVECs more angiogenic. Many chemokynes and their receptors also seemed to be altered, both up and donwregulated. It is known that, for example, CXC chemokines have both anti-and pro-angiogenic effects. Those with an ELR motif promote angiogenesis and those that are inducible by interferons and do not contain the ELR motif inhibit angiogenesis (Belperio *et al*., 2000). Members of both groups were up and downregulated. Microarray results should be interpreted carefully and together with other experimental evidence. It is suggested that more cell based assays are performed, such as Boyden chamber to evaluate any role of ECSCR in myosin II-

mediated contraction and then, based on a specific context, the tables produced from the microarray analysis can be used to suggest what other genes can be measured or visualised.

3.6.4 siRNA duplexes titration and transfection stability assessment

The expression of ECSCR was silenced in HUVECs using a regulatory cellular pathway known as RNA interference (RNAi). In the eukaryotic cell, long dsRNA are cleaved by Dicer, a ribonuclease III–like enzyme, into short RNA duplexes, small interfering RNA (siRNA). Synthetic siRNA can be generated and introduced into cells to knockdown the expression of a particular gene. After entering into cells by lipofection, the siRNA is assembled into an endoribonuclease-containing complex, known as RNA-induced silencing complex (RISC) and unwinds to become single stranded. The siRNA strand incorporated into RISC base pairs to its complementary mRNA sequence, resulting in its cleavage and degradation. This blocks the translation of mRNA into protein thus silencing its expression in the cell (Xia *et al*., 2002).

Cells can sometimes display an innate immune interferon response to double stranded siRNA duplexes used in RNAi technology, because double stranded RNA is sometimes present in virus-infected cells (Anderson *et al*., 2008). Also, siRNA duplexes can trigger off-target effects such that they can knock down unintended mRNAs with high silencing efficacy (Sledz *et al*., 2003). In order to minimize both the interferon response and off-target effects, the lowest concentration of siRNA required to knockdown ECSCR expression was determined. In addition, it had been shown by Armstrong *et al*. (2008) that ECSCR siRNA with D1 does not elicit interferon response (by quantifying the expression of OAS1 and ISG20 by qPCR).

3.6.5 *In silico* analysis of conserved ECSCR putative functional motifs

ECSCR is a unique protein that does not share domain homologies with any known protein when analysed *in silico*. To find those similarities and confirm the functionality of such conserved domains usually constitutes the first step when trying to characterize a novel protein.

Therefore, to have some insights on possible functions or protein interactions, other *in silico* analyses for the ECSCR primary structure have been done, such as the search for conserved predicted functional sites using the human, mouse and zebrafish sequences.

This was done using Eukaryotic Linear Motif (ELM) resource for predicting functional sites in eukaryotic proteins. For the intracellular domain several possible functional sites conserved in all three species were found and could be investigated: PKA (protein kinase A) and CK1 (casein kinase 1) phosphorylation sites and GSK3 (glycogen synthase kinase 3) phosphorylation recognition site, class III PDZ domains binding motif (in the C terminus of the protein) and a sorting and internalisation signal found in the cytoplasmic juxtamembrane region of type I transmembrane proteins (figure 3.15).

The endosomes play key roles in the cell such as sorting and recycling of membranes and cargo and the intracellular delivery of proteins, toxins and viruses by endocytosis. In addition to these classical functions, it has become clear over the last few years that endosomes are also involved in cell signalling (by internalising receptors or facilitating the recruitment and integration of signalling cascades on the surface of endocytic vesicles), cytokinesis, polarity and migration (Gould and Lippincott-Schwartz, 2009). So far, ECSCR-GFP seems to localize to the plasma membrane and filopodia, rather than organelles. However, in the MS analysis of proteins that co-precipitated with ECSCR, some proteins regulating trafficking related to endosomes have been identified.

CK1 is involved in cytoskeleton remodelling by, for example, phosphorylating RhoB and thus impeding actin stress fibre organization and epidermal growth factor receptor (EGF) stabilization (Tillement *et al.*, 2008). In quiescent cells, β-catenin in association with cytoskeletal components (such as E-cadherin), orchestrates actin dynamics and regulates cell

adhesion, cell-cell interactions, and intercellular communication. CK1 phosphorylation of β-catenin primes it for additional phosphorylation by GSK3, which targets it for proteasomal destruction (Kim and Kimmel, 2006). PKA activity regulates integrin activation and actin cytoskeletal organization. In neutrophils asymmetrical PKA activity is necessary and sufficient for actin cytoskeletal polarization and migration during chemotaxis (Jones and Sharief, 2005). Furthermore, PKA is needed for syndecan-2 induced filopodia formation via Enabled (Ena) and vasodilator-stimulated phosphoprotein (VASP) (Lin *et al.*, 2007). There is a conserved cysteine residue in ECSCR located three amino acids upstream from the putative serine to be phosphorylated by PKA (figure 6.1). Palmitoylation of a cysteine near the transmembrane region, either up or downstream from the serine residue seems to be fundamental for PKA phosphorylation modulatory functions (Moffett *et al*., 1996; Tian *et al.*, 2008). The interaction of ECSCR with these kinases (or proteins phosphorylated by GSK3) could be investigated by the use of kinase inhibitors.

PDZ domains recognize specific motifs that occur at the C-termini of target proteins and act as modules for protein-protein interactions. The PDZ motifs are common in the cytoplasmic tails of transmembrane receptors and channels (Niethammer *et al*., 1996), although they can also recognize internal sequences (Xu e*t al*., 1998). By recruiting downstream proteins in a signaling pathway, PDZ domains mediate assembly of specific multi-protein complexes. PDZ domains containing proteins perform functions such as maintaining epithelial cell polarity and morphology (Bredt, 1998), organizing the postsynaptic density in neuronal cells, and regulating the activity and trafficking of membrane proteins (Harris and Lim, 2001). Since the putative class III PDZ domains binding motif is located in the C terminus of ECSCR, being ECSCR a type I transmembrane protein, the existence of this binding motif is possible to be true and could be investigated.

3.6.6 Glycosylation paterns of ECSCR

Glycosylation is one of the most frequent post-translational modifications of proteins. It is well documented that altered glycosylation is a feature of cancer cells and some glycan types can even be used as markers of tumour progression (Dall'Olio, 1996; Varki, 2008). The altered glycosylation profiles of tumour-associated endothelium, however, are not well characterized. Peng *et al*. (2010) have recently found that beta-1,6-GlcNAc branching modification of PECAM-1 leads to cytoskeletal conformational changes that result in cell contraction, which facilitates tumour cell extravasation.

ECSCR is predicted to be heavily glycosylated, due to containing multiple O-glycosylation and one consensus N-glycosylation sites and also because on a western blot it is detected at around 55 kDa and the predicted size is 21.6 kDa (Armstrong *et al.,* 2008). An attempt was made to immunoprecipitate ECSCR and then digest it using different combinations of glycosidases. Changes in size of the protein would be detected both by western blot (proteins) and using a kit containing the Schiff reagent, based on the periodic acid reaction, that recognizes carbohydrates. However, all antibodies are glycosylated and the heavy chain has the same size as ECSCR. The positive control (fetuin) has been successfully deglycosylated, but the analysis of ECSCR was not conclusive. All samples were incubated with five different glycosidases(PNGase F, sialidase, beta-glycosidase, glucosaminidase and O-glycosidase) from the DeGlycoMx kit (QA-Bio). It was not possible to know if the (incompletely digested) band around 50 kDa was ECSCR or the heavy chain of the antibody. As an alternative, a kit containing different lectins that will bind to and allow the identification of specific carbohydrate groups could be used, rather than trying to remove specific carbohydrate groups. Another alternative would be to overexpress ECSCR- GFP in HUVECs using a lentiviral

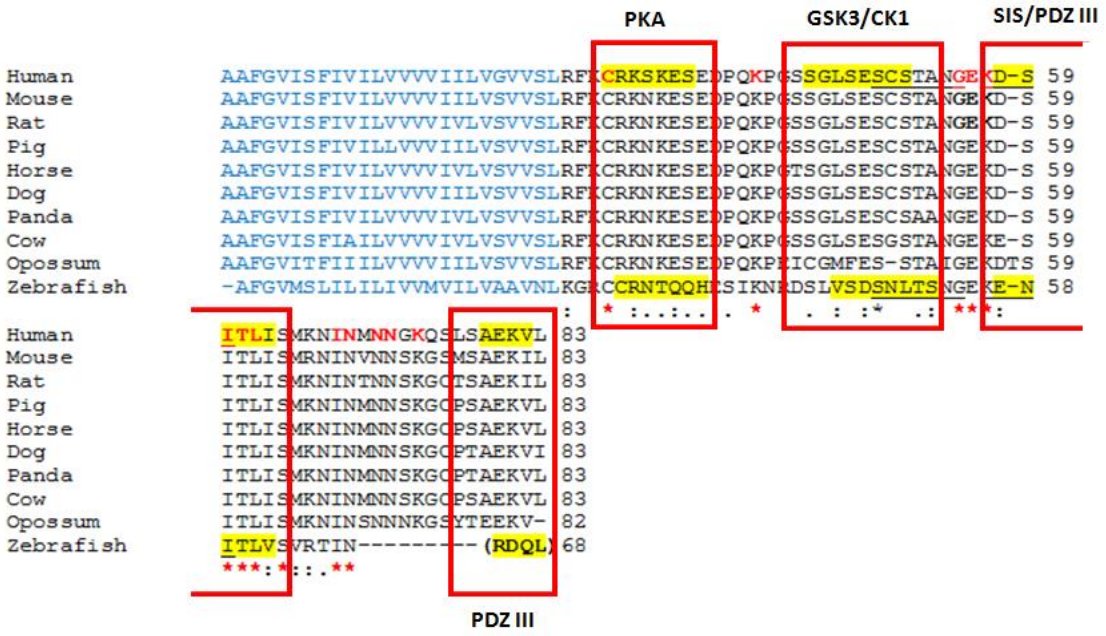

Figure 3.15 –Putative conserved predicted functional sites on ECSCR.

The transmembrane domain is depicted in blue. The predicted functional sites are highlighted in yellow or underlined, when overlapping. The terminal predicted PDZ III domain binding motif for zebrafish was manually added, as it locates to the end of the C-terminus, but this protein is longer and has a part of the sequence that doesn't align with the other orthologs.

system and subsequent immunoprecipitation and deglycosylation. This would remove ECSCR from the 50 kDa range, so that it could be distinguished from the antibody heavy chain. It is important to use HUVEC cells, as glycosylation patters in endothelial cells are very specific. For example, an antibody against the extracellular domain of ECSCR was raised by a company in Belfast (appendix 1). They have used the bacterially expressed naked protein as an immunogen and the antibody was able to recognize ECSCR-GFP overexpressed in HEK 293T cells. However, this protein was not as glycosylated as it would have been in HUVECs, as it runs at a much lower molecular weight on an SDS-PAGE. This was also observed by Shi *et al*., (2011), when an ECSM2-FLAG fusion protein was observed at ~40 kDa, compared to the ~55 kDa from HUVECs)

Shi *et al*., (2011) have immunoprecipitated ECSCR from HUVECs using a monoclonal antibody and treated the purified protein with a glycosidase mix. They were able to produce some lighter bands, but the full length ECSCR did not disappear, which may indicate that ECSCR has a very specific type of carbohydrate or there are other post-translational modifications contributing to its molecular weight.

3.6.7 What regulates ECSCR?

A quick promoter analysis of the region 2000 bp upstream of ECSCR and intron 1 using a program available online, TFSEARCH (http://www.cbrc.jp/research/db/TFSEARCH.html), has found some interesting conserved potential transcription factors. These could be narrowed down to a small number and all seem to be related to haematopoiesis and endothelial cells (table 3.1). In the future it would be interesting to knock some of these transcription factors down (the ones more specific to endothelial cell biology) and assess their effect on the expression of ECSCR and angiogenesis.

Table 3.1 – Conserved transcription factors potentially regulating ECSCR

Transcription factor	Function
SRY (SOX11)	Spermatogenesis, developing nervous system, developmental tissue remodelling (upregulated 4x in the microarray)
Gata-1	Erythroid development
Gata-2	Activator which regulates endothelin-1 gene expression in endothelial cells (EDNRB is 3x downregulated in the microarray)
Gata-3	T-cell development and plays an important role in endothelial cell biology
AML-1a (Runx-1)	Haematopoiesis (runx1T1 2x downregulated in the microarray)
Nkx-2.5	Heart formation and development
c-Ets-1 (ETS1)	stem cell development, cell senescence and death, and tumorigenesis; turns endothelial cells angiogenic by upregulating MMPs and ITGB3 (upregulated 4x in the microarray, 2 probes)
CdxA	Tumour suppressor (migration, proliferation, apoptosis)
Evi-1	Haematopoiesis and vascular patterning
Oct-1 (POU2F1)	Transcription factor for IL8 (POU2F2 is upregulated 5x in the microarray and IL8 19x)
MZF-1	Induces cancer migration and invasion through Axl

4 THE ROLE OF ECSCR IN DEVELOPMENTAL ANGIOGENESIS OF THE ZEBRAFISH (*DANIO RERIO*)

4.1 Introduction

HUVECs primary cells were used as a human *in vitro* model to perform signalling and interaction studies. As a complement, *in vivo* studies were also performed, using zebrafish and an Ecscr knockout mouse as models. Mouse and zebrafish orthologs for ECSCR have been identified by Armstrong *et al*. (2008). Zebrafish are very easy to use, as they reproduce often and quickly and the embryos are transparent and develop rapidly, which allows direct observation. In addition, there are several transgenic lines available suitable for angiogenesis studies, such as tg[fli1:EGFP] (Lawson and Weinstein, 2002). In this line, friend leukaemia integration 1 (fli1) is fused to enhanced green fluorescent protein (EGFP), which allows the visualisation, study and manipulation of the vasculature. Fli1 is an E-twenty six (ETS)-domain transcription factor that is present in vasculature since the appearance of the haemangioblasts (Brown *et al*. 2000).

Blood and endothelial cells derive from a mesodermal common precursor, the haemangioblast (Keller, 2001). In the developing zebrafish embryo two populations of haemangioblasts arise at the lateral plate mesoderm to form the primitive vasculature. The anterior population forms the head vasculature and the posterior originates the dorsal aorta and posterior cardinal vein, the axial vessels of the tail and trunk (Fouquet *et al*., 2007). The latter starts migrating into the midline at the 14 hours post fertilization (hpf) stage (10 somites) and coalesces to form a tube. Soon after, the anterior angioblasts also migrate to locate ventrally to the dorsal aorta and by 13-15 hpf (7-12 somites) the arterial and venous fates are already determined (Zhong *et al*., 2001). Cell fate is controlled by neighbouring tissues. The dorsal aorta is located ventrally to the notochord and hypocord and dorsally to the posterior cardinal vein, being laterally flanked by the somites (Fouquet *et al*., 2007; Zhong *et al*., 2001). The posterior cardinal vein is dorsally flanked by the aorta and ventrally by the endoderm. The midline structures secrete hedgehog

towards the dorsal aorta, which controls important signalling pathways, including Vegf and Notch (Lawson *et al*., 2002). Hedgehog signalling is required in vascular development at three stages: medial migration of dorsal aorta progenitors, arterial-specific gene expression and sprouting of intersegmental vessels (Gering and Patient, 2005). By 22 hpf primary intersegmental vessels sprout upwards from the dorsal aorta and soon after, by 24 hpf, the primitive vascular loop is formed and circulation starts (Isogai *et al*., 2003). Secondary sprouting from the posterior cardinal vein starts at 32 hpf and gives rise to venous intersegmental vessels and the lymphatic system. Through remodelling of the trunk vasculature, primary arterial sprouts contribute to the formation of both arterial and venous intersegmental vessels (Isogai *et al.*, 2003). Arterial sprouting depends on Vegfa, kdr and kdr-1, whereas venous intersegmental vessels require Vegfc. Delta-like ligand 4 supresses the ability of developing intersegmental arteries to respond to Vegfc-driven Flt4 signalling (Hogan *et al.*, 2009).

At 22 hpf, the sprouting of primary intersegmental vessels from the dorsal aorta occurs by angiogenesis and has been widely used as a model to study that process. Sprouting starts with arterial cells migrating out and overlapping. Then, they form a multicellular tube. After undergoing several complex rearrangements, such as division, rearrangement and changes in cell-cell contacts, the dorsal-most cell (tip cell) acquires a T-shape and joins with its anterior and posterior neighbours to form the dorsal longitudinal anastomotic vessel. The lumen of the vessel is formed through the formation and fusion of vacuoles from contiguous cells (Blum *et al*., 2008).

4.2 Zebrafish Ecscr expression pattern

Armstrong *et al*. (2008) reported that an uncharacterised putative zebrafish protein showed similarity to human ECSCR, especially in the intracellular domain. The endothelial specificity in zebrafish embryos of this protein is now investigated. RNA whole mount *in situ* hybridization was performed. RNA antisense (and sense, as a control) probes were made by extracting total RNA from 24 hours post-fertilization (hpf) zebrafish embryos. RNA was converted into cDNA, putative Ecscr was amplified by PCR and inserted into the PCR TOPO blunt vector using *Eco*RI and *BamH*I restriction enzymes. The orientation of the insert was confirmed by sequencing and the plasmid was linearised using *Not*I (for the sense probe, synthesised using the SP6 RNA polymerase promoter) and *BamH*I (for the antisense probe, synthesised using the T7 RNA polymerase promoter) restriction enzymes. The RNA probes were synthesised using the mMessagemMachine kit and subsequently purified, so that they could be used for detection of the Ecscr transcript by whole mount *in situ* hybridization.

Figure 4.1 shows that zebrafish Ecscr is specifically expressed in the vasculature, namely in the major head and trunk vessels. No expression in the intersegmental vessels was detected.

Subsequently, the message levels of Ecscr were detected by reverse-transcription PCR using lysates from AB* wild type embryos at different developmental stages, from 1 cell to 72 hpf (Figure 4.2). Ecscr is maternally expressed and the levels decrease up to the 12-somite stage. By the 16-somite stage, transcription levels increase substantially and remain high at 72 hpf. This suggests that Ecscr may play a part in the developing vasculature. A second transcript of Ecscr was detected. This transcript seems to have a role between 12 and 30 hpf, as it is not detectable on samples from other stages. Elongation factor 1 alpha was used as a housekeeping gene and a -RT PCR was performed using the samples not converted into cDNA to assess possible contamination with genomic DNA.

Although the gels shown on figure 4.2 allow a more visual assessment and the detection of a second transcript, real-time quantitative PCR was also performed on the same samples (figure 4.3). The Ecscr expression was normalised to that of EF1-alpha. The pattern observed on figure 4.3 is the same as on figure 4.2.

To further investigate the presence of two Ecscr bands, full-length Ecscr was amplified by PCR from cDNA and the two bands were excised from an agarose gel, purified and sequenced. The sequencing results have revealed two alternative transcripts, differing on the presence/absence of exon 2 (figure 4.4).

Figure 4.1 - Zebrafish Ecscr mRNA expression pattern in 24 hpf zebrafish AB* wild type embryos

The zebrafish Ecscr transcript was detected by whole mount *in situ* hybridization. At 24 hpf Ecscr is expressed in the head and major trunk vessels, as indicated by the black arrows. The two inserts below the main image are a magnification of the head and trunk regions where the transcript was detected. This staining has been repeated 3 times with similar results, on 10 embryos each time.

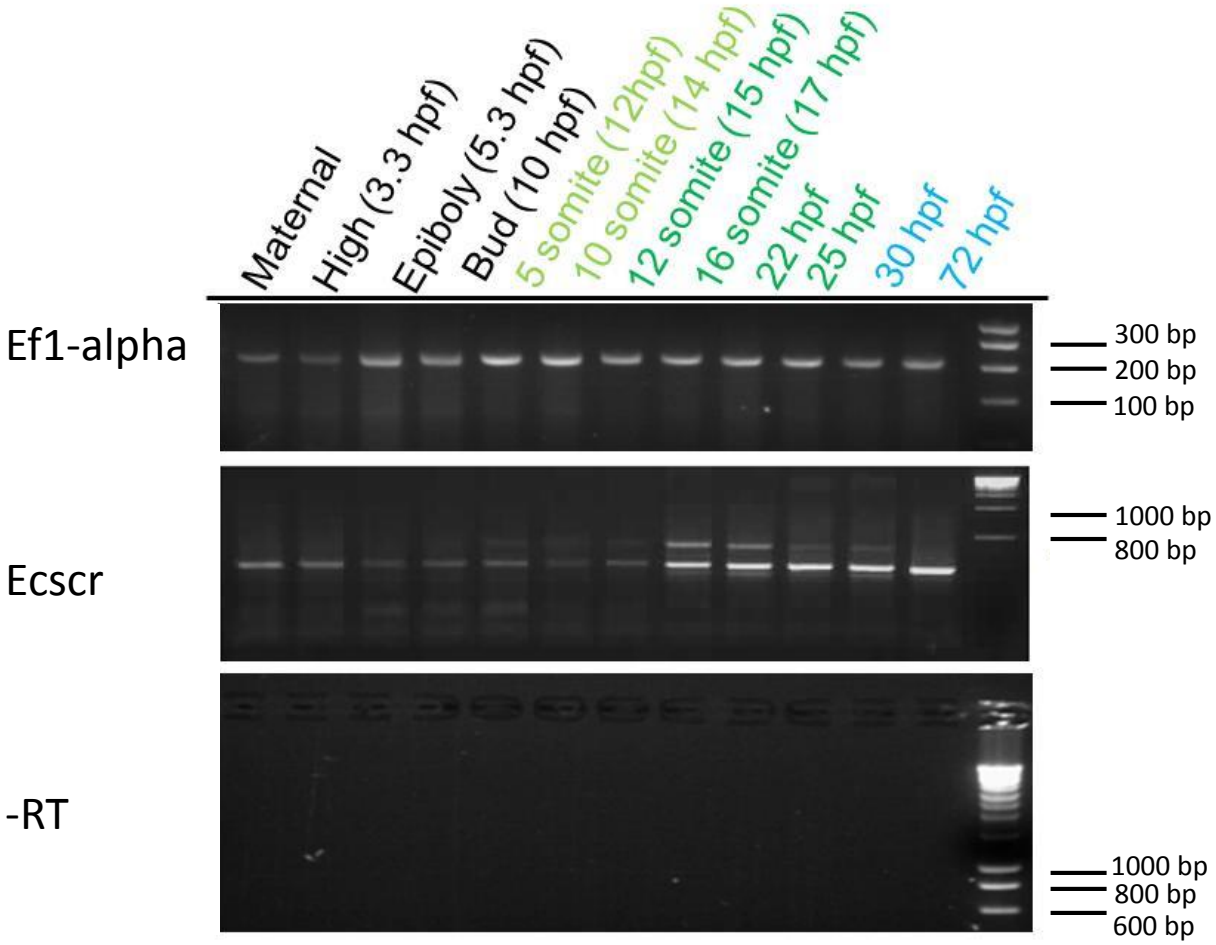

Figure 4.2 - Ecscr transcript levels during zebrafish embryonic development using reverse transcriptase-PCR

Wild type zebrafish embryos were collected at different stages, from 1 cell (maternal) to 72 hpf. PCR reactions for Ecscr, Ef1-alpha and –RT were performed (from cDNA) and repeated 3 times with similar results. The Ecscr transcript is maternally expressed and levels decrease up to the 12-somite stage. By the 16-somite stage, transcription levels increase substantially and remain high at 72 hpf. A second transcript was detected. hpf – hours post fertilization; Ef1-alpha – elongation factor 1 alpha ; -RT – negative control for the reverse transcriptase reaction.

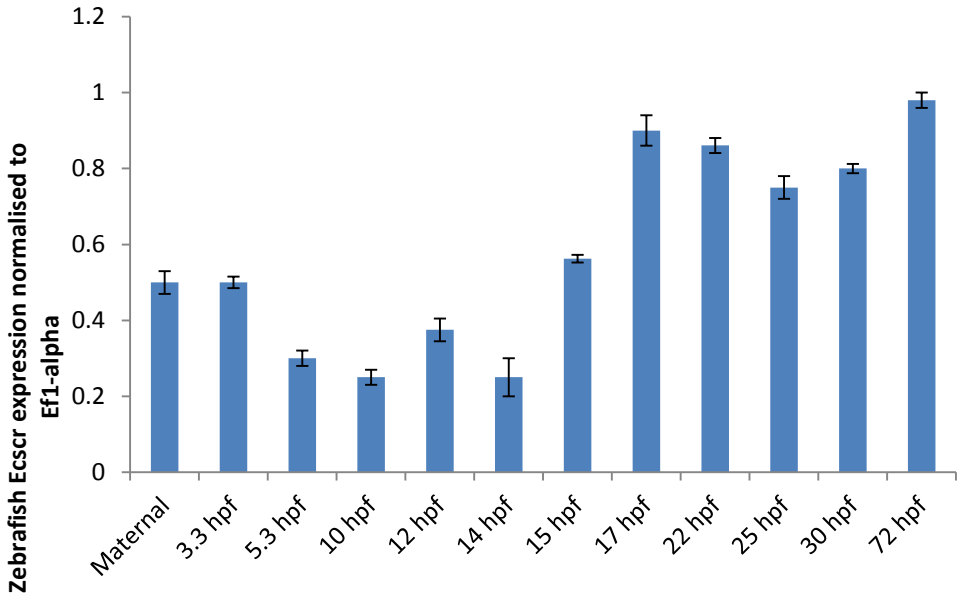

Figure 4.3 – Ecscr transcript levels during zebrafish embryonic development using real time quantitative PCR.

Wild type zebrafish embryos were collected at different stages, from 1 cell (maternal) to 72 hpf. Total RNA was extracted and converted to cDNA. qPCR reactions were performed and the expression levels of Ecscr were normalised to those of Ef1-alpha. Each reaction was performed in triplicate and repeated 3 times with similar results. As observed for figure 4.2, Ecscr transcript is maternally expressed and levels decrease up to the 14 hpf stage. By the 15 hpf stage, transcription levels increase and remain high at 72 hpf. Statistical variation is shown as standard deviation. hpf – hours post fertilization.

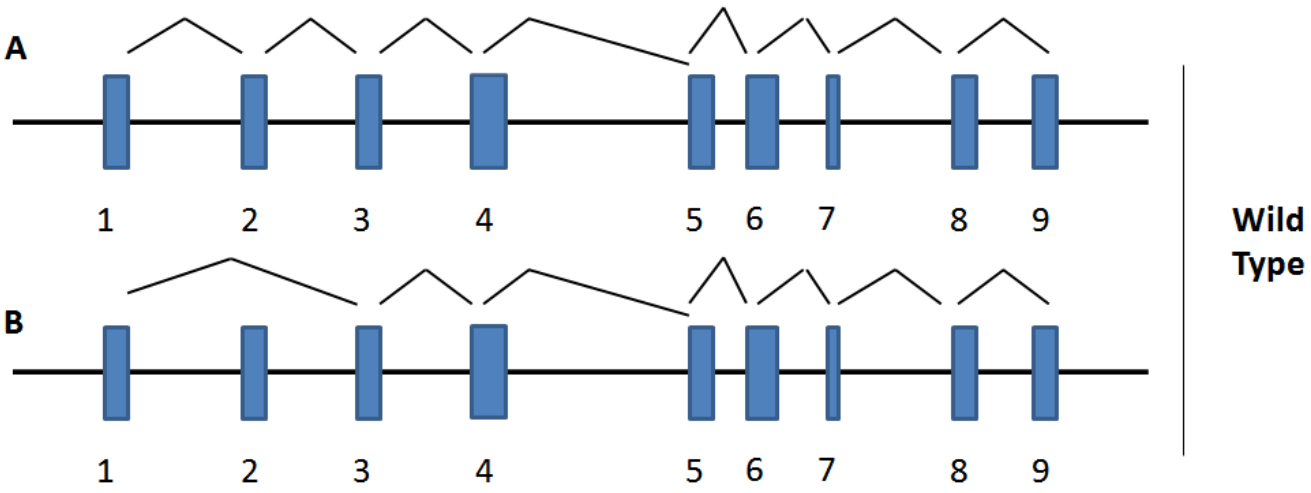

Figure 4.4 - Alternative splicing of the zebrafish Ecscr transcript

When analysing the Ecscr expression during embryonic development by reverse-transcriptase PCR (figure 4.2), the gel has revealed a second band for the stages between 12 and 30 hpf that are not present before or after these points. This was further investigated by excising and sequencing the two bands. The results have shown that there are two alternatively spliced Ecscr variants in wild type zebrafish, differing in the presence/absence of exon 2 (A and B).

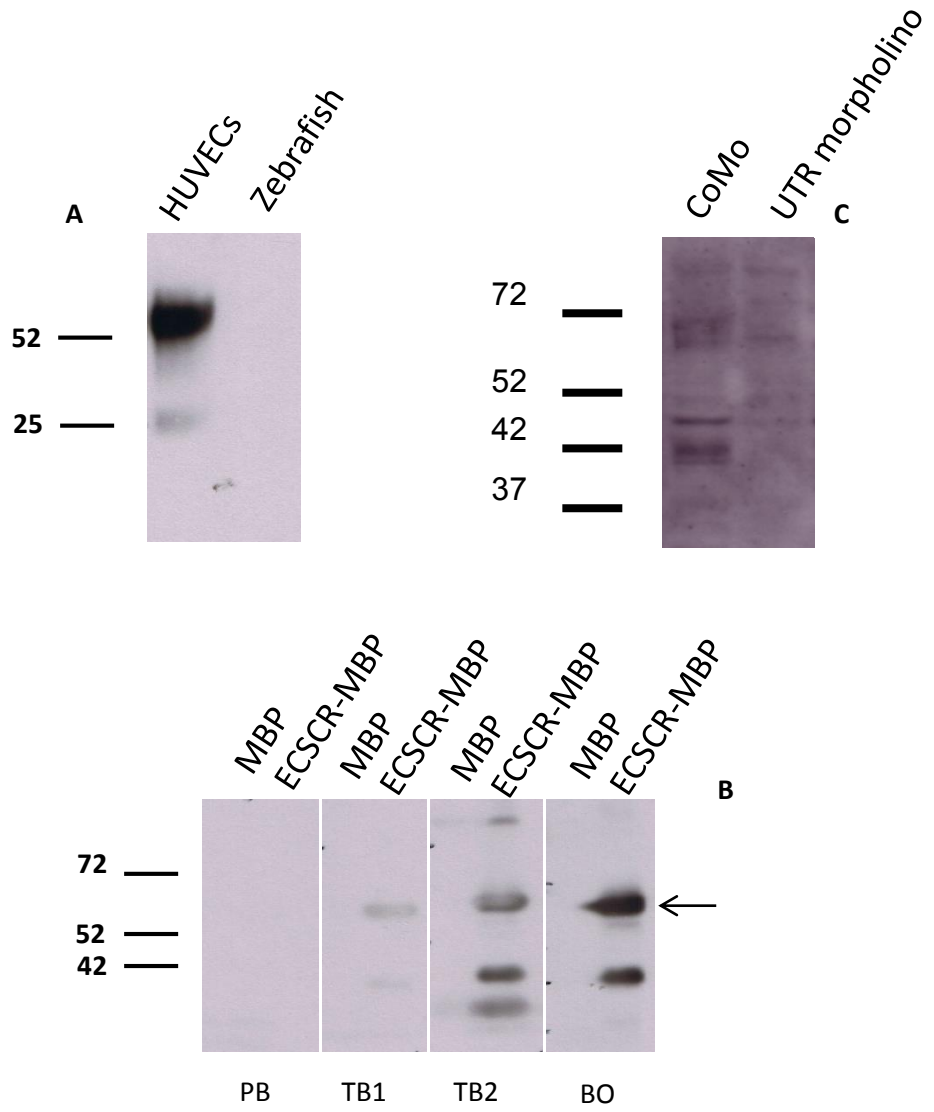

Figure 4.5 – Test of antibodies suitable to detect zebrafish Ecscr

To be able to detect the zebrafish Ecscr protein, the polyclonal antibody against human ECSCR was tested on HUVECs (positive control) and 24 hpf zebrafish lysate. This antibody did not detect the fish protein (A). Therefore, a new antibody was produced in rabbit, using Ecscricd-MBP. The different test bleeds were able to detect the immunogen (B, arrow), as well as the endogenous protein (C). the MBP – maltose-binding protein; Ecscricd-MBP – zebrafish Ecscr intracellular domain fused to MBP; PB – pre-bleed; TB1 – test bleed 1; TB2 – test bleed 2; BO – bleed out; CoMo – negative control morpholino; UTR Mo – morpholino targeting Ecscr 5' UTR region.

4.3 Raising an antibody against the zebrafish Ecscr intracellular domain (icd)

Many antibodies have the ability to detect ortholog proteins from different species, when the regions used as immunogens show sufficient conservation. Since a polyclonal antibody against the whole human ECSCRicd (conserved across species) was available, total protein from wild type zebrafish embryos was extracted and analysed by western blot. Total protein from HUVECs was used as a positive control. This antiserum did not recognise the zebrafish protein (figure 4.5 A). In order to detect Ecscr on a western blot or to use it for immunoprecipitation studies in the future, the production of a suitable antibody was necessary. A zebrafish Ecscricd-MBP (maltose binding protein) fusion protein was produced and purified. A rabbit was immunised and the bleeds were tested against the protein that was sent to CRUK for antisera production, as well as against zebrafish embryos lysates (injected with control or UTR morpholino, as described on the next section). Prior to being tested, the antiserum was incubated with PVDF membrane where containing MBP, so that it could be depleted from these antibodies. The antibody successfully recognised both the bacterially produced fusion protein and endogenous zebrafish Ecscr (figure 4.5 B and C). This validates not only the antibody, but also the morpholino, as the double band (~40-47 kDa) is present in the negative control and absent in samples from embryos treated with an Ecscr 5' UTR-targeting morpholino.

4.4 Loss of Ecscr function causes defects in intersegmental vessels sprouting

One of the most commonly used strategies to study the function of a given gene consists of removing it from the system, either by knockdown or knockout techniques. To study the loss

of Ecscr function antisense morpholino technology was used (Nasevicius and Ekker, 2000). Two different morpholinos were designed to target Ecscr: one that binds to the 5' UTR region immediately before the start codon and another one that binds between the end of exon 5 and the beginning of intron 5. The first should interfere with and block translation, whereas the latter should impair splicing between exons 5 and 6. As controls for specificity, a mismatch morpholino was designed for each targeting one, differing in five nucleotides, which causes them not to bind to the specific target. Transgenic tg[Fli1:EGFP] one cell embryos were injected with 8, 4 and 2 ng of each morpholino, which correspond to 1 nl of 1, 0.5 and 0.25 mM, respectively. The amount of morpholino that caused a phenotype for the Ecscr-targeting sequence and no alterations for the mismatch controls was 4 ng for both pairs. In the light of this result, 4 ng per embryo was the amount chosen for further loss of function studies. The embryos were observed and counted at 30 hpf. Three independent experiments were performed for each morpholino and at least 100 viable embryos were counted and assessed for each condition. Figure 4.6 depicts the basic anatomy of a zebrafish embryo and shows what region has been used for imaging. The embryos injected with control morpholinos were not affected (Figure 4.7). The specifically targeted morphants displayed a range of intersegmental vessel effects due to Ecscr loss of function. In general, Ecscr knockdown caused defects in the sprouting of intersegmental vessels from the main trunk vasculature. The range of phenotypes observed was divided into four categories: no abnormal effects detectable (the embryos look like the controls), mild (one or two intersegmental vessels disrupted), intermediate (three or four abnormal intersegmental vessels) and severe effects (more than five intersegmental vessels disrupted) (Figure 4.7). The embryos were counted for each category and are represented on figures 4.8 A and 4.8 B as a percentage of the total. Upon morpholino injection, approximately 75% of the embryos presented vessel defects in both conditions.

The specificity of the targeting morpholinos was also tested by using *in vitro* transcribed Ecscr mRNA, where neither of the morpholinos can bind. The construct used to make the transcript contained only the open reading frame (so the 5'UTR morpholino cannot bind) and, since the mRNA was already spliced, the splicing-interfering morpholino was also unable to target this molecule. The injection of this message alone caused a similar phenotype to the one inflicted by the morpholino when used at high concentrations (1, 100 and 1000 ng/µl were tested). The concentration chosen for the assay was 100 ng/µl). When co-injected with the morpholino, a rescue of the phenotype was achieved, reflected by the significant decrease ($p < 0.05$) in the number of embryos displaying mild and especially severe abnormalities (figures 4.9 A and 4.9 B). Even in the few cases where significance of decrease was not achieved, those categories still showed a decreasing trend. A western blot was also performed for protein samples from embryos injected with the various morpholinos and mRNA, to assess changes in Ecscr protein expression (figure 4.10). The injection of mRNA alone has produced an increase in Ecscr expression, whereas the injection of either morpholino has produced a considerable decrease. The injection of either mismatch negative control morpholino has not affected the amount of Ecscr compared to the uninjected control. A co-injection of either targeting morpholino and Ecscr mRNA has restored the protein levels back to those of the uninjected control. An antibody against mouse actin was used as a loading control. This antibody can still recognise the fish protein but, probably due to evolutionary distance, the bands are faint and somewhat diffused.

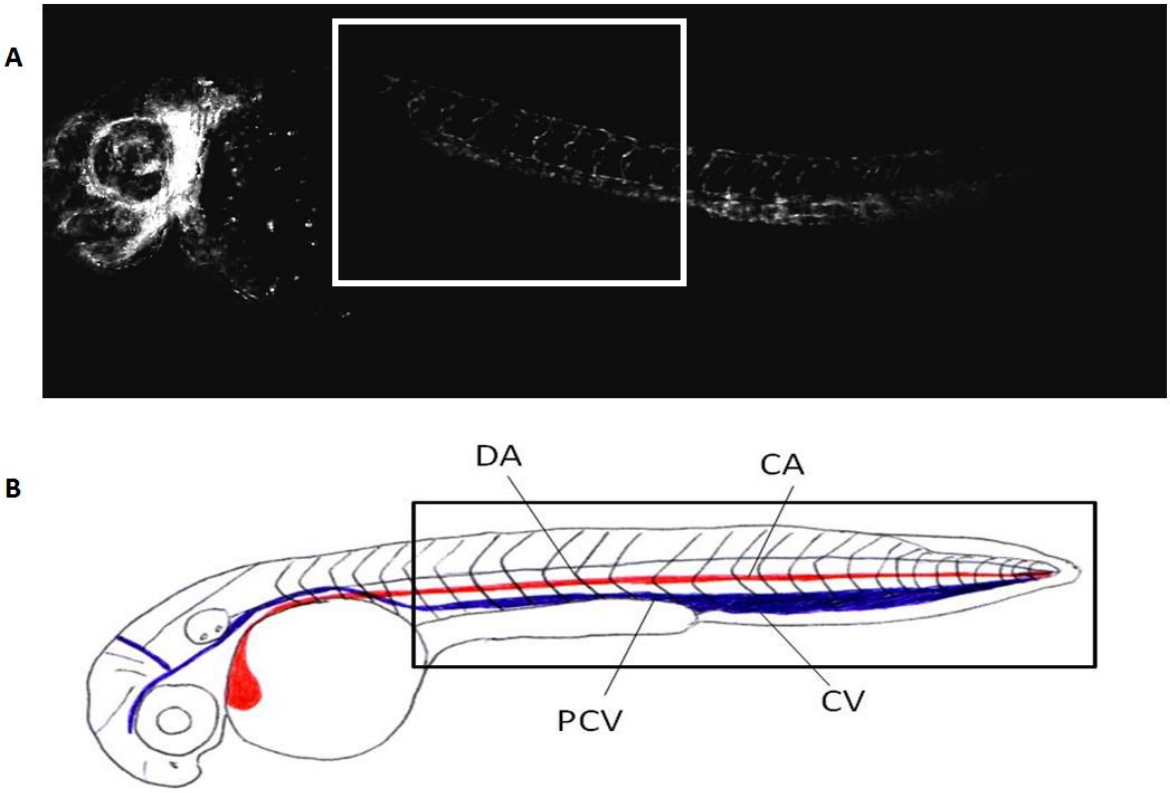

Figure 4.6 – The zebrafish vasculature at 36 hours post fertilization

To illustrate the typical vasculature of a 36 hpf zebrafish embryo, a transgenic tg[fli1:EGFP] embryo was imaged (A). The white rectangle represents the area of the trunk that was selected for further imaging and comparisons. The main zebrafish axial vessels are schematically represented in (B). The black rectangle highlights the main trunk axial vessels. DA – dorsal aorta; CV – cardinal vein; ISV – intersegmental vessels.

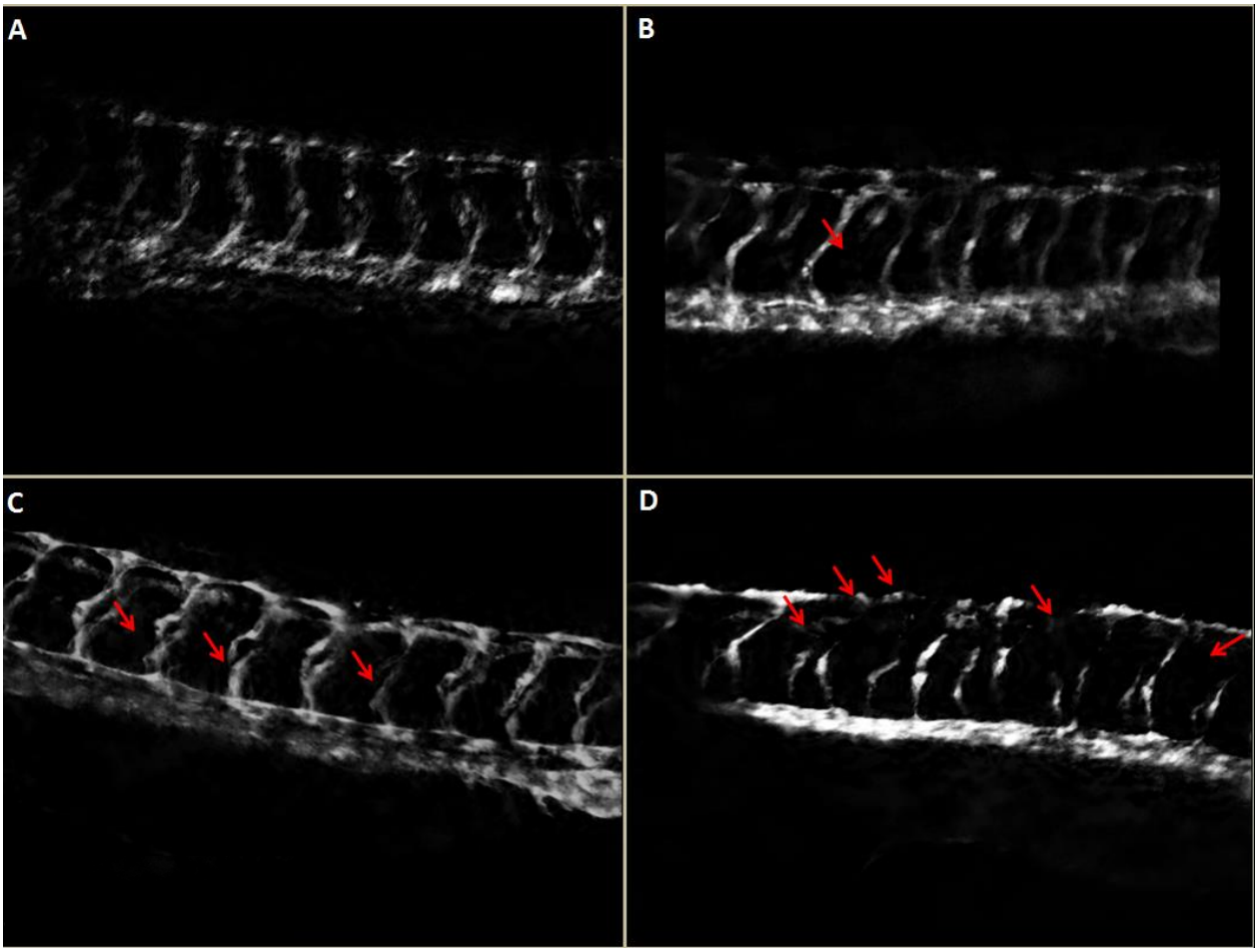

Figure 4.7 – Ecscr loss of function in transgenic tg[Fli1:EGFP] 30 hpf zebrafish embryos. At 30 hpf zebrafish embryos injected with Ecscr-targeting morpholinos displayed intersegmental vessel formation abnormalities, that ranged from no abnormal phenotype (A) to more than 5 vessels disrupted (D). This was quantified in at least 100 viable embryos, 3 times. The red arrows indicate the disrupted vessels and their number in each panel is proportional to the severity of the abnormal phenotype. A – No abnormal phenotype; B – mild (1-2 disrupted vessels); C – intermediate (3-4 disrupted vessels); D – severe (more than 5 disrupted vessels).

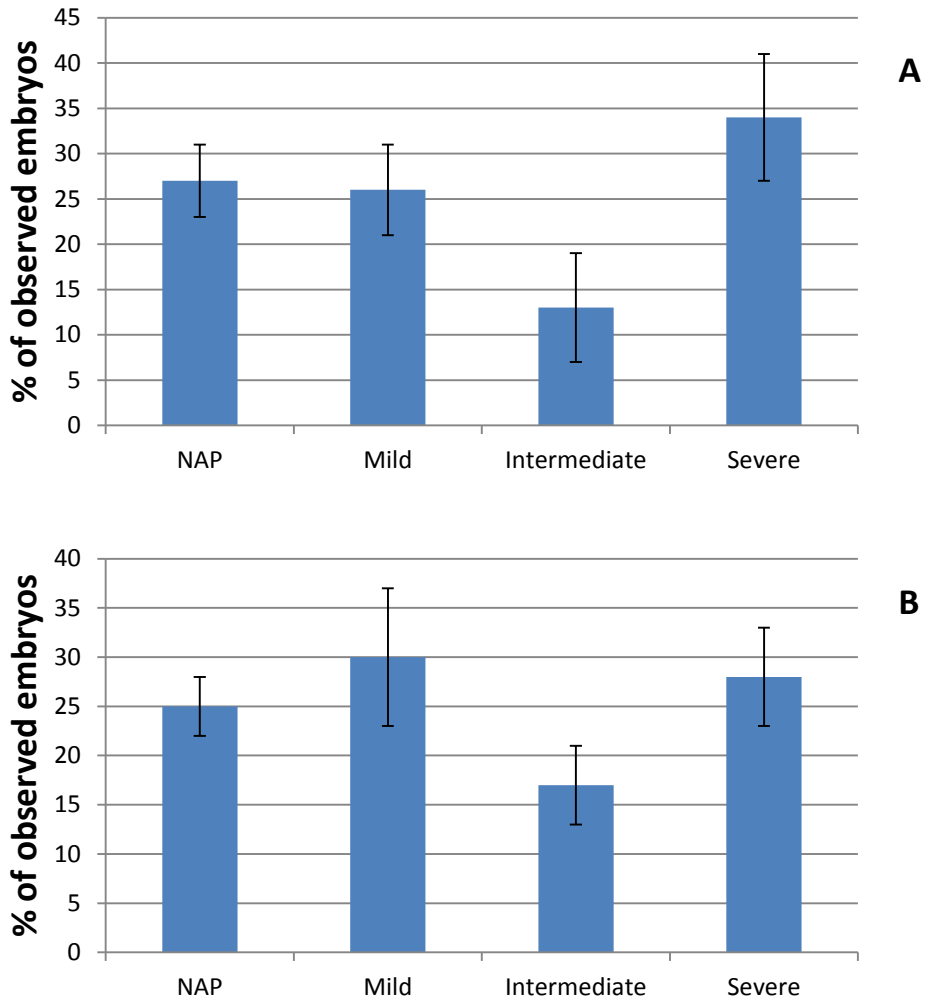

Figure 4.8 - Quantification of the defects in intersegmental vessels sprouting resulting from Ecscr loss of function.

The morpholino-injected embryos for each category represented on figure 4.7 were counted and divided by the total number of embryos observed (at least 100, 3 times).

A – proportions of embryos in each category of the range of effects caused by the splice morpholino injection. B – proportions of embryos in each category of the range of effects caused by the 5' UTR morpholino injection. NAP – no abnormal phenotype. Statistical variation is shown as standard deviation.

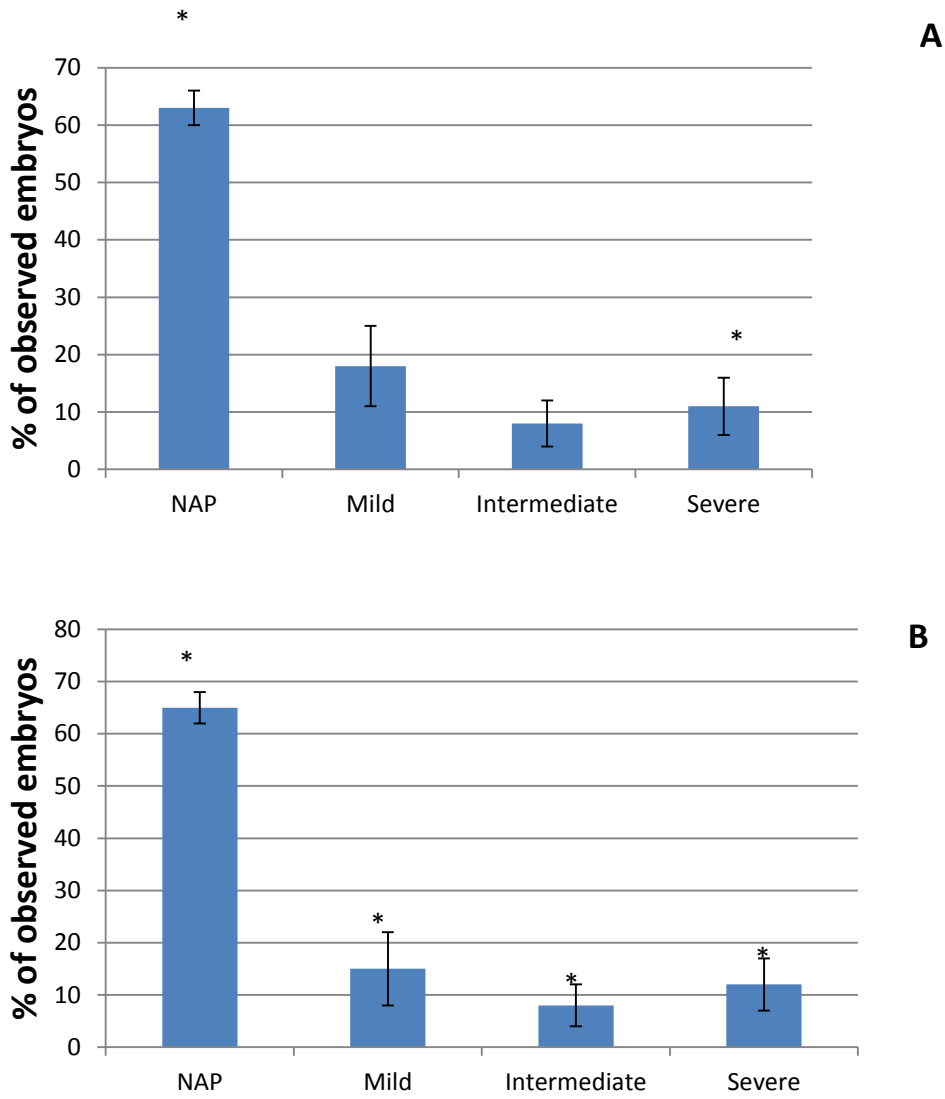

Figure 4.9 - Quantification of the defects in intersegmental vessels sprouting after mRNA rescue

To verify the specificity of the targeting morpholinos, these were co-injected with Ecscr RNA and the same counts were performed as for figure 4.8. A chi-square test was done to determine significant differences between counts of morpholino-injected embryos and rescued embryos, for the same category. A p-value < 0.05 is represented by *. A – proportions of embryos in each category of the range of effects caused by the splice morpholino and zebrafish Ecscr mRNA co-injection. B – proportions of embryos in each category of the range of effects caused by the 5' UTR morpholino and zebrafish Ecscr mRNA co-injection injection. NAP – no abnormal phenotype. Statistical variation is shown as standard deviation.

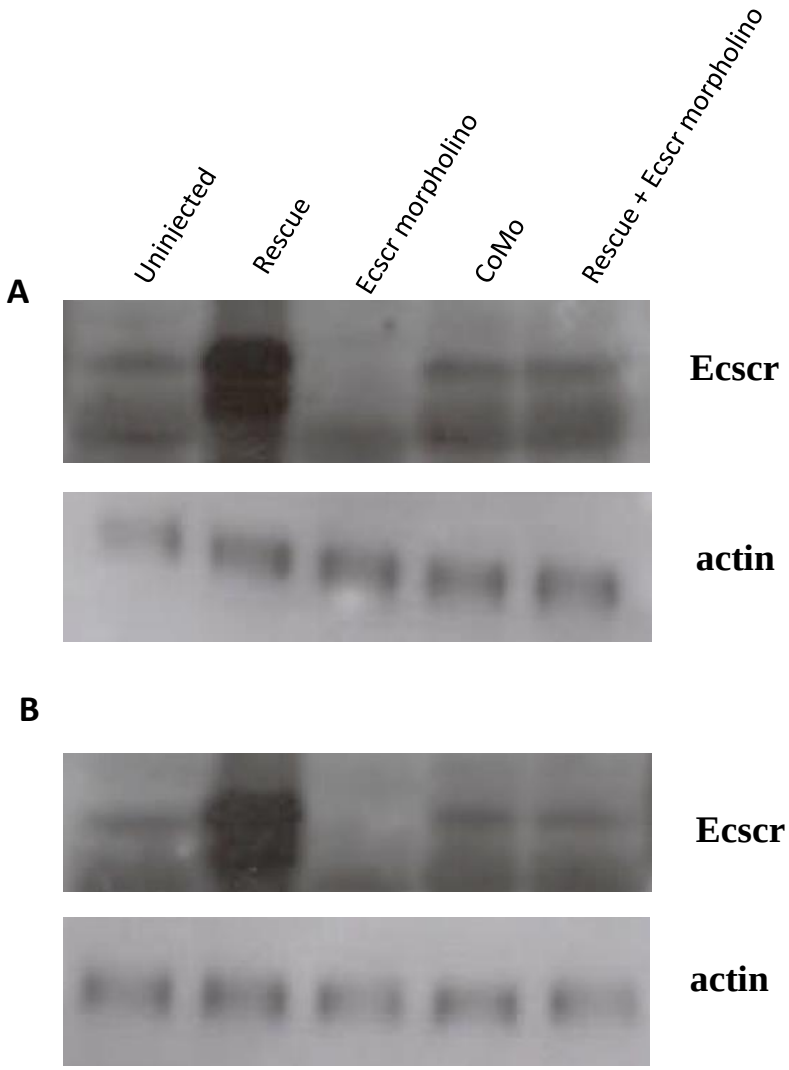

Figure 4.10 – Ecscr protein assessment by western blot of zebrafish embryos injected with morpholinos and mRNA

A western blot was performed for protein samples from embryos injected with the various morpholinos and mRNA, to assess changes in Ecscr protein expression. The injection of mRNA alone has produced an increase in Ecscr expression, whereas the injection of either morpholino has produced a considerable decrease. The injection of either mismatch negative control morpholino has not affected the amount of Ecscr compared to the uninjected control. A co-injection of either targeting morpholino and Ecscr mRNA has restored the protein levels back to those of the uninjected control. An antibody against mouse actin was used as a loading control. A – Ecscr splice morpholino; B – Ecscr 5' UTR morpholino. CoMo – mismatch control morpholino

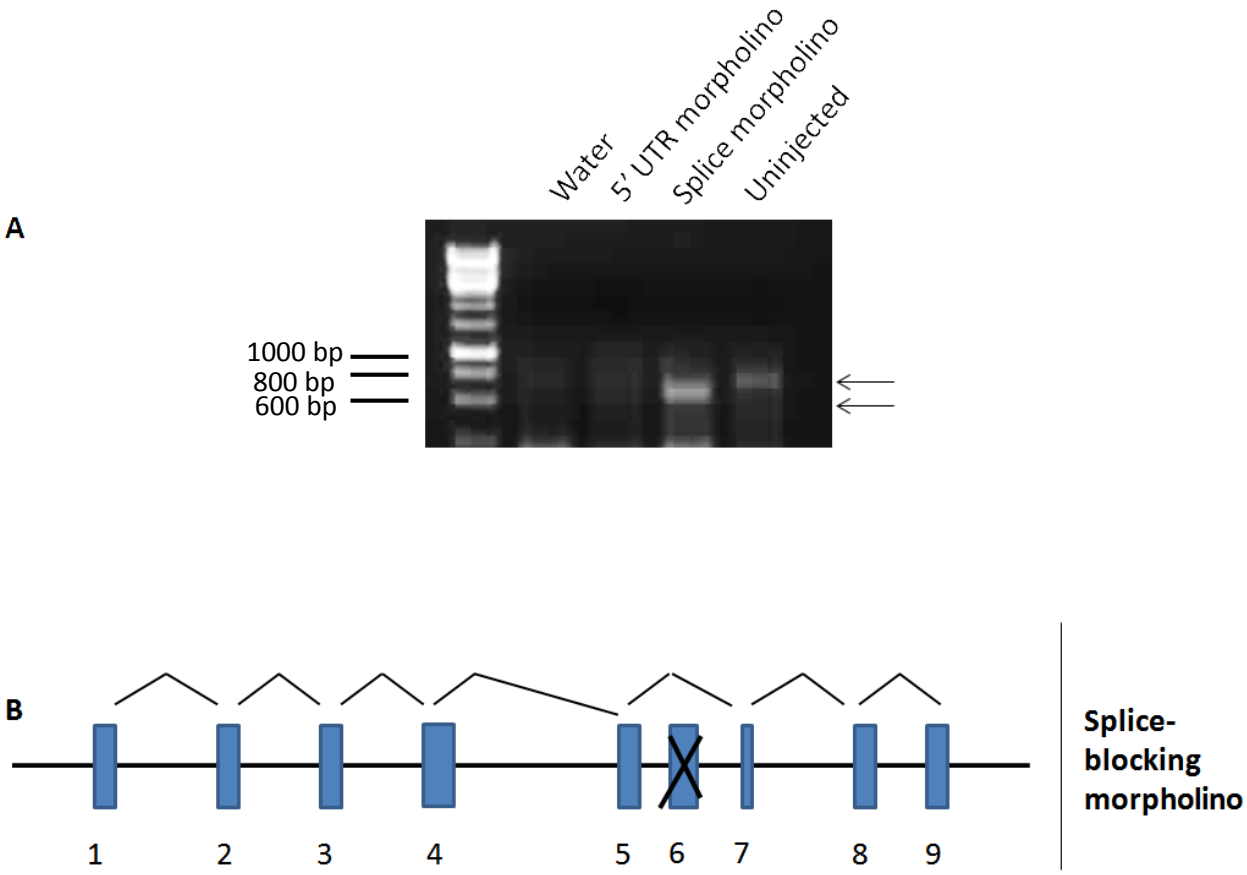

Figure 4.11 – Effects of ECSCR knockdown at the transcript level.

After injection of the morpholinos, RNA was purified and cDNA was synthesised. This was used to amplify the full length zebrafish Ecscr (A). The 5'UTR morpholino resulted in no transcript being made and the splice morpholino resulted in a smaller transcript. The difference in sizes is shown by the black arrows. The two transcripts were sequenced and the smaller one lacked exon 6 (B).

After injection of the morpholinos, RNA was purified and cDNA was synthesised. This was used to amplify the full length zebrafish Ecscr. The 5'UTR morpholino resulted in no transcript being made and the splice morpholino resulted in a smaller transcript (figure 4.11 A). The two transcripts were sequenced and the smaller one lacked exon 6 (figure 4.11 B).

The intersegmental vessels are known to sprout from both the dorsal aorta and the cardinal vein (Isogai *et al*., 2003). Using specific markers for artery (Ephb2) and vein (Efn4) endothelial cells, the major trunk vessels seem to be intact when Ecscr is depleted (figure 4.12). These markers do not stain intersegmental vessels. MyoD, a marker for myogenesis, was used to assess endoderm integrity, to attest that the intersegmental vessel phenotype was specific and other structures deriving from the mesoderm were not affected. The somites, as the blood vessels, originate from the mesoderm. There may be a slight ventral expansion of the cardinal vein in embryos injected with Ecscr morpholino. However, these are preliminary data that need to be repeated, as the experiment was performed only once.

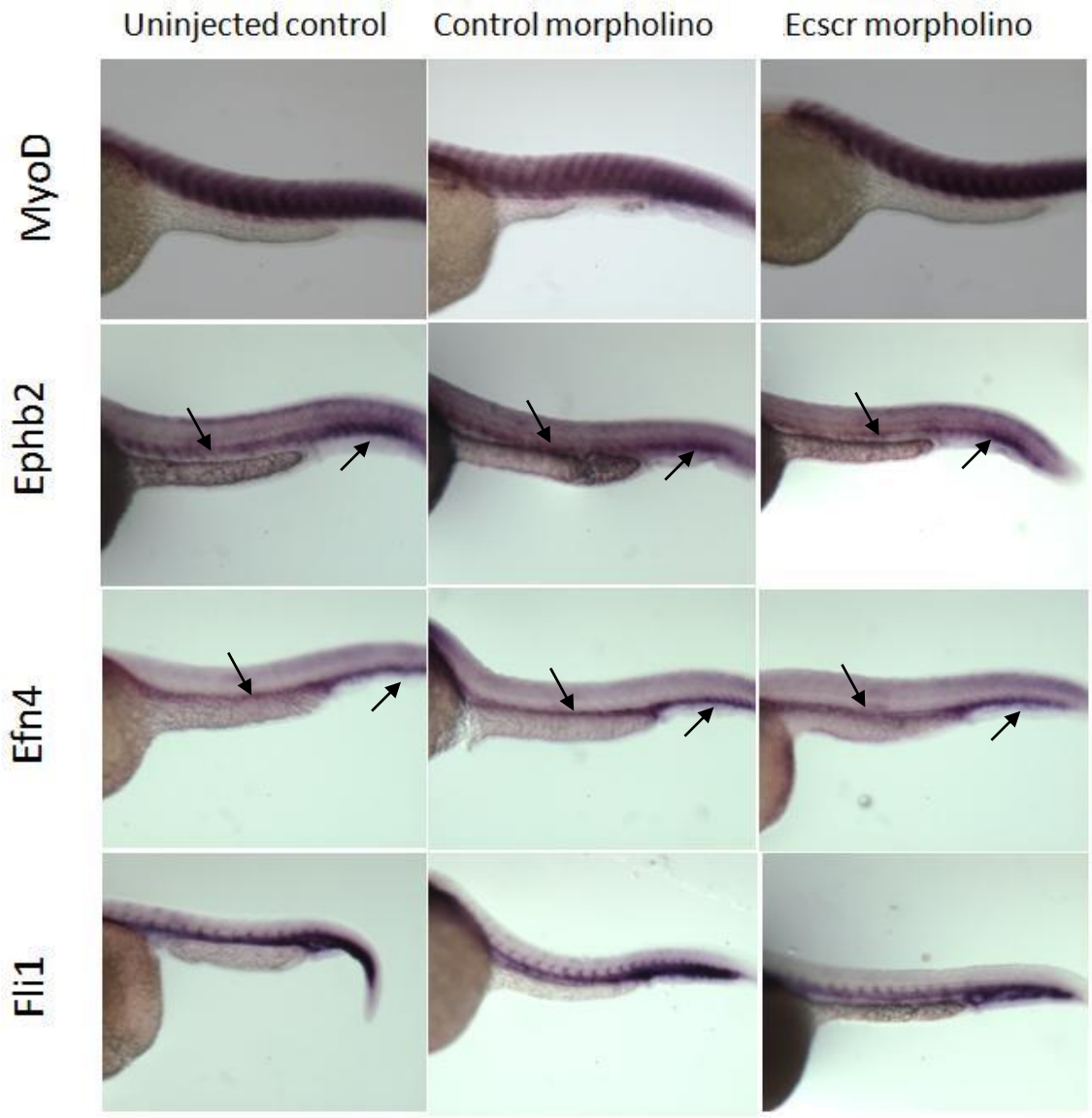

Figure 4.12 - RNA staining for vascular markers in zebrafish embryos with depleted Ecscr by morpholino injection.

Zebrafish embryos were injected with 5' UTR morpholino and the transcripts of blood vessel markers were detected by *in situ* hybridization. The arrows indicate specific staining for the dorsal aorta (Ephb2) and cardinal vein (Efn4). MyoD was used to make sure that mesoderm-derived structures were developing normally. Fli1 is a marker for endothelial differentiation, which is present in both veins and arteries.

4.5 Discussion

4.5.1 Spatial and temporal distribution of zebrafish Ecscr

Zebrafish has been recognised as a good genetic and developmental biology model to study vessel development. Many genetic mutants and transgenic lines of endothelial lineages have been created and are currently available. Importantly, developmental mechanisms including those of blood vessels are conserved between higher vertebrates and zebrafish (Davidson and Zon, 2004).

A zebrafish orthologue for ECSCR has been found by Armstrong *et al*. (2008). In order to determine its endothelial specificity and therefore study its role in developmental angiogenesis, *in situ* hybridization was performed using 24 hpf wild type embryos. This revealed that Ecsr is expressed in the major head and trunk vessels exclusively (figure 4.1). Later others have independently confirmed these results. Furthermore, they have detected the message at as early as 10 somites in the lateral plate mesoderm, at positions where endothelial precursors are expressed. From 16-18 somites Ecscr message is present at midline vascular structures and at 24 hpf it is detected on both trunk axial vessels (dorsal aorta and cardinal vein) and main head vessels (Verma *et al*., 2010). As in the present study, they have not detected Ecscr in the intersegmental vessels. This can be because the transcript is not there or it is expressed at such low levels that the technique is not powerful enough to detect it.

Many other genes that are endothelial specific and play a role in vascular development have been identified in zebrafish by genome-wide analysis and *in situ* hybridization screening. GA2692 (orthologue of mammalian HspA12B, a distant member of the heat shock protein 70 family) mRNA expression was detected in zebrafish ventral hematopoietic and vasculogenic mesoderm and later throughout the vasculature up to 48 hours post fertilization. Morpholino-

mediated knockdown of this protein resulted in multiple defects in vasculature, particularly at sites undergoing active capillary sprouting (intersegmental vessels, sub-intestinal vessels and the capillary sprouts of the pectoral fin vessel). HspA12B is highly expressed in HUVECs *in vitro* and knockdown by siRNAs blocked wound healing, migration and tube formation, whereas overexpression enhanced migration and accelerated wound healing (Hu *et al*., 2006). Another example are the transcription factors from the ETS family members erg, fli1 and etsrp. Loss-of-function analyses have demonstrated that erg and fli1 are required for angiogenesis, acting cooperatively, possibly by regulating VE-cadherin. Etsrp, on the other hand, is essential for haemangioblasts and vasculogenesis (Liu and Patient, 2010; Sumanas and Lin 2006).

Some proteins are expressed during transient distinct developmental periods to perform functions that are only required during development, such as GA2692, which is only expressed up to 48 hpf (Hu *et al*., 2006). Others are important during the whole lifetime of an individual. This seems to be the case of ECSCR. It is expressed during embryonic stages (in HUVECs) and *in situ* hybridization has detected ECSCR in human adult vessels from paraffin-embedded tissue arrays (appendix 2, figure A4). Temporal expression of zebrafish Ecscr was studied from 1 cell to 72 hpf (figures 4.2 and 4.3). It is maternally expressed, as it is present already at the 1-cell stage. Maternal gene products drive early development when the embryo is transcriptionally inactive. It only begins to produce its own RNA after the maternal-zygotic transition, which occurs at the blastula stage (Schier 2007). This suggests that Ecscr may have a role in very early development. However, it does not seem to be a determinant of embryonic survival, as Ecscr-targeting morpholino injected embryos do not present lethal phenotypes. The transcript starts expression remains low until 12 somites and then increases and remains high. This coincides with the period when vasculogenesis occurs (Baldessari and Mione, 2008), which implies that Ecscr may have a role during this stage. If it does, again, it does not appear

to be crucial, as both dorsal aorta and cardinal vein seem fairly normal when Ecscr is knocked down (figure 4.12). However, this *in situ* hybridization should be repeated and examined carefully, to confirm if there is a slight ventral vein expansion. Alternatively, because there is a temporal gap between mRNA and protein, this increase in transcript may be in preparation for a role in intersegmental vessel sprouting, that starts at around 22 hpf. Studies in the present work show that loss of Ecscr results in intersegmental vessel sprouting disruption (figure 4.7). Temporal expression of Ecscr was quantified using qPCR, which shows the pattern described above (figure 4.3). Additionally, a reverse-transcriptase PCR was also performed and the products were run on a gel. This allowed the identification of a second transcript that otherwise would have not been seen (figure 4.2). What is interesting about this transcript (lacking exon 2, figure 4.4) is that it is only transiently expressed, between 5 somites (12 hpf) and 30 hpf. Its peak of expression is between 16 somites (17 hpf) and 22 hpf (figure 4.2). This coincides with the period during which the intersegmental vessels sprout from the axial vessels (at 22 hpf and then the second wave at 30 hpf) (Isogai *et al*., 2003). Others have also reported the existence of two mouse Ecscr transcripts, differing from each other in the first and second exons (Wu *et al*., 2012). The human protein is also known to present two distinct bands on an SDS-PAGE gel (figure 3.10; Armstrong 2005). Further investigations should be carried out to determine the role of this transcript in intersegmental vessel sprouting, as discussed below.

4.5.2 Effects of zebrafish Ecscr loss of function in zebrafish embryos

Tg[Fli:EGFP] is a zebrafish transgenic line, in which the endothelium and its precursors are labelled with GFP (Weinstein, 2002). These embryos were used to rapidly assess the effect of Ecscr loss by targeting morpholino injections. Two Ecscr-specific morpholinos were used, one targeting the 5' UTR (translation-blocking morpholino) and another one targeting a region between exon 5 and intron 5 (splice-blocking morpholino). For each one of those, a mismatch

control was used, where 5 nucleotides were altered so that the sequences are very similar but these do not bind to the targets. When Ecscr is depleted the intersegmental vessels don't form properly (figure 4.7). The injected embryos displayed a variety of intersegmental vessel disruption, ranging from no abnormal phenotype to mild (1-2 vessels disrupted), moderate (3-4 disrupted vessels) and severe (more than 5 abnormal vessels). Approximately 75% of the observed embryos presented an altered phenotype (figure 4.8). Although mismatch controls that had no effect on vascular development were used, there is always concern about off-target effects of the Ecscr-specific morpholino. While the underlying mechanism of these effects is unknown, one well-described and relatively consistent phenotype is p53-dependent neural toxicity, which is dose-dependent and has been estimated to be apparent in 15–20% of all morpholinos when injected at standard efficacy doses (Bedell *et al*., 2011). A possible solution is to co-inject a p53-targeting morpholino, to eliminate this toxicity. Another common phenotype is known as the "monster phenotype", where embryos display overall severe deformities, such as shortened and gnarled tails, massive body curvatures and small heads and eyes (Bedell *et al*., 2011). Minimum morpholino doses that would cause a vascular-only phenotype were carefully optimised, to avoid non-specific morphological abnormalities. Most of the embryos injected displayed overall normal anatomy and morphology. Therefore, any embryo with abnormal morphology was considered a non-specific effect and was not used when counting embryos and assigning them to the various intersegmental vessel defects categories. Furthermore, to assess the integrity of the mesoderm, where endothelial cells derive from (Gilbert, 2006), *in situ* hybridization was performed for MyoD, which shows normal somites in morpholino-injected embryos (figure 4.12). To additionally attest Ecscr specificity of the morpholinos, these were co-injected with Ecscr mRNA, which has resulted in the rescue of the phenotype towards milder defects or no abnormal vasculature (figure 4.9).

In the developing zebrafish embryo angioblasts arise from the lateral plate mesoderm at the 5-somite stage (Gilbert, 2006). Then, they migrate to the midline and form the dorsal aorta and cardinal vein by vasculogenesis. A recent study (Herbert *et al.*, 2009), however, suggests that only the dorsal aorta is formed by vasculogenesis from a common precursor vessel and the cardinal vein is formed by venous fated endothelial cells that segregate and migrate ventrally. Subsequently, intersegmental vessels sprout from the dorsal aorta and cardinal vein by angiogenesis, forming the dorsal longitudinal anastomotic vessels. Haemangioblasts are the common precursors of endothelial cells, haematopoietic cells and the cells that form the heart tube. After trans-differentiation and migration, each of these lines expresses specific markers. Friend leukaemia integration (fli1) is expressed only in the endothelial lineage, and ephrin B2a (Efnb2a) and ephrin 4 (Eph4) are arterial and venous markers, respectively. Transcription factors such as stem cell leukaemia (Scl) or Gata1 are markers for the erythroid lineage. Blood cell development occurs in two phases, termed primitive and definitive haematopoiesis. The first one is transitory and occurs in the blood islands in the ventral mesoderm close to the yolk sac and the latter takes place in the mesodermal region surrounding the aorta (Davidson and Zon, 2004). Given this common origin of vascular endothelial cells and blood cells, the effect of Ecscr loss could be evaluated in haematopoiesis by *in situ* hybridization using Ecscr morpholino injected embryos and haematopoiesis specific RNA probes.

The intersegmental vessels are known to sprout from both dorsal aorta and cardinal vein. Using specific markers for artery and vein endothelial cells, the major trunk vessels seem to be intact when Ecscr is depleted (figure 4.12), although these observations need to be repeated and confirmed carefully. Therefore, Ecscr may be more important for angiogenesis (the formation of new blood vessels from pre-existing ones) than it is to vasculogenesis. However, Ecscr is present in zebrafish at all times (as the transcript was detected from the 1-cell stage) and

morpholino knockdown studies by Verma *et al*. (2010) have shown that loss of this protein results in slower migration of the angioblasts to the midline, which is part of vasculogenesis, not angiogenesis. It is possible that there are proteins with a redundant function, or that can be upregulated to compensate for the loss of Ecscr at this stage, as vascular development is not arrested. Because it is maternally expressed, it may have other unknown roles in early development, as it may regulate the availability of filamin A, which is involved in a multitude of processes (Zhou *et al*., 2009). Also, other binding partners have recently been discovered, such as moesin (this study) and cIAP (Ikeda *et al*., 2009). Survivin, a member of the IAP family conserved in zebrafish, has been demonstrated to be an essential regulator of neurogenesis, vasculo-angiogenesis, haematopoiesis and cardiogenesis (Delvaeye *et al*., 2009; Ma *et al*., 2007). Regarding angiogenesis, it would be interesting to keep observing the morpholino-injected Tg[Fli:EGFP] embryos over time to assess if the loss of Ecscr causes permanent damages in the vasculature. Also, the role of the second transcript of Ecscr that is only produced in the embryo from 12 to 30 hpf with a peak that coincides with intersegmental vessel sprouting should be investigated. For that, a translation-blocking morpholino could be used to abolish all Ecscr expression, in conjunction with mRNA specific for either transcript. This would evaluate if they have distinct roles at different stages. Additionally, a morpholino could be designed to specifically eliminate this transcript. Similar studies, as well as protein interaction studies could be performed in HUVECs using both proteins, to possibly uncover distinct binding partners and pathways in an isoform-dependent manner.

In addition to visually assessing the effects of Ecscr loss via morpholino injection, the Ecscr transcript and protein levels were also monitored. PCR products were visualised on an agarose gel, which showed the absence of Ecscr in embryos injected with the 5' UTR morpholino and a smaller transcript in splice morpholino injected embryos compared to controls (figure 4.11).

Sequencing of this band shows lack of exon 6, which was expected, as the morpholino binds between exon 5 and intron 5, resulting in mis-splice between exons 5 and 6. Verma *et al*. (2010) have performed the same experiment for younger embryos and have observed several bands smaller than the original transcript, instead of just one. This can be due to the fact that embryos at different developmental stages process the transcript differently or respond to the morpholino in a distinct manner. Another possibility is that they may have used more cDNA template and therefore detected low copy transcripts that were not observed in the present study. In order to detect the zebrafish protein, that was shown to display the same pattern as the transcript (figure 4.10), a rabbit polyclonal antibody was generated from a fusion protein containing maltose binding protein and zebrafish Ecscr intracellular domain. Before doing so, the polyclonal antibody against human ECSCR was tested, but failed to recognise the zebrafish protein (figure 4.5). Relatively few zebrafish antibodies are available, so usually the first step is to identify antibodies raised for other species that cross-react with the zebrafish antigen (Akhtar *et al*., 2009). Typically, a panel of different antibodies can be tested, but at the time our group possessed the only available anti-ECSCR antibody, which had also been custom made from ECSCR-GST produced in our laboratory. Having an antibody that recognises the zebrafish protein provides the opportunity for further zebrafish studies, such as co-immunoprecipitation, immunofluorescence and even the possibility of it working as a blocking antibody.

4.5.3 Further directions

A recent study in zebrafish has shown that moesin 1 knockdown results in intersegmental vessel sprouting and lumen formation defects. Furthermore, this has led to the loss of VE-cadherin in cell-cell junctions. During embryonic angiogenesis, the primary lumen elongates along cell-cell junctions and moesin 1 is enriched in intracellular vacuoles that fuse with the

luminal membrane during expansion of the primary lumen (Wang *et al.*, 2010). In the future, Ecscr morpholino injected zebrafish embryos could be analysed in greater detail and stained for VE-cadherin, as Ecscr knockdown results in intersegmental vessel formation disruption and ECSCR has been shown to be present at cell-cell adhesions and interacts with moesin (Shi *et al*., 2011; this study). Although the initial staining (that needs repeating) for VE-cadherin in HUVECs where ECSCR was knocked down shows that VE-cadherin doesn't seem to change (figure 3.6), this *in vitro* model does not contain the rich pro-angiogenic environment that the sprouting vessels are exposed to *in vivo*. This difference could be essential to uncover a role for Ecscr *in vivo* that cannot be easily reproduced *in vitro*.

The tg[fli:GFP::gata1:dsRed] zebrafish transgenic line displays green vessels (GFP-tagged Fli1) and red erythrocytes (dsRed-tagged gata1) (Gering and Patient, 2001). Using time-lapse fluorescence microscopy imaging of this line, the defects in vascular development in these embryos can be imaged and therefore any flow disturbances or missed effects in haematopoiesis can be analysed. Time-lapse high magnification imaging of tip endothelial cells in sprouting intersegmental vessels from controls and embryos lacking Ecscr could provide insights on the impact this molecule on, for example, filopodia (number, length, turnover), or cell-cell interactions.

5 PRODUCTION AND PRELIMINARY CHARACTERIZATION OF AN ECSCR KNOCKOUT MOUSE

5.1 **Introduction**

In the previous chapter, RNA antisense oligonucleotides, morpholinos, were used to assess the role of ECSCR in angiogenesis. Morpholino-mediated knockdown of genes is a quick and relatively easy and cheap way of obtaining a fast answer that has been largely used in the zebrafish model. However, these changes are neither permanent nor complete. Homologous disruption has not yet been found to be efficient in zebrafish, mainly because of the difficulty in isolating and cultivating ES cells from this organism (Wienholds and Plasterk, 2004). To overcome this barrier a new gene targeting approach is starting to be used in zebrafish, employing synthetic zinc finger nucleases (Doyon *et al*., 2008; Ekker 2008; Meng *et al*., 2008). Nevertheless, the mouse is still the most widely used model to study the function of genes and to model human disease. As it is a mammal, it is closer to humans than the zebrafish is.

Presently, the International Knockout Mouse Consortium (IKMC), that comprises large-scale efforts from the Knockout Mouse Project (KOMP), European Conditional Mouse Mutagenesis (EUCOMM), North American Conditional Mouse Mutagenesis Project NorCOMM and the International Gene Trap Consortium, aims to mutate all protein-coding genes in the mouse using C57BL/6 embryonic stem (ES) cells. They have employed a selection of techniques, such as gene traps and conditional and non-conditional gene targeting strategies. In the past, researchers would make their own constructs, with the desired particularities or they would be available from heterogeneous sources, such as BayGenomics. This consortium of research groups focuses mainly on genes relevant to cardiovascular and pulmonary development and disease (Stryke *et al.*, 2003). At the KOMP, by creating the same types of constructs for different genes, the project aims to generate alleles that are as uniform as possible, to allow accurate comparisons. However, because of the nature of the studies to be performed or the severity of effects, constructs made available allow the creation of both null and conditional

knockouts. If nothing is known about the function of a gene or the severity of its absence is not thought to be lethal, a null knockout can be generated. The insertion of a reporter gene, such as β-galactosidase, allows the visualization of where the gene of interest would be expressed (Austin *et al*., 2004).

In Europe, the EUCOMM is contributing to the mouse genome mutagenesis programme by establishing and integrating mutagenesis platforms, phenotyping units, gene expression resources, storage and distribution centres and bioinformatics resources. They are applying conditional strategies for the rapid creation of conditional alleles in ES cells (Auwerx *et al*., 2004).

In recent years many important advances have been made in improving strategies and efficiency of gene targeting and gene trapping. The KOMP provides constructs for these two strategies, transfected into ES cells. Gene targeting comprises the insertion of a drug-resistance selection cassette into a specific region of the genome by homologous recombination, thus resulting in the interruption of the target gene. Gene trapping is achieved by random integration of a promoterless reporter construct and is restricted to genes expressed in ES cells (Skarnes, 2005). A clever strategy developed by Friedel *et al*. (2005) and named "targeted trapping" combines both. This was adopted by the KOMP to make their constructs to produce null knockouts. The null knockout produced for the present study was prepared using ES cells containing such a construct. There are two homologous recombination arms, 5' and 3', so that the sequences contained between them can be integrated into determined specific locations in the genome (figure 5.1). In the case of the Ecscr construct, the whole cassette was inserted between the 24 first nucleotides of exon 1 (in the untranslated (UTR) region) and the first 6 nucleotides of exon 9, immediately before the stop codon. A promoterless β-galactosidase open reading frame followed by a simian virus 40 polyadenylation signal (SV40 PolyA) will both

interrupt the gene and indicate in which cells that has happened upon LacZ staining. This happens because the inserted promoterless beta- galactosidase will be expressed under the control of the Ecscr promoter. The SV40 polyA has the ability to terminate transcription and add a polyA tail to mRNA (Li *et al.*, 2012). In order to select which ES cells were successfully transfected with the construct, it contains a Neomycin-resistance (Neo) cassette with an mPkg polyA that has the same function as the SV40 polyA. This cassette is under the control of a hybrid promoter between human ubiquitin C (that permits its expression in mammalian cells, such as ES cells) and a prokaryote promoter EM7, that allows the expression in bacteria for positive selection when the construct is being made and purified before going into the ES cells (Liu *et al*., 2003). The Neo cassette (promoter, open reading frame and polyA) is flanked by two loxP sites in the same orientation. This allows for further removal of the cassette, if required, using a Cre recombinase. LoxP sites (locus of X-over P1) from bacteriophage P1 are a 34 base pair long region consisting of two flanking 13 base pair palindromic sequences and an 8 base pair central sequence that is asymmetric. If the two sites are in the same orientation, the recombinase will produce a deletion; if the LoxP sites are in opposite orientations, then an inversion will be obtained (Nagy, 2000).

Once a null knockout mouse is produced using the method mentioned above, the alteration will be permanent. However, if the knockout is lethal, either embryonically or during any other time early in life, some studies may not be possible. To overcome this problem, as well as allow gene function studies in mice under challenging conditions, in specific cell types or age, conditional knockout mice can be created instead. The KOMP provides constructs to produce conditional gene knockout in mice that they termed "knockout-first". As for the previous construct, two homologous recombination arms are present (figure 5.2). This is a multi-purpose construct, that in the first instance works like the null one and a LacZ cassette will report if and

where the trap occurs. However, it differs in the way the LacZ cassette is inserted, as RNA processing signals have been added to the design. The promoterless beta-galactosidase cassette with its polyA tail starts with a splice acceptor from the gene engrailed homeobox 2, which allows it to be spliced onto the preceding mouse exon. In the case of the construct available for Ecscr, it would be exon 1. To prevent an accidental in frame stop codon between the mouse sequence for the gene of interest and the lacZ open reading frame (which would result in no beta-galactosidase expression), or a frameshift, or a fusion protein that might not be active, an encephalomyocarditis virus (EMCV) internal ribosomal entry site (IRES) has been included. This ensures that, regardless of the transcript, the enzyme will be fully and independently produced and can act as a reporter in the cells where the protein of interest is ablated. The Neo cassette under the control of the human beta-actin promoter and with its polyA tail has the same function as that mentioned for the null construct. The construct described is a modification of the one developed by Testa *et al*. (2003).

In order to produce a conditional knockout mouse, the two cassettes (LacZ and Neo) have been flanked by FLP (flipase) recognition target (FRT) sites. Flipase is a recombinase that works in the same fashion as Cre, but recognises a different sequence. Upon removal of the cassette, the mice need to be subsequently crossed with a Cre-expressing deleter strain to finally remove the genomic information between the LoxP sites.

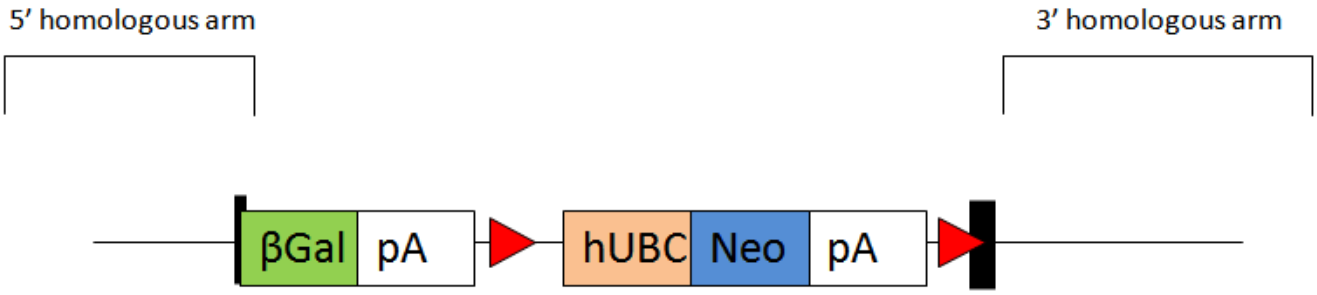

Figure 5.1 - Targeting trap construct produced by the KOMP, used to make an Ecscr null knockout mouse.

In this type of construct there are two homologous recombination arms, 5' and 3', so that the sequences contained between them can be integrated into determined specific locations in the genome. In the case of the Ecscr construct, the whole cassette was inserted between the 24 first nucleotides of exon 1 (in the untranslated region) and the first 6 nucleotides of exon 9, immediately before the stop codon. A promoterless β-galactosidase open reading frame followed by a simian virus 40 polyadenylation signal will both interrupt the gene and indicate in which cells that has happened upon LacZ staining. The construct also contains an ES cell selection Neomycin-resistance (Neo) cassette. The two loxP sites flanking this cassette allow for further removal, if desired, using a Cre recombinase.

βGal – beta-galactosidase; pA – polyadenylation signal; hUBC – human ubiquitin C promoter (the box represents a hybrid promoter, containing mostly sequence from hUBC promoter and 67 nucleotides from the EM7 promoter); Neo – neomycin resistance cassette; red triangles – loxP sites; vertical black rectangles – exons.

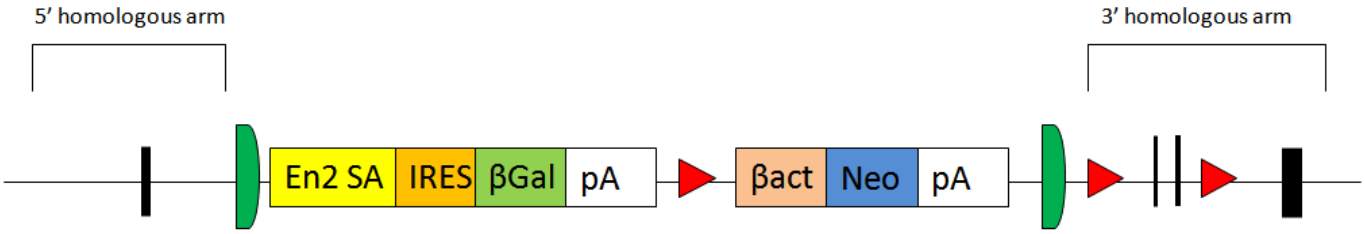

Figure 5.2 - Knockout-first allele construct produced by the KOMP, used to make a conditional knockout mouse.

In this type of construct two homologous recombination arms are present. When it is introduced into cells, it produces a null knockout and a LacZ cassette will report if and where the trap occurs. The promoterless beta-galactosidase cassette will be spliced onto the preceding exon due to the insertion of a splice acceptor. An internal ribosomal entry site was added so that the enzyme produced is not fused to any fraction of the trapped protein. This construct also comprises a Neo cassette for ES cell selection. To produce a conditional knockout mouse, the two cassettes are flanked by flipase recognition target (FRT) sites. Upon their removal, the mice will subsequently be crossed with a Cre-expressing deleter strain to finally remove the genomic information between the LoxP sites.

En2 SA – engrailed homeobox 2 splice acceptor; IRES – internal ribosomal entry site; βGal – beta-galactosidase; pA – polyadenylation signal; βact – human beta-actin promoter; Neo – neomycin resistance cassette; red triangles – loxP sites; green rectangles – FRT sites; vertical black rectangles – exons.

There are currently two effective flipase deleter strains available. The first, Flpo, was produced in a C56BL/6 background with a codon-optimised Flpo gene, which showed higher recombination efficacy compared to Flpe deleter mice. A complete removal of the FRT-flanked Neo cassette was observed in the first generation, that was then passed on to further generations (Wu *et al*., 2009). If the construct used has the FRT sites in opposite orientations, then an inversion rather than a deletion is necessary to make a conditional knockout mouse. For that purpose, a ROSA26Flpo deleter strain has been successfully created, using the codon-optimised Flpo at the ROSA26 locus. Like the previous one, this line is also more efficient than the traditional Flpe (Raymond and Soriano, 2010). As for Cre deleter strains, there are many available, that produce constitutive knockouts in specific tissues or inducible ones, activated by drugs. This offers many possibilities and applications.

5.2 Ecscr expression in mouse

In order to assess if Ecscr displayed the same endothelial specific distribution as in zebrafish and human tissues, an RNA *in situ* hybridization was performed. The mouse protein seemed to be expressed in the trunk, intersegmental and brain vasculature (figure 5.3). Although there was no staining with the sense probe (figure 5.3 A), there is much background produced with the antisense probe, which needs optimization. However, the observed pattern was similarly described by Ikeda *et al*. (2009).

5.3 Initial attempt produce a conditional knockout mouse

As Ecscr seemed to have a vascular distribution in the mouse, a conditional knockout was attempted, to characterise the role of the protein using this model. The original project

encompassed the in-house production of the construct and its subsequent electroporation into ES cells.

A construct was designed as shown on figure 5.4. In short, a *Sna*BI-*Age*I fragment from the mouse BAC clone bMQ121H10 would be cloned into the *Sma*I site of pBluescript by blunt-end ligation. This fragment consists of 5.2 kb of genomic DNA upstream of the first exon, all 9 exons and 7.3 kb of genomic DNA downstream of the last exon. Unique restriction enzyme sites within this fragment were selected to incorporate loxP sites as well as a neomycin selection cassette.

To delete the exons 1-7, a loxP site would be inserted at *Hpy*99I site before exon-1 and at *Pme*I site after exon-7. A neomycin cassette flanked by FRT sites would be excised from pMyb3.0H vector (provided by Dr. Paloma Garcia, University of Birmingham) and cloned into the *Afe*I site after exon-9 by blunt-end ligation (Garcia *et al*., 2005). A thymidine kinase (TK) gene would be cloned into the *Xho*I site of pBluescript. The targeting construct would be linearized with *Not*I (which does not cut the 20.6 kb Ecscr fragment) before electroporation into the ES cells.

To detect homologous recombination, two probes (one each at upstream and downstream of the recombination arm) could be used. To do the southern blot using the upstream probe, the genomic DNA would be digested with *Cla*I. For detection using the downstream probe the DNA would be digested with *Mfe*I.

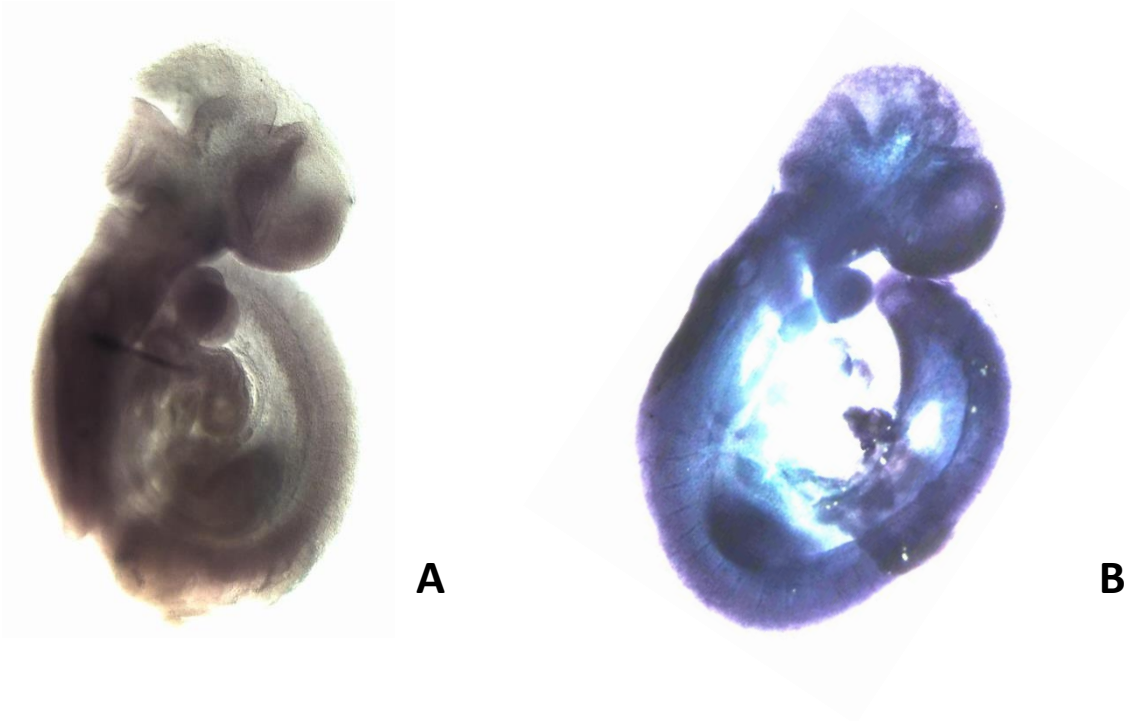

Figure 5.3 – Ecscr transcript distribution pattern detected by whole mount *in situ* hybridization

The mouse Ecscr transcript was detected in E9.5 C57bl/6 wild type mouse embryos. Although excessive background is present in embryos treated with the Ecscr-specific (antisense) probe, there seems to be specific staining on the main trunk and head vessels, as well as the intersegmental vessels. (A) Sense probe, (B) Antisense probe.

The strategy described above was put into practise, but all the attempts to obtain the fragment of interest from the BAC have failed. Both restriction digestion and combined PCR amplification and ligation were not successful in obtaining the desired fragment. Despite Professor Gerard Eberl's (Pasteur Institute, France) advice on BAC extraction, purification and handling, it was impossible to even amplify a small fragment (800 bp) from the original vial by PCR-colony.

As an alternative, embryonic stem (ES) cells were purchased from the Sanger Institute to generate a conditional knock out mouse for Ecscr. These cells for the conditional knockout mouse were produced by the knockout mouse project – KOMP (http://www.knockoutmouse.org). The line JM8A1.N3 is subcloned from JM8 parental line, derived from C57BL/6N mice. These ES cells have been modified to correct the black mutation on the Agouti allele and originated an Agouti coat colour (Pettit *et al*., 2009). This work has been carried out at the University of Birmingham's MRC centre for immune regulation by the centre's animal resource manager Andrea Bacon.

Recipient blastocysts were harvested from C57BL/6OlaHsd pregnant black mice and injected with the JM8A1.N3 ES cells containing a construct with potential to obtain an Ecscr conditional knockout (figure 5.2). In total 160 correctly injected blastocysts were implanted in the uteri of CD-1 pseudopregnant white mice (16 per mouse, 8 on each side). Only four chimeras were born in total, 3 males and one female. The coat colour chimerism was about 50% for each mouse, but no germline transmission was observed. One of the males has never successfully had a female producing a plug and a second one had to be culled before germline testing, due to severe skeletal malformations (the necropsy revealed a protruding xyphoid process and a much arched spine when compared to a sex and age-matched littermate). The

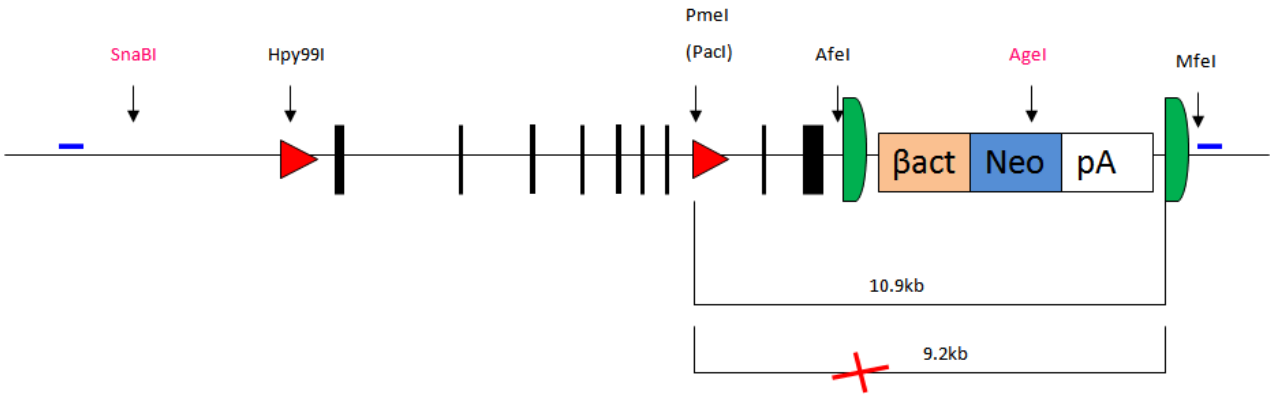

Figure 5.4 - Diagram showing the original construct design to generate a conditional Ecscr knockout mouse.

To make this construct, a fragment consisting of 5.2 kb of genomic DNA upstream of the first exon, all 9 exons and 7.3 kb of genomic DNA downstream of the last exon would be excised and inserted into pBluescript. Unique restriction enzyme sites within this fragment were selected to incorporate loxP sites, as well as a neomycin selection cassette. To detect homologous recombination by southern blot using the upstream probe, genomic DNA would be digested with *Cla*I. For detection using the downstream probe the DNA would be digested with *Mfe*I. The wild type and transgenic fragments would have different sizes, depending on whether the cassette had been incorporated or not.

βact – beta-actin promoter; pA – polyadenylation signal; Neo – neomycin resistance cassette; red triangles – loxP sites; vertical black rectangles – exons; green rectangles – FRT sites

remaining male and the female have only ever produced descendents with a black coat.

In order to assess that the construct had been built according to its design, critical regions were amplified by PCR and sequenced (figure 5.5, table 5.1). Samples from FVB/N white mice and C57BL/6OlaHsd black mice were used as wild type. All the tested regions of the construct were successfully amplified and identified. However, since there was no germline transmission observed, the ES cells were compared to those used to make a full knockout mouse in our laboratory, which have given rise to germline transmission (for Clec14a). Overall, the morphology of both types of ES cells was similar, as well as the chromosome spreads (both contained 40 chromosomes) (Figure 5.6).

In the KOMP website, a different type of clone was available for purchase. This is the one that was used to create Clec14a null knockout mice and its design is less complex. Basically, upon homologous recombination, the whole Ecscr gene will be replaced with a LacZ cassette (figure 5.1). The genotyping strategy is also simpler, as depicted on table 5.4. This clone has produced germline transmission, as shown on the next chapter.

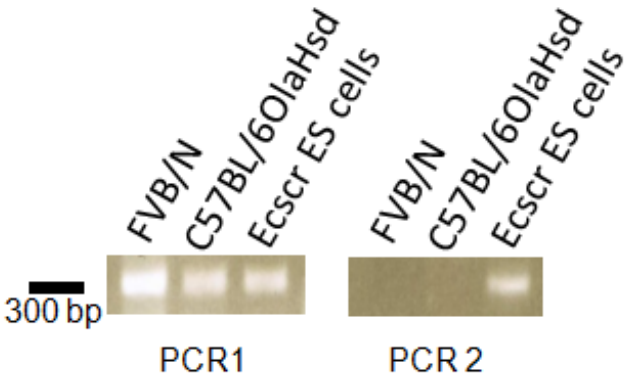

Figure 5.5 - Example of the PCR strategy used to identify the different components of the knockout-first construct.

PCR 1 was performed using the pair of primers 3armF + 3armR (table 5.1). This corresponds to a region in the wild type genome. As the ES cells are heterozygous, all there samples were positive. PCR2 refers to a region within the cassette introduced by homologous recombination, amplified with the pair Universal5F + Common-n2R. Therefore, only the ES cells provided amplification of a band.

Table 5.1 - PCR strategy to identify critical regions in the KOMP construct to originate a conditional knockout mouse for Ecscr.

The numbers correspond to the amplicon size in base pairs.

Primers	FVB/N	C57BL/6OlaHsd	ES cells	Homozygous
5armF + 5armR	330	330	330	330
5beforeInsF + 3afterInsR	328	328	-	328
Universal5F + Common-n2R	-	-	303	303
3IRES5F + LacZR	-	-	279	279
Common3F + BactR	-	-	368	368
RAF5F + FRTLoxR	-	-	386	386
mECSCRinSituF + WTintron3R	382	382	382	382
CommonLoxPF + Universal3R	-	-	359	359
3armF + 3armR	303	303	303	303

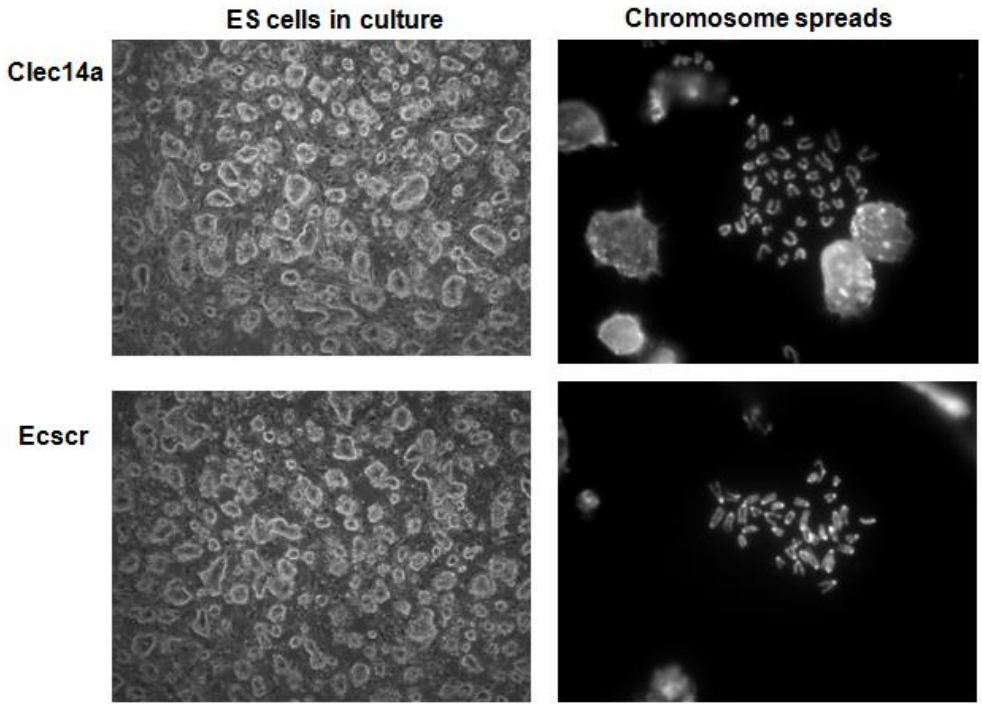

Figure 5.6 - Comparison between ES cells purchased from the KOMP containing constructs for Clec14a and ECSCR knockout mice.

ES cells containing a conditional construct for Ecscr were compared to those used to make a full knockout mouse in our laboratory, which have given rise to germline transmission (for Clec14a). Overall, the morphology of both types of ES cells was similar, as well as the chromosome spreads (both contained 40 chromosomes).

5.4 Producing a null Ecscr knockout mouse

ES cells containing the conditional knockout-first construct (figure 5.2) were initially bought from the KOMP, as they offer the possibility of making both a null and a conditional knockout. However, the number of chimeras produced was very low (only 4 in total, having one suddenly died) and there was no germline transmission. Alternatively, ES cells containing the construct to produce a null Ecscr knockout mouse (figure 5.1) were purchased.

These ES cells were expanded and injected into blastocysts by the MRC transgenic facility manager at the University of Birmingham, Dr. Andrea Bacon. The ES cells derived from the (black) C57BL/6NTac strain, so they were injected into blastocysts from an albino black 6 strain B6(Cg)-*Tyr*$^{c-2J}$/J (or B6-albino) and implanted into the uteri of pseudopregnant females also from the latter strain. As, in very simplistic terms, black is dominant over white, the degree of chimerism observed in the mice's coat colour is an indicator of how well the ES cells have integrated into the embryos. The higher the percentage of black compared to white, the higher the probability of germline transmission. To test for germline transmission two male chimeras with over 50% black coat were chosen to be crossed with B6-albino females. One male has produced several litters of all-white pups and another one has produced both white and black pups, which confirms germline transmission for the latter male, but not the former.

A detailed description of the litters produced by the male chimera is shown on table 5.2. Ten litters were produced, with 25 black pups in total. 60% of the pups were heterozygous and 40% were wild type. The sex ratio was 48% males and 52% females. Of the heterozygous, 66.7% were males and 33.3% females. Interestingly, as more litters were produced, the number of black pups in each increased (table 5.2).

Table 5.2 - Ecscr clone AB8 chimera #2 germline transmission progeny F1 (into B6-albino background)

Litter number	Date of birth	Pups born	Black pups	% black pups	Sex, ID of black pups	Genotype
LN1	16.05.2012	9	1	11.1	1 male	het
LN2	20.05.2012	8	1	12.5	1 male	het
LN3	01.06.2012	8	2	25.0	2 females	het; het
LN4	08.06.2012	9	2	22.2	2 females	het; het
LN5	14.06.2012	8	2	25.0	1 male, 1 female	wt; wt
LN6	19.06.2012	7	2	28.5	1 male, 1 female	het; het
LN7	04.07.2012	9	2	22.2	2 males	het; het
LN8	11.07.2012	8	4	50.0	1 male, 3 females	het; wt; wt; wt
LN9	15.07.2012	9	5	55.6	3 males, 2 females	het; wt; het; wt; wt
LN10	16.07.2012	8	4	50	2 males, 2 females	het; het; wt; wt

LN – litter number; het – heterozygous; wt – wild type; the male heterozygous mice are highlighted in blue and the females in pink. The wild type mice of both sexes are depicted in black, as they are not required to proceed with the creation of a knockout mouse at this stage. However, in the "genotype" column, the mice are in the same order as in the previous column.

Once the heterozygous mice were old enough to breed (6-8 weeks), they were crossed using males and females from different litters, as depicted on table 5.3. Not all litters have produced knockout mice but, once positive males and females are mature, they will be crossed to produce a pure knockout colony. As this work is currently ongoing, it is yet unknown if the knockout mice can survive until reaching maturity and old age, if they are fertile and what phenotype the absence of Ecscr causes.

5.5 Genotyping strategy

The most well-known inbred mouse strain is C57BL/6. From this one, nine other substrains have been created, including the C57BL/6J (from the Jackson Laboratory) and C57BL/6N (from the National Institutes of Health). A study has found genetic differences between these two major substrains while genotyping for single nucleotide polymorphisms (SNP) at eleven loci. Even among C57BL/6J substrains there are more substantial differences. For example, the same group has found a deletion of exons 7-11 from the nicotinamide nucleotide transhydrogenase gene in C57BL/6J strains and 1,446 SNPs genotyping among seven C57BL/6 strains (Mekada *et al*., 2008). For this reason, the first step before injecting the ES cells into B6-albino blastocysts was to check that the Ecscr gene was present in the strain of choice (C57BL/6JOlaHsd). A positive band obtained by PCR served both to optimise the PCR conditions for genotyping and to be able to proceed, as Ecscr is present in this strain.

PCR of small fragments from genomic DNA (up to 400 base pairs) was chosen as the genotyping strategy, over the more traditional southern blot. The tissue samples used for genotyping were ear clippings (that serve this purpose, as well as numbering of the pups).

Table 5.3- Crosses between Ecscr clone AB8 chimera #2 heterozygous progeny to obtain knockouts

Litter number	Parents	Date of birth	Pups born	Sex, ID of pups	Genotype	White pups
LNA	LN3F#1 x LN1M#1	12.08.2012	5	2 males, 3 females	het; het; wt; wt; het	0
LNB	LN3F#2 x LN2M#1	09.08.2012	(8)/6	5 males, 1 female	wt; het; wt; het; ko; het	1 male
LNC	LN4F#2 x LN6M#1	07.09.2012	(11)/10	5 males, 5 females	het; wt; het; ko; ko; wt; wt; het; ko; het	(4)/3
LND	LN4F#1 x LN7M#1	20.09.2012	8	Not yet known	Not yet known	0

LN – litter number; F – female; M – male; het – heterozygous; wt – wild type; ko – knockout; the male knockout mice are highlighted in blue and the females in pink. In the "genotype" column, the mice are in the same order as in the previous column. The numbers in brackets represent the total of pups born in a given litter and the number next to them represents the how many of pups were in the litter after a death.

Table 5.4- Genotyping strategy

The primer combinations and respective expected amplicon sizes for wild type, heterozygous and knockout mice are presented.

Primers	WT band (bp)	Het band (bp)	KO band (bp)
5armF + ULacZ-Rev	-	445	445
UNeo-Fw + mECSCR-in situR	-	432	432
mECSCR-in situF + WTintron3R	382	382	-

WT – wild type; Het – heterozygous; KO – knockout; bp – base pairs.

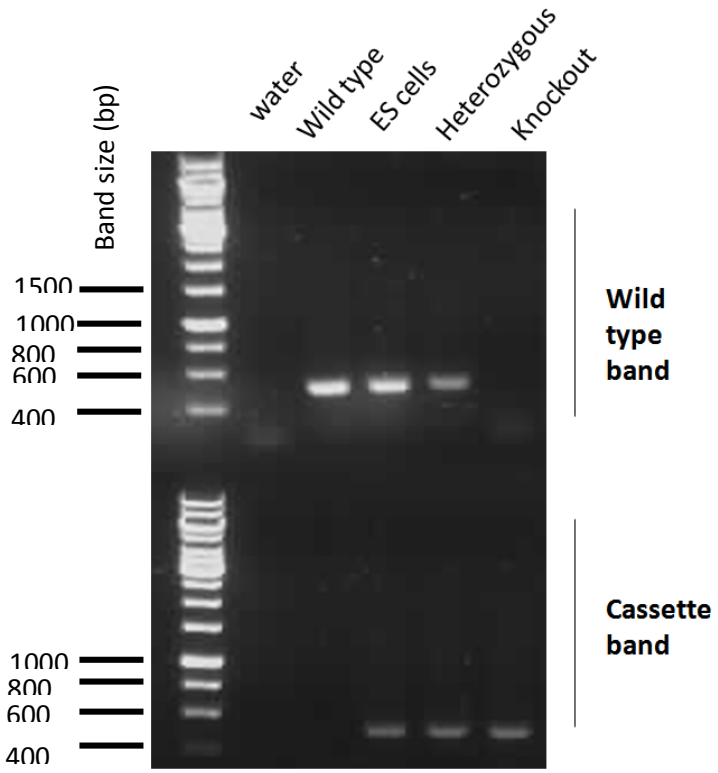

Figure 5.7 - Example of genotyping results for wild type, heterozygous and knockout mice

In order to determine zygosity, a biopsy from each pup has to be submitted to PCR analysis for both wild type and cassette bands. Wild type mice are expected to have only the wild type band, samples from knockout mice should contain only the cassette band and heterozygous will have both. The wild type band is the resulting amplicon from mECSCR-in situF and WTintron3R primers and the cassette band is obtained using the primers 5armF and ULacZ-Rev. DNA from the ES cells used to produce the chimeras (heterozygous) was extracted and submitted to PCR analysis, as a positive control to check band sizes.

Primers were designed to amplify both wild type bands (present in wild type and heterozygous mice) and cassette bands (present in heterozygous and knockout mice) (table 5.4). The primers to amplify the cassette bands were planned so that one of them would bind to the mouse genomic sequence and the other would bind to a region in the cassette. As they should provide the same answer, one pair for each side of the cassette was tested. The combination of UNeo-Fw + mECSCR-in situR provided a single, clearer band, compared to 5armF + ULacZ-Rev, so this was chosen for further genotyping. The ES cells were used to optimise the primers for the cassette.

As illustrated on figure 5.7, both bands are needed to interpret the genotyping results. The wild type mice should only have the wild type band (as the cassette was engineered and inserted by homologous recombination), the heterozygous mice should have both bands, as they have one wild type allele and another one that is modified. The ES cells purchased from the KOMP are also heterozygous. The knockout mice should have a complete replacement of the wild type band by the cassette.

5.6 Monitoring and mapping the replacement of Ecscr by beta-galactosidase

As previously discussed, the knockout-first construct includes a gene trap that expresses beta-galactosidase when and wherever it replaces the target gene. The location of this enzyme can easily be identified by LacZ staining. Litter number C (table 5.3) was suddenly left orphan and rejected by a possible foster mother. As the pups were too old to foster and too young to survive on their own (11 days post-natal), they had to be culled. This provided an opportunity to perform a LacZ stain. Briefly, after genotyping the pups (results shown on table 5.3) the heart

and lungs were removed and rapidly fixed. Then, they were incubated with X-Gal, a substrate for beta-galactosidase, fixed overnight and examined under the microscope.

The degradation of X-gal produced a blue product, easily identifiable. It was possible to see a dose-dependent effect, and no stain was observed for the wild type organs, some staining was observed in the organs from heterozygous mice and strong staining was noted in organs belonging to knockout mice. The lungs of the knockout mice were very strong blue (figure 5.8). After being stained for LacZ activity, the lungs were included in paraffin, sectioned and stained with hematoxylin and eosin to analyse tissue morphology. Lungs from knockout mice seemed to be denser, containing more cells and less air space than those from wild type (figure 5.9). As for the hearts, a very interesting distribution pattern for the Ecscr has emerged (figure 5.10). It doesn't seem to be present in large vessels and it seems to be found only on (some but not all) small capillaries around the heart. Also, in the hearts from knockout and, to a lesser extent, heterozygous mice, there seems to be an asymmetry, where the right atria look enlarged.

5.7 Monitoring the Ecscr protein and transcript amounts in wild type, heterozygous and knockout mice

To further confirm the deletion of Ecscr, a small sample of lung, kidney, liver and blood was taken from a specimen of each category. The tissues were macerated using a homogeniser and the total protein was extracted and analysed by western blot, using the anti-human ECSCR polyclonal antiserum. Unfortunately, in spite of the homology between the human and mouse proteins, this antiserum didn't seem to detect the murine version. Alternatively, small samples of lung had also been taken and snap frozen. Total RNA was extracted, converted into cDNA and a qPCR (real-time quantitative polymerase chain reaction) was performed. The data were normalised to actin and are represented as relative expression compared to the wild type (figure 5.11). As observed for the colour gradient in the LacZ staining, Ecscr is no longer present in

the lungs from knockout mice and it is present in approximately half the amount of the wild type in heterozygous mice. As these are preliminary data, only one specimen per category was analysed for qPCR. Each sample was analysed in triplicates for Ecscr and actin.

A B C

Figure 5.8 - LacZ staining of lungs from wild type (A), heterozygous (B) and knockout (C) mice

The construct used to produce an Ecscr knockout mouse contains a gene trap LacZ cassette, that prevents Ecscr from being transcribed and uses its promoter to produce beta-galactosidase instead. This way, the deletion of Ecscr and replacement by this enzyme can be monitored through lacZ staining, via the conversion of Xgal into a blue product. Lungs from wild type mice do not contain beta-galactosidase, therefore, there was no blue colour observed. Lungs from knockout mice displayed a bright blue coloration, due to enzymatic activity. Lungs from heterozygous mice exhibited a pale blue colour, resulting from less beta-galactosidase being present.

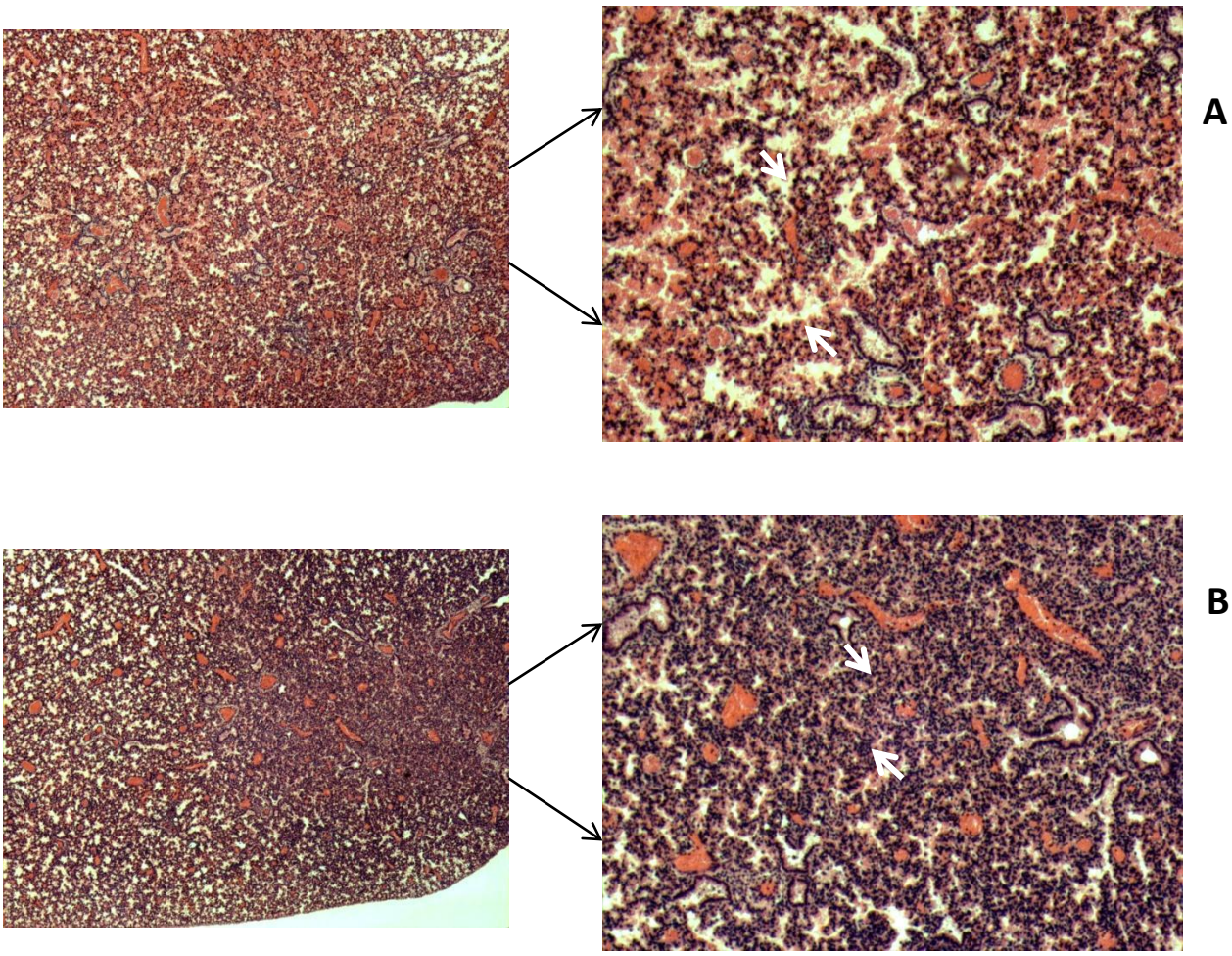

Figure 5.9 – Hematoxylin and eosin staining of lung paraffin sections from wild type (A), and knockout (B) mice

After being stained for LacZ activity, the lungs were included in paraffin, sectioned and stained with hematoxylin and eosin to analyse tissue morphology. Lungs from knockout mice seemed to be denser, containing more cells and less air space than those from wild type.

Total magnification of the images on the left hand side is 2.5x and 7.2x on the right.

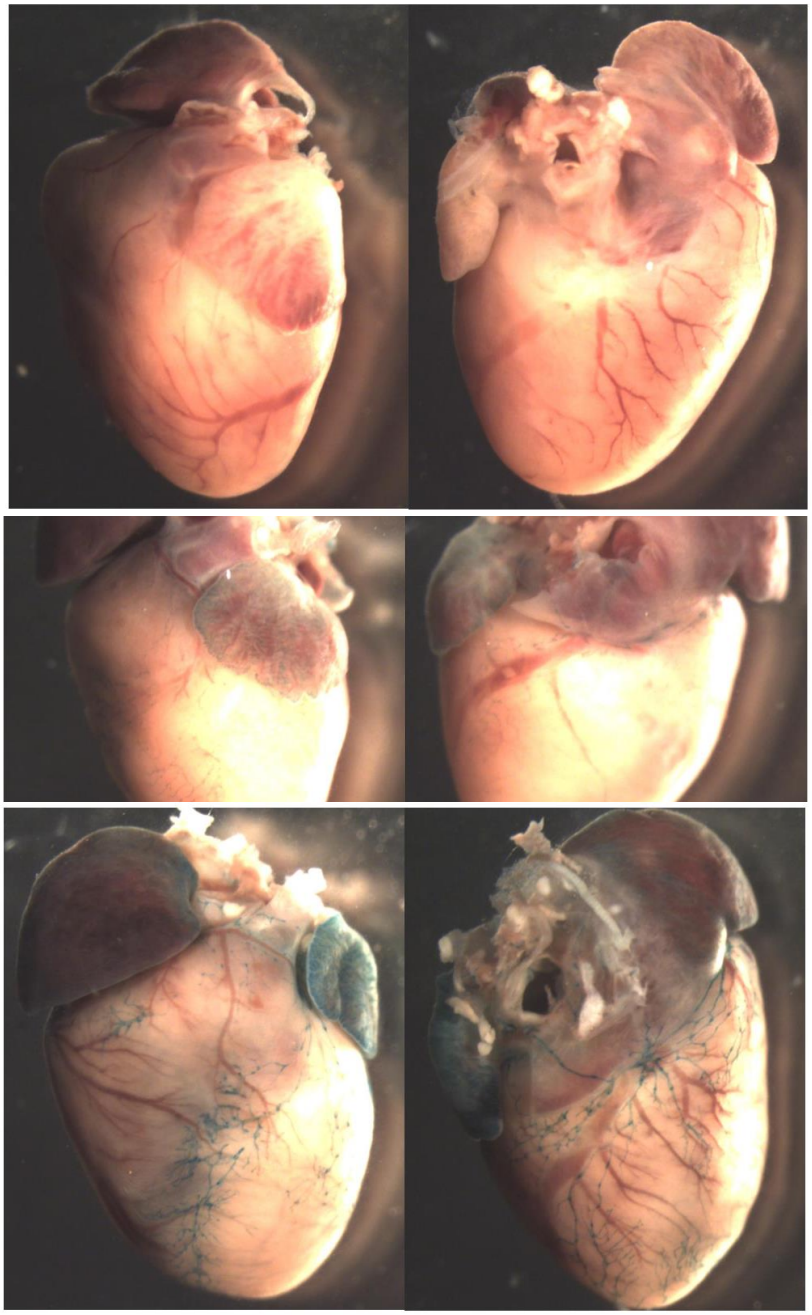

Figure 5.10 - LacZ staining of hearts from wild type (A), heterozygous (B) and knockout (C) mice

As described on figure 5.4 for lungs, hearts from wild type, heterozygous and knockout mice were also stained for LacZ activity. Wild type hearts have no blue stain, hearts from knockout mice show some external vessels (but not all) stained in blue and heterozygous hearts display the same pattern as the knockouts, with a weaker signal. The right atria of knockout mice and, to a lesser extent, heterozygous, seem to be enlarged compared to those of wild type mice.

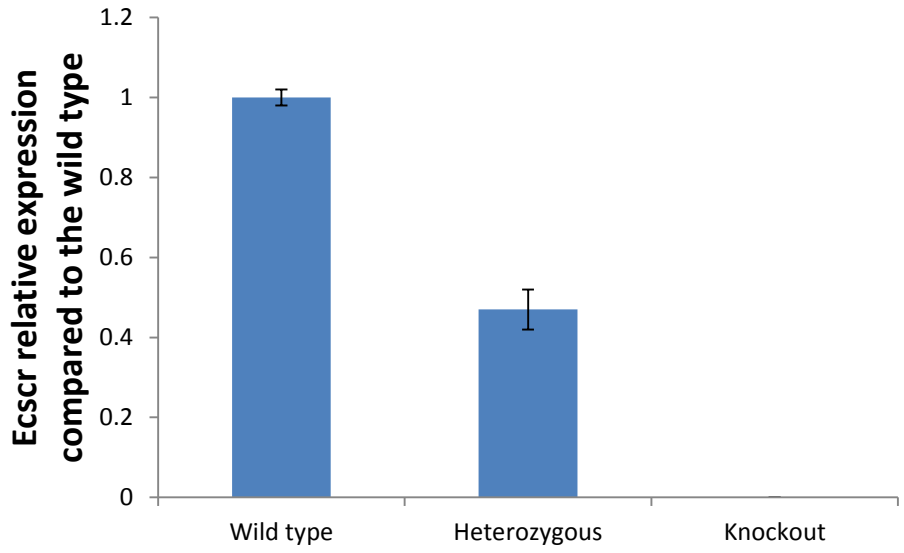

Figure 5.11 - Ecscr relative expression in lung from wild type, heterozygous and knockout mice

RNA was extracted from lungs of wild type, heterozygous and knockout pups and quantitative PCR was performed for Ecscr and actin (3 times for each sample). Ecscr expression was normalised to that of actin and the relative expression compared to the wild type are represented. As expected, heterozygous mice have approximately half of Ecscr expression compared to the wild type and no Ecscr was detected in knockout mice. The error bars represent the standard deviation of the mean of the 3 replicates. No statistical analysis was performed to obtain significant differences between categories, as the aim is purely to observe that Ecscr expression is consistent with the genotyping results.

5.8 Discussion

5.8.1 Ecscr transcript expression patterns in mouse E9.5 embryos

Initial results from Ecscr *in situ* hybridization of E9.5 wild type embryos show that the mouse protein seems to be expressed in the trunk, intersegmental and brain vasculature (figure 5.3). Ikeda *et al*. (2009) found a similar distribution using the same technique and also E9.5 embryos. Their images for the entire embryo were even less clear than those in this thesis. They have then sectioned the embryos, which revealed more conclusive staining results. These authors described that Ecscr transcript is present in the intersegmental arteries, dorsal aorta and blood vessels of the yolk sac. Furthermore, they have generated an antibody against mouse Ecscr, which has detected the protein in bronchial epithelial cells, artery and vein in lung, as well as blood vessels in spleen. In blood vessels, they claimed Ecscr is expressed in both endothelial and smooth muscle cells. No further detail is provided regarding the age of the mice or what artery(ies) or vein(s) have been stained.

The antisense probe has produced much background. This can be because the probe was too concentrated, in which case it should be diluted for further experiments. Probes can be re-used and tend to produce too much staining the first time they are used and work better in subsequent cycles of usage. Also, the protocol optimised by Thisse and Thisse (2008) for zebrafish was applied to mouse embryos. Because these are thicker and of different nature, they may not have been completely digested, which may have resulted in incomplete penetration of the probe. A protocol dedicated to mouse embryos should be applied, such as the one described by Piette *et al*. (2008). This protocol is largely similar to that described for zebrafish, but contains incubation times specific for the various mouse developmental stages and an additional

permeabilization step with RIPA buffer after the proteinase K digestion, which may contribute for better results.

As Ecscr appeared to have an endothelial distribution, a knockout mouse model was generated to study its role in vascular development.

5.8.2 Generation of an Ecscr knockout mouse model

In order to create an Ecscr knockout mouse model, different approaches were adopted, as it was not a straightforward procedure. Firstly, a construct to obtain a conditional knockout mouse was designed (figure 5.4). Exons 1-7 would be deleted, as loxP sites would be inserted at *Hpy*99I site before exon-1 and at *Pme*I site after exon-7. A neomycin cassette flanked by FRT sites (used to screen positive ES cells once electroporated with the linearized construct) would be cloned into the *Afe*I site after exon-9 by blunt-end ligation (Garcia *et al*., 2005). The design of this construct could have been improved by the insertion of a reporter gene, such as β-galactosidase, which allows the visualization of where the gene of interest would be deleted (Austin *et al*., 2004). At the time Ecscr expression in mouse embryos seemed to be endothelial-specific, but the *in situ* hybridization technique had to be much improved to have a more definitive answer (figure 5.3). Making a conditional knockout mouse meant that even if Ecscr expression was not restricted to the endothelium, its role in endothelial cells could still be studied by crossing these mice with, for example, the Tie-1-Cre delete strain. In these mice Cre recombinase is expressed in endothelial cells of embryoid bodies and transgenic mice driven by the Tie-1 promoter (Gustafsson *et al*., 2000). To confirm endothelial specificity, these mice were crossed with Rosa26R reporter mice. The Rosa26R mice have the lacZ gene inserted into the ubiquitously expressed Rosa locus that is preceded by a transcriptional stop cassette flanked

by loxP sites (Mao *et al*., 1999; Soriano, 1999). LacZ staining showed that the Tie-1-Cre transgenic strain can efficiently direct deletion of floxed genes in endothelial cells *in vivo* (Gustafsson *et al*., 2000). Another advantage of a floxed strain is the possibility of halting expression of the gene of interest at a specific point in the animal's life. This was achieved with the creation of CreER inducible strains, where ligand-dependent Cre recombinases can be activated by administration of tamoxifen to the animal, which binds to the oestrogen receptor (ER) and prevents expression of the gene of interest. Cre is fused to a mutant ER that binds to tamoxifen but not endogenous ligands and translocates into the nucleus upon tamoxifen induction. CreER tissue-specific strains have also been produced (Feil *et al*., 2009).

The production of this construct was, however, unsuccessful, as all components were correctly inserted into the backbone plasmid, but the genomic insert containing Ecscr full length and 5.2 kb of genomic DNA upstream of the first exon, as well as 7.3 kb of genomic DNA downstream of exon 9 was not effectively excised or amplified to be included in the final construct. This was probably due to inexperience and lack of expertise in this area. As an alternative strategy, ES cells were purchased from the KOMP that contained a knockout-first construct, with the potential to also generate a conditional knockout mouse (figure 5.2). This approach is less time-consuming and potentially yields more successful results, as the constructs and ES cell handling and electroporation are done by a team of experienced experts. The first step was to confirm that indeed the construct had all the elements as described. For that purpose, several PCR reactions were performed to amplify and sequence small key sequences such as LoxP sites, LacZ cassette or the actual Ecscr gene (figure 5.5; table 5.1). As the identity of all of them was confirmed, these ES cells were then injected into recipient blastocysts to generate chimeras. The number of chimeras created was low and no germline transmission was observed. In an attempt to understand why this strategy had failed, chromosome spreads were

done for these ES cells compared to ES cells containing a targeting trap construct used to successfully produce Clec14a null knockout mice, under the guidance of Dr. Laura O'Neil (University of Birmingham, UK). No evident abnormalities were observed (figure 5.6).

Generating transgenic mice from genetically modified ES cells injected into blastocyst hosts produces chimeras that are only partially derived from the ES cells. These chimeras have to be tested for germline transmission of the mutant features and then the offspring need to be further crossed to obtain homozygosity. This is a long and expensive process and germline transmission is not guaranteed. An alternative strategy was proposed by Poueymirou *et al*. (2007): laser-assisted injection of transgenic ES cells into 8-cells embryos (rather than blastocysts). This has efficiently yielded F0 generation mice that are fully ES cell-derived and healthy, have 100% germline transmission and allow immediate phenotypic assessment (Poueymirou *et al*., 2007). This alternative route could be explored by the University of Birmingham transgenics unit, however it requires specialised equipment, training and high level of skill.

Finally, ES cells containing a targeting trap construct to produce a null knockout mouse were purchased from the KOMP (figure 5.1). Injection of these cells into blastocysts has produced chimeras that yielded germline transmission of the engineered inserted cassette. The first generation was heterozygous and by the time of completion of this thesis heterozygous mice had just been crossed and produced the first homozygous pups (tables 5.2 and 5.3). To distinguish between homozygous, heterozygous and wild type mice, a combination of two PCR reactions had to be analysed (table 5.4; figure 5.7). Homozygous (knockout) mice had the cassette interrupting Ecscr successfully inserted in both alleles, as confirmed by the presence of an amplicon for the cassette and complete absence of the wild type band. This is because the primers designed to detect the wild type band bind to a region that was replaced by the cassette

by homologous recombination. Conversely, in samples from wild type mice only the wild type band is detected. This is because the cassette was engineered and its elements do not naturally occur in the mouse genome. Heterozygous mice contain one wild type allele and one allele where the cassette has been inserted by recombination. Therefore, both products are amplified by PCR.

Apart from a less complex construct than the knockout-first, the targeting trap was also electroporated into different ES cells. The conditional construct was inserted into JM8A1.N3 cells, subcloned from JM8 parental line, derived from C57BL/6N mice. These ES cells have been modified to correct the black mutation on the Agouti allele and originated an Agouti coat colour (Pettit *et al*., 2009). For this reason, recipient blastocysts had to be harvested from C57BL/6OlaHsd pregnant black mice rather than white mice. This has produced black and brown chimeras rather than the traditionally white and black ones. In this case, the less black coat coverage (and more brown), the more likely chimeras are to produce germline transmission. The opposite is true for the null knockout mice. Since the ES cells derived from the (black) C57BL/6NTac strain, they were injected into blastocysts from an albino black 6 strain B6(Cg)-*Tyr*$^{c\text{-}2J}$/J (white). Therefore, the more black hair patches compared to white, the more likely a chimera will be to yield germline transmission. It can be hypothesised that simpler constructs somehow have a higher rate of recombination compared to longer, more complex ones, resulting in faster or more successful germline transmission. So far, in our laboratory, two knockout strains have been successfully produced using the targeting trap construct. Another reason can be related to the nature of the ES cells. It is possible that line specific features determine the success of integration into blastocysts, producing more or less chimeric animals. On the other hand, assuming equal integration potential, the key may lie in recipient blastocysts from different strains being more or less amenable to allow foreign ES

cells to integrate, survive, migrate, and differentiate. To finalise, still regarding the different nature of the ES cells, these were cultured and manipulated in the same way, which may have favoured one line in detriment of the other, that may have been grown under suboptimal conditions, resulting in less efficiency.

Traditionally, white mice from strains other than black 6 were used as blastocyst donors, as well as white mice that were crossed with chimeras to check for the presence of black pups in case of germline transmission (Nagy *et al*., 2003). This would mean that pups from these crossings would be discarded, as they were in a mixed background, which is not desirable. The use of the black 6 albino strain represents an advantage, as it allows an easy method to create knockout mice on the C57BL/6J genetic background and pups from the germline transmission confirmation crossings can be used instead of culled. This is a spontaneous mutation in the tyrosinase gene and when the mice are homozygous for the mutation the coat color is albino rather than black (this information was obtained from the Jackson Laboratory webpage at http://jaxmice.jax.org/strain/000058.html).

5.8.3 Preliminary characterisation of the Ecscr null knockout mouse model

As unfortunately this first litter containing some knockout pups was left orphan too old to be adopted by another female and too young to be weaned, they had to be culled. This has made it impossible to know whether they would be fertile, survive through adulthood or even develop a disease at old age. However, it has created the opportunity to do a preliminary analysis of 11 days old wild type, heterozygous and homozygous knockout Ecscr littermate pups.

Hearts and lungs from the three genotypes were chosen to perform LacZ staining to confirm the loss of Ecscr, as well as observe its location. The targeting trap construct contains a reporter

gene, β-galactosidase, which allows the visualization of a blue enzymatic product coincident with its location (Austin *et al*., 2004). Lungs from wild type pups displayed no LacZ staining, whereas lungs from knockout mice were intensely blue and lungs from heterozygous pups presented an intermediate colour (figure 5.8). This gradient is consistent with the expected amount of Ecscr being expressed, which was confirmed by qPCR (figure 5.11). Lung staining is also consistent with this organ containing 30% of endothelial cells in the body (Atochina *et al.*, 1998). Furthermore, Ikeda *et al*. (2009) have reported Ecscr staining in lung epithelial cells, additionally to endothelial cells, which could explain such an intense and apparently homogeneous staining for lungs from knockout mice. This would also explain why the paraffin sections from knockouts seemed to have a pale blue-green colour throughout the whole tissue, compared to the white (paraffin colour) seen for the wild type. These sections were made from the lungs stained for LacZ. To further investigate this and compare morphology, hematoxylin and eosin staining was performed. Lungs from knockout mice seemed to have less air space and more cells, as evidenced by a much stronger dark purple hematoxylin stain of nuclei (Fischer *et al*., 2008) (figure 5.9). Lung hyperplasia has also been reported by Xian *et al*. (2001) in Dutt1/Robo1 knockout mice. This phenotype is evident since E15.5 and the newborns die within 24h due to breathing difficulties. Ecscr knockout mice live at least until the age of 11 days. Ecscr heterozygous can reach breeding age and are fertile. However, the mother of the pups that has died was heterozygous and the same has been reported for other females by the technicians at the animal facility. According to animal welfare guidelines, because there may be a harmful phenotype that was previously unaccounted for, only heterozygous females were allowed to breed, which slows down the process of obtaining a knockout line. Not all heterozygous females died soon after giving birth, but a higher than normal number did. This needs to be investigated in greater detail. Giving birth to approximately 8-9 pups is a big effort,

that requires intense breathing. Although the LacZ staining was performed only once, as well as sectioning and hematoxylin and eosin, all the observations taken together seem to indicate that the loss of Ecscr may cause breathing problems due to changes in lung morphology and efficiency.

In addition to lungs, hearts from the three genotypes were also stained for beta-galactosidase activity. Surprisingly, only some (but not all) superficial cardiac smaller vessels were stained (figure 5.10). Large vessels, such as the aorta, were not stained. Given that in both zebrafish and mouse embryos Ecscr transcript is found in the dorsal aorta, this was not expected. However, as discussed in section 4, Ecscr may have a more prominent role in the sprouting of smaller vessels and its role in larger vessels may be limited to a specific period during embryonic vascular development. To shed some light into this matter, LacZ staining could be performed in embryos at different stages. Koide *et al*. (2011) have also produced an Ecscr knockout mouse model, where the first three exons were deleted. Although bleeding was observed in embryos, mice were viable and fertile and had an overall otherwise normal development. Small vessel (< 10 μm) density was increased and no change was found in larger vessels. Accordingly, in a critical limb ischaemic model, blood flow recovery and capillary density was significantly increased in knockout mice compared to the wild type.

Additionally, right atria from knockout pups seemed enlarged compared to those of wild types. Again, this can be linked to the phenotype observed in the lungs. Causes of right atrial enlargement include COPD, mitral stenosis, mitral regurgitation, or pulmonary emboli. Most cases of right atrial enlargement are associated with right ventricular hypertrophy (Harrigan and Jones, 2002). This was not as evident, but could be explored by comparing sections of hearts from knockout and wild type mice. In the results from pathway analysis of the microarray data there was a cluster called “cardiac hypertrophy”, where MEF2C is

downregulated. According to Zhao *et al*. (2002) myocyte enhancer factor-2 (MEF2) is more abundant in atria than ventricles and upregulated in the atria in response to hypertrophic stimuli. VEGF induces the expression of and MEF2 is an important mediator of VEGF in endothelial cells (Maiti *et al*., 2008).

5.8.4 Further directions

One of the aims when creating a conditional knockout mouse was to characterise the expression patterns and mechanism of action of Ecscr during embryonic development and tumour angiogenesis. In order to do that, Ecscr knockouts could be compared to the wild type. Namely, cryosections of different developmental stages could be done and immunostained with antibodies against Ecscr and general and specific vessel markers. Other markers may be found relevant from future results obtained with the other models (HUVECs or zebrafish). The embryos could be analysed anatomically and histologically to uncover any defect caused by the loss of Ecscr. The culture of wild type and Ecscr knock out endothelial cells could be attempted in order to assess the behaviour of these cells in angiogenesis assays such as the scratch wound and tube formation on Matrigel. In adult mice (as so far the knockout does not seem to be lethal) a piece of sponge could be inserted subcutaneously and the blood vessel growth into it could be assessed by analysing parameters such as vessel density, number, calibre, morphology (Andrade and Ferreira, 2009). In order to uncover any role for Ecscr in tumour angiogenesis, cancer cells (such as Lewis lung carcinoma) could be injected subcutaneously and tumour growth as well as vascularisation could be assessed (Dudek *et al*., 2007).

6 GENERAL CONCLUSIONS

Angiogenesis, although a normal process during development and wound healing, is also involved in pathological conditions, such as cancer. ECSCR has been identified as an endothelial-specific protein that binds to filamin A and is involved in tube formation and cell migration, possibly via modulation of the actin cytoskeleton. This makes ECSCR a potentially interesting marker for therapy. In the beginning of this project the mechanisms by which ECSCR regulates the cytoskeleton were unknown and required further investigation. Therefore, the aims were to 1) identify ECSCR binding partners and subsequent downstream signalling, 2) determine a putative role in zebrafish vascular development, 3) produce and characterise an Ecscr knockout mouse model and 4) assess whether ECSCR function is conserved across species.

Identification of proteins interacting with ECSCR was done using two *in vitro* approaches, co-immunoprecipitation combined with mass spectrometry and GST pull-down followed by western blotting. Two proteins were chosen for further investigations using yeast-two-hybrid: moesin and filamin A. Yeast-two-hybrid failed to show any association between ECSCR and moesin (as the yeast did not express the latter protein) and confirmed the interaction with filamin A. An alternative method, luciferase complementation assay, has demonstrated an interaction between ESCR intracellular domain and moesin. To determine the effects of ECSCR loss, siRNA knockdowm was performed. Several cytoskeletal proteins were visualised by immunofluorescent staining and lack of ECSCR resulted in disorganised stress fibres and uncoupling of the cytoskeleton from the plasma membrane. Overexpression of ECSCR-GFP in HEK 293T cells induced the formation of filopodia. This was not replicated in filamin A-deficient M2 cells, which implies that filamin A is necessary for the formation of filopodia and the two proteins probably associate to form these structures. A microarray to compare expression of HUVECs treated with ECSCR-targeting siRNA and a negative control duplex

was also performed. Altered gene expression was observed for proteins involved in migration, apoptosis and cytoskeletal processes.

After confirming endothelial specificity by *in situ* hybridization (mainly in head and major trunk vessels), the role of Ecscr in zebrafish developmental angiogenesis was explored using morpholino knockdown. Loss of Ecscr results in disrupted intersegmental vessels sprouting, which can be rescued by co-injection of Ecscr mRNA and morpholino. Two splice variants were identified, one of particular interest, which is only present during intersegmental vessel sprouting, possibly indicating a crucial role in this process.

Mouse endothelial specificity of Ecscr was also confirmed by *in situ* hybridization, which has detected the transcript in trunk and head vessels, as well as intersegmental vessels. Three strategies were attempted to produce an Ecscr knockout mouse model. Initially, the construct to make a conditional knockout mouse was going to be made, electroporated into ES cells, selected and injected into blastocysts to produce chimeras. Most of the construct was successfully made, but an essential element containing the genomic DNA could not be inserted. Alternatively, ES cells were purchased to make the same type of knockout, but no germline transmission was observed. Finally, ES cells containing a construct for a null knockout have produced chimeras with germline transmission. Preliminary analyses show that Ecscr is expressed in lung and some but not all heart superficial vessels. It seems to be absent from the aorta. Initial observations of the lung histology indicate less air space and more cells, which can be indicative of respiratory problems. This seems to be supported by the presence of enlarged right atria and the fact that some heterozygous females have died a few days after giving birth.

ECSCR endothelial specificity seems to be conserved across species (human, zebrafish and mouse), as demonstrated by qPCR and *in situ* hybridization (this work and published literature). Regarding specific vessels, Ecscr seems to be present in the major trunk vessels in both zebrafish and mouse embryos, but absent from the murine aorta in 11 days old pups. The presence of Ecscr in large calibre vessels was not studied in older zebrafish or in humans. A role in smaller vessels seems evident. However, there seem to be differences between species, as loss of Ecscr results in incorrect formation of intersegmental vessels in zebrafish, but it has been reported to induce the growth of microvasculature in knockout mice (Koide *et al*., 2011). Nevertheless, caution must be taken when interpreting these results, as these phenomena were observed at different developmental stages. Additionally, Verma *et al*. (2010) suggest a role for Ecscr in angioblast migration in zebrafish, which was not studied in in mouse.

A considerable part of this thesis involved the development and validation of techniques and reagents, which has proved challenging. Some of the aims were fulfilled more successfully than others but, when unsuccessful, techniques were replaced by logical alternatives which in the end proved to be more efficient to accomplish the goal. This was the case, for example, of the yeast-two-hybrid technique which was replaced by the luciferase complementation assay. The latter has confirmed the interaction between moesin and ECSCR. Three strategies were attempted to produce an Ecscr knockout mouse. In the end, this mouse model was successfully generated.

APPENDICES

APPENDIX 1: LISTS OF UP AND DOWNREGULATED GENES UPON ECSCR KNOCKDOWN IN HUVECS

Table A1 – Genes that are upregulated when ECSCR is knocked down

FC – fold change; the numbers in brackets after the gene name are the fold change for that gene found in other probes, as the chip contains more than one probe for some genes

Gene Symbol	Gene name	FC
CCL20	chemokine (C-C motif) ligand 20	69,27775
IL1B	interleukin 1, beta" (50, 50, 44, 43, 41, 40, 37, 36)	55,58571
CXCL5	chemokine (C-X-C motif) ligand 5 (5)	51,55574
SELE	selectin E	45,62285
CXCL3	chemokine (C-X-C motif) ligand 3 (19)	43,1904
BIRC3	baculoviral IAP repeat-containing 3	39,29428
LINCR	likely ortholog of mouse lung-inducible Neutralized-related C3HC4 RING domain protein	35,91131
KYNU	kynureninase (L-kynurenine hydrolase) (19)	35,25836
CXCL2	chemokine (C-X-C motif) ligand 2 (12)	26,25162
IFI44L	interferon-induced protein 44-like	23,43921
LTB	lymphotoxin beta (TNF superfamily, member 3)"	22,39423
C6orf58	chromosome 6 open reading frame 58 (15)	22,16312
CXCL1	chemokine (C-X-C motif) ligand 1 (melanoma growth stimulating activity, alpha)"	22,14715
ATF3	activating transcription factor 3 (16)	18,71241
IL8	interleukin 8	18,58318
CD69	CD69 molecule (18, 18, 17, 17, 17, 15, 15, 14,12)	18,06872
NR0B1	nuclear receptor subfamily 0, group B, member 1"	17,81812
FAM129A	family with sequence similarity 129, member A" (10)	17,73367
NR4A3	nuclear receptor subfamily 4, group A, member 3"	17,54172
CEBPD	CCAAT/enhancer binding protein (C/EBP), delta	17,47981
CX3CL1	chemokine (C-X3-C motif) ligand 1	17,32104

UBD	ubiquitin D	16,71386
IL6	interleukin 6 (interferon, beta 2)" (14, 13, 13, 13, 13, 12, 11, 11, 11)	15,82812
CSF3	colony stimulating factor 3 (granulocyte)	14,69577
RRAD	Ras-related associated with diabetes (11)	14,46713
TNIP3	TNFAIP3 interacting protein 3	13,40016
CLDN1	claudin 1	12,99483
IL20RB	interleukin 20 receptor beta	12,98884
RSAD2	radical S-adenosyl methionine domain containing 2 (5)	12,40548
TRAF1	TNF receptor-associated factor 1 (11)	12,26445
C15orf48	chromosome 15 open reading frame 48	12,2139
IL1A	interleukin 1, alpha" (11, 11, 10, 10, 10, 9, 9, 9, 9)	12,11216
MX1	myxovirus (influenza virus) resistance 1, interferon-inducible protein p78 (mouse)"	11,93219
ICAM1	intercellular adhesion molecule 1 (11, 10,10, 10, 9, 8)	11,49177
TSLP	thymic stromal lymphopoietin	11,48282
TAC1	tachykinin, precursor 1 (8)	11,47063
IL13RA2	interleukin 13 receptor, alpha 2"	11,46244
NKD2	naked cuticle homolog 2 (Drosophila)	11,24896
ETV7	ets variant 7	11,24188
IFI6	interferon, alpha-inducible protein 6"	11,17219
LOC344887	similar to hCG2041270 (9)	10,93561
RASGRF2	Ras protein-specific guanine nucleotide-releasing factor 2	10,12908
EBI3	Epstein-Barr virus induced 3 (3)	10,12063
KCNA7	potassium voltage-gated channel, shaker-related subfamily, member 7	9,942975
GAL	galanin prepropeptide	9,67776
FOXF1	forkhead box F1	9,476391
FOXF2	forkhead box F2	9,372928
DDIT4L	DNA-damage-inducible transcript 4-like	9,327639
PTGS2	prostaglandin-endoperoxide synthase 2 (prostaglandin G/H synthase and cyclooxygenase) (9, 9, 8, 8, 8, 8, 7, 7, 7, 4)	9,198848
TUBB2B	tubulin, beta 2B"	9,191147
FGF13	fibroblast growth factor 13 (6)	8,862905

CLDN14	claudin 14	8,828304
CCL2	chemokine (C-C motif) ligand 2 (9, 9, 9, 8, 8, 8, 6)	8,810368
HOXB9	homeobox B9	8,671537
TRIB3	tribbles homolog 3 (Drosophila) (4)	8,443915
IL23A	interleukin 23, alpha subunit p19"	8,419675
NEFM	neurofilament, medium polypeptide"	8,411503
EPSTI1	epithelial stromal interaction 1 (breast) (4)	8,375842
CSF2	colony stimulating factor 2 (granulocyte-macrophage)	8,360494
SLC7A11	solute carrier family 7, (cationic amino acid transporter, y+ system) member 11" (4, 4)	8,256422
CD70	CD70 molecule	8,229235
TNFRSF9	tumor necrosis factor receptor superfamily, member 9"	8,17885
DDIT3	DNA-damage-inducible transcript 3	8,141426
C8orf4	chromosome 8 open reading frame 4 (5)	7,844324
TNC	tenascin C	7,838327
IRS1	insulin receptor substrate 1	7,838222
LAMP3	lysosomal-associated membrane protein 3	7,703025
RCSD1	RCSD domain containing 1	7,612539
NFKBIZ	nuclear factor of kappa light polypeptide gene enhancer in B-cells inhibitor, zeta	7,609051
OLAH	oleoyl-ACP hydrolase	7,510173
IGFBP3	insulin-like growth factor binding protein 3 (7, 7, 6, 6, 6, 6, 5, 5)	7,506168
XAF1	XIAP associated factor 1 (6)	7,504867
IFIT1	interferon-induced protein with tetratricopeptide repeats 1	7,332894
TNFAIP2	tumor necrosis factor, alpha-induced protein 2	7,329811
CEBPA	CCAAT/enhancer binding protein (C/EBP), alpha" (6)	7,300273
RGS16	regulator of G-protein signaling 16	7,266498
LSM14B	LSM14B, SCD6 homolog B (S. cerevisiae)"	7,246722
RASD1	RAS, dexamethasone-induced 1" (5)	7,178346
CXCL6	chemokine (C-X-C motif) ligand 6 (granulocyte chemotactic protein 2)	7,102826
MX2	myxovirus (influenza virus) resistance 2 (mouse)	7,085482
PLA2G4C	phospholipase A2, group IVC (cytosolic, calcium-independent)" (4)	7,081566

IL7R	interleukin 7 receptor	7,035184
OAS1	2',5'-oligoadenylate synthetase 1, 40/46kDa"	6,923822
TNFRSF11B	tumor necrosis factor receptor superfamily, member 11b" (6, 5, 5, 4, 4, 4, 4, 4, 4, 4, 3)	6,869461
FAM150B	family with sequence similarity 150, member B"	6,783794
RELB	v-rel reticuloendotheliosis viral oncogene homolog B	6,686273
CXCL12	chemokine (C-X-C motif) ligand 12 (stromal cell-derived factor 1) (6, 6, 6, 6, 5, 5, 5, 5, 4)	6,63401
PAPLN	papilin, proteoglycan-like sulfated glycoprotein"	6,546394
LPL	lipoprotein lipase	6,513617
TNFAIP6	tumor necrosis factor, alpha-induced protein 6"	6,463195
CEBPB	CCAAT/enhancer binding protein (C/EBP), beta" (6, 6, 6, 6, 6, 5, 5, 5)	6,44158
PRRX2	paired related homeobox 2	6,388108
SLC15A3	solute carrier family 15, member 3	6,239996
CXCL10	chemokine (C-X-C motif) ligand 10	6,202999
SLC12A7	solute carrier family 12 (potassium/chloride transporters), member 7" (3)	6,169221
TLR2	toll-like receptor 2 (4, 3, 3)	6,165808
FLJ45422	FLJ45422 protein	6,096475
KCTD16	potassium channel tetramerisation domain containing 16	6,084301
PITX2	paired-like homeodomain 2	6,051326
LOC645638	similar to WDNM1-like protein	5,975268
ITGA9	integrin, alpha 9 (4)	5,931367
SLC10A4	solute carrier family 10 (sodium/bile acid cotransporter family), member 4	5,916113
HLA-B	major histocompatibility complex, class I, B"	5,911434
SH2D5	SH2 domain containing 5	5,896935
OASL	2'-5'-oligoadenylate synthetase-like	5,862833
CITED4	Cbp/p300-interacting transactivator, with Glu/Asp-rich carboxy-terminal domain, 4 (4)	5,815169
HMOX1	heme oxygenase (decycling) 1 (5, 5, 5, 5, 5, 5, 5, 5, 5, 5)	5,76187
OAS2	2'-5'-oligoadenylate synthetase 2, 69/71kDa (4)	5,754087
HERC6	hect domain and RLD 6	5,740996
SQSTM1	sequestosome 1	5,73985
SOD2	superoxide dismutase 2, mitochondrial"	5,735423

ISG20	interferon stimulated exonuclease gene 20kDa	5,687222
PTCHD1	patched domain containing 1	5,684286
UNC5B	unc-5 homolog B (C. elegans)	5,601578
COL8A2	collagen, type VIII, alpha 2"	5,560278
MC5R	melanocortin 5 receptor	5,555165
MMP1	matrix metallopeptidase 1 (interstitial collagenase) (5, 5, 5, 5, 4, 4, 4, 4)	5,527686
LOC100126784	hypothetical LOC100126784	5,510926
CLIP4	CAP-GLY domain containing linker protein family, member 4"	5,503133
NUAK2	NUAK family, SNF1-like kinase, 2"	5,486645
SPINK1	serine peptidase inhibitor, Kazal type 1"	5,394292
AREG	Amphiregulin	5,373462
NOG	Noggin	5,250764
HES4	hairy and enhancer of split 4 (Drosophila)	5,148451
IFIT3	interferon-induced protein with tetratricopeptide repeats 3	5,105371
KCNN2	potassium intermediate/small conductance calcium-activated channel, subfamily N, member 2"	5,069032
IFI27	interferon, alpha-inducible protein 27" (4, 4, 4, 4, 4, 3, 3, 3, 3, 3, 3)	5,067551
ATP1B1	ATPase, Na+/K+ transporting, beta 1 polypeptide" (4)	5,004399
MAFF	v-maf musculoaponeurotic fibrosarcoma oncogene homolog F (avian)	4,972289
HIST1H3D	histone cluster 1, H3d"	4,962294
SLC7A2	solute carrier family 7 (cationic amino acid transporter, y+ system), member 2"	4,883991
CD83	CD83 molecule	4,870915
DUSP5P	dual specificity phosphatase 5 pseudogene (4)	4,861522
TNFRSF4	tumor necrosis factor receptor superfamily, member 4"	4,851218
RAB3IL1	RAB3A interacting protein (rabin3)-like 1	4,788185
PCK2	phosphoenolpyruvate carboxykinase 2 (mitochondrial) (3)	4,775168
CBS	cystathionine-beta-synthase	4,752131
LOC728855	hypothetical LOC728855	4,659575
BDKRB2	bradykinin receptor B2	4,656202
BATF3	basic leucine zipper transcription factor, ATF-like 3	4,645409
DNER	delta/notch-like EGF repeat containing	4,63993

GPC6	glypican 6	4,598506
HLA-F	major histocompatibility complex, class I, F"	4,588335
ICAM4	intercellular adhesion molecule 4 (Landsteiner-Wiener blood group)	4,587044
AKAP12	A kinase (PRKA) anchor protein 12	4,581684
CEBPE	CCAAT/enhancer binding protein (C/EBP), epsilon"	4,578664
ICOSLG	inducible T-cell co-stimulator ligand	4,560733
POU2F2	POU class 2 homeobox 2	4,555146
FAM148B	family with sequence similarity 148, member B"	4,55495
CAMTA1	calmodulin binding transcription activator 1 (3)	4,544532
FOXA3	forkhead box A3	4,532092
BMP8B	bone morphogenetic protein 8b	4,528976
SLC7A5	solute carrier family 7 (cationic amino acid transporter, y+ system), member 5"	4,501349
MAMDC2	MAM domain containing 2	4,490658
ADRA2C	adrenergic, alpha-2C-, receptor"	4,46032
MMP10	matrix metallopeptidase 10 (stromelysin 2)	4,445137
LOC345630	similar to hCG1641252	4,377962
MT1M	metallothionein 1M	4,374825
ZC3H12A	zinc finger CCCH-type containing 12A	4,362434
DDIT4	DNA-damage-inducible transcript 4	4,353625
BMPR1B	bone morphogenetic protein receptor, type IB"	4,336013
IFITM1	interferon induced transmembrane protein 1 (9-27)	4,335091
PMAIP1	phorbol-12-myristate-13-acetate-induced protein 1 (4, 4, 4, 3, 3, 3, 3, 3)	4,238996
PPARG	peroxisome proliferator-activated receptor gamma (3, 2)	4,237915
ATP13A3	ATPase type 13A3 (4)	4,177427
VEGFA	vascular endothelial growth factor A (3)	4,167951
MT1JP	metallothionein 1J (pseudogene)	4,12442
SPATA13	spermatogenesis associated 13	4,106179
CTHRC1	collagen triple helix repeat containing 1	4,103684
IRX2	iroquois homeobox 2	4,090886
TNF	tumor necrosis factor (TNF superfamily, member 2)"	4,087982

TRA@	T cell receptor alpha locus	4,086858
RGAG4	retrotransposon gag domain containing 4	4,074331
LOR	Loricrin	4,071845
E2F7	E2F transcription factor 7	4,04478
YPEL2	yippee-like 2 (Drosophila)	4,040712
ISG15	ISG15 ubiquitin-like modifier	4,012287
FLJ10490	hypothetical protein FLJ10490	3,993195
ID2	inhibitor of DNA binding 2, dominant negative helix-loop-helix protein" (3)	3,991321
LL22NC03-75B3.6	KIAA1644 protein	3,965081
MSX1	msh homeobox 1 (3)	3,963032
ABTB2	ankyrin repeat and BTB (POZ) domain containing 2	3,95733
IER5	immediate early response 5	3,951198
SLC2A6	solute carrier family 2 (facilitated glucose transporter), member 6"	3,926804
ALOX5AP	arachidonate 5-lipoxygenase-activating protein	3,923313
SLC12A2	solute carrier family 12 (sodium/potassium/chloride transporters), member 2"	3,870077
SOX11	SRY (sex determining region Y)-box 11	3,835315
OAS3	2'-5'-oligoadenylate synthetase 3, 100kDa (3)	3,810113
SPPL2B	signal peptide peptidase-like 2B	3,793562
PTPRH	protein tyrosine phosphatase, receptor type, H"	3,786373
CDV3	CDV3 homolog (mouse)	3,726423
IL32	interleukin 32	3,714886
NAT8L	N-acetyltransferase 8-like (GCN5-related, putative)"	3,708802
NF-E4	transcription factor NF-E4	3,702473
F2RL3	coagulation factor II (thrombin) receptor-like 3	3,700633
CBLN2	cerebellin 2 precursor	3,692642
CXCL11	chemokine (C-X-C motif) ligand 11	3,679541
ZNF644	zinc finger protein 644 (3)	3,661652
EIF2AK2	eukaryotic translation initiation factor 2-alpha kinase 2	3,655188
GADD45G	growth arrest and DNA-damage-inducible, gamma"	3,644449
ETS1	v-ets erythroblastosis virus E26 oncogene homolog 1 (avian) (4)	3,641341

HRK	harakiri, BCL2 interacting protein (contains only BH3 domain)	3,596273
CTH	cystathionase (cystathionine gamma-lyase)	3,582555
ITPR1	inositol 1,4,5-triphosphate receptor, type 1"	3,572426
HIST1H2AC	histone cluster 1, H2ac"	3,548782
TNFAIP3	tumor necrosis factor, alpha-induced protein 3"	3,544287
LOC644135	hypothetical LOC644135	3,537164
FBXO6	F-box protein 6	3,53669
KCNIP3	Kv channel interacting protein 3, calsenilin"	3,531159
IFI35	interferon-induced protein 35	3,526616
F2RL1	coagulation factor II (thrombin) receptor-like 1	3,521476
PPAP2C	phosphatidic acid phosphatase type 2C	3,512899
S100A3	S100 calcium binding protein A3	3,496241
PHLDA1	pleckstrin homology-like domain, family A, member 1 (3)	3,48519
EIF5	eukaryotic translation initiation factor 5	3,466144
GPR150	G protein-coupled receptor 150	3,462558
VCAM1	vascular cell adhesion molecule 1	3,451567
TIFA	TRAF-interacting protein with forkhead-associated domain	3,446937
SLC3A2	solute carrier family 3 (activators of dibasic and neutral amino acid transport), member 2"	3,444901
DCBLD2	discoidin, CUB and LCCL domain containing 2" (2)	3,425845
C10orf63	chromosome 10 open reading frame 63	3,416924
NFKB2	nuclear factor of kappa light polypeptide gene enhancer in B-cells 2 (p49/p100) (3, 3, 3)	3,408586
GBA3	glucosidase, beta, acid 3 (cytosolic)"	3,398055
GEM	GTP binding protein overexpressed in skeletal muscle	3,396345
STC2	stanniocalcin 2	3,394851
LOC401317	hypothetical LOC401317	3,387634
TAP1	transporter 1, ATP-binding cassette, sub-family B (MDR/TAP)"	3,370895
TXNL4B	thioredoxin-like 4B	3,355144
GATA5	GATA binding protein 5	3,353586
TMEM217	transmembrane protein 217 (3)	3,348653
NFIL3	nuclear factor, interleukin 3 regulated	3,334935

STX6	syntaxin 6	3,323307
LOC646626	hypothetical LOC646626	3,302352
WWC1	WW and C2 domain containing 1	3,284061
RAB12	RAB12, member RAS oncogene family	3,273459
ZNF365	zinc finger protein 365	3,270699
SNX26	sorting nexin 26	3,266806
FBXL13	F-box and leucine-rich repeat protein 13	3,263564
HIST1H2BG	histone cluster 1, H2bg	3,259872
IFIT5	interferon-induced protein with tetratricopeptide repeats 5 (3)	3,250025
PARD6G	par-6 partitioning defective 6 homolog gamma (C. elegans)	3,246163
EMILIN2	elastin microfibril interfacer 2	3,24535
PKN2	protein kinase N2	3,240875
LARS	leucyl-tRNA synthetase	3,232565
OR11G2	olfactory receptor, family 11, subfamily G, member 2"	3,218494
RSL1D1	ribosomal L1 domain containing 1	3,204735
S100P	S100 calcium binding protein P	3,202209
ESM1	endothelial cell-specific molecule 1	3,19416
ZBED1	zinc finger, BED-type containing 1	3,184566
PTPRK	protein tyrosine phosphatase, receptor type, K"	3,179771
DUX4	double homeobox, 4"	3,179511
USHBP1	Usher syndrome 1C binding protein 1	3,170622
SYNGR3	synaptogyrin 3	3,140811
ZFP91	zinc finger protein 91 homolog (mouse)	3,131078
GVIN1	GTPase, very large interferon inducible 1" (3)	3,110038
C5orf41	chromosome 5 open reading frame 41	3,106751
IFI30	interferon, gamma-inducible protein 30"	3,103898
TPM1	tropomyosin 1 (alpha)	3,094334
ADAM12	ADAM metallopeptidase domain 12	3,092041
JUNB	jun B proto-oncogene	3,081591
SIK1	salt-inducible kinase 1	3,079149

ZDHHC11	zinc finger, DHHC-type containing 11"	3,064191
CTSS	cathepsin S	3,063559
SP5	Sp5 transcription factor	3,062138
CD274	CD274 molecule	3,050084
SGK1	serum/glucocorticoid regulated kinase 1	3,042282
LOC100127983	hypothetical protein LOC100127983	3,038411
CDH24	cadherin-like 24	3,03514
MT2A	metallothionein 2A	3,032209
HES2	hairy and enhancer of split 2 (Drosophila)	3,030875
OBFC2A	oligonucleotide/oligosaccharide-binding fold containing 2A	3,018
EVC2	Ellis van Creveld syndrome 2	3,015805
CRCP	CGRP receptor component	3,007095
FTH1	ferritin, heavy polypeptide 1"	2,963964
OSGIN1	oxidative stress induced growth inhibitor 1	2,957198
KITLG	KIT ligand	2,9491
IRF7	interferon regulatory factor 7	2,933232
RCOR2	REST corepressor 2	2,922273
TNFSF15	tumor necrosis factor (ligand) superfamily, member 15"	2,90531
DHX58	DEXH (Asp-Glu-X-His) box polypeptide 58	2,899787
N4BP3	Nedd4 binding protein 3	2,89582
HDAC9	histone deacetylase 9	2,892829
LOC644189	similar to peroxisomal long-chain acyl-coA thioesterase	2,88748
NFKBIA	nuclear factor of kappa light polypeptide gene enhancer in B-cells inhibitor, alpha"	2,867977
KCNJ14	potassium inwardly-rectifying channel, subfamily J, member 14	2,867113
MAFA	v-maf musculoaponeurotic fibrosarcoma oncogene homolog A (avian)	2,860308
CFTR	cystic fibrosis transmembrane conductance regulator (ATP-binding cassette sub-family C, member 7)"	2,851662
PDGFA	platelet-derived growth factor alpha polypeptide	2,842574
RHBDF2	rhomboid 5 homolog 2 (Drosophila)	2,84253
FCRLB	Fc receptor-like B	2,833371
NUPL1	nucleoporin like 1	2,832407

KBTBD11	kelch repeat and BTB (POZ) domain containing 11	2,821291
DTX3L	deltex 3-like (Drosophila)	2,799295
PLXNA1	plexin A1	2,793375
OCIAD2	OCIA domain containing 2	2,789949
UBE2E1	ubiquitin-conjugating enzyme E2E 1 (UBC4/5 homolog, yeast)"	2,776083
WNT5A	wingless-type MMTV integration site family, member 5A"	2,772922
KITLG	KIT ligand	2,76321
PARP9	poly (ADP-ribose) polymerase family, member 9	2,757096
SPON2	spondin 2, extracellular matrix protein"	2,755371
GPR68	G protein-coupled receptor 68	2,749564
SIX1	SIX homeobox 1	2,732723
PAG1	phosphoprotein associated with glycosphingolipid microdomains 1	2,728033
GRPEL2	GrpE-like 2, mitochondrial (E. coli)"	2,728015
ZNF697	zinc finger protein 697	2,716183
AIFM2	apoptosis-inducing factor, mitochondrion-associated, 2"	2,716176
FOSL2	FOS-like antigen 2	2,711685
AADAC	arylacetamide deacetylase (esterase)	2,710489
MYLK	myosin light chain kinase	2,707101
TCF7	transcription factor 7 (T-cell specific, HMG-box)"	2,704893
FAM132A	family with sequence similarity 132, member A	2,68782
ADFP	adipose differentiation-related protein	2,662066
MT2A	metallothionein 2A	2,660903
IL4I1	interleukin 4 induced 1	2,658979
UTS2R	urotensin 2 receptor	2,645053
HIST1H2AE	histone cluster 1, H2ae	2,631659
PRDM10	PR domain containing 10	2,627767
CIDECP	cell death-inducing DFFA-like effector c pseudogene	2,62727
ZNF322B	zinc finger protein 322B	2,624297
TLR7	toll-like receptor 7	2,620025
ERRFI1	ERBB receptor feedback inhibitor 1	2,613644

VAV3	vav 3 guanine nucleotide exchange factor	2,612158
NPBWR1	neuropeptides B/W receptor 1	2,578884
SOX7	SRY (sex determining region Y)-box 7	2,576394
CKB	creatine kinase, brain"	2,49131
EIF1	eukaryotic translation initiation factor 1	2,487807
GBP1	guanylate binding protein 1, interferon-inducible, 67kDa	2,478448
G0S2	G0/G1switch 2	2,464977
AKIRIN1	akirin 1	2,454619
DEAF1	deformed epidermal autoregulatory factor 1 (Drosophila)	2,446047
C9orf150	chromosome 9 open reading frame 150	2,423348
HIST2H2AA4	histone cluster 2, H2aa4	2,417622
BCAN	Brevican	2,402919
SYNCRIP	synaptotagmin binding, cytoplasmic RNA interacting protein"	2,385486
MT1G	metallothionein 1G	2,382322
C3orf52	chromosome 3 open reading frame 52	2,378354
CTSK	cathepsin K	2,369672
LIPG	lipase, endothelial	2,368038
SRGN	Serglycin	2,367863
KLF11	Kruppel-like factor 11	2,360476
PSMB8	proteasome (prosome, macropain) subunit, beta type, 8 (large multifunctional peptidase 7)"	2,354499
CLDN23	claudin 23	2,313628
CUEDC1	CUE domain containing 1	2,288127
MAFK	v-maf musculoaponeurotic fibrosarcoma oncogene homolog K (avian)	2,278666

Table A2 – Genes that are downregulated when ECSCR is knocked down

FC – fold change; the numbers in brackets after the gene name are the fold change for that gene found in other probes, as the chip contains more than one probe for some genes

Gene Symbol	Gene name	FC
CYP26B1	cytochrome P450, family 26, subfamily B, polypeptide 1"	24,59053
LYVE1	lymphatic vessel endothelial hyaluronan receptor 1	13,12212
SEPP1	selenoprotein P, plasma, 1"	12,15971
METTL7A	methyltransferase like 7A	10,99246
SELP	selectin P (granule membrane protein 140kDa, antigen CD62)"	9,65395
MATN2	matrilin 2	9,515602
CCL15	chemokine (C-C motif) ligand 15	9,117793
AK5	adenylate kinase 5	8,991111
IL33	interleukin 33	8,245166
MYCN	v-myc myelocytomatosis viral related oncogene, neuroblastoma derived (avian)"	8,125842
CD36	CD36 molecule (thrombospondin receptor)	7,961454
SGCD	sarcoglycan, delta (35kDa dystrophin-associated glycoprotein)"	7,878169
COL3A1	collagen, type III, alpha 1"	7,645113
AGTPBP1	ATP/GTP binding protein 1	7,417495
PKNOX2	PBX/knotted 1 homeobox 2	7,40154
MEST	mesoderm specific transcript homolog (mouse)	7,063699
AQP1	aquaporin 1 (Colton blood group) (6)	7,014114
ECSM2	endothelial cell-specific molecule 2	6,358596
ALDH1A1	aldehyde dehydrogenase 1 family, member A1"	6,182551
NKAIN2	Na+/K+ transporting ATPase interacting 2	6,160984
LIMCH1	LIM and calponin homology domains 1	5,903961
CCRL1	chemokine (C-C motif) receptor-like 1	5,860797

MAN1C1	mannosidase, alpha, class 1C, member 1"	5,814218
ACP5	acid phosphatase 5, tartrate resistant"	5,77145
CCL3L3	chemokine (C-C motif) ligand 3-like 3	5,76664
CCNE2	cyclin E2	5,625399
LEPR	leptin receptor	5,61404
E2F8	E2F transcription factor 8	5,571739
ABCG2	ATP-binding cassette, sub-family G (WHITE), member 2	5,535094
PCDH10	protocadherin 10	5,530232
SLC40A1	solute carrier family 40 (iron-regulated transporter), member 1"	5,287551
PLAT	plasminogen activator, tissue" (5, 5,5, 5, 5, 5,4, 4)	5,287475
KIAA0644	KIAA0644 gene product	5,275179
MRAP2	melanocortin 2 receptor accessory protein 2	5,238853
METTL7A	methyltransferase like 7A	5,222575
ST6GALNAC1	ST6 (alpha-N-acetyl-neuraminyl-2,3-beta-galactosyl-1,3)-N-acetylgalactosaminide alpha-2,6-sialyltransferase 1	5,183783
MMP7	matrix metallopeptidase 7 (matrilysin, uterine)"	5,165852
GUCY1A3	guanylate cyclase 1, soluble, alpha 3"	5,073154
FRY	furry homolog (Drosophila)	5,057096
MALAT1	metastasis associated lung adenocarcinoma transcript 1 (non-protein coding)	5,052179
PCDH7	protocadherin 7	5,047044
ACSM2B	acyl-CoA synthetase medium-chain family member 2B	5,043029
ACSM2A	acyl-CoA synthetase medium-chain family member 2A	4,975459
KCNMB2	potassium large conductance calcium-activated channel, subfamily M, beta member 2"	4,939225
GPR126	G protein-coupled receptor 126	4,853051
SULF1	sulfatase 1	4,766119
PROS1	protein S (alpha)	4,764287
C5orf4	chromosome 5 open reading frame 4	4,721733
ITGA11	integrin, alpha 11	4,673621
MGP	matrix Gla protein	4,665341
SLC14A1	solute carrier family 14 (urea transporter), member 1 (Kidd blood group)"	4,550198
SGCD	sarcoglycan, delta (35kDa dystrophin-associated glycoprotein)"	4,550033

THBD	Thrombomodulin	4,512136
RNF125	ring finger protein 125	4,503208
GLT8D2	glycosyltransferase 8 domain containing 2	4,501765
CMAH	cytidine monophosphate-N-acetylneuraminic acid hydroxylase (CMP-N-acetylneuraminate monooxygenase) pseudogene	4,487061
KLRG1	killer cell lectin-like receptor subfamily G, member 1"	4,442692
ELMOD1	ELMO/CED-12 domain containing 1	4,406717
HTR2B	5-hydroxytryptamine (serotonin) receptor 2B	4,400674
COL3A1	collagen, type III, alpha 1"	4,305804
GIMAP1	GTPase, IMAP family member 1	4,302009
KIAA1524	KIAA1524	4,301181
CROT	carnitine O-octanoyltransferase	4,280991
ABCA6	ATP-binding cassette, sub-family A (ABC1), member 6	4,261901
PLXDC2	plexin domain containing 2	4,224135
MST150	MSTP150	4,213687
TP53TG1	TP53 target 1 (non-protein coding)	4,212748
THSD7A	thrombospondin, type I, domain containing 7A"	4,175809
NTN4	netrin 4	4,139463
ANGPT1	angiopoietin 1	4,131439
TSPAN7	tetraspanin 7	4,127978
C17orf58	chromosome 17 open reading frame 58	4,093107
ACSM3	acyl-CoA synthetase medium-chain family member 3	4,078574
GUCY1A3	guanylate cyclase 1, soluble, alpha 3"	4,073248
SETBP1	SET binding protein 1	4,068339
CD36	CD36 molecule (thrombospondin receptor)	4,056686
OLFML2A	olfactomedin-like 2A	4,05054
ADAM22	ADAM metallopeptidase domain 22	4,043939
FAM63A	family with sequence similarity 63, member A"	4,019929
MAN1C1	mannosidase, alpha, class 1C, member 1	4,00291
AMIGO2	adhesion molecule with Ig-like domain 2	3,994552
ITLN1	intelectin 1 (galactofuranose binding)	3,976707

PCDH17	protocadherin 17	3,971997
DNAJB4	DnaJ (Hsp40) homolog, subfamily B, member 4"	3,970255
CYP4X1	cytochrome P450, family 4, subfamily X, polypeptide 1"	3,933246
KLHL13	kelch-like 13 (Drosophila)	3,926297
LIMCH1	LIM and calponin homology domains 1	3,901281
CASP12	caspase 12 (gene/pseudogene)	3,859531
NPHS2	nephrosis 2, idiopathic, steroid-resistant (podocin)	3,839631
ZNF608	zinc finger protein 608	3,831042
COL1A2	collagen, type I, alpha 2"	3,81778
KIAA1377	KIAA1377	3,801961
GDF6	growth differentiation factor 6	3,789169
SP8	Sp8 transcription factor	3,789124
C10orf10	chromosome 10 open reading frame 10	3,785241
DNAJB4	DnaJ (Hsp40) homolog, subfamily B, member 4"	3,776615
KCNMB4	potassium large conductance calcium-activated channel, subfamily M, beta member 4	3,756521
PIK3C2B	phosphoinositide-3-kinase, class 2, beta polypeptide"	3,746364
COL1A2	collagen, type I, alpha 2"	3,737154
PXMP2	peroxisomal membrane protein 2, 22kDa	3,706716
RAD51AP1	RAD51 associated protein 1	3,697544
ENTPD1	ectonucleoside triphosphate diphosphohydrolase 1	3,696764
STON1	stonin 1	3,687482
CYP4X1	cytochrome P450, family 4, subfamily X, polypeptide 1"	3,681587
TTC13	tetratricopeptide repeat domain 13	3,667282
LOC339483	hypothetical LOC339483	3,659573
FAM107A	family with sequence similarity 107, member A	3,65268
C4orf49	chromosome 4 open reading frame 49	3,642848
COL1A2	collagen, type I, alpha 2"	3,634113
SDPR	serum deprivation response (phosphatidylserine binding protein)	3,628161
DSCC1	defective in sister chromatid cohesion 1 homolog (S. cerevisiae)	3,617317
GCNT1	glucosaminyl (N-acetyl) transferase 1, core 2 (beta-1,6-N-acetylglucosaminyltransferase)	3,613131

MMRN1	multimerin 1	3,597911
CDKN2C	cyclin-dependent kinase inhibitor 2C (p18, inhibits CDK4)"	3,581516
ATAD2	ATPase family, AAA domain containing 2"	3,576729
MYO5C	myosin VC	3,567839
FABP4	fatty acid binding protein 4, adipocyte"	3,548161
ALDH6A1	aldehyde dehydrogenase 6 family, member A1"	3,525673
RACGAP1	Rac GTPase activating protein 1	3,517794
FAM107A	family with sequence similarity 107, member A	3,514274
KLHL3	kelch-like 3 (Drosophila)	3,513667
GIPC2	GIPC PDZ domain containing family, member 2	3,512596
SCN9A	sodium channel, voltage-gated, type IX, alpha subunit"	3,502842
FCRL3	Fc receptor-like 3	3,492753
NAP1L3	nucleosome assembly protein 1-like 3	3,491722
CCDC80	coiled-coil domain containing 80	3,484302
COL1A2	collagen, type I, alpha 2"	3,458554
NDC80	NDC80 homolog, kinetochore complex component (S. cerevisiae)"	3,449489
C6orf142	chromosome 6 open reading frame 142	3,449136
GIPC2	GIPC PDZ domain containing family, member 2	3,42513
CDO1	cysteine dioxygenase, type I"	3,414906
KIF20B	kinesin family member 20B	3,414889
TRERF1	transcriptional regulating factor 1	3,399105
COL1A2	collagen, type I, alpha 2"	3,390621
COL1A2	collagen, type I, alpha 2"	3,381495
GJA4	gap junction protein, alpha 4, 37kDa"	3,377162
CLDN22	claudin 22	3,364727
VWA5A	von Willebrand factor A domain containing 5A	3,346545
CLEC14A	C-type lectin domain family 14, member A	3,331307
DSCC1	defective in sister chromatid cohesion 1 homolog (S. cerevisiae)	3,328079
LOC643733	hypothetical LOC643733	3,325942
HAPLN1	hyaluronan and proteoglycan link protein 1	3,320056

SORT1	sortilin 1	3,31407
SPTLC3	serine palmitoyltransferase, long chain base subunit 3	3,309382
KAL1	Kallmann syndrome 1 sequence	3,302677
SELENBP1	selenium binding protein 1	3,287307
PTGIS	prostaglandin I2 (prostacyclin) synthase	3,286498
CFH	complement factor H	3,272152
TMEM71	transmembrane protein 71	3,262596
CCL3L3	chemokine (C-C motif) ligand 3-like 3	3,26022
GPR126	G protein-coupled receptor 126	3,258217
C18orf34	chromosome 18 open reading frame 34	3,250303
KCNJ15	potassium inwardly-rectifying channel, subfamily J, member 15"	3,238777
ABLIM1	actin binding LIM protein 1	3,235758
CGNL1	cingulin-like 1	3,234857
KCND2	potassium voltage-gated channel, Shal-related subfamily, member 2"	3,234167
LUM	Lumican	3,231183
TMSB15A	thymosin beta 15a	3,231081
TRERF1	transcriptional regulating factor 1	3,230042
GRB14	growth factor receptor-bound protein 14	3,220014
CALCRL	calcitonin receptor-like	3,219786
SESN3	sestrin 3	3,209932
SLC22A5	solute carrier family 22 (organic cation/carnitine transporter), member 5"	3,207387
KBTBD6	kelch repeat and BTB (POZ) domain containing 6	3,207162
FILIP1	filamin A interacting protein 1	3,19257
GALNTL2	UDP-N-acetyl-alpha-D-galactosamine:polypeptide N-acetylgalactosaminyltransferase-like 2	3,188781
HMCN1	hemicentin 1	3,186536
STAB2	stabilin 2	3,166811
B3GNT1	UDP-GlcNAc:betaGal beta-1,3-N-acetylglucosaminyltransferase 1"	3,165542
ACOX2	acyl-Coenzyme A oxidase 2, branched chain"	3,163547
ALS2CR4	amyotrophic lateral sclerosis 2 (juvenile) chromosome region, candidate 4"	3,147664
SLC9A9	solute carrier family 9 (sodium/hydrogen exchanger), member 9"	3,132598

COL1A2	collagen, type I, alpha 2"	3,128723
FAT4	FAT tumor suppressor homolog 4 (Drosophila)	3,120981
SORT1	sortilin 1	3,118484
KIAA0101	KIAA0101	3,118215
HEPH	Hephaestin	3,117348
MAP2K6	mitogen-activated protein kinase kinase 6	3,1117
TTK	TTK protein kinase	3,111003
AMPH	Amphiphysin	3,105592
KLRG1	killer cell lectin-like receptor subfamily G, member 1"	3,101475
TMEM106C	transmembrane protein 106C	3,096738
UBA5	ubiquitin-like modifier activating enzyme 5	3,095758
FUCA1	fucosidase, alpha-L- 1, tissue"	3,093508
GGTA1	glycoprotein, alpha-galactosyltransferase 1"	3,090182
TBC1D8B	TBC1 domain family, member 8B (with GRAM domain)"	3,086032
ATAD2	ATPase family, AAA domain containing 2"	3,083222
TBC1D8B	TBC1 domain family, member 8B (with GRAM domain)"	3,069616
NCAPG	non-SMC condensin I complex, subunit G	3,064876
SPEG	SPEG complex locus	3,036352
RNFT2	ring finger protein, transmembrane 2	3,034193
EDNRB	endothelin receptor type B	3,033874
SAMD13	sterile alpha motif domain containing 13	3,032893
SATB1	SATB homeobox 1	3,029964
RRM2	ribonucleotide reductase M2 polypeptide	3,029954
ATP6V0A4	ATPase, H+ transporting, lysosomal V0 subunit a4"	3,027554
LMO7	LIM domain 7	3,023999
SLC1A1	solute carrier family 1 (neuronal/epithelial high affinity glutamate transporter, system Xag), member 1"	3,013368
TRO	Trophinin	3,007376
NHLRC3	NHL repeat containing 3	3,003075
MYH10	myosin, heavy chain 10, non-muscle	3,000197
ASAH1	N-acylsphingosine amidohydrolase (acid ceramidase) 1	2,996805

KLHL4	kelch-like 4 (Drosophila)	2,987169
ANGPT1	angiopoietin 1	2,98547
ETV1	ets variant 1	2,983133
RBP1	retinol binding protein 1, cellular"	2,98245
TCF19	transcription factor 19 (SC1)	2,980965
GIMAP8	GTPase, IMAP family member 8"	2,977004
RNASE1	ribonuclease, RNase A family, 1 (pancreatic)"	2,975943
ATAD2	ATPase family, AAA domain containing 2"	2,962574
MELK	maternal embryonic leucine zipper kinase	2,961678
DCLK1	doublecortin-like kinase 1	2,960902
DEPDC1B	DEP domain containing 1B	2,959885
E2F2	E2F transcription factor 2	2,959335
BEND5	BEN domain containing 5	2,944889
HFE	Hemochromatosis	2,942213
C1orf21	chromosome 1 open reading frame 21	2,939498
MGC16121	hypothetical protein MGC16121	2,938651
C17orf76	chromosome 17 open reading frame 76	2,929663
RICH2	Rho-type GTPase-activating protein RICH2	2,925252
FAM64A	family with sequence similarity 64, member A"	2,925092
TXNDC16	thioredoxin domain containing 16	2,922002
CD46	CD46 molecule, complement regulatory protein"	2,921294
GNA14	guanine nucleotide binding protein (G protein), alpha 14	2,919711
PCDH17	protocadherin 17	2,916579
NUDT7	nudix (nucleoside diphosphate linked moiety X)-type motif 7	2,916499
LOC54492	neuralized-2	2,910138
ATAD2	ATPase family, AAA domain containing 2"	2,907876
COL1A2	collagen, type I, alpha 2"	2,905537
C6orf114	chromosome 6 open reading frame 114	2,904462
METTL2A	methyltransferase like 2A	2,897252
ATAD2	ATPase family, AAA domain containing 2"	2,894996

COL1A2	collagen, type I, alpha 2"	2,893378
GPR124	G protein-coupled receptor 124	2,889106
GIMAP1	GTPase, IMAP family member 1"	2,888239
ATAD2	ATPase family, AAA domain containing 2"	2,881836
ANGPTL5	angiopoietin-like 5	2,881786
KIF18A	kinesin family member 18A	2,875793
MAGEH1	melanoma antigen family H, 1	2,873733
THRA	thyroid hormone receptor, alpha (erythroblastic leukemia viral (v-erb-a) oncogene homolog, avian)"	2,861482
PLS1	plastin 1 (I isoform)	2,854548
EPHA4	EPH receptor A4	2,853894
SMARCA2	SWI/SNF related, matrix associated, actin dependent regulator of chromatin, subfamily a, member 2"	2,851817
FGGY	FGGY carbohydrate kinase domain containing	2,849485
ITGB3	integrin, beta 3 (platelet glycoprotein IIIa, antigen CD61)"	2,847288
KBTBD7	kelch repeat and BTB (POZ) domain containing 7	2,815308
ATAD2	ATPase family, AAA domain containing 2"	2,812275
FAM74A3	family with sequence similarity 74, member A3"	2,807836
MRAP2	melanocortin 2 receptor accessory protein 2	2,806959
FADS2	fatty acid desaturase 2	2,804734
FAM64A	family with sequence similarity 64, member A"	2,803523
EPHX2	epoxide hydrolase 2, cytoplasmic	2,802932
FAM64A	family with sequence similarity 64, member A"	2,802722
FAM113B	family with sequence similarity 113, member B	2,795731
NR1H3	nuclear receptor subfamily 1, group H, member 3"	2,786837
FAM83D	family with sequence similarity 83, member D	2,771843
CEP192	centrosomal protein 192kDa	2,769905
KCNMA1	potassium large conductance calcium-activated channel, subfamily M, alpha member 1"	2,747961
GUCY1B3	guanylate cyclase 1, soluble, beta 3	2,739744
DZIP1	DAZ interacting protein 1	2,735478
NPAL3	NIPA-like domain containing 3	2,719882
SEMA3D	sema domain, immunoglobulin domain (Ig), short basic domain, secreted, (semaphorin) 3D	2,719666

TLR4	toll-like receptor 4	2,719458
GLRXL	glutaredoxin (thioltransferase)-like	2,718919
ATAD2	ATPase family, AAA domain containing 2"	2,717136
NEIL3	nei endonuclease VIII-like 3 (E. coli)	2,712439
PIR	pirin (iron-binding nuclear protein)	2,701644
TXNDC12	thioredoxin domain containing 12 (endoplasmic reticulum)	2,701128
FAM74A3	family with sequence similarity 74, member A3"	2,699797
LOC151878	hypothetical protein LOC151878	2,697855
TYMS	thymidylate synthetase	2,696464
KAT2B	K(lysine) acetyltransferase 2B	2,690971
PCNA	proliferating cell nuclear antigen	2,690725
RRM1	ribonucleotide reductase M1	2,68714
RCAN2	regulator of calcineurin 2	2,686817
ATAD2	ATPase family, AAA domain containing 2"	2,684398
HMMR	hyaluronan-mediated motility receptor (RHAMM)	2,683695
ZDHHC13	zinc finger, DHHC-type containing 13	2,682936
DMTF1	cyclin D binding myb-like transcription factor 1	2,678654
GPSM2	G-protein signaling modulator 2 (AGS3-like, C. elegans)	2,677193
CPE	carboxypeptidase E	2,675854
KIF20A	kinesin family member 20A	2,670471
ERCC6L	excision repair cross-complementing rodent repair deficiency, complementation group 6-like"	2,669791
RIBC2	RIB43A domain with coiled-coils 2	2,648765
POLQ	polymerase (DNA directed), theta"	2,643268
RP5-1022P6.2	hypothetical protein KIAA1434	2,630018
SPINK5	serine peptidase inhibitor, Kazal type 5"	2,629796
KIAA0485	hypothetical LOC57235	2,629308
E2F1	E2F transcription factor 1	2,618136
LOX	lysyl oxidase	2,617217
ATAD2	ATPase family, AAA domain containing 2"	2,612732
C12orf48	chromosome 12 open reading frame 48	2,608701

LMO7	LIM domain 7	2,60593
TLR4	toll-like receptor 4	2,594917
PLEKHA6	pleckstrin homology domain containing, family A member 6"	2,591856
LGR4	leucine-rich repeat-containing G protein-coupled receptor 4	2,589069
CCDC3	coiled-coil domain containing 3	2,579823
C4orf12	chromosome 4 open reading frame 12	2,578949
RACGAP1	Rac GTPase activating protein 1	2,571524
FLJ30901	hypothetical protein FLJ30901	2,570284
LOX	lysyl oxidase	2,569416
RNASEL	ribonuclease L (2',5'-oligoisoadenylate synthetase-dependent)	2,56885
ERLIN2	ER lipid raft associated 2	2,566741
MTSS1	metastasis suppressor 1	2,565103
NCAM2	neural cell adhesion molecule 2	2,56095
CFH	complement factor H	2,558314
SGIP1	SH3-domain GRB2-like (endophilin) interacting protein 1	2,557269
KIAA1522	KIAA1522	2,554842
ALDH5A1	aldehyde dehydrogenase 5 family, member A1"	2,550732
FAM64A	family with sequence similarity 64, member A"	2,547409
INHBB	inhibin, beta B"	2,540446
C16orf75	chromosome 16 open reading frame 75	2,537688
KIF20A	kinesin family member 20A	2,534352
MYH10	myosin, heavy chain 10, non-muscle	2,527407
LTA4H	leukotriene A4 hydrolase	2,525544
ADSS	adenylosuccinate synthase	2,519818
PLK4	polo-like kinase 4 (Drosophila)	2,518215
CCL23	chemokine (C-C motif) ligand 23	2,512078
C10orf58	chromosome 10 open reading frame 58	2,507434
KIF20A	kinesin family member 20A	2,495433
PBX1	pre-B-cell leukemia homeobox 1	2,487947
C3orf64	chromosome 3 open reading frame 64	2,479864

PAM	peptidylglycine alpha-amidating monooxygenase	2,475382
LOX	lysyl oxidase	2,467707
PTGER4	prostaglandin E receptor 4 (subtype EP4)	2,464955
DIAPH3	diaphanous homolog 3 (Drosophila)	2,460108
LOC100129406	hypothetical protein LOC100129406	2,448051
RAB38	RAB38, member RAS oncogene family"	2,446264
RUNX1T1	runt-related transcription factor 1; translocated to, 1 (cyclin D-related)"	2,442814
ALDH2	aldehyde dehydrogenase 2 family (mitochondrial)	2,440793
KIAA0586	KIAA0586	2,434786
CASC5	cancer susceptibility candidate 5	2,424181
C1R	complement component 1, r subcomponent"	2,420773
LOC100134119	similar to hCG2018924	2,420194
CD302	CD302 molecule	2,413478
SGOL2	shugoshin-like 2 (S. pombe)	2,410969
DYNC1I1	dynein, cytoplasmic 1, intermediate chain 1"	2,410772
FAM64A	family with sequence similarity 64, member A"	2,409291
TM7SF3	transmembrane 7 superfamily member 3	2,40264
EXO1	exonuclease 1	2,378808
NAIP	NLR family, apoptosis inhibitory protein"	2,374909
C18orf56	chromosome 18 open reading frame 56	2,374383
FLJ14213	protor-2	2,37244
GIMAP8	GTPase, IMAP family member 8"	2,368156
ITGB2	integrin, beta 2 (complement component 3 receptor 3 and 4 subunit)"	2,366366
BRCA1	breast cancer 1, early onset"	2,35691
MALL	mal, T-cell differentiation protein-like"	2,353596
SAMD12	sterile alpha motif domain containing 12	2,336493
LIPA	lipase A, lysosomal acid, cholesterol esterase"	2,33034
MEF2C	myocyte enhancer factor 2C	2,325836
P2RY5	purinergic receptor P2Y, G-protein coupled, 5"	2,32418
HNRNPA0	heterogeneous nuclear ribonucleoprotein A0	2,323535

NUDT15	nudix (nucleoside diphosphate linked moiety X)-type motif 15	2,308787
EXO1	exonuclease 1	2,306251
DPY19L4	dpy-19-like 4 (C. elegans)	2,28757

APPENDIX 2: TESTING THE EFFECTS OF AN ANGIOGENESIS-BLOCKING ANTIBODY

A1.1 Angiogenesis assays

Wound healing usually depends on a combination of both cell migration and proliferation (Boamah, 2007). Mitomycin C is an antibiotic that is activated *in vivo* into an alkylating agent that binds to DNA, blocking DNA synthesis and inhibiting cell growth (Yarrow *et al*., 2004). Therefore, mitomycin C was added to the scratch wound assay to ensure that closure of the wound was not due to cell division but to migration solely. Some care needs to be taken in order to have a uniform width of the scratch. An alternative may be to grow the cells in special inserts that contain a separation and remove the insert by the time of the assay. In this way, all the scratches would be directly comparable.

Matrigel is a mixture of extracellular and basement membrane proteins derived from the mouse Engelbreth–Holm–Swarm sarcoma on which endothelial cells attach and rapidly form tubes (Lawley, 1898). Matrigel stimulates attachment, migration and differentiation of endothelial cells into tubes mimicking *in vivo* angiogenesis (Auerbach *et al*., 2003). Electron microscopy showed that tight junctions are formed between the endothelial cells during these assays. Therefore, *in vitro* 2-dimensional tube formation assays are considered a model of capillary development and represent the differentiation stage of angiogenesis (Auerbach *et al*., 2003; Staton *et al*., 2006).

The ECSCR siRNA-mediated knockdown with duplex 1 (D1) was used as a control for further experiments. An antibody company based in Belfast (Northern Ireland), Fusion Antibodies, has produced a monoclonal antibody in mouse against the extracellular domain of ECSCR (13G11). The naked protein, produced in bacteria, was used as an immunogen. This antibody was employed in two angiogenesis assays: the scratch wound assay and the tube formation on Matrigel^{TM}.

A1.1.1 Scratch wound assay

Cell migration was observed over a period of 24h after making a scratch on siRNA knocked down HUVECs (and controls, mock and negative control duplex) or HUVECs treated with 4.5, 23 and 45 nM of 13G11 antibody (and IgG controls). siRNA knocked down cells, after a period of 24h seemed to be able to close the wound, but slower compared to the controls. In the controls it was impossible to trace the scratch and the treated cells still showed a migration phenotype. However, it is not quantitatively significant (figure A1). On the other hand, as little as 4.5 nM of 13G11 antibody seemed to inhibit cell migration, since the wound is still not closed after 24h (figure A1). All the used concentrations of blocking antibody have had an effect on cell migration, which seems to be dose dependent.

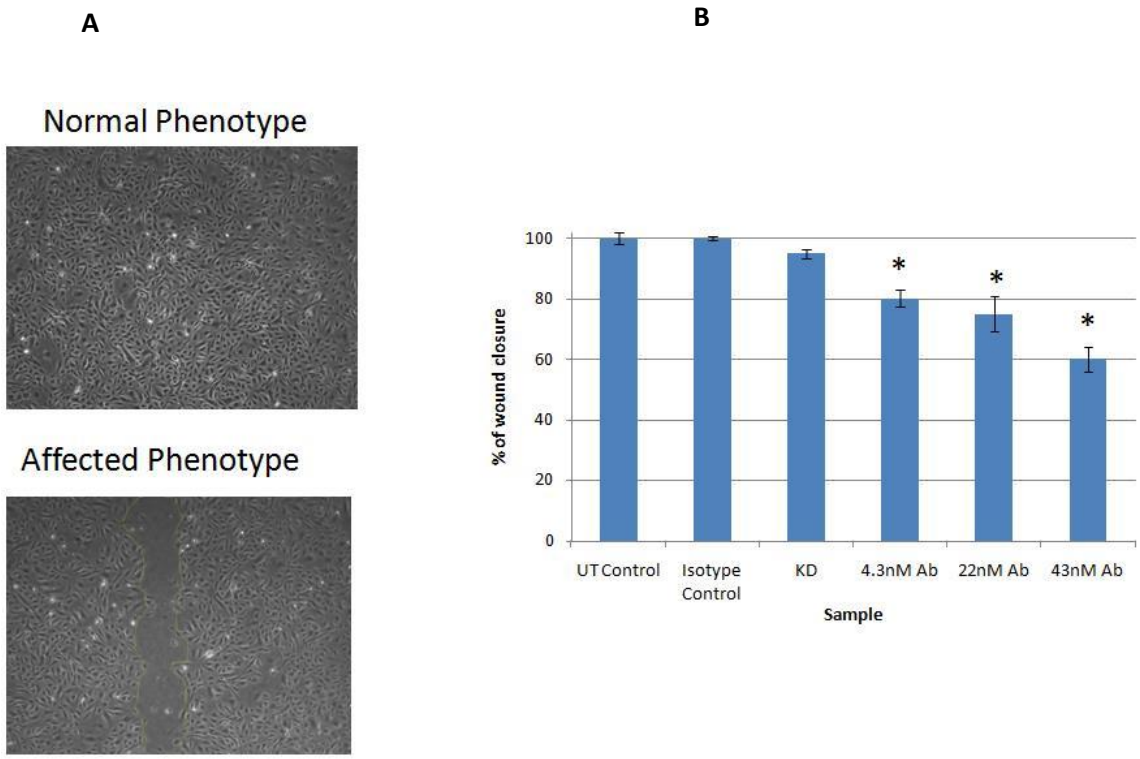

Figure A 1 Wound closure capacity of HUVECs on Matrigel™ measured over a period of 24h

A – representative pictures of normal and abnormal wound closing after 24h. B – quantification of wound closure for the different treatments after 24h. All the images analysed contained a scratch width not significantly different within and between treatments ($-p < 0.05$). UT – untransfected; KD – knockdown; Ab – 13G11 antibody. * significantly different from the respective controls ($-p < 0.05$).

A1.1.2 Matrigel tube formation assay

For the same treatments as on section A1.1.1, the ability of forming tubular structures on Matrigel™ was assessed (Arnaoutova *et al.*, 2009). Both siRNA knock down and 13G11 antibody at all concentrations had a negative effect on tube formation in contrast to the controls (figure A2 B). The quantification of this effect was done by counting the number of nodes per image, which was not significantly different (figure A2 B, blue bars). However, the images of the phenotypes caused by either the 13G11 blocking antibody or siRNA looked quite different from the respective controls. Therefore, the number of branches radiating from each node was not only quantified but also qualified. Strong branches are those which are thick and connect two nodes; weak branches still connect two nodes, but are very thin; broken branches were also counted because they budded from one particular node, but did not connect it to any other. Compared to the respective controls both siRNA and increasing concentrations of 13G11 antibody caused a decreased number of strong branches and an increased number of weak and broken branches sprouting from the nodes (figure A2 B).

Previous work (Bicknell and Nagy, unpublished) had suggested that ECSCR might be upregulated at the transcript level in some types of human cancer, compared to matched normal tissue (figure A3). The 13G11 antibody was used to stain tissue sections of normal *versus* cancer, using a variety of tissues. No significant differences were found between the two types of samples. The antibody seemed to recognise vessels and could be used for both immunohistochemistry and immunofluorescence. Figure A4 illustrates an example of these two techniques using 13G11. Interestingly, the staining seems to co-localise with ULEX (a vascular marker) only on the lumen of the vessels.

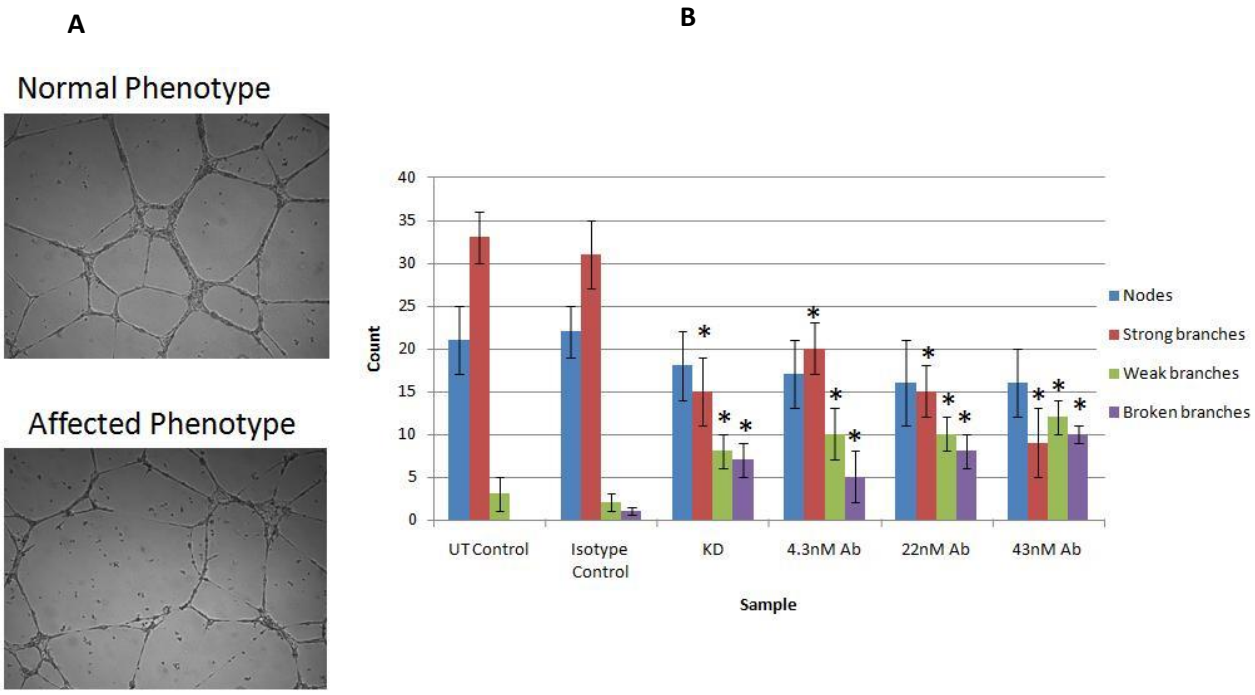

Figure A 2 - Tube formation capacity of HUVECs on Matrigel measured over a period of 24h.

A – representative pictures of normal and abnormal tube formation on Matrigel^{TM} after 24h. B – quantification of tube formation through the count of the number of nodes and branches per image. UT – untransfected; KD – knock down; Ab – 13G11 antibody. * significantly different from the respective controls (-$p < 0.05$, unpaired two-tailed t-test).

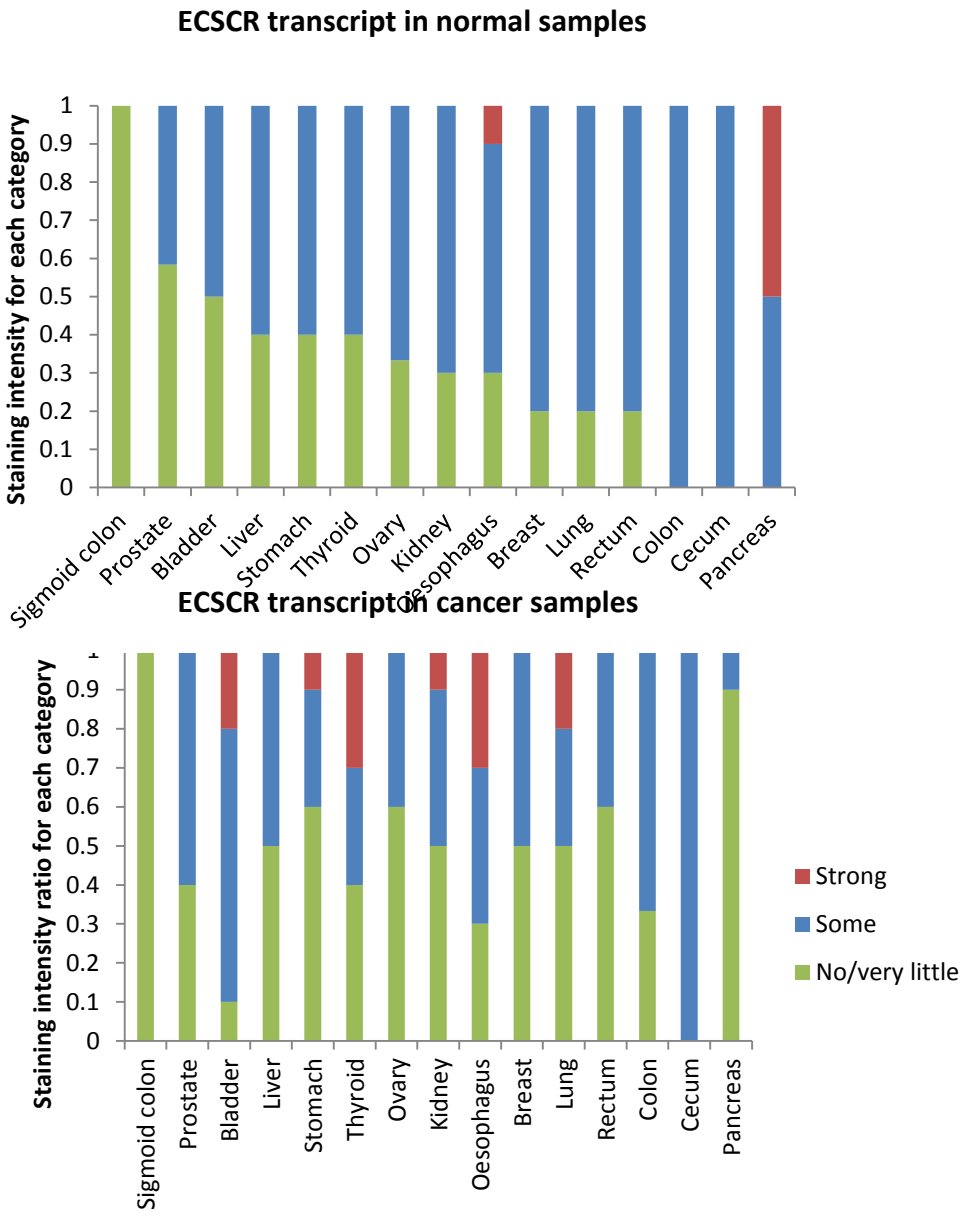

Figure A 3 - Qualitative analysis of ECSCR transcript by *in situ* hybridization in normal and cancer human tissues.

An ECSCR RNA probe was produced to detect and quantify the ECSCR transcript in human normal and cancer tissues (tissue arrays, SuperBioChips Laboratoties). The results were divided into three categories: strong staining, some staining and no or very little staining detected. Due to the fact that not all tissues/types of cancer were represented by the same number of paraffin-embedded spots, the total counts for each category were divided by the total number of spots analysed. For each vertical bar, the different colours represent each category and the sum is 100%.

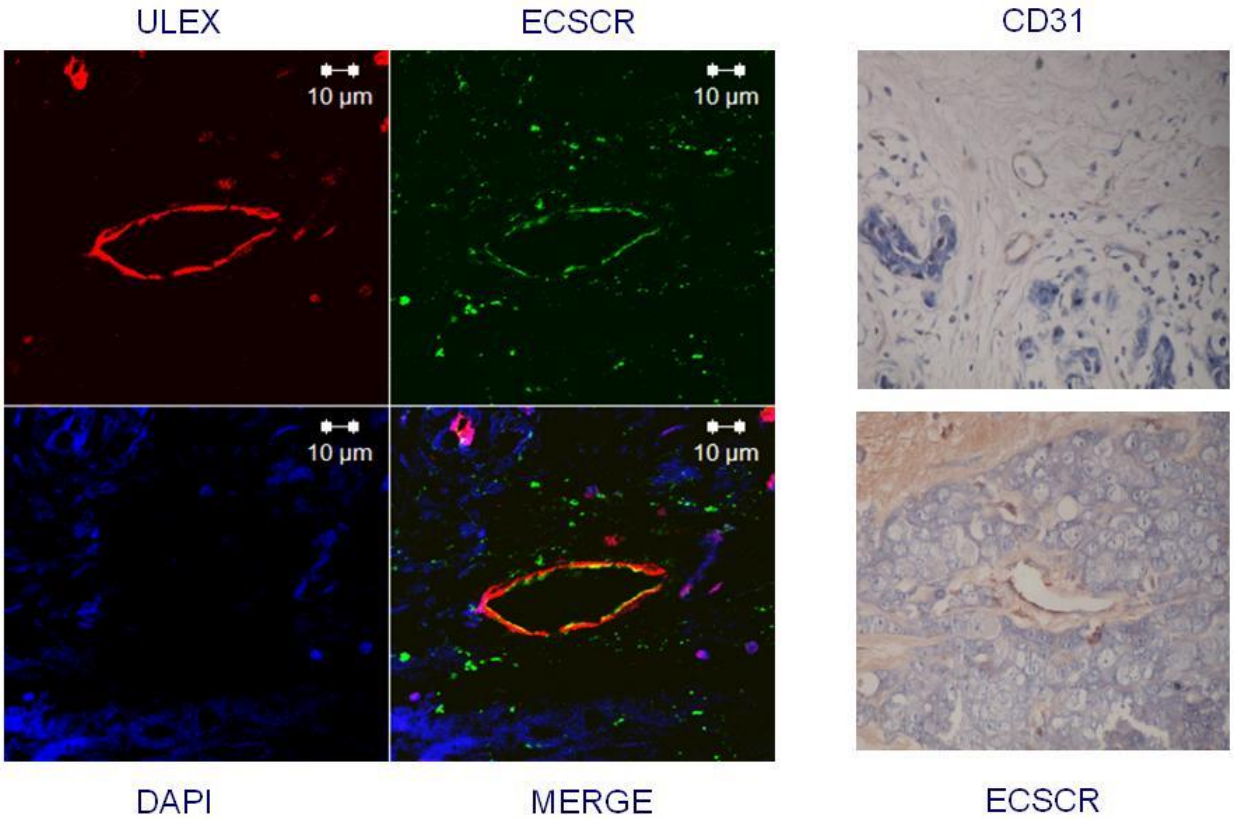

Figure A 4 - Breast cancer paraffin sections stained with 13G11.

Since ECSCR transcript seemed to be upregulated in some cancer types (figure A3), an antibody against ECSCR (13G11) produced by our collaborators at Phusion Antibodies (Belfast) was used to assess the protein levels in human paraffin samples (SuperBioChips Laboratories) by immunofluorescence and immunohistochemistry. The qualitative results of staining are shown on tables A3-A9. This figure shows an example of 13G11 endothelial-specific staining in samples from human breast cancer. Panels on the left – immunofluorescence; panel on the right immunohistochemistry. Endothelial cell markers were used (Ulex, CD31) to confirm endothelial specificity of the 13G11 staining. All staining and image analysis were performed with Dr. Stephanie Maloney, who has acquired these images and kindly allowed their inclusion in this thesis.

Table A3 – Analysis of ECSCR antibody staining on whole (human) tissue sections by immunohistochemistry (IHC) and immunofluorescence (IF). + strong staining; +/- some staining; - no staining detected.

	Tissue	IHC	IF		Tissue	IHC	IF
Normals	Placenta	+	+	Tumours	Colon	-	-
	Adrenal gland	-	-		Ovary	-	-
	Breast skin	-	-		Rectal	+/-	-
	Colon	-	-		Sq Cervix	-	-
	Foreskin	-	-		Ad Cervix	+	+
	Heart	+/-	+/-		Bladder	+	-
	Kidney	-	+/-		Endometrial	+	+
	Liver	-	-		Breast	+	+
	Lung	-	-				
	Lymph gland	-	-				
	Pancreas	-	-				
	Spleen	-	-				
	Stomach	-	+/-				
	Tonsil	-	-				
	Scalp	+/-	+/-				
	Prostate	+	-				
	Brain	+	+				

Table A4 – Analysis of ECSCR antibody staining on human cancer tissue array MA2 (SuperBioChips Laboratories) by immunohistochemistry. + strong staining; +/- some staining; - no staining detected. The numbers on the first column represent each spot for each sample type. The cells with no annotation mean that either that specific spot got lost or damaged during processing or there were less spots present in the chip for that specific tissue.

	Tissue microarray MA2 common cancers					
#	**stomach**	**esophagus**	**lung**	**colon**	**thyroid**	**Kidney**
1	-	-	-	-	+/-	-
2	-	+/-	-	-	-	+/-
3	+	-	+	-	+	-
4	+	-	-	+	+/-	-
5	+/-	+	+	-	+/-	+/-
6	-	-	-	-	-	-
7	-	+/-	+/-	-	-	-
8	-	+	-	-	+	+/-
9	-	-	-	-	-	
10	-	+/-	+/-	-	-	

Table A5 – Analysis of ECSCR antibody staining on human normal tissue array MAN2 (SuperBioChips Laboratories) by immunohistochemistry. + strong staining; +/- some staining; - no staining detected. The numbers on the first column represent each spot for each sample type. The cells with no annotation mean that either that specific spot got lost or damaged during processing or there were less spots present in the chip for that specific tissue.

	Tissue microarray MAN2 matching normals					
#	**stomach**	**esophagus**	**lung**	**colon**	**thyroid**	**kidney**
1	-	+/-	+	+	+	+
2	+	+/-	+/-	-	-	+/-
3	-	+	-	+	+/-	+
4	-	+	+/-	+	-	+/-
5	+	+	+	-	+/-	-
6	-	+	+	-	+	-
7	+/-	+/-	+	-	-	+/-
8	-	-	+	+	+/-	-
9	-	+	+	-	-	-
10	-	-	+/-	+	-	

Table A6 – Analysis of ECSCR antibody staining on human cancer tissue array MB3 (SuperBioChips Laboratories) by immunohistochemistry. + strong staining; +/- some staining; - no staining detected. The numbers on the first column represent each spot for each sample type. The cells with no annotation mean that either that specific spot got lost or damaged during processing or there were less spots present in the chip for that specific tissue.

	Tissue microarray MB3 common cancers					
#	**breast**	**liver**	**bladder**	**ovary**	**pancreas**	**prostate**
1	+	+/-	-	-	+/-	-
2	-	-	+/-	+	-	-
3	+/-	-	-	+	-	+/-
4	+/-	-	-	+	-	-
5	-	+/-	+	-	-	-
6	-	-	-	-	-	+/-
7	+	+/-	-	-	-	+/-
8	-	-	-	+	-	-
9	-	-	+/-	+	-	-
10	-	-	-	-	-	

Table A7 – Analysis of ECSCR antibody staining on human normal tissue array MBN3 (SuperBioChips Laboratories) by immunohistochemistry. + strong staining; +/- some staining; - no staining detected. The numbers on the first column represent each spot for each sample type. The cells with no annotation mean that either that specific spot got lost or damaged during processing or there were less spots present in the chip for that specific tissue.

	Tissue microarray MBN3 matching normals					
#	**breast**	**liver**	**bladder**	**ovary**	**pancreas**	**prostate**
1	+/-	-		-	+/-	+/-
2	+	+/-	-	+	+	+/-
3	-	+	-	+/-	-	+
4	+	-	+/-	+	+	-
5	-	-	+/-	+/-	-	+
6	+	-	-	+	+	-
7	+/-	-	+	-	-	-
8	+/-	-	+	-	-	+
9	+	+/-	-	+	-	+
10	+/-	-	-	+	+/-	

Table A8 – Analysis of ECSCR antibody staining on human cancer tissue array MC4 (SuperBioChips Laboratories) by immunohistochemistry. + strong staining; +/- some staining; - no staining detected. The numbers on the first column represent each spot for each sample type. The cells with no annotation mean that either that specific spot got lost or damaged during processing or there were less spots present in the chip for that specific tissue.

	Tissue microarray MC4 common cancers					
#	**Endometrium**	**Gall-bladder**	**Larynx**	**Cervix**	**Lymphoma**	**Melanoma**
1	+/-	-	-	-	-	-
2	+/-	+/-	-	-	+/-	-
3	-	-		+/-	-	-
4	-	-	-	-	+	-
5	-	-	-	+/-	-	-
6	-	+/-	-	-	-	+/-
7	-	-	-	-	+/-	+
8	-	-	-	-	-	-
9	-	-	+/-	+/-	+/-	-
10	+/-		-	+/-	-	

Table A9 – Analysis of ECSCR antibody staining on human normal tissue array MCN4 (SuperBioChips Laboratories) by immunohistochemistry. + strong staining; +/- some staining; - no staining detected. The numbers on the first column represent each spot for each sample type. The cells with no annotation mean that either that specific spot got lost or damaged during processing or there were less spots present in the chip for that specific tissue.

	Tissue microarray MCN4 matching normals					
#	**Endometrium**	**Gall-bladder**	**Larynx**	**Cervix**	**Lymphoma**	**Melanoma**
1	-	+	-	+	+/-	-
2	-	-	+	+/-	+/-	+
3	-	-	+	+	+	-
4	-	-	+/-	+	+	+/-
5	-	+		+	+/-	+/-
6	+	+	+	+/-	-	+/-
7	-	+/-		+	-	
8	-	+/-	+/-	+/-	-	
9	+	+	+		+	
10	+/-	+/-	+/-	-	+/-	

While the functional assays and tissue staining were being done in Birmingham, the isotype (IgG1) and epitope of 13G11 were being determined in Belfast. In order to map the epitope, several constructs were made, lacking segments of the protein (figure A5) and subsequent western blots were performed to assess where the antibody would bind or not. The epitope recognised by 13G11, QTVPPNSTTM, is located between amino acids 91 and 100.

To test the specificity of 13G11 for ECSCR, in Belfast, HEK 293T cells were transfected with ECSCR-GFP (and untransfected HEK 293T cells were used as a control). The antibody has recognised a protein at about 55 kDa in the transfected lysate. This corresponds to the size of a fusion protein between GFP and unglycosylated or very little glycosylated ECSCR.

Several attempts were made to use 13G11 to detect ECSCR in HUVEC lysate, but they were unsuccessful. In order to further test for specificity, HUVECs were transfected with ECSCR siRNA (and respective controls) and analysed by FACS. This analysis has shown that the antibody binds to HUVECs, but does not recognise ECSCR (figure A 7), as there is a shift from the population not treated with 13G11 to the populations exposed to the antibody, but there are no differences between mock, negative control duplex and ECSCR siRNA.

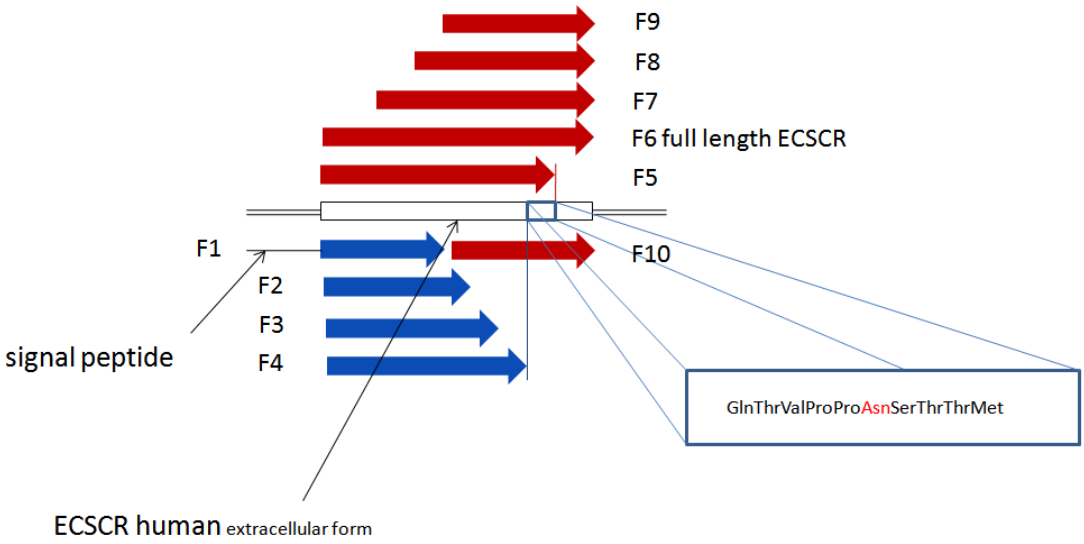

Figure A 5 – Epitope mapping strategy of 13G11

In order to map the epitope recognised by 13G11, several constructs were made, lacking segments of the protein and subsequent western blots were performed to assess where the antibody would bind or not. The epitope recognised by 13G11 is QTVPPNSTTM.

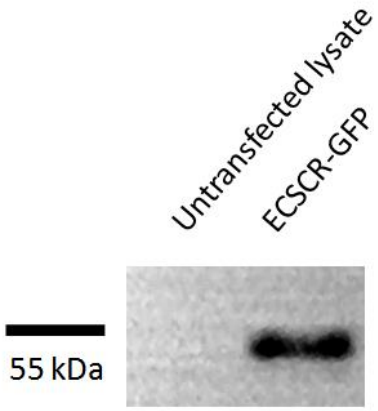

Figure A 6 – 13G11 recognises an ECSCR-GFP fusion.protein produced in HEK 293T cells

To test the specificity of 13G11 for ECSCR, HEK 293T cells were transfected with ECSCR-GFP (and untransfected HEK 293T cells were used as a control). The antibody has recognised a protein at about 55 kDa in the transfected lysate.

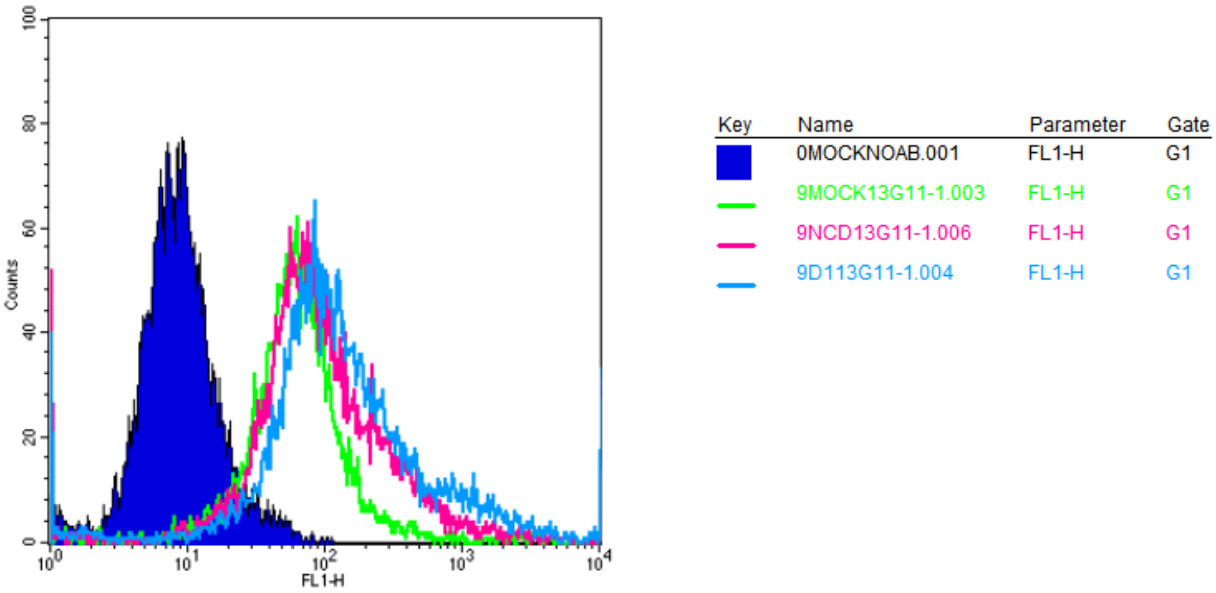

Figure A 7 – FACS analysis of 13G11 in HUVECs.

HUVECs were transfected with ECSCR siRNA (and respective controls) and analysed by FACS. This analysis has shown that the antibody produced in Belfast by Phusion Antibodies binds to HUVECs, but doesn't recognise ECSCR (figure A 7), as there is a shift from the population not treated with 13G11 (dark blue) to the populations exposed to the antibody, but there are no differences between mock (green), negative control duplex (pink) and ECSCR siRNA (light blue).

APPENDIX 3: RE-PRINT OF THE THESIS-RELATED PUBLICATION

Verissimo AR, Herbert JMJ, Heath VL, Legg JA, Sheldon H, Andre M, Swain RK and Bicknell R. (2009). Functionally defining the endothelial transcriptome, from Robo4 to ECSCR. *Biochem Soc Trans*. 37: 1214-1217

APPENDIX 4: LIST OF PRESENTED ABSTRACTS

1. Poster presentations

2011 – The role of ECSCR in endothelial cell biology. Gordon Research Conference on Vascular Cell Biology, Ventura, CA, USA.

2010 – Regulation of zebrafish developmental angiogenesis by endothelial cell specific chemotaxis regulator (ECSCR). 9th International Zebrafish Development and Genetics Conference, Madison, WI, USA.

2009 – Endothelial cell specific molecule 2 is involved in actin cytoskeleton modulation. Molecular and Cellular Mechanisms of Angiogenesis (Biochemical Society meeting), Chester, UK.

2009 – Endothelial cell specific molecule 2 is involved in actin cytoskeleton modulation. Angionet Meeting, Dundee, UK.

2. Oral presentations

2010 – Functional characterisation of ECSCR. EMBO mouse anatomy and embryology practical course, Split, Croatia – award for best oral presentation.

2009 – The role of endothelial cell specific molecule 2 in angiogenesis. VITA seminars, University of Birmingham, UK.

REFERENCES

Akhtar T, Li J, Olden T, and Wallace KN. (2009). Use of Phospholipase A2 for Antigen Retrieval in Zebrafish Whole-Mount Immunohistochemistry. *Zebrafish.* 6(3): 223–227.

Akinc A, Thomas M, Klibanov AM, Langer R. (2004). Exploring polyethylenimine-mediated DNA transfection and the proton sponge hypothesis. *J Gene Med.* 7 (5): 657–663.

Anderson EBQ, Khvorova A, Karpilow J. (2008) Identifying siRNA-induced offtargets by microarray analysis. *Methods Mol Biol*. 442: 45-63.

Andrade SP, Ferreira MA. (2009). The sponge implant model of angiogenesis. Methods Mol Biol. 467:295-304.

Armstrong L-J, Heath VL, Sanderson S, Kaur S, Beesley JFJ, Herbert JM, Legg JA, Poulsom R and Bicknell R. (2008)**.** ECSM2, an endothelial specific filamin A binding protein that mediates chemotaxis. *Arterioscler Thromb Vasc Biol*. 28:1640-1646.

Armstrong L-J. (2005). Characterisation of the endothelial specific molecule ECSM2. D.Phil. Thesis, University of Oxford, Oxford, U.K.

Arnaoutova I, George J, Kleinman HK, Benton G. (2009). The endothelial cell tube formation assay on basement membrane turns 20: state of the science and the art. *Angiogenesis.* 12(3):267-74.

Atochina EN, Balyasnikova IV, Danilov SM, Granger DN, Fisher AB, Muzykantov VR. (1998). Immunotargeting of catalase to ACE or ICAM-1 protects perfused rat lungs against oxidative stress. *Am J Physiol*. 275(4 Pt 1):L806-17.

Auerbach R, Lewis R, Shinners B, Kubai L, and Aktar N. (2003) Angiogenesis assays: a critical overview. *Clin. Chem.* 49: 32-40.

Baker M, Robinson SD, Lechertier T, Barber PR, Tavora B, D'Amico G, Jones DT, Vojnovic B and Hodivala-Dilke K. (2012). Use of the mouse aortic ring assay to study angiogenesis. *Nature Protocols*. 7(1): 89-104.

Baldessari D and Mione M. (2008). How to create the vascular tree? (Latest) help from the zebrafish. *Pharmacology and Therapeutics*. 118: 206-230.

Bazzoni G and Dejana E. (2004). Endothelial cell to cell junctions: molecular organisation and role in vascular homeostasis. *Physiol Rev.* 84: 869-901.

Bedell VM, Westcot SE, Ekker SC. (2011). Lessons from morpholino-based screening in zebrafish. *Brief Funct Genomics*. 10(4):181-8.

Bergers G and Hanahan D. (2008). Models of resistance to anti-angiogenic therapy. *Nat Rev Cancer*. 8: 592-603.

Blaser H, Reichman-Fried M, Castanon I, Dumstrei K, Marlow FL, Kawakami K, Solnica-Krezel L, Heisenberg CP and Raz E. (2006). Migration of zebrafish primordial germ cells: a role for myosin contraction and cytoplasmic flow. *Dev. Cell.* 11(5): 613–627.

Boamah EK. (2007). Mitomycin-DNA adducts induce p53 dependant and p53 independant cell death pathways. *ACS Chemical Biology*, 399-407.

Bredt DS. (1998). Sorting out genes that regulate epithelial and neuronal polarity. *Cell.* 94:691–694.

Bretscher A, Edwards K and Fehon RG. (2002). ERM proteins and merlin: Integrators at the cell cortex. *Nat Rev Mol Cell Biol*, 3:586–599.

Brown JM and Wilson WR. (2004). Exploiting tumour hypoxia in cancer treatment. *Nat Rev*

Cancer. 4:437-447.

Carmeliet P. (2005). Angiogenesis in life, disease and medicine. *Nature*. 438 (15): 932-936.

Castets M, Mehlen P. (2010). Netrin-1 role in angiogenesis: to be or not to be a pro-angiogenic factor? *Cell Cycle*. 15;9(8):1466-71.

Cha YR and Weinstein BM. (2007). Visualization and experimental analysis of blood vessel formation using transgenic zebrafish. *Birth Defects Research (Part C)*. 81: 286-296.

Childs S, Chen JN, Garrity DM and Fishman MC. (2002). Patterning of angiogenesis in the zebrafish embryo. *Development*. 129: 973-982.

Coultas L, Chawengsaksophak K and Rossant J. (2005). Endothelial cells and VEGF in vascular development. *Nature Insights*. 937-945.

Davidson AJ and Zon LI. (2004). The definitive (and primitive) guide to zebrafish hematopoiesis. *Oncogene*. 23: 7233-7146.

Delvaeye M, De Vriese A, Zwerts F, Betz I, Moons M, Autiero M, Conway EM. (2009). Role of the 2 zebrafish survivin genes in vasculo-angiogenesis, neurogenesis, cardiogenesis and hematopoiesis. *BMC Dev Biol*. 26;9:25.

Denekamp J. (1982). Endothelial cell proliferation as a novel approach to targeting tumour therapy. *Br. J. Cancer.* 45: 136-139.

Dennis G, Sherman BT, Hosack DA, Yang J, Baseler MW, Lane HC, Lempicki RA. (2003). DAVID: Database for Annotation, Visualization, and Integrated Discovery. *Genome Biology.* 4(5): p3.

Dewhirst MW, Cao Y and Moeller B. (2008). Cycling hypoxia and free radicals regulate angiogenesis and radiotherapy response. *Nat Rev Cancer*. 8: 425-437.

Doyon Y, McCammon J, Miller JC, Faraji F, Ngo C, Katibah GE, Amora R, Hocking TD, Zhang L, Rebar EJ, Gregory PD, Urnov FD and Amacher SL. (2008). Heritable targeted gene disruption in zebrafish using designed zinc finger nucleases. *Nat Biotechnol*. 26(6): 702-708.

Dudek AZ, Bodempudi V, Welsh BW, Jasinski P, Griffin RJ, Milbauer L, Hebbel RP. (2007). Systemic inhibition of tumour angiogenesis by endothelial cell-based gene therapy. *Br J Cancer*. 97(4):513-22.

Ekker SC. (2000). Morphants: a new systemic vertebrate functional genomics approach. *Yeast* 17: 302-306.

Ekker SC. (2008). Zinc finger-based knockout punches for zebrafish genes. *Zebrafish*. 5(2): 121-123.

Fang K, Bruce M, Pattillo CB, Zhang S, Stone R 2nd, Clifford J and Kevil CJ. (2011). Temporal genomewide expression profiling of DSS colitis reveals novel inflammatory and angiogenesis genes similar to ulcerative colitis. *Physiol. Genomics*. 43: 43-56.

Feil S, Valtcheva N and Feil R. (2009). Inducible Cre mice. *Methods Mol Biol.* 530:343-63.

Felty Q. (2011). Proteomic 2D DIGE profiling of human vascular endothelial cells exposed to environmentally relevant concentration of endocrine disruptor PCB153 and physiological concentration of 17β-estradiol. *Cell Biol Toxicol*. 27(1):49-68.

Ferrara N. (2002). VEGF and the quest for tumour angiogenesis factors. *Nat Rev Cancer*. 2: 795-803.

Ferrara N and Kerbel RS. (2005). Angiogenesis as a therapeutic target. *Nature Insights*. 967-974.

Fischer AH, Jacobson KA, Rose J, Zeller R. (2008). Hematoxylin and eosin staining of tissue and cell sections. *CSH Protoc*. doi: 10.1101/pdb.prot4986.

Flamme I, Frolich T and Risau W. (1997). Molecular Mechanisms of Vasculogenesis and Embryonic Angiogenesis. *J Cell Physiol*. 173:206–210.

Folkman J. (1971) Tumor angiogenesis: therapeutic implications. *N Eng J Med.* 285: 1182-1186.

Folkman J and Klagsbrun M. (1987) Angiogenic factors. *Science* 235: 442-447.

Fouquet B, Weinstein BM, Serluca FC and Fishman MC. (1997). Vessel Patterning in the Embryo of the Zebrafish: Guidance by Notochord. *Developmental Biology.* 183: 37-48.

Friedel RH, Plump A, Lu X, Spilker K, Jolicoeur C, Wong K, Venkatesh TR, Yaron A, Hynes M, Chen B, Okada A, McConnell SK, Rayburn H and Tessier-Lavigne M. (2005). Gene targeting using a promoterless gene trap vector. *Proc Natl Acad Sci U S A.* 102: 13188-13193.

Fukumura D, Kashiwagi S and Jain R. (2006). The role of nitric oxide in tumour progression. *Nat Rev Cancer*. 6: 521-534.

Garcia P, Berlanga O, Watson R and Frampton J. (2005). Generation of a conditional allele of the B-myb gene. *Genesis*. 43: 189-195.

Gariano RF and Gardner TW. (2005). Retinal angiogenesis in development and disease. *Nature insights*. 960-966.

Gering M and Patient P. (2005). Hedgehog signalling is required for adult blood stem cell formation in zebrafish embryos. *Dev. Cell*. 8:389-400.

Giganti A, Plastino J, Janji B, Van Troys M, Lentz D, Ampe C, Sykes C, Friederich E. (2005). Actin-filament cross-linking protein T-plastin increases Arp2/3-mediated actin-based movement. *J Cell Sci*. 118(Pt 6):1255-65.

Gilbert SF. (2006). Developmental Biology. 8th Edition. Sinauer Associates, Inc. Sunderland, Massachussets, USA. 817 pp.

Gomez TS, Kumar K, Medeiros RB, Shimizu Y, Leibson PJ, Billadeau DD. Immunity. (2007). Formins regulate the actin-related protein 2/3 complex-independent polarization of the centrosome to the immunological synapse. 26(2):177-90.

Gould GW and Lippincott-Schwartz J. (2009). New roles for endosomes: from vesicular carriers to multi-purpose platforms. *Nat Rev Cancer*. 10: 287-292.

Graf T. (2002). Differentiation plasticity of hematopoietic cells. *Blood.* 99: 3089-3101.

Green AR, Salvaris E and Begley CG. (1991). Erythroid expression of the 'helix-loop-helix' gene, SCL. *Oncogene*. 6(3): 475-479.

Greenberg DA and Jin K. (2005). From angiogenesis to neuropathy. *Nature Insights*. 954-959.

Gustafsson E, Brakebusch C, Hietanen K and Fässler R. (2000). Tie-1-directed expression of Cre recombinase in endothelial cells of embryoid bodies and transgenic mice. *J Cell Sci*. 114(4): 671-676.

Harrigan RA and Jones K. (2002). ABC of clinical electrocardiography - conditions affecting the right side of the heart. *BMJ*. 324: 1201-1204.

Harris BZ and Lim WA. (2001). Mechanism and role of PDZ domains in signalling complex assembly. *J Cell Sci.* 114: 3219–3231.

Herbert JM, Stekel D, Sanderson S, Heath VL and Bicknell R. (2008) A novel method of differential gene expression analysis using multiple cDNA libraries applied to the identification of tumour endothelial genes. *BMC Genomics* 9:153-173.

Herbert SP, Huisken J, Kim TN, Feldman ME, Houseman BT, Wang RA, Shokat KM and Stainier DYR. (2009). Arterial-Venous Segregation by Selective Cell Sprouting: An Alternative Mode of Blood Vessel Formation. *Science.* 326 (5950): 294-298.

Hsia N and Zon LI. (2005). Transcriptional regulation of hematopoietic stem cell development in zebrafish. *Exp Hematol.* 33(9): 1007-1014.

Hu G., Tang J, Zhang B., Lin Y, Hanai J, Galloway J, Bedell V, BaharyN, Han Z, Ramchandran R, Thisse B, Thisse C, Zon LI and Sukhatme1 VP. (2006). A novel endothelial-specific heat shock protein HspA12B is required in both zebrafish development and endothelial functions in vitro. *J Cell Sci.* 119: 4117-4126

Huminiecki L and Bicknell R. (2000). *In silico* cloning of novel endothelial-specific genes. *Genome Res*. 10 (11): 1796-1806.

Huttlin EL, Jedrychowski MP, Elias JE, Goswami T, Rad R, Beausoleil SA, Villén J, Haas W, Sowa ME, Gygi SP. (2010). A tissue-specific atlas of mouse protein phosphorylation and expression. *Cell*. 143(7):1174-89.

Ikeda K, Nakano R, Uraoka M, Nakagawa Y, Koide M, Katsume A, Minamino K, Yamada E, Yamada H, Quetermous T and Matsubara H. (2009). Identification of ARIA regulating

endothelial apoptosis and angiogenesis by modulating proteasomal degradation of cIAP-1 and cIAP-2. *Proc Nat Acad Sci USA*. 106(20): 8227-8232.

Isogai S, Horiguchi M and Weinstein BM. (2001). The vascular anatomy of the developing zebrafish: an atlas of embryonic and early larval development. *Dev Biol.* 230(2): 278-301.

Isogai S, Lawson ND, Torrealday S, Horiguchi M, Weinstein BM. (2003). Angiogenic network formation in the developing vertebrate trunk. *Development.* 130(21):5281-90.

Jaffe, EA, Nachman, RL, Becker CG, and Minick R. (1973). Culture of human endothelial cells derived from umbilical veins. Identification by morphologic and immunologic criteria. *J Clin Invest.* 52(11): 2745-2756.

Jia J, Wang J, Teh M, Sun W, Zhang J, Kee I, Chow PK, Liang RC, Chung MC, Ge R. (2010). Identification of proteins differentially expressed between capillary endothelial cells of hepatocellular carcinoma and normal liver in an orthotopic rat tumor model using 2-D DIGE. *Proteomics.* 10(2):224-34.

Jones SL and Sharif Y. (2005). Asymmetrical protein kinase A activity establishes neutrophil cytoskeletal polarity and enables chemotaxis. *J Lekocyte Biol*. 78

Jong JLO and Zon LI. (2005). Use of the zebrafish system to study primitive and definitive hematopoiesis. *Annu Rev Genet.* 39: 481-501.

Kaczmarek E, Erb L, Koziak K, Jarzyna R, Wink MR, Guckelberger O, Blusztajn JK, Trinkaus-Randall V, Weisman GA and Robson SC. (2005). Modulation of endothelial cell migration by extracellular nucleotides: involvement of focal adhesion kinase and phosphatidylinositol 3-kinase-mediated pathways. *Thromb Haemost*. 93(4):735-42.

Kidd KR and Weinstein BM. (2003) Fishing for novel angiogenic therapies. *Br. J.Pharmacol.* 140: 585-594.

Kim, L and Kimmel AR. (2006). GSK3 at the Edge: Regulation of Developmental Specification and Cell Polarization. *Curr Drug Targets*. 7: 1411-1419.

Kimmel CB, Ballard WW, Kimmel SR, Ullmann B and Schilling TF. (1995). Stages of Embryonic Development of the zebrafish. *Developmental Dynamics.* 203:253-310.

Koide, M., Ikeda, K., Akakabe, Y., Kitamura, Y., Ueyama, T., Matoba, S., Yamada, H., Okigaki, M. and Matsubara, H. (2011). Apoptosis regulator through modulating IAP expression (ARIA) controls the PI3K/Akt pathway in endothelial and endothelial progenitor cells. *Proc. Natl. Acad. Sci. U.S.A.* 108: 9472–9477.

Krupke DM, Begley DA, Sundberg JP, Bult CJ and Eppig JT. (2008). The mouse tumour biology database. *Nat Rev Cancer*. 8: 459-465.

Kurosaka S and Kashina A. (2009). Cell Biology of Embryonic Migration. *Birth Defects Res C Embryo Today*. 84(2): 102–122.

Lämmermann T, Bader BL, Monkley SJ, Worbs T, Wedlich-Söldner R, Hirsch K, Keller M, Förster R, Critchley DR, Fässler R, Sixt M. (2008). Rapid leukocyte migration by integrin-independent flowing and squeezing. *Nature*. 453(7191):51-5.

Lawley TJ. (1989) Induction to morphologic differentiation of endothelial cells in culture. *J. Invest. Dermatol.* 93: 595-615.

Liang CC, Park AY, Guan JL. (2007). *In vitro* scratch assay: a convenient and inexpensive method for analysis of cell migration in vitro. *Nat Protoc*. 2(2):329-33.

Liao EC, Paw BH, Oates AC, Pratt SJ, Postlethwait JH and Zon LI. (1998). SCL/Tal-1 transcription factor acts downstream of cloche to specify hematopoietic and vascular progenitors in zebrafish. *Genes Dev.* 12(5):621-626.

Liu F and Patient R. (2008). Genome-wide analysis of the zebrafish ETS family identifies three genes required for hemangioblast differentiation or angiogenesis. *Circulation Research*. 103: 1147-1154.

Livak KJ, Schmittgen TD. (2001). Analysis of relative gene expression data using real-time quantitative PCR and the 2(-Delta Delta C(T)) Method. *Methods.* 25(4):402-8.

Loy CJ, Sim KS and Young EL. (2003). Filamin-A fragment localises to the nucleus to regulate androgen receptor and coactivator functions. *Proc. Natl. Acad. Sci. USA*. 100: 4562-4567.

Luo Y, Batalao A, Zhou H and Zhu L. (1997). Mammalian Two-Hybrid System: A Complementary Approach to the Yeast Two-Hybrid System. *BioTechniques*. 22:350-352.

Ma AC, Lin R, Chan PK, Leung JC, Chan LY, Meng A, Verfaillie CM, Liang R, Leung AY. (2007). The role of survivin in angiogenesis during zebrafish embryonic development. *BMC Dev Biol*. 18;7:50.

Ma F, Zhang D, Yang H, Sun H, Wu W, Gan Y, Balducci J, Wei Y, Zhao X and Huang Y. (2009). Endothelial cell-specific molecule 2 (ECSM2) modulates actin remodelling and epidermal growth factor receptor signalling. *Genes to Cells*. 14:281-293.

Maciag T, Cerundolo J, Ilsley S, Kelley PR and Forand R. (1979). An endothelial cell growth factor from bovine hypothalamus: identification and partial characterization. *Proc Natl Acad Sci U S A*. 76(11): 5674-8.

Madri JA, Graesser D. (2000). Cell migration in the immune system: the evolving inter-related roles of adhesion molecules and proteinases. *Dev Immunol*. 7(2-4):103-16.

Maiti D, Xu Z, Duh EJ. (2008). Vascular endothelial growth factor induces MEF2C and MEF2-dependent activity in endothelial cells. *Invest Ophthalmol Vis Sci*. 49(8):3640-8

Mao X, Fujiwara Y, Orkin SH. (1999). Improved reporter strain for monitoring Cre recombinase-mediated DNA excisions in mice. *Proc Natl Acad Sci USA*. 96:5037–5042.

Martin, S. and Murray, C. (Eds) (2009). Angiogenesis Protocols. 2nd Edition. Humana Press. New York, USA. 358pp.

McClatchey AI and Fehon RG. (2009). Merlin and the ERM proteins--regulators of receptor distribution and signaling at the cell cortex. *Trends Cell Biol*. 19(5):198-206.

McCormick CJ, Newbold CI, Berendt AR. (2000). Sulfated glycoconjugates enhance CD36-dependent adhesion of Plasmodium falciparum-infected erythrocytes to human microvascular endothelial cells. *Blood.* 96(1):327-33.

Meng X, Noyes MB, Zhu L, Lawson ND, Wolfe, SA. (2008). Targeted gene inactivation in zebrafish using engineered zinc finger nucleases. *Nat Biotechnol*. 26(6): 695-701.

Mignatti, P and Rifkin DB. (1996) Plasminogen activators and matrix metalloproteinases in angiogenesis. *Enzyme protein* 49 (1-3): 117-137.

Murre C. (2009). Developmental trajectories in early hematopoiesis. *Genes and Development*. 23: 2366-2370.

Naldini L, Blömer U, Gallay P, Ory D, Mulligan R, Gage FH, Verma IM, Trono D. 1996. *In vivo* gene delivery and stable transduction of nondividing cells by a lentiviral vector. Science. 272(5259):263-7.

Neri D and Bicknell R. (2005). Tumour vascular targeting. *Nat Rev Cancer*. 5: 436-446.

Niethammer M, Kim E and Sheng M. (1996). Interaction between the C terminus of NMDA receptor subunits and multiple members of the PSD-95 family of membrane-associated guanylate kinases. *J Neurosci* 16:2157–2163.

Pandya NM, Dhalla NS and Santan DD. (2006). Angiogenesis—a new target for future therapy. *Vascular Pharmacology*. 44: 265-274.

Passman JN, Dong XR, Wu SP, Maguire CT, Hogan KA, Bautch VL, Majesky MW. (2008). A sonic hedgehog signaling domain in the arterial adventitia supports resident Sca1+ smooth muscle progenitor cells. *Proc Natl Acad Sci.* 105(27):9349-54.

Pelosi E, Valtieri M, Coppola S, Botta R, Gabbianelli M, Lulli V, Marziali G, Masella B, Muller R, Sgadari C, Testa U, Bonanno G and Peschle C. (2002) Identification of the hemangioblast in postnatal life. *Blood*. 100:3203–3208.

Pettit SJ, Liang Q, Rairdan XY, Moran JL, Prosser HM, Beier DR, Lloyd KC, Bradley A and Skarnes WC. (2009). Agouti C57BL/6N embryonic stem cells for mouse genetic resourced. *Nat Methods*. 6: 493-495.

Piette D, Hendrickx M, Willems E, Kemp CR, Leyns L. (2008). An optimized procedure for whole-mount *in situ* hybridization on mouse embryos and embryoid bodies. *Nat Protoc*. 3(7):1194-201.

Poueymirou WT, Auerbach W, Frendewey D, Hickey JF, Escaravage JM, Esau L, Doré AT, Stevens S, Adams NC, Dominguez MG, Gale NW, Yancopoulos GD, DeChiara TM, Valenzuela DM. (2007). F0 generation mice fully derived from gene-targeted embryonic stem cells allowing immediate phenotypic analyses. *Nat Biotechnol.* 25(1):91-9.

Raffii S, Lyden D, Benezra R, Hattori K and Heissig B. (2002). Vascular and haematopoietic stem cells: novel targets for anti-angiogenesis therapy? *Nat Rev Cancer*. 2: 826-835.

Raymond C and Soriano P. (2010). ROSA26Flpo delete mice promote efficient inversion of conditional gene traps *in vivo*. *Genesis*. 48: 603-606.

Reynolds, A, Leake, D, Boese Q, Scaringe S, Marshall WS and Khvorova A. (2004) Rational siRNA design for RNA interference. *Nature Biotechnol.* 22: 326-330

Risau W and Flamme I. (1995). Vasculogenesis. *Annu Rev Cell Dev Biol*. 11: 73-91.

Risau, W. (1997) Mechanisms of angiogenesis. *Nature.* 386**:** 671-674.

Roman BL and Weinstein BM. (2000). Building the vertebrate vasculature: research is going swimmingly. *Bioassays*. 22: 882-893.

Rouslahti E. (2002). Specialization of tumour vasculature. *Nat Rev Cancer*. 2002. 2: 83-90.

Rudolph C, Lausier J, Naundorf S, Müller RH, Rosenecker J. (2000). *In vivo* gene delivery to the lung using polyethylenimine and fractured polyamidoamine dendrimers. *J Gene Med*. 2(4): 269–78.

Sacewicz I, Wiktorska M, Wysocki T, Niewiarowska J. (2009). Mechanisms of cancer angiogenesis. *Postepy Hig Med Dosw*. 63:159-68.

Sambrook J and Russel D. (2001). SDS-Polyacrylamide Gel Electrophoresis of Proteins. Molecular Cloning. J. Sambrook and D. Russel. New York, Cold Spring Harbor Laboratory Press. 3: A8.40-A8.45.

Schier AF. 2007. The maternal-zygotic transition: death and birth of RNAs. *Science*. 316(5823):406-7.

Seol HJ, Chang JH, Yamamoto J, Romagnuolo R, Suh Y, Weeks A, Agnihotri S, Smith CA, Rutka JT. (2012). Overexpression of CD99 Increases the Migration and Invasiveness of Human Malignant Glioma Cells. *Genes Cancer*. 3(9-10):535-49.

Shi C, Lu J, Wu W, Ma F, Georges J, Huang H, Balducci J, Chang Y and Huang Y. (2011) Endothelial Cell- Specific Molecule 2 (ECSM2) localizes to cell-cell junctions and modulates bFGF-directed cell migration via the ERK-FAK pathway. *PloS ONE*. 6(6): e21482

Sledz C, de Veer M, Silverman R and Williams B. (2003) Activation of the interferon system by short-interferring RNAs. *Nat. Cell Biol.* 5: 834-839.

Söldera E, Böckle BC, Nguyen VA, Fürhapter C, Obexer P, Erdel M, Stössel H, Romani N, Sepp NT. (2012). Isolation and characterization of CD133 + CD34 + VEGFR-2 + CD45 − fetal endothelial cells from human term placenta. Microvascular Research. 84(1): 65–73.

Soriano P. (1999). Generalized lacZ expression with the ROSA26 Cre reporter strain. *Nat Genet.* 21:70–71.

Sparwasser T, Gong S, Li JY and Eberl G. (2004). General method for the modification of different BAC types and the rapid generation of BAC transgenic mice. *Genesis*. 38 (1): 39-50.

Staton CA, Lewis C and Bicknell, R. (Eds.) (2006). Angiogenesis Assays, a critical appraisal of current techniques. John Wiley and Sons, Ltd. Chippenham, UK. 390pp.

Stossel TP, Condeelis J, Cooley L, Hartwig JH, Noegel A, Schleicher M and Shapiro SS. (2001). Filamins as integrators of cell mechanics and signalling. *Nat. Rev. Mol. Cell Biol*. 2: 138-145.

Sumanas S, Lin S. (2006). Ets1-related protein is a key regulator of vasculogenesis in zebrafish. *PLoS Biol.* 4(1):e10.

Sumanas S, Gomez G, Zhao Y, Park C, Choi K and Lin S. (2008). Interplay among Etsrp/ER71, Scl and Alk8 signalling controls endothelial and myeloid cell formation. *Blood*. 111: 4500-4510.

Swiers G, Patient R and Loose M. (2006). Genetic regulatory networks programming hematopoietic stem cells and erythroid lineage specification. *Developmental Biology*. 294: 525-540.

Testa G, Schaft J, van der Hoeven F, Glaser S, Anastassiadis K, Zhang Y, Hermann T, Stremmel W and Stewart F. (2004). A reliable lacZ expression reporter cassette for multipurpose, knockout first alleles. *Genesis* 38: 151-158.

Thisse C and Thisse B (2008). High resolution *in situ* hybridization to whole-mount zebrafish embryos. *Nature Protocols*. 3(1): 59-69.

Thomas P and Smart TG. (2005). HEK293 cell line: a vehicle for the expression of recombinant proteins. *J Pharmacol Toxicol Methods*. 51(3):187-200.

Thompson MA, Ransom DG, Pratt SJ, MacLennan H, Kieran MW, Detrich III HW, Vail B, Huber TL, Paw B, Brownlie AJ, Oates AC, Fritz A, Gates MA, Amores A, Bahary N, Talbot WS, Her H, Beier DR, Postlethwait JH, Zon LI. (1998). The *cloche* and *spadetail* genes differentially affect hematopoiesis and vasculogenesis. *Developmental Biology*. 197: 248-269.

Tillement V, Lajoie-Mazenc I, Casanova A, Froment C, Penary M, Tovar D, Marquez R, Monsarrat B, Favre G and Pradines A.(2008). Phosphorylation of RhoB by CK1 impedes actin stress fiber organization and epidermal growth factor receptor stabilization. *Exp Cell Res*. 314 (15): 2811-2821.

Toledo JR, Prieto Y, Oramas N, Sánchez O. (2009). Polyethylenimine-based transfection method as a simple and effective way to produce recombinant lentiviral vectors. *Appl Biochem Biotechnol*. 157(3):538-44.

Tozer GM, Kanthou C and Baguley, BC. (2005) Disrupting tumour blood vessels. *Nature Rev Cancer*. 5: 423-435.

Valle-Perez B, Martinez VG, Lacasa-Salavert C, Figueras A, Shapiro SS, Takafuta T, Casanovas O, Capella G, Ventura F and Vinals F. (2010). Filamin B plays a key role in VEGF-induced endothelial cell motility through its interaction with Rac-1 and Vav-2. *JBC*. 285(14):10748-60.

Verissimo AR, Herbert JMJ, Heath VL, Legg JA, Sheldon H, Andre M, Swain RK and Bicknell R. (2009). Functionally defining the endothelial transcriptome, from Robo4 to ECSCR. *Biochem Soc Trans*. 37: 1214-1217.

Verma A, Bhattacharya R, Remadevi I, Li K, Pramanik K, Samant GV, Horswill M, Chun CZ, Zhao B, Wang E, Miao RQ, Mukhopadhyay D, Ramchandran R and Wilkinson GA. (2010). Endothelial cell specific chemotaxis receptor (ecscr) promotes angioblast migration during vasculogenesis and enhances VEGF receptor sensitivity. *Blood*.

Visvader JE, Fujiwara Y and Orkin SH. (1998). Unsuspected role for the T-cell leukemia protein SCL/tal-1 in vascular development. *Genes and Development.* 12: 473–479.

Wang Y, Kreisberg JI, Bedolla RG, Mikhailova M, de Vere White RW and Ghosh PM. (2007). A 90kDa fragment of filamin A promotes Caosdex-induced growth inhibition in Casodex-resistant androgen receptor positive C4-2 prostate cancer cells. *Oncogene*. 26:6061-6070.

Wang Y, Kaiser MS, Larson JD, Nasevicius A, Clark KJ, Wadman SA, Roberg-Perez SE, Ekker SC, Hackett PB, McGrail M and Essner JJ. (2010). Moesin1 and Ve-cadherin are required in endothelial cells during in vivo tubulogenesis. *Development*. 137(18):3119-28.

Weinstein B. (2000). Plumbing the mysteries of vascular development using the zebrafish. *Semin. Cell Dev Biol.* 13: 515-522.

Wienholds E and Plasterk RH. (2004). Target-selected gene inactivation in zebrafish, *in Methods Cell Biol*. 77: 69-90.

Wu W, Shi C, Ma F, Balducci J, Huang H, Ji H-L, Chang Y and Huang Y. (2012) Structural and functional characterisation of two novel mouse endothelial cell-specific molecule 2 (ECSM2) isoforms. *Int J Mol Sci.* 13(4): 4920–4936.

Wu Y, Wang C, Sun H, LeRoith D and Yakar S. (2009). High-efficient FLPo delete mice in C57BL/6J background. *Plos One*. 4:11.

Xia H, Mao Q, Paulson HL and Davidson BL. (2002). siRNA-mediated gene silencing *in vitro* and *in vivo*. *Nat. Biotehnol.* 20: 1006-1010.

Xian J, Clark KJ, Fordham R, Pannell R, Rabbitts TH and Rabbitts PH. (2001). Inadequate lung development and bronchial hyperplasia in mice with a targeted deletion in the Dutt1/Robo1 gene. *Proc Natl Acad Sci U S A*. 98(26):15062-6.

Xu XZ, Choudhury A, Li X and Montell C. (1998) Coordination of an array of signaling proteins through homo and heteromeric interactions between PDZ domains and target proteins. *J Cell Biol.* 142 (2): 545–555.

Yarrow JC, Periman NJ, Westwood NJ and Mitchison TJ. (2004) A high-throughput cell migration assay using scratch wound healing, a comparison of image based readout methods. *BMC Biotehnol.* 4: 21-30.

Zhao, Xiao-Song, Teresa D. Gallardo, Ling Lin, Jeoffrey J. Schageman, and Ralph V. Shohet. (2002). Transcriptional mapping and genomic analysis of the cardiac atria and ventricles. *Physiol Genomics*.12: 53–60.

Zhong TP. (2005). Zebrafish genetics and formation of embryonic vasculature. *Curr Top Dev Biol*. 71: 53-81.

Zhuang X, Cross D, Heath VL and Bicknell R. (2012). Shear stress, tip cells and regulators of endothelial migration. *Biochem Soc Trans*. 39: 1571-1575.

Zon, L. (1995). Developmental biology of hematopoiesis. *Blood.* 86: 2876-2891.